The Dissertation Committee for Stephen James Shannon
certifies that this is the approved version of the following dissertation:

Hybridized Discontinuous Galerkin Methods for Magnetohydrodynamics

Committee:

Tan Bui-Thanh, Supervisor

Todd Arbogast

Leszek Demkowicz

Omar Ghattas

John Shadid

François Waelbroeck

Hybridized Discontinuous Galerkin Methods for Magnetohydrodynamics

by

Stephen James Shannon

Dissertation

Presented to the Faculty of the Graduate School of

The University of Texas at Austin

in Partial Fulfillment

of the Requirements

for the Degree of

Doctor of Philosophy

The University of Texas at Austin

December 2018

Acknowledgments

I would like to extend special thanks to the following people.

- Tan Bui-Thanh, for sharing his knowledge and for providing direction and support
- John Shadid, for the Summer internship at Sandia National Laboratories in Albuquerque where his guidance helped me to set up the nonlinear time-dependent MHD problems
- John Lee, for significant contributions to the error analysis in this work
- my colleagues, Sriram Krishnan and Shinhoo Kang, for helpful discussions
- my wife, Prapti Neupane, for being patient and supportive
- the Institute for Computational Engineering and Sciences (ICES) for accepting me into their PhD program and for the generous financial support

This work was partially supported by DOE grants DE-SC0010518, DE-SC0011118, and DE-SC0018147 NSF Grant DMS-1620352, and by DOE NNSA ASC Algorithms effort, the DOE Office of Science AMR program at Sandia National Laboratory under contract DE-AC04-94AL85000.

Hybridized Discontinuous Galerkin Methods for Magnetohydrodynamics

by

Stephen James Shannon, Ph.D.
The University of Texas at Austin, 2018

Supervisor: Tan Bui-Thanh

Discontinuous Galerkin (DG) methods combine the advantages of classical finite element and finite volume methods. Like finite volume methods, through the use of discontinuous spaces in the discrete functional setting, we automatically have local conservation, an essential property for a numerical method to behave well when applied to hyperbolic conservation laws. Like classical finite element methods, DG methods allow for higher order approximations with compact stencils. For time-dependent problems with implicit time stepping and for steady-state problems, DG methods give a larger globally coupled linear system than continuous Galerkin methods (especially for three dimensional problems and low polynomial orders). The primary motivation of the hybridized (or hybridizable) discontinuous Galerkin (HDG) methods is to reduce the number of globally coupled DG unknowns when implicit time stepping or direct-to-steady-state solutions are desired. This is accomplished by the introduction of new "trace unknowns" defined on the mesh skeleton, the definition of one-sided numerical fluxes, and the enforcement of local conservation. This results in a globally coupled linear system where the local "volume unknowns" can be eliminated in a

Schur complement procedure, resulting in a reduced globally coupled system in terms of only the trace unknowns. The extent to which the condensed global HDG system is smaller than the global DG system is greater with higher polynomial orders. For this reason, HDG methods can be seen as "high order, implicit" methods, as their benefits are more readily seen when applied to problems that benefit from implicit treatment, and applied with a high spatial (and temporal) resolution.

Magnetohydrodynamics (MHD) is the study of the flow of electrically conducting fluids under the influence of magnetic fields. The MHD equations are used to describe important physical phenomena including laboratory plasmas (plasma confinement in fusion energy devices), astrophysical plasmas (solar coronas, planetary magnetospheres) and liquid metal flows (metallurgy processes, the Earth's molten core, cooling for nuclear reactors). Incompressible MHD, which is the main focus of this work, is relevant in low Lundquist number liquid metals, in high Lundquist number large guide field fusion plasmas, and in low flow-Mach-number compressible flows. The equations of MHD are highly nonlinear, and are characterized by physical phenomena spanning wide ranges of length and time scales. For numerical methods, this presents challenges in both spatial and temporal discretizations. In terms of temporal discretization, fully implicit numerical methods are attractive in their robustness; they allow for stable, high-order time integration over long time scales of interest.

In this work, we employ an upwind framework to first construct HDG schemes for the induction equation and the Oseen equations, which make up the subsystems of the linearized visco-resistive incompressible MHD equations, and prove their well-posedness. Using these schemes, we construct a family of HDG schemes for the MHD equations, each member of the family having a different *minimal* set of trace variables. For one specific choice of trace variables, we prove well-posedness of the scheme and

perform a rigorous a priori error analysis. Finally, we use the scheme to solve a set of benchmark problems in linear and nonlinear, steady state and transient MHD.

Table of Contents

Acknowledgments **iv**

Abstract **v**

List of Tables **x**

List of Figures **xi**

Chapter 1. Introduction **1**
1.1 A General Upwind HDG Framework 5
1.2 Outline 13

Chapter 2. Stokes Equations **15**
2.1 Construction of Upwind HDG Schemes 15
2.2 HDG Schemes Using the $\widehat{\boldsymbol{u}}_h$ Flux 23
2.2.1 Modifications for Local Solver Invertibility 27
2.2.1.1 The Augmented Lagrangian Approach 28
2.2.1.2 The Average Edge Pressure Approach 30
2.3 HDG Schemes Using the $(\widehat{\boldsymbol{u}}_h^t, \widehat{f}_h)$ Flux 32
2.4 Numerical Results 38
2.5 Discussion 42

Chapter 3. Oseen Equations **44**
3.1 Construction of Upwind HDG Schemes 44
3.2 HDG Schemes Using the $\widehat{\boldsymbol{u}}_h$ Flux 53
3.3 HDG Schemes Using the $(\widehat{\boldsymbol{u}}_h^t, \widehat{f}_h)$ Flux 58
3.4 Numerical Results 64
3.5 Discussion 69

Chapter 4. Induction Equation **73**
4.1 Construction of Upwind HDG Schemes 74
4.2 Discussion 84

Chapter 5. Incompressible Magnetohydrodynamics **86**
5.1 Construction of Upwind HDG Schemes 86
5.2 HDG Schemes Using the $(\widehat{\boldsymbol{u}}_h, \widehat{\boldsymbol{b}}_h)$ Flux 96
5.3 HDG Schemes Using the $(\widehat{\boldsymbol{u}}_h^t, \widehat{f}_h, \widehat{\boldsymbol{b}}_h^t, \widehat{r}_h)$ Flux 101
5.4 HDG Schemes Using the $(\widehat{\boldsymbol{u}}_h, \widehat{\boldsymbol{b}}_h^t, \widehat{r}_h)$ Flux 107
5.5 Error Analysis 117
5.5.1 Auxiliary Lemmas 120
5.5.2 Definition of Projections and Their Properties 122
5.5.3 The Error Equations and an Energy Estimate 124
5.5.4 The Adjoint Equations and a Regularity Assumption 130
5.5.5 Definition of Adjoint Projections and Their Properties 131
5.5.6 An Estimate for $\varepsilon_{\boldsymbol{u}}^h$ and $\varepsilon_{\boldsymbol{b}}^h$ 132
5.5.7 Putting It Together 137
5.6 A Nonlinear Solver 141
5.7 Time Integration 143
5.8 Numerical Results 144
5.8.1 Smooth Solution 144
5.8.2 Singular Solution 145
5.8.3 Hartmann Flow 147
5.8.4 Rayleigh Flow 152
5.8.5 Magnetic Reconnection - Island Coalescence 154

Chapter 6. Conclusions and Future Work **172**

Appendices **178**

Appendix A. Common Notation **179**

Appendix B. Characterization of HDG Schemes for the Stokes Equations **183**
B.1 Characterization of Formulation 2.2 184
B.2 Characterization of Formulation 2.3 187
B.3 Characterization of Formulation 2.4 191

Appendix C. Additional Fluxes for the Oseen Equations **198**

Appendix D. Proofs of Properties of Projections **201**

Bibliography **210**

List of Tables

1.1 Ratio of DG to HDG globally coupled unknowns for a scalar variable. 10

5.1 HDG fluxes for the linearized incompressible visco-resistive MHD equations. 95

List of Figures

1.1 DG unknowns (left) and HDG unknowns (right). 10

2.1 Stokes HDG schemes: Kovasznay flow problem solution - $\boldsymbol{u}_{h1}$ (top left), $\boldsymbol{u}_{h2}$ (top right), and p_h (bottom). 40

2.2 Stokes HDG schemes: Kovasznay flow problem L^2 convergence of volume unknowns using $\widehat{\boldsymbol{u}}_h$ flux (2.16) (left), using $(\widehat{\boldsymbol{u}}_h^t, \widehat{f}_h)$ flux (2.18) (right). 41

3.1 Oseen HDG schemes: Kovasznay flow problem solution - $\boldsymbol{u}_{h1}$ (top left), $\boldsymbol{u}_{h2}$ (top right), and p_h (bottom). 66

3.2 Oseen HDG schemes: Kovasznay flow problem L^2 convergence of volume unknowns using $\widehat{\boldsymbol{u}}_h$ flux (3.21) (left), using $(\widehat{\boldsymbol{u}}_h^t, \widehat{f}_h)$ flux (3.23) (right). 67

3.3 Oseen HDG schemes: Kovasznay flow problem nonlinear solution with Picard iteration - L^2 convergence of volume unknowns using $\widehat{\boldsymbol{u}}_h$ flux (3.21) (left), using $(\widehat{\boldsymbol{u}}_h^t, \widehat{f}_h)$ flux (3.23) (right). 70

5.1 Geometry of the non-convex domain with a mesh at refinement level $l = 4$. 145

5.2 MHD smooth solution problem: L^2 convergence. 146

5.3 MHD singular solution problem: L^2 convergence. 148

5.4 Hartmann flow problem: numerical and exact solution for u_1 (left) and b_1 (right). 151

5.5 Hartmann flow problem: numerical and exact solution for u_1 (left) and b_1 (right), scaled to reveal boundary layers. 151

5.6 Hartmann flow problem: spatial convergence in L^2 norm for velocity and magnetic field. 152

5.7 Rayleigh flow problem: numerical and exact solution for u_1 (left) and b_1 (right) for $b_0 = 10$. 154

5.8 Rayleigh flow problem: numerical and exact solution for u_1 (left) and b_1 (right) for $b_0 = 100$. 155

5.9 Rayleigh flow problem: temporal convergence in L^2 norm for u_1 (left) and b_1 (right). 155

5.10 Rayleigh flow problem: spatial convergence in L^2 norm for u_1 (left) and b_1 (right). 156

5.11 Magnetic island coalescence problem: initial magnetic vector potential (left), and initial current (right). 160
5.12 Magnetic island coalescence problem: initial magnetic field configuration. 160
5.13 Magnetic island coalescence problem: initial pressure profile. 161
5.14 Magnetic island coalescence problem: perturbation in the initial magnetic vector potential (left), and perturbation in the initial current (right). 163
5.15 Magnetic island coalescence problem: perturbation in the initial magnetic field configuration. 164
5.16 Magnetic island coalescence problem: reconnection rates. 166
5.17 Magnetic island coalescence problem: peak reconnection rates. 167
5.18 Magnetic island coalescence problem: current density $\boldsymbol{J}_h$ in x_3 direction with $Re = Rm = 10^{3.5}$ for $t = 0, 5, 6, 7, 8$ (top to bottom). 168
5.19 Magnetic island coalescence problem: pressure p_h with $Re = Rm = 10^{3.5}$ for $t = 0, 5, 6, 7, 8$ (top to bottom). 169
5.20 Magnetic island coalescence problem: current density $\boldsymbol{J}_h$ in x_3 direction with $Re = Rm = 10^{4.5}$ for $t = 0, 5, 6, 7, 8$ (top to bottom). 170
5.21 Magnetic island coalescence problem: pressure p_h with $Re = Rm = 10^{4.5}$ for $t = 0, 5, 6, 7, 8$ (top to bottom). 171

Chapter 1

Introduction

Our interest in magnetohydrodynamics (MHD) is primarily motivated by advances in nuclear fusion. Decades of scientific advances in the field of nuclear fusion have brought us closer and closer to a revolutionary large-scale renewable energy source. A promising method by which to achieve nuclear fusion is sustaining a deuterium-tritium reaction in a high temperature, magnetically confined plasma. Among the many challenges in realizing this goal is understanding the instabilities that lead to plasma disruption (a termination of plasma discharge, which can be accompanied by damage to plasma-facing components). MHD is a single-fluid model of the magnetized plasma that is used as a base model for simulations to assess macroscopic, long-time instabilities in fusion plasmas.

Physically, MHD is the study of the flow of electrically conducting fluids under the influence of magnetic fields. Mathematically, MHD is described by the coupling of the Navier-Stokes equations of fluid flow (mass, momentum, and energy balance) with a reduced form of Maxwell's equations of electromagnetism. Specifically, the fluid momentum balance equation is altered by the additional consideration of the Lorentz force, and the system is closed by the low frequency Maxwell's equations and Ohm's law. In addition to laboratory plasmas, the MHD equations are used to describe important physical phenomena [31, 48, 49], including astrophysical plasmas (solar coronas, planetary magnetospheres) and liquid metal flows (metallurgy processes, the Earth's molten core, cooling for nuclear reactors). Incompressible MHD, which is the

main focus of this work, is relevant in low Lundquist number liquid metals, in high Lundquist number, large guide field fusion plasmas, and in low flow-Mach-number compressible flows [64].

The MHD equations are highly nonlinear, and are characterized by physical phenomena spanning wide ranges of length and time scales. For numerical methods, this presents challenges in both spatial and temporal discretizations. In terms of temporal discretization, fully implicit numerical methods are attractive in their robustness; they allow for stable, high-order time integration over long time scales of interest [64]. However, fully implicit methods for MHD systems lead to large, highly nonlinear systems of equations. Because of this limitation, the prevailing computational strategy in solving MHD systems numerically has been to employ explicit or partially implicit methods. However, these methods make concessions in the form of conditional stability limits, operator splitting errors, and temporal order of convergence limits. With modern computers and modern linear/nonlinear solvers, fully implicit methods have seen an increase in relevance (see, e.g. [38, 42, 70, 14, 15, 67, 12, 44, 13, 65, 68, 39, 63]). High order spatial discretizations for MHD can handle extreme anisotropies without the need for a specific mesh orientation, and coupled with a numerical scheme with some form of imposition of the solenoidal constraint, high order methods are useful in imposing the constraint to high accuracy. See, e.g., [69] for discussions related to high order methods and dealing with these discretization challenges.

As mentioned, one of the challenges in spatial discretization of the MHD equations is the enforcement of the divergence-free constraint on the magnetic field. Recent finite element methods for incompressible MHD can be put into three categories based on the way they deal with the divergence-free constraint: methods derived from the exact penalty [33, 28], or weighted exact penalty [34] formulation of the continuous

weak form, methods derived from the double saddle-point form of the continuous weak form, [61, 25, 37, 5, 64] and methods derived from a vector potential form of the PDE [62]. Galerkin methods [33] (that is, methods that use the same linear, bilinear, and trilinear forms as in the continuous weak formulation) and stabilized methods [28] posed in $H^1(\Omega)$ on the exact penalty formulation do not converge to solutions on domains that have reentrant corners; that is, they converge only for solutions on sufficiently smooth domains or on convex domains. The same can be said in general about stabilized methods based on the saddle point formulation of the magnetic subproblem [25, 64]. The Galerkin method in [34] based on a weighted exact penalty formulation is proven to converge to singular solutions with proper tuning of a weighting parameter with a priori knowledge about the location of the singularities. The stabilized method in [5] based on the saddle point formulation of the magnetic subproblem is proven to converge to singular solutions with strategically defined stabilization parameters and the use of a particular macro-element structure. The Galerkin method in [61] utilizing inf-sup stable pairs for the fluid and magnetic subproblems and the mixed order interior penalty DG method in [37] converge unconditionally to singular solutions. The stabilized methods and the DG methods have benefits in implementational considerations; they employ equal order polynomial basis functions (or mixed order, in the case of [37]), as opposed to inf-sup stable vector basis functions, which have increased complexity in the computational implementation.

The Discontinuous Galerkin (DG) method was introduced by Reed and Hill [59] for the neutron transport problem. DG combines the advantages of classical finite element and finite volume methods [36]. Like finite volume methods, through the use of discontinuous spaces in the discrete functional setting, DG methods automatically achieve local conservation, an essential property for a numerical method to behave well when applied to hyperbolic conservation laws. Like classical finite element methods,

DG methods allow for higher order approximations with compact stencils. DG is also naturally suited to handle adaptive mesh refinement.

For time-dependent problems with implicit time stepping and for steady-state problems, DG methods give a larger globally coupled linear system than CG methods (especially for three dimensional problems and low polynomial orders). The primary motivation of the hybridized (or hybridizable) discontinuous Galerkin (HDG) methods is to reduce the number of globally coupled DG unknowns when implicit time stepping or direct-to-steady-state solutions are desired. This is accomplished by the introduction of new "trace unknowns" defined on the mesh skeleton, the definition of one-sided numerical fluxes, and the enforcement of local conservation. This results in a globally coupled linear system where the local "volume unknowns" can be eliminated in a Schur complement procedure, resulting in a reduced globally coupled system in terms of only the trace unknowns. The extent to which the condensed global HDG system is smaller than the global DG system is greater with higher polynomial orders (and with lower spatial dimension) [10]. For this reason, HDG methods can be seen as "high order, implicit" methods, as their benefits are more readily seen when applied to problems that benefit from implicit treatment, and applied with a high spatial (and temporal) resolution. Additional benefits of HDG schemes include [56]

- better convergence properties for flux variables than for existing DG methods,
- the ability to perform a local post-processing, which for incompressible flow problems, gives a velocity that is divergence free and globally $H(div)$ conforming and gains an order of convergence, and
- a natural framework through which to apply different types of boundary conditions.

HDG schemes have been introduced for many different PDEs including elliptic problems [21], linear convection-diffusion [55], Stokes equations [53, 16, 23, 24], Oseen equations [11], and incompressible Navier-Stokes equations [56]. The reference [16] studies the Stokes equations in vorticity form with multiple sets of boundary conditions, which have an identical structure to the saddle point form of the magnetic subproblem of the resistive MHD equations. In [9], Bui-Thanh presents a systematic framework, based on a Godunov approach, through which to construct HDG schemes for a broad class of PDEs, and in [10], the author presents an alternate framework using the Rankine-Hugoniot condition. Using these frameworks, we can derive new HDG methods, and we can re-derive most existing HDG methods in their parameter-free upwind form.

1.1 A General Upwind HDG Framework

In this section, we outline the basic concepts of HDG in the context of a general class of PDEs and review the upwind HDG framework [9]. The reader can refer to Appendix A for the common notation used throughout this work. Consider the abstract first order system of PDEs

$$\frac{\partial \boldsymbol{u}}{\partial t} + \nabla \cdot \mathbf{F}(\boldsymbol{u}) + \mathbf{C}\boldsymbol{u} := \frac{\partial \boldsymbol{u}}{\partial t} + \sum_{\ell=1}^{d} \frac{\partial \mathbf{F}_\ell(\boldsymbol{u})}{\partial x_\ell} + \mathbf{C}\boldsymbol{u} = \boldsymbol{f} \quad \text{in } \Omega, \tag{1.1}$$

where the vector $\mathbf{F}_\ell = \mathbf{A}^\ell \boldsymbol{u}$ is the ℓth component of the flux, $\boldsymbol{u} \in \mathbb{R}^m$ is the unknown solution, and $\boldsymbol{f}$ is a forcing term. For simplicity, the matrices $\mathbf{A}^\ell$ are assumed to be continuous across Ω.

Formally, multiplying (1.1) by an elementwise continuous test function, integrating over every element K of a finite element mesh $\mathcal{T}_h$, and integrating by parts,

we have

$$\left(\frac{\partial \boldsymbol{u}}{\partial t}, \boldsymbol{v}\right)_K - (\mathbf{F}(\boldsymbol{u}), \nabla \boldsymbol{v})_K + (\mathbf{C}\boldsymbol{u}, \boldsymbol{v})_K + \langle \mathbf{F}(\boldsymbol{u}) \cdot \boldsymbol{n}, \boldsymbol{v} \rangle_{\partial K} = (\boldsymbol{f}, \boldsymbol{v})_K \,. \tag{1.2}$$

The boundary term $\mathbf{F}(\boldsymbol{u}) \cdot \boldsymbol{n}$ can be written as $\mathbf{F}(\boldsymbol{u}) \cdot \boldsymbol{n} = \mathbf{A}\boldsymbol{u}$, where

$$\mathbf{A} := \sum_{\ell=1}^{d} \mathbf{A}^{\ell} n_{\ell}. \tag{1.3}$$

The treatment of this boundary term in the numerical scheme is what differentiates HDG and traditional DG. Working now with discrete (polynomial) function spaces, replacing the boundary term by a single-valued flux that depends on the solution $\boldsymbol{u}_h$ on each side of the interface, $\mathbf{F}_h^* = \mathbf{F}_h^*(\boldsymbol{u}_h^-, \boldsymbol{u}_h^+)$ gives a semidiscrete DG scheme

$$\left(\frac{\partial \boldsymbol{u}_h}{\partial t}, \boldsymbol{v}\right)_K - (\mathbf{F}(\boldsymbol{u}_h), \nabla \boldsymbol{v})_K + (\mathbf{C}\boldsymbol{u}_h, \boldsymbol{v})_K + \left\langle \mathbf{F}_h^*(\boldsymbol{u}_h^-, \boldsymbol{u}_h^+) \cdot \boldsymbol{n}, \boldsymbol{v} \right\rangle_{\partial K} = (\boldsymbol{f}, \boldsymbol{v})_K \,. \tag{1.4}$$

For steady-state problems and time-dependent problems with implicit time discretization, the DG scheme (1.4) leads to a sparse matrix system where all the unknowns are globally coupled. Instead, to construct an HDG scheme, we introduce the trace quantity $\widehat{\boldsymbol{u}}_h$ and replace the flux on the boundary in (1.2) by a one sided HDG flux $\widehat{\mathbf{F}}_h = \widehat{\mathbf{F}}_h(\boldsymbol{u}_h^-, \widehat{\boldsymbol{u}}_h)$, which gives

$$\left(\frac{\partial \boldsymbol{u}_h}{\partial t}, \boldsymbol{v}\right)_K - (\mathbf{F}(\boldsymbol{u}_h), \nabla \boldsymbol{v})_K + (\mathbf{C}\boldsymbol{u}_h, \boldsymbol{v})_K + \left\langle \widehat{\mathbf{F}}_h\left(\boldsymbol{u}_h, \widehat{\boldsymbol{u}}_h\right) \cdot \boldsymbol{n}, \boldsymbol{v} \right\rangle_{\partial K} = (\boldsymbol{f}, \boldsymbol{v})_K \,. \tag{1.5}$$

To close the system, we enforce that the normal flux is (weakly) continuous across element interfaces,

$$\left\langle \widehat{\mathbf{F}}_h\left(\boldsymbol{u}_h, \widehat{\boldsymbol{u}}_h\right) \cdot \boldsymbol{n}, \widehat{\boldsymbol{v}} \right\rangle_{\partial \mathcal{T}_h \setminus \partial \Omega} = 0 \tag{1.6}$$

for test functions $\widehat{\boldsymbol{v}}$ that reside in the same space as $\widehat{\boldsymbol{u}}_h$. The HDG scheme comprises the local solver (1.5), the transmission or conservation conditions (1.6), and boundary

conditions, which are prescribed through the trace unknowns on the domain boundary. The main point of the upwind HDG framework [9] is the definition of the HDG flux. The Godunov flux is traditionally written as

$$\mathbf{F}^* \cdot \boldsymbol{n}^- = \frac{1}{2}\left[\mathbf{F}(\boldsymbol{u}^-) + \mathbf{F}(\boldsymbol{u}^+)\right] \cdot \boldsymbol{n}^- + \frac{1}{2}\left|\mathbf{A}\right|\left(\boldsymbol{u}^- - \boldsymbol{u}^+\right), \tag{1.7}$$

but can also be written in terms of the upwind state $\boldsymbol{u}^*$ as

$$\mathbf{F}^* \cdot \boldsymbol{n} = \mathbf{F}(\boldsymbol{u}) \cdot \boldsymbol{n} + \left|\mathbf{A}\right|\left(\boldsymbol{u} - \boldsymbol{u}^*\right). \tag{1.8}$$

This one-sided expression of the Godunov flux leads naturally to the definition of the HDG flux by treating the upwind state $\boldsymbol{u}^*$ as an unknown $\widehat{\boldsymbol{u}}$,

$$\widehat{\mathbf{F}}_h \cdot \boldsymbol{n} = \mathbf{F}(\boldsymbol{u}_h) \cdot \boldsymbol{n} + \left|\mathbf{A}\right|\left(\boldsymbol{u}_h - \widehat{\boldsymbol{u}}_h\right). \tag{1.9}$$

We assume that $\mathbf{A}$ admits an eigendecomposition $\mathbf{R}\mathbf{D}\mathbf{R}^{-1}$, and define $\left|\mathbf{A}\right| := \mathbf{R}\left|\mathbf{D}\right|\mathbf{R}^{-1}$, where $\left|\mathbf{D}\right|$ is a matrix obtained by taking the absolute values of the entries of $\mathbf{D}$. Thus, the upwind HDG framework provides a unified methodology by which to derive parameter-free HDG schemes by hybridizing the Godunov flux. We refer the reader to [9] for more details. It may appear that we have as many trace variables as variables in the first order PDE system, but we can reduce the number of trace variables when we consider each PDE specifically, as will be demonstrated in chapters 2, 3, and 4.

For linear systems, the HDG scheme (1.5) and (1.6) gives rise to the following matrix equations, where $\mathbb{U}$ represents the vector degrees of freedom of $\boldsymbol{u}_h$, and $\widehat{\mathbb{U}}$ represents the vector degrees of freedom of $\widehat{\boldsymbol{u}}_h$,

$$\begin{bmatrix} \mathbb{A} & \mathbb{B} \\ \mathbb{C} & \mathbb{D} \end{bmatrix} \begin{Bmatrix} \mathbb{U} \\ \widehat{\mathbb{U}} \end{Bmatrix} = \begin{Bmatrix} \mathbb{F}_l \\ \mathbb{F}_g \end{Bmatrix}. \tag{1.10}$$

Here, the subscripts l and g stand for local and global, respectively. Nonzero terms in $\mathbb{F}_g$ may result, for example, depending on the boundary conditions and how they are enforced.

The power of HDG comes from the following.

- The HDG flux is one-sided, i.e., for a given element, the flux depends only on the solution in that element and the neighboring skeleton faces. Together with the fact that the discontinuous basis functions are local to one element, this implies that $\mathbb{A}$ is *block diagonal*.
- If the local solver $(\widehat{\boldsymbol{u}}_h, \boldsymbol{f}) \mapsto \boldsymbol{u}_h$ given by (1.5) is well-posed, then $\mathbb{A}$ is *invertible*.

A consequence of these two points is that we can easily eliminate $\mathbb{U}$ from (1.10) by a static condensation procedure, and write

$$\mathbb{U} = \mathbb{A}^{-1}\left[\mathbb{F}_l - \mathbb{B}\widehat{\mathbb{U}}\right]. \tag{1.11}$$

The global system (1.10) then reduces to

$$\underbrace{\left(\mathbb{D} - \mathbb{C}\left[\mathbb{A}\right]^{-1}\mathbb{B}\right)}_{\mathbb{K}}\widehat{\mathbb{U}} = \underbrace{\mathbb{F}_g - \mathbb{C}\left[\mathbb{A}\right]^{-1}\mathbb{F}_l}_{\mathbb{F}}. \tag{1.12}$$

In practice, $\mathbb{K}$ and $\mathbb{F}$ are formed by a local assembly procedure, $\widehat{\mathbb{U}}$ is solved for from the reduced global system (1.12), and then $\mathbb{U}$ is recovered in an element by element fashion from (1.11).

Figure 1.1 shows a schematic of the DG and HDG unknowns for a conforming mesh, with the globally coupled unknowns in red. For steady-state schemes or time dependent schemes with implicit time stepping, the DG discretization leads to a sparse matrix system where the all of the unknowns are coupled, whereas only the trace unknowns in HDG are globally coupled. It is useful to explicitly write the ratio

of globally coupled DG to HDG unknowns. If we assume a periodic domain (or a sufficiently fine mesh such that the number of boundary skeleton faces is negligible compared to the number of interior skeleton faces) and that the mesh is geometrically conforming (no hanging nodes), then knowing that each skeleton face has exactly two neighboring elements, we can make a geometrical argument as to the ratio of DG unknowns to HDG unknowns. For polynomial degree k and spatial dimension d, the ratio for simplicial meshes with total degree polynomials becomes

$$\frac{\#\text{DG}_k \text{ unk}}{\#\text{HDG}_k \text{ unk}} = \frac{\#\text{vol elmts}}{\#\text{skel elmts}} \frac{\left\lceil \frac{\#\text{unk}}{\text{vol elmt}} \right\rceil}{\left\lceil \frac{\#\text{unk}}{\text{skel elmt}} \right\rceil} = \frac{2}{d+1} \frac{\left\lceil \frac{(k+d)!}{k!d!} \right\rceil}{\left\lceil \frac{(k+d-1)!}{k!(d-1)!} \right\rceil} = \frac{2(k+d)}{d(d+1)}, \tag{1.13}$$

and the ratio for quadrilateral/hexahedral meshes with tensor-product polynomial basis functions becomes

$$\frac{\#\text{DG}_k \text{ unk}}{\#\text{HDG}_k \text{ unk}} = \frac{\#\text{vol elmts}}{\#\text{skel elmts}} \frac{\left\lceil \frac{\#\text{unk}}{\text{vol elmt}} \right\rceil}{\left\lceil \frac{\#\text{unk}}{\text{skel elmt}} \right\rceil} = \frac{2}{2d} \frac{(k+1)^d}{(k+1)^{d-1}} = \frac{k+1}{d}. \tag{1.14}$$

These ratios are explicitly written in Table 1.1 for polynomial orders 1 through 10. As can be seen, the ratio is higher (and thus the benefits of HDG are more readily seen) for tensor-product elements and for lower spatial dimension. The cross-over point where the number of coupled HDG unknowns is smaller than the number of coupled DG unknowns is shown in blue. In particular, for hexahedral elements the ratio is one for $k = 2$ and for tetrahedral elements the ratio is one at $k = 3$.

An additional reduction of unknowns beyond the above geometrical argument is possible for certain equations. Local discontinuous Galerkin (LDG) methods for incompressible flow problems [18, 19] result in a global coupling of the velocity $\boldsymbol{u}_h$ and pressure p_h unknowns over the whole domain, whereas HDG formulations in the literature [53, 11, 56] have globally coupled unknowns related to the trace velocity only, or the trace velocity and an elementwise constant edge-pressure. In the former, another $\frac{d+1}{d}$ reduction in trace unknowns is achieved, but the system is solved

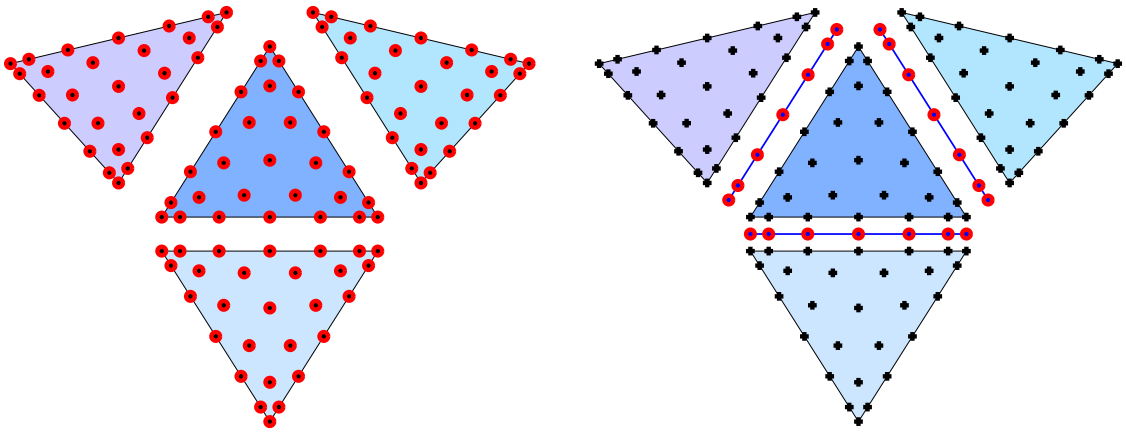

Figure 1.1: DG unknowns (left) and HDG unknowns (right).

	1D	2D		3D	
poly. order		quad	tri	hex	tet
1	**2.00**	**1.00**	**1.00**	0.67	0.67
2	**3.00**	**1.50**	**1.33**	**1.00**	0.83
3	**4.00**	**2.00**	**1.67**	**1.33**	**1.00**
4	**5.00**	**2.50**	**2.00**	**1.76**	**1.17**
5	**6.00**	**3.00**	**2.33**	**2.00**	**1.33**
6	**7.00**	**3.50**	**2.67**	**2.33**	**1.50**
7	**8.00**	**4.00**	**3.00**	**2.67**	**1.67**
8	**9.00**	**4.50**	**3.33**	**3.00**	**1.83**
9	**10.00**	**5.00**	**3.67**	**3.33**	**2.00**
10	**11.00**	**5.50**	**4.00**	**3.67**	**2.17**
k	$k+1$	$\frac{k+1}{2}$	$\frac{k+2}{3}$	$\frac{k+1}{3}$	$\frac{k+3}{6}$

Table 1.1: Ratio of DG to HDG globally coupled unknowns for a scalar variable.

iteratively. In the latter, the elementwise scalar becomes negligible *in terms of the number of coupled unknowns* in 3D and with high polynomials order. Later in this work we introduce schemes for the Stokes and Oseen equations that have d scalar trace variables without the need to solve the system iteratively, thus achieving the $\frac{d+1}{d}$ reduction without qualification.

Even though we hinted at the possibility of using the Godunov flux as a the numerical flux in a traditional DG scheme, this leads to impractical schemes for PDE systems. Thus, HDG allows the use of numerical fluxes that DG does not practically allow, and HDG has the mathematical benefits that come with these fluxes. To illustrate this, we consider the example of the Poisson equation in first order form,

$$\boldsymbol{q} - \nabla u = 0, \tag{1.15a}$$

$$-\nabla \cdot \boldsymbol{q} = f. \tag{1.15b}$$

A DG scheme takes the following form for some numerical fluxes u_h^* and $\boldsymbol{q}_h^*$ that are single-valued by definition,

$$(\boldsymbol{q}_h, \boldsymbol{r})_{\mathcal{T}_h} + (u_h, \nabla \cdot \boldsymbol{r})_{\mathcal{T}_h} - \langle u_h^*, \boldsymbol{r} \cdot \boldsymbol{n} \rangle_{\partial \mathcal{T}_h} = 0, \tag{1.16a}$$

$$(\boldsymbol{q}_h, \nabla v)_{\mathcal{T}_h} - \langle \boldsymbol{q}_h^* \cdot \boldsymbol{n}, v \rangle_{\partial \mathcal{T}_h} = (f, v)_{\mathcal{T}_h}. \tag{1.16b}$$

In general, and in the case of the Godunov flux, $u_h^* = u_h^*({u_h}^-, {u_h}^+, {\boldsymbol{q}_h}^-, {\boldsymbol{q}_h}^+)$ and $\boldsymbol{q}_h^* = \boldsymbol{q}_h^*({u_h}^-, {u_h}^+, {\boldsymbol{q}_h}^-, {\boldsymbol{q}_h}^+)$, which, in general, leads to a scheme where $\boldsymbol{q}_h$ and u_h are coupled across the entire domain. The prevailing DG schemes in the literature are such that $\boldsymbol{q}_h$ can be eliminated locally [4, 36], avoiding that all primal and auxiliary unknowns are globally coupled. This is possible if u_h^* is not a function of $\boldsymbol{q}_h$, i.e., $\boldsymbol{u}_h^* = u_h^*({u_h}^-, {u_h}^+)$. On the other hand, the local equations of an HDG scheme look the same as above, but the Godunov flux can be manipulated so that the numerical flux takes $u_h^* = \widehat{u}_h$, $\boldsymbol{q}_h^{*-} = \boldsymbol{q}_h^*({u_h}^-, {\boldsymbol{q}_h}^-, \widehat{u}_h)$, and $\boldsymbol{q}_h^{*+} = \boldsymbol{q}_h^*({u_h}^+, {\boldsymbol{q}_h}^+, \widehat{u}_h)$, with the

scheme being closed by $\langle \boldsymbol{q}_h^* \cdot \boldsymbol{n}, \widehat{v} \rangle_{\partial \mathcal{T}_h \setminus \partial\Omega} = 0$. A similar limitation for the DG flux extends to other PDEs; the $\boldsymbol{u}_h^*$ term in the auxiliary equation must not be a function of the auxiliary variable, otherwise the auxiliary variable will be coupled globally to the rest of the unknowns. Thus, if we limit ourselves to the Godunov flux, we see a very significant reduction in the number of globally coupled unknowns; for the Poisson equation this reduction is a factor of $d+1$.

This is not a fair or practical comparison, however. A better comparison is as follows. In general, LDG methods for the second order elliptic problem are known to give L^2 convergence of $k+1$ and k for the primal and auxiliary variable, respectively, when both variables are approximated by kth order polynomials. HDG methods for this problem have been shown to converge at a rate of $k+1$ for both the primal and auxiliary variable. Furthermore, through a local procedure, a postprocessed primal variable $u^\star$ can be computed which converges at a rate of $k+2$ for $k \geq 1$. Thus, at the cost of solving a globally coupled primal trace system of polynomial order k, we ultimately can recover approximations of order $k+2$ and $k+1$ for the primal and auxiliary variable, respectively. So, to recover an HDG solution of the same order of accuracy as an LDG solution, the globally coupled system for the LDG system must be associated with unknowns of one polynomial order higher. In this scenario, HDG effectively gives an additional reduction of globally coupled unknowns. For simplicial elements, the factor of this reduction is $\frac{k+1+d}{k+1}$ and for tensor-product elements, this factor is $\left[\frac{k+2}{k+1}\right]^d$, where k is the polynomial order of the HDG solution. These factors multiply the factors in Table 1.1 so that the ratio of DG to HDG unknowns is greater than one for all cases. Similar statements can be made regarding HDG and LDG methods for the Stokes and incompressible Navier-Stokes equations. In these cases, LDG methods give an L^2 convergence rate of $k+1$, k, and k for the velocity, auxiliary variable, and pressure, respectively, whereas HDG methods give an L^2 convergence

rate of $k+2$, $k+1$, and $k+1$ for the postprocessed velocity, the auxiliary variable, and the pressure, respectively.

1.2 Outline

In this work, we introduce a a family of high order, implicit numerical methods for solving problems in MHD. Specifically, we have developed the *first known HDG schemes for MHD equations*. Attractive features of these HDG schemes include the ability to use *equal order* Lagrange polynomial (simplicial or tensor product) basis functions, the *lack of mesh-dependent parameters*, and *convergence to solutions on nonconvex domains and singular solutions*. We employ the upwind framework [9] to construct an upwind-like HDG scheme for a linearization of the double saddle point form of the viscous, resistive, incompressible MHD equations.

The rest of this work is outlined as follows. In Chapter 2, we apply the upwind HDG framework to the velocity-pressure-gradient form of the Stokes equations to derive four HDG schemes, which differ from each other by the choice of unknowns for the trace variable. One of the schemes is related to existing schemes in the literature, whereas the other three are new methods. One of the new schemes provides the advantage that no modifications to the basic scheme to ensure uniqueness of the pressure in the local solver. We perform well-posedness analysis for these two schemes and provide numerical convergence results. In Chapter 3, we extend the schemes for the Stokes equations to the Oseen equations. We again prove well-posedness for two schemes. Numerical results are provided for linear problems and for nonlinear problems using a Picard iteration. In Chapter 4, we apply the upwind HDG framework to the induction equation and define four HDG schemes that take the same form as existing schemes for the velocity-pressure-vorticity form of the Stokes equations. In

Chapter 5, we define HDG schemes for the viscous, resistive, incompressible MHD equations by strategically combining the numerical fluxes for the Oseen equations and the induction equation. For one resulting scheme, we prove well-posedness and perform a rigorous projection-based L^2 error analysis. Numerical studies are performed for linear, steady state problems with smooth and singular solutions, and for nonlinear steady-state and time dependent problems in liquid metal flow and in plasma physics. Finally, in Chapter 6 we summarize the work and provide directions for future research.

Chapter 2

Stokes Equations

In this chapter, we construct HDG methods for the Stokes equations based on the upwind HDG framework proposed in [9]. The HDG methods are based on the first order Stokes system defined through an auxiliary variable based on the velocity gradient. Through the use of this framework, we derive four different HDG schemes. One of the schemes is related to or is precisely the one defined in [53, 9]. The other schemes are new in this work. We prove well-posedness of two schemes that seem to be particularly useful, and present numerical results for these two schemes, showing that they give practically identical results. The HDG schemes developed in this chapter serve as logical starting points for developing schemes for the Oseen equations, which are used as building blocks in our MHD schemes.

2.1 Construction of Upwind HDG Schemes

For notation used in this chapter and throughout this work, see Appendix A. The Stokes equations in dimensionless form reads

$$-\frac{1}{\mathrm{Re}}\Delta \boldsymbol{u} + \nabla p = \boldsymbol{f}, \tag{2.1a}$$

$$\nabla \cdot \boldsymbol{u} = 0, \tag{2.1b}$$

where $\mathrm{Re} := \frac{\rho u_0 l_0}{\mu}$ is the Reynolds number, ρ is the fluid density, u_0 is a characteristic speed, l_0 is a characteristic length scale, and μ is the dynamic viscosity of the fluid. All parameters are assumed to be constant. In the construction of HDG schemes, we

consider the boundary conditions

$$\boldsymbol{u} = \boldsymbol{u}_D \quad \text{on } \partial\Omega_D, \tag{2.2a}$$

$$-\frac{1}{\mathrm{Re}}\nabla u \cdot \boldsymbol{n} + p\boldsymbol{n} = \boldsymbol{f}_N \quad \text{on } \partial\Omega_N, \tag{2.2b}$$

where $\partial\Omega_D \cap \partial\Omega_N = \emptyset$ and $\partial\Omega_D \cup \partial\Omega_N = \partial\Omega$. In the case that $\partial\Omega_N = \emptyset$, the compatibility condition on the Dirichlet boundary data $\int\limits_{\partial\Omega} \boldsymbol{u}_D \cdot \boldsymbol{n} = 0$ should be satisfied, and we have to impose an additional constraint on the pressure. We choose this constraint to be the zero mean pressure $\int\limits_{\Omega} p = 0$. For simplicity, we consider the case where $\partial\Omega_D \neq \emptyset$.

Toward applying the upwind HDG framework outlined in [9], we first put (2.1a) into first order form through the definition of an auxiliary variable. We have multiple choices as to how to define the auxiliary variable, leading to different HDG formulations. In this work, we define the auxiliary variable $\mathbf{L}$ through the velocity gradient, leading to a velocity-gradient-pressure formulation:

$$\mathrm{Re}\mathbf{L} - \nabla\boldsymbol{u} = 0, \tag{2.3a}$$

$$-\nabla \cdot \mathbf{L} + \nabla p = \boldsymbol{f}, \tag{2.3b}$$

$$\nabla \cdot \boldsymbol{u} = 0. \tag{2.3c}$$

To define a general HDG scheme for the Stokes equations, we multiply (2.3) by a test function, integrate over the computational domain, integrate by parts, replace the boundary terms with a not-necessarily-single-valued HDG flux, then weakly enforce the single valuedness of the HDG flux. HDG schemes defined in this manner for (2.3) will take a general form consisting of the local equations

$$\mathrm{Re}\,(\mathbf{L}_h, \mathbf{G})_{\mathcal{T}_h} + (\boldsymbol{u}_h, \nabla \cdot \mathbf{G})_{\mathcal{T}_h} - \langle \boldsymbol{u}_h^* \otimes \boldsymbol{n}, \mathbf{G}\rangle_{\partial\mathcal{T}_h} = 0, \tag{2.4a}$$

$$(\mathbf{L}_h, \nabla\boldsymbol{v})_{\mathcal{T}_h} - (p_h, \nabla \cdot \boldsymbol{v})_{\mathcal{T}_h} + \langle -\mathbf{L}_h^*\boldsymbol{n} + p_h^*\boldsymbol{n}, \boldsymbol{v}\rangle_{\partial\mathcal{T}_h} = (\boldsymbol{f}, \boldsymbol{v})_{\mathcal{T}_h}, \tag{2.4b}$$

$$-(\boldsymbol{u}_h, \nabla q)_{\mathcal{T}_h} + \langle \boldsymbol{u}_h^* \cdot \boldsymbol{n}, q\rangle_{\partial\mathcal{T}_h} = 0, \tag{2.4c}$$

the conservation equations

$$\left\langle \boldsymbol{u}_h^* \otimes \boldsymbol{n}, \widehat{\mathbf{G}} \right\rangle_{\partial\mathcal{T}_h \setminus \partial\Omega} = 0, \tag{2.4d}$$

$$-\left\langle -\mathbf{L}_h^* \boldsymbol{n} + p_h^* \boldsymbol{n}, \widehat{\boldsymbol{v}} \right\rangle_{\partial\mathcal{T}_h \setminus \partial\Omega} = 0, \tag{2.4e}$$

$$-\left\langle \boldsymbol{u}_h^* \cdot \boldsymbol{n}, \widehat{q} \right\rangle_{\partial\mathcal{T}_h \setminus \partial\Omega} = 0, \tag{2.4f}$$

and the boundary conditions

$$\left\langle \boldsymbol{u}_h^*, \widehat{\boldsymbol{w}} \right\rangle_{\partial\Omega_D} = \left\langle \boldsymbol{u}_D, \widehat{\boldsymbol{w}} \right\rangle_{\partial\Omega_D}, \tag{2.4g}$$

$$\left\langle -\mathbf{L}_h^* \boldsymbol{n} + p_h^* \boldsymbol{n}, \widehat{\boldsymbol{w}} \right\rangle_{\partial\Omega_N} = \left\langle \boldsymbol{f}_N, \widehat{\boldsymbol{w}} \right\rangle_{\partial\Omega_N}. \tag{2.4h}$$

In the above, $(\mathbf{L}_h, \boldsymbol{u}_h, p_h)$ will be sought in some discontinuous polynomial spaces on the volume of the domain, and $(\mathbf{G}, \boldsymbol{v}, q)$ are test functions in those same spaces. The quantities $\boldsymbol{u}_h^*$ and $-\mathbf{L}_h^* \boldsymbol{n} + p_h^* \boldsymbol{n}$ are yet-to-be-defined, not-necessarily-single-valued numerical fluxes, which are function of the volume unknowns $(\mathbf{L}_h, \boldsymbol{u}_h, p_h)$ and trace variables $\left(\widehat{\mathbf{L}}_h, \widehat{\boldsymbol{u}}_h, \widehat{p}_h\right)$. The trace variables reside in discontinuous polynomial spaces defined on the mesh skeleton, as do the interior test functions $\left(\widehat{\mathbf{G}}, \widehat{\boldsymbol{v}}, \widehat{q}\right)$ and boundary test function $\widehat{\boldsymbol{w}}$. In what follows, we derive different choices for $\boldsymbol{u}_h^*$ and $-\mathbf{L}_h^* \boldsymbol{n} + p_h^* \boldsymbol{n}$ and analyze schemes that result from some specific choices. The fluxes we derive will have a minimal number of trace unknowns (d scalar unknowns) so that not all of the trace unknowns $\left(\widehat{\mathbf{L}}_h, \widehat{\boldsymbol{u}}_h, \widehat{p}_h\right)$ (and their corresponding test functions) will exist as unknowns (and test functions). Related to this is the fact that not all of the conservation equations (2.4d) – (2.4f) must be explicitly enforced, as some will be automatically satisfied depending on the choice of the numerical flux. Additionally, the boundary test function $\widehat{\boldsymbol{w}}$ will have a natural association with the interior skeleton test functions among $\left(\widehat{\mathbf{G}}, \widehat{\boldsymbol{v}}, \widehat{q}\right)$ that do exist in the scheme. These points will be made clearer after we derive the HDG numerical fluxes.

The first order system (2.3) fits into the general framework (1.1), and is symmetric hyperbolic. Indeed, choosing the ordering of unknowns as the column vector $\boldsymbol{U} := (\mathrm{vec}\,(\mathbf{L})\,;\boldsymbol{u};p)$, we have

$$\mathbf{A} = \begin{bmatrix} \mathbf{0} & -\boldsymbol{n}\otimes_K \mathbf{I} & \mathbf{0} \\ -\boldsymbol{n}^\top \otimes_K \mathbf{I} & \mathbf{0} & \boldsymbol{n} \\ \mathbf{0} & \boldsymbol{n}^\top & 0 \end{bmatrix}. \tag{2.5}$$

We can perform the eigendecomposition $\mathbf{A} = \mathbf{R}\mathbf{D}\mathbf{R}^{-1}$, where $\mathbf{D}$ is a diagonal matrix comprising the eigenvalues of $\mathbf{A}$, and $\mathbf{R}$ is a matrix whose columns are the eigenvectors corresponding those eigenvalues. Defining $|\mathbf{D}|$ by taking the absolute value of each eigenvalue in $\mathbf{D}$, we can define $|\mathbf{A}| := \mathbf{R}\,|\mathbf{D}|\,\mathbf{R}^{-1}$. It can be shown that for the Stokes system we have

$$|\mathbf{A}| = \begin{bmatrix} \mathbf{N}\otimes_K \left(\frac{1}{\tau_t^S}\mathbf{T} + \frac{1}{\tau_n^S}\mathbf{N}\right) & \mathbf{0} & -\frac{1}{\tau_n^S}\boldsymbol{n}\otimes_K \boldsymbol{n} \\ \mathbf{0} & \tau_t^S\mathbf{T} + \tau_n^S\mathbf{N} & \mathbf{0} \\ -\frac{1}{\tau_n^S}\boldsymbol{n}^\top \otimes_K \boldsymbol{n}^\top & \mathbf{0} & \frac{1}{\tau_n^S} \end{bmatrix}, \tag{2.6}$$

where

$$\tau_t^S := 1 \quad \text{and} \quad \tau_n^S := \sqrt{2}. \tag{2.7}$$

Later, we will consider more general parameters τ_t and τ_n than τ_t^S and τ_n^S which give the upwind flux. This allows us to generalize the upwind scheme, to define simpler schemes, and to make connections to existing HDG methods. We define the normal upwind flux $\boldsymbol{F}_n^*$ as a column vector $\boldsymbol{F}_n^* := (\mathrm{vec}\,(-\boldsymbol{u}^* \otimes \boldsymbol{n})\,; -\mathbf{L}^*\boldsymbol{n} + p^*\boldsymbol{n}; \boldsymbol{u}^* \cdot \boldsymbol{n})$. Since there is a one-to-one correspondence between $\mathrm{vec}\,(-\boldsymbol{u}^* \otimes \boldsymbol{n})$ and $-\boldsymbol{u}^* \otimes \boldsymbol{n}$, we also identify $\boldsymbol{F}_n^*$ with the triple

$$\boldsymbol{F}_n^* = \begin{pmatrix} -\boldsymbol{u}^* \otimes \boldsymbol{n}, \\ -\mathbf{L}^*\boldsymbol{n} + p^*\boldsymbol{n}, \\ \boldsymbol{u}^* \cdot \boldsymbol{n} \end{pmatrix}. \tag{2.8}$$

In this way, we can write the exact upwind flux in its one-sided form, $\boldsymbol{F}_n^* = \mathbf{A}\boldsymbol{U} + |\mathbf{A}|(\boldsymbol{U} - \boldsymbol{U}^*)$, as

$$\boldsymbol{F}_n^* = \begin{pmatrix} -\boldsymbol{u}\otimes\boldsymbol{n} + \left(\frac{1}{\tau_t^S}\mathbf{T} + \frac{1}{\tau_n^S}\mathbf{N}\right)(\mathbf{L} - \mathbf{L}^*)\,\mathbf{N} - \frac{1}{\tau_n^S}(p - p^*)\,\mathbf{N}, \\ -\mathbf{L}\boldsymbol{n} + p\boldsymbol{n} + \left(\tau_t^S\mathbf{T} + \tau_n^S\mathbf{N}\right)(\boldsymbol{u} - \boldsymbol{u}^*), \\ \boldsymbol{u}\cdot\boldsymbol{n} - \frac{1}{\tau_n^S}\boldsymbol{n}\cdot(\mathbf{L} - \mathbf{L}^*)\,\boldsymbol{n} + \frac{1}{\tau_n^S}(p - p^*) \end{pmatrix}. \tag{2.9}$$

At this point, we can eliminate "starred quantities" from the right side of (2.9) with the aim of defining an HDG flux with minimal trace unknowns. It turns out that we can do so in a way that naturally leads to four different forms of the upwind flux, each with d scalar starred quantities. The key to reducing the number of trace unknowns is the following relations between the upwind states.

Lemma 2.1. *The following relationships between the upwind states hold:*

$$\tau_t^S\mathbf{T}(\boldsymbol{u} - \boldsymbol{u}^*) = \mathbf{T}(\mathbf{L} - \mathbf{L}^*)\,\boldsymbol{n}, \tag{2.10a}$$

$$\tau_n^S\mathbf{N}(\boldsymbol{u} - \boldsymbol{u}^*) = -\mathbf{N}\left[-(\mathbf{L} - \mathbf{L}^*)\,\boldsymbol{n} + (p - p^*)\,\boldsymbol{n}\right]. \tag{2.10b}$$

Proof. The claims follow directly from equating the tangential components of the left and right sides of the second term of (2.9), and doing the same for the normal components. □

Note that we arrive at the same expressions by equating the left and right sides of the first term of (2.9). Equating the third term gives the expression (2.10b). That is to say that (2.10a) and (2.10b) are the only two relations we can discover from (2.9).

Using (2.10a) to eliminate either $\mathbf{T}\boldsymbol{u}^*$ or $\mathbf{T}\mathbf{L}^*\boldsymbol{n}$, and using (2.10b) to eliminate either $\mathbf{N}\boldsymbol{u}^*$ or $\mathbf{N}(-\mathbf{L}^*\boldsymbol{n} + p^*\boldsymbol{n})$, we arrive at the following four forms of the upwind flux.

The $\boldsymbol{u}^*$ flux: The quantity $-\mathbf{L}^*\boldsymbol{n}+p^*\boldsymbol{n}$ can be eliminated from (2.9) so that (2.9) can be written as

$$\boldsymbol{F}_n^* = \begin{pmatrix} -\boldsymbol{u}^*\otimes\boldsymbol{n}, \\ -\mathbf{L}\boldsymbol{n}+p\boldsymbol{n}+\left(\tau_t^S\mathbf{T}+\tau_n^S\mathbf{N}\right)(\boldsymbol{u}-\boldsymbol{u}^*), \\ \boldsymbol{u}^*\cdot\boldsymbol{n} \end{pmatrix}. \tag{2.11}$$

The $-\mathbf{L}^*\boldsymbol{n}+p^*\boldsymbol{n}$ flux: The quantity $\boldsymbol{u}^*$ can be eliminated from (2.9) so that (2.9) can be written as

$$\boldsymbol{F}_n^* = \begin{pmatrix} -\boldsymbol{u}\otimes\boldsymbol{n}+\left(\frac{1}{\tau_t^S}\mathbf{T}+\frac{1}{\tau_n^S}\mathbf{N}\right)(\mathbf{L}-\mathbf{L}^*)\mathbf{N}-\frac{1}{\tau_n^S}(p-p^*)\mathbf{N}, \\ -\mathbf{L}^*\boldsymbol{n}+p^*\boldsymbol{n}, \\ \boldsymbol{u}\cdot\boldsymbol{n}-\frac{1}{\tau_n^S}\boldsymbol{n}\cdot(\mathbf{L}-\mathbf{L}^*)\boldsymbol{n}+\frac{1}{\tau_n^S}(p-p^*) \end{pmatrix}. \tag{2.12}$$

The $(\mathbf{T}\boldsymbol{u}^*, f^*)$ flux: The quantities $\mathbf{T}\mathbf{L}^*\boldsymbol{n}$ and $\mathbf{N}\boldsymbol{u}^*$ can be eliminated from (2.9) so that (2.9) can be written as

$$\boldsymbol{F}_n^* = \begin{pmatrix} -\mathbf{N}\boldsymbol{u}\otimes\boldsymbol{n}-\mathbf{T}\boldsymbol{u}^*\otimes\boldsymbol{n}-\frac{1}{\tau_n^S}(-\boldsymbol{n}\cdot\mathbf{L}\boldsymbol{n}+p-f^*)\mathbf{N}, \\ -\mathbf{T}(\mathbf{L}\boldsymbol{n})+f^*\boldsymbol{n}+\tau_t^S\mathbf{T}(\boldsymbol{u}-\boldsymbol{u}^*), \\ \boldsymbol{u}\cdot\boldsymbol{n}+\frac{1}{\tau_n^S}(-\boldsymbol{n}\cdot\mathbf{L}\boldsymbol{n}+p-f^*) \end{pmatrix}, \tag{2.13}$$

where $f^* := -\boldsymbol{n}\cdot\mathbf{L}^*\boldsymbol{n}+p^*$.

The $(\mathbf{N}\boldsymbol{u}^*, \mathbf{T}\mathbf{L}^*\boldsymbol{n})$ flux: The quantities $\mathbf{N}(-\mathbf{L}^*\boldsymbol{n}+p^*\boldsymbol{n})$ and $\mathbf{T}\boldsymbol{u}^*$ can be eliminated from (2.9) so that (2.9) can be written as

$$\boldsymbol{F}_n^* = \begin{pmatrix} -\mathbf{N}\boldsymbol{u}^*\otimes\boldsymbol{n}-\mathbf{T}\boldsymbol{u}\otimes\boldsymbol{n}-\frac{1}{\tau_t^S}\mathbf{T}(-\mathbf{L}+\mathbf{L}^*)\mathbf{N}, \\ (-\boldsymbol{n}\cdot\mathbf{L}\boldsymbol{n}+p)\boldsymbol{n}+\mathbf{T}(-\mathbf{L}^*\boldsymbol{n})+\tau_n^S\mathbf{N}(\boldsymbol{u}-\boldsymbol{u}^*), \\ \boldsymbol{u}^*\cdot\boldsymbol{n} \end{pmatrix}. \tag{2.14}$$

Finally, in order to define numerical fluxes

$$\boldsymbol{F}_{n,h}^* := \begin{pmatrix} -\boldsymbol{u}_h^*\otimes\boldsymbol{n}, \\ -\mathbf{L}_h^*\boldsymbol{n}+p_h^*\boldsymbol{n}, \\ \boldsymbol{u}_h^*\cdot\boldsymbol{n} \end{pmatrix} \tag{2.15}$$

to be used in the HDG scheme (2.4), we append a subscript h to the terms in (2.11) – (2.14) and replace the starred quantities on the right side of (2.11) – (2.14) with hatted unknown quantities residing on the mesh skeleton. Additionally we replace τ_t^S

and τ_n^S with τ_t and τ_n, which, from the well-posedness analysis, can be freely chosen positive values. This gives the following numerical fluxes.

The $\widehat{\boldsymbol{u}}_h$ flux:

$$\boldsymbol{F}^*_{n,h} := \begin{pmatrix} -\widehat{\boldsymbol{u}}_h \otimes \boldsymbol{n}, \\ -\mathbf{L}_h\boldsymbol{n} + p_h\boldsymbol{n} + (\tau_t\mathbf{T} + \tau_n\mathbf{N})\left(\boldsymbol{u} - \widehat{\boldsymbol{u}}_h\right), \\ \widehat{\boldsymbol{u}}_h \cdot \boldsymbol{n} \end{pmatrix}. \tag{2.16}$$

The $\widehat{\boldsymbol{f}}_h$ flux (where $\widehat{\boldsymbol{f}}_h$ approximates $-\mathbf{L}^*\tilde{\boldsymbol{n}} + p^*\tilde{\boldsymbol{n}}$):

$$\boldsymbol{F}^*_{n,h} := \begin{pmatrix} -\left(\boldsymbol{u}_h + \left(\frac{1}{\tau_t}\mathbf{T} + \frac{1}{\tau_n}\mathbf{N}\right)\left(-\mathbf{L}_h\boldsymbol{n} + p_h\boldsymbol{n} - \mathrm{sgn}\widehat{\boldsymbol{f}}_h\right)\right) \otimes \boldsymbol{n}, \\ \mathrm{sgn}\widehat{\boldsymbol{f}}_h, \\ \boldsymbol{u}_h \cdot \boldsymbol{n} + \frac{1}{\tau_n}\left(-\boldsymbol{n} \cdot \mathbf{L}_h\boldsymbol{n} + p_h - \widehat{\boldsymbol{f}}_h \cdot \tilde{\boldsymbol{n}}\right) \end{pmatrix}. \tag{2.17}$$

The $(\widehat{\boldsymbol{u}}^t_h, \widehat{f}_h)$ flux (where $\widehat{f}_h$ approximates $-\boldsymbol{n} \cdot \mathbf{L}^*\boldsymbol{n} + p^*$):

$$\boldsymbol{F}^*_{n,h} := \begin{pmatrix} -\left(\widehat{\boldsymbol{u}}^t_h + \mathbf{N}\boldsymbol{u}_h + \frac{1}{\tau_n}\left(-\boldsymbol{n} \cdot \mathbf{L}_h\boldsymbol{n} + p_h - \widehat{f}_h\right)\boldsymbol{n}\right) \otimes \boldsymbol{n}, \\ \widehat{f}_h\boldsymbol{n} - \mathbf{T}\mathbf{L}_h\boldsymbol{n} + \tau_t\left(\boldsymbol{u}^t_h - \widehat{\boldsymbol{u}}^t_h\right), \\ \boldsymbol{u}_h \cdot \boldsymbol{n} + \frac{1}{\tau_n}\left(-\boldsymbol{n} \cdot \mathbf{L}_h\boldsymbol{n} + p_h - \widehat{f}_h\right) \end{pmatrix}. \tag{2.18}$$

The $(\widehat{u}^{\tilde{n}}_h, \widehat{\boldsymbol{f}}^t_h)$ flux (where $\widehat{\boldsymbol{f}}^t_h$ approximates $-\mathbf{T}\mathbf{L}^*\tilde{\boldsymbol{n}}$):

$$\boldsymbol{F}^*_{n,h} := \begin{pmatrix} -\left(\widehat{u}^{\tilde{n}}_h\tilde{\boldsymbol{n}} + \boldsymbol{u}^t_h + \frac{1}{\tau_t}\left(-\mathbf{T}\mathbf{L}_h\boldsymbol{n} - \mathrm{sgn}\widehat{\boldsymbol{f}}^t_h\right)\right) \otimes \boldsymbol{n}, \\ \mathrm{sgn}\widehat{\boldsymbol{f}}^t_h + \mathbf{N}\left(-\mathbf{L}_h\boldsymbol{n} + p_h\boldsymbol{n}\right) + \tau_n\left(\mathbf{N}\boldsymbol{u}_h - \widehat{u}^{\tilde{n}}_h\tilde{\boldsymbol{n}}\right), \\ \mathrm{sgn}\widehat{u}^{\tilde{n}}_h \end{pmatrix}. \tag{2.19}$$

In (2.17) and (2.19), we rely on an arbitrarily chosen normal direction $\tilde{\boldsymbol{n}}$ associated with a skeleton face e, and

$$\mathrm{sgn} := \mathrm{sgn}(\boldsymbol{n}) = \begin{cases} 1, & \text{if } \boldsymbol{n} = \tilde{\boldsymbol{n}}, \\ -1, & \text{if } \boldsymbol{n} = -\tilde{\boldsymbol{n}} \end{cases}$$

associated with each face of each element K in order to allow the unknowns on the mesh skeleton to be single-valued.

It can be shown that any of the fluxes (2.16) – (2.19) are suitable for use in the HDG scheme (2.4), some being more practical than others. It should also be noted

that it is not necessary to use the same flux on all skeleton faces. It may be convenient to use one flux on the skeleton faces that are on the interior of the computational domain and a different flux for each part of the boundary corresponding to a different boundary condition. For example, the $\widehat{\boldsymbol{u}}_h$ flux (2.16) can be used to directly prescribe Dirichlet boundary conditions of type (2.2a), the $\widehat{\boldsymbol{f}}_h$ flux (2.17) can be used to directly prescribe boundary conditions of type (2.2b), and the $(\widehat{u}_h^{\tilde{n}}, \widehat{\boldsymbol{f}}_h^t)$ flux (2.19) can be used to directly prescribe the conditions for "mirror" symmetry boundary conditions. If it is possible to treat the boundary conditions in this manner, all boundary skeleton unknowns decouple from the interior skeleton unknowns, thereby keeping the number of coupled unknowns in the system to a minimum.

Recall that in order to realize one of the advantages of HDG, the volume unknowns must be uniquely defined by the trace unknowns; that is, the local solver must be well posed. We will show in Section 2.2 that, without modifications, (2.16) only defines the pressure p_h up to an elementwise constant. This is also the case for (2.19). Similarly, (2.17) only defines the velocity $\widehat{\boldsymbol{u}}_h$ up to constant. On the other hand, (2.18) defines the all of the volume unknowns uniquely. In the following sections, we explicitly define schemes based on $\widehat{\boldsymbol{u}}_h$ flux (2.16) and modifications that ensure uniqueness of the local solver. This is the "standard" flux for the velocity gradient based HDG scheme for the Stokes equations. We also define a new scheme based on the flux (2.18) that requires no modifications for well-posedness of the local solver. We do not pursue HDG schemes based on (2.17) and (2.19), as they do not appear to offer benefits compared to the other schemes.

2.2 HDG Schemes Using the $\widehat{\boldsymbol{u}}_h$ Flux

In this section, we define an upwind HDG scheme based on (2.16), which recovers schemes developed in [16, 9]. For the sake of this discussion, we use (2.16) on all skeleton faces. The discontinuous polynomial spaces in which we seek the volume unknowns $(\mathbf{L}_h, \boldsymbol{u}_h, p_h)$ are as follows:

$$\mathbf{G}_h := \left\{ \mathbf{G} \in \left[L^2(\Omega)\right]^{d\times d} \ : \ \mathbf{G}|_K \in \mathbf{G}_h(K) \right\}, \tag{2.20a}$$

$$\boldsymbol{V}_h := \left\{ \boldsymbol{v} \in \left[L^2(\Omega)\right]^{d} \ : \ \boldsymbol{v}|_K \in \boldsymbol{V}_h(K) \right\}, \tag{2.20b}$$

$$Q_h := \left\{ q \in L^2(\Omega) \ : \ q|_K \in Q_h(K) \right\}, \tag{2.20c}$$

where $\mathbf{G}_h(K)$, $\boldsymbol{V}_h(K)$, $Q_h(K)$ are polynomial spaces defined on K that we assume to be of equal polynomial order $k \geq 1$. The discontinuous polynomial space in which we seek the trace unknowns $\widehat{\boldsymbol{u}}_h$ is

$$\widehat{\boldsymbol{V}}_h := \left\{ \widehat{\boldsymbol{v}} \in \left[L^2(\mathcal{E}_h)\right]^{d} \ : \ \widehat{\boldsymbol{v}}|_e \in \widehat{\boldsymbol{V}}_h(e) \right\}, \tag{2.21}$$

where $\widehat{\boldsymbol{V}}_h(e)$ is a polynomial space defined on e that is assumed to be of the same polynomial order k as the volume unknowns.

With the numerical flux (2.16), the enforcement of the Dirichlet boundary condition (2.4g) simplifies to an L^2 projection of the Dirichlet boundary data to the trace unknown on $\partial\Omega_D$, thereby decoupling the trace unknowns on $\partial\Omega_D$ from the rest of the unknowns. Then we can decompose the trace unknown

$$\widehat{\boldsymbol{u}}_h = \widehat{\boldsymbol{u}}_h^i + \widehat{\boldsymbol{u}}_h^D \tag{2.22}$$

where $\widehat{\boldsymbol{u}}_h^D$ is defined on $\partial\Omega_D$ as the L^2 projection of the boundary data,

$$\left\langle \widehat{\boldsymbol{u}}_h^D, \widehat{\boldsymbol{v}} \right\rangle_{\partial\Omega_D} = \langle \boldsymbol{u}_D, \widehat{\boldsymbol{v}} \rangle_{\partial\Omega_D} \quad \text{for all } \widehat{\boldsymbol{v}} \in \widehat{\boldsymbol{V}}_h(e) \text{ for all } e \in \partial\Omega_D, \tag{2.23}$$

and $\widehat{\boldsymbol{u}}_h^i$ is the trace unknown $\widehat{\boldsymbol{u}}_h$ restricted to $\mathcal{E}_h \backslash \partial\Omega_D$. Note that in writing (2.22) we identify $\widehat{\boldsymbol{u}}_h^i$ and $\widehat{\boldsymbol{u}}_h^D$ with their extensions by zero to $\mathcal{E}_h$. Then $\widehat{\boldsymbol{u}}_h^i$ resides in the polynomial space

$$\widehat{\boldsymbol{V}}_h^i := \left\{ \widehat{\boldsymbol{v}} \in \left[L^2(\mathcal{E}_h \backslash \partial\Omega_D) \right]^d \,:\, \widehat{\boldsymbol{v}}|_e \in \widehat{\boldsymbol{V}}_h(e) \right\}. \tag{2.24}$$

With this in place, we write the HDG scheme as follows.

Formulation 2.1. *Find* $(\mathbf{L}_h, \boldsymbol{u}_h, p_h, \widehat{\boldsymbol{u}}_h^i)$ *in* $\mathbf{G}_h \times \boldsymbol{V}_h \times Q_h \times \widehat{\boldsymbol{V}}_h^i$ *such that the local equations*

$$\mathrm{Re}\,(\mathbf{L}_h, \mathbf{G})_{\mathcal{T}_h} + (\boldsymbol{u}_h, \nabla \cdot \mathbf{G})_{\mathcal{T}_h} - \left\langle \widehat{\boldsymbol{u}}_h^i, \mathbf{G}\boldsymbol{n} \right\rangle_{\partial\mathcal{T}_h \backslash \partial\Omega_D} = \left\langle \widehat{\boldsymbol{u}}_h^D, \mathbf{G}\boldsymbol{n} \right\rangle_{\partial\Omega_D}, \tag{2.25a}$$

$$-(\nabla \cdot \mathbf{L}_h, \boldsymbol{v})_{\mathcal{T}_h} + (\nabla p_h, \boldsymbol{v})_{\mathcal{T}_h} + \langle \mathbf{S}\boldsymbol{u}_h, \boldsymbol{v} \rangle_{\partial\Omega_D}$$

$$+ \left\langle \mathbf{S}\left(\boldsymbol{u}_h - \widehat{\boldsymbol{u}}_h^i\right), \boldsymbol{v} \right\rangle_{\partial\mathcal{T}_h \backslash \partial\Omega_D} = (\boldsymbol{f}, \boldsymbol{v})_{\mathcal{T}_h} + \left\langle \mathbf{S}\widehat{\boldsymbol{u}}_h^D, \boldsymbol{v} \right\rangle_{\partial\Omega_D}, \tag{2.25b}$$

$$-(\boldsymbol{u}_h, \nabla q)_{\mathcal{T}_h} + \left\langle \widehat{\boldsymbol{u}}_h^i \cdot \boldsymbol{n}, q \right\rangle_{\partial\mathcal{T}_h \backslash \partial\Omega_D} = -\left\langle \widehat{\boldsymbol{u}}_h^D \cdot \boldsymbol{n}, q \right\rangle_{\partial\Omega_D}, \tag{2.25c}$$

and the conservation equation and Neumann boundary condition

$$-\left\langle -\mathbf{L}_h\boldsymbol{n} + p_h\boldsymbol{n} + \mathbf{S}\left(\boldsymbol{u}_h - \widehat{\boldsymbol{u}}_h^i\right), \widehat{\boldsymbol{v}} \right\rangle_{\partial\mathcal{T}_h \backslash \partial\Omega_D} = -\langle \boldsymbol{f}_N, \widehat{\boldsymbol{v}} \rangle_{\partial\Omega_N} \tag{2.25d}$$

hold for all $(\mathbf{G}, \boldsymbol{v}, q, \widehat{\boldsymbol{v}})$ *in* $\mathbf{G}_h \times \boldsymbol{V}_h \times Q_h \times \widehat{\boldsymbol{V}}_h^i$*, where*

$$\mathbf{S} := \tau_t \mathbf{T} + \tau_n \mathbf{N}, \tag{2.26}$$

and $\widehat{\boldsymbol{u}}_h^D$ *is defined by* (2.23)*. If* $\partial\Omega_N = \emptyset$*, we additionally require the zero mean pressure conditions for the uniqueness of the pressure*

$$(p_h, 1)_{\mathcal{T}_h} = 0. \tag{2.27}$$

Some comments are in order. First, using the flux (2.16), the conservation conditions (2.4d) and (2.4f) are automatically satisfied, and so we do not need to

explicitly include these equations in the formulation. Second, the conservation condition (2.4e) and the Neumann boundary condition (2.4h) (where we associate $\widehat{\boldsymbol{w}}$ with $\widehat{\boldsymbol{v}}$) are combined in (2.25d). Third, we have integrated by parts the terms in (2.4e) in order to write the scheme in a concise manner that reveals the symmetric and skew symmetric terms. Finally, it is not necessary to decompose $\widehat{\boldsymbol{u}}_h$ into the coupled "interior" unknowns and the decoupled Dirichlet boundary unknowns in (2.25a) – (2.25c). We can recouple (2.23) to the rest of the system, but that would change the matrix structure of the trace system that we comment on in the following discussions.

In the following, we discuss the well-posedness of Formulation 2.1.

Theorem 2.2. *(well-posedness of Formulation 2.1)*
Suppose that $\tau_t > 0$ and $\tau_n > 0$ (which is true in particular for $\tau_t = \tau_t^S$ and $\tau_n = \tau_n^S$). Then Formulation 2.1 is well-posed in the sense that given $\boldsymbol{f}$, $\boldsymbol{u}_D$, and $\boldsymbol{f}_N$, there exists a unique solution $(\mathbf{L}_h, \boldsymbol{u}_h, p_h, \widehat{\boldsymbol{u}}_h)$ in $\mathbf{G}_h \times \boldsymbol{V}_h \times Q_h \times \widehat{\boldsymbol{V}}_h$.

Proof. It is sufficient to prove that if $\boldsymbol{f} = \mathbf{0}$, $\boldsymbol{u}_D = \mathbf{0}$, and $\boldsymbol{f}_N = \mathbf{0}$, then the solution $(\mathbf{L}_h, \boldsymbol{u}_h, p_h, \widehat{\boldsymbol{u}}_h)$ is zero. We can rewrite Formulation 2.1 as: find $(\mathbf{L}_h, \boldsymbol{u}_h, p_h, \widehat{\boldsymbol{u}}_h^i)$ in $\mathbf{G}_h \times \boldsymbol{V}_h \times Q_h \times \widehat{\boldsymbol{V}}_h^i$ such that

$$\begin{aligned} &a_{sym}\left(\left(\mathbf{L}_h, \boldsymbol{u}_h, \widehat{\boldsymbol{u}}_h^i\right), (\mathbf{G}, \boldsymbol{v}, \widehat{\boldsymbol{v}})\right) \\ &\quad + a_{skew}\left(\left(\mathbf{L}_h, \boldsymbol{u}_h, p_h, \widehat{\boldsymbol{u}}_h^i\right), (\mathbf{G}, \boldsymbol{v}, q, \widehat{\boldsymbol{v}})\right) = \ell\left(\mathbf{G}, \boldsymbol{v}, q, \widehat{\boldsymbol{v}}\right) \end{aligned} \tag{2.28}$$

for all $(\mathbf{G}, \boldsymbol{v}, q, \widehat{\boldsymbol{v}})$ in $\mathbf{G}_h \times \boldsymbol{V}_h \times Q_h \times \widehat{\boldsymbol{V}}_h^i$, where

$$\begin{aligned} a_{sym}\left(\left(\mathbf{L}_h, \boldsymbol{u}_h, \widehat{\boldsymbol{u}}_h^i\right), (\mathbf{G}, \boldsymbol{v}, \widehat{\boldsymbol{v}})\right) &= \mathrm{Re}\left(\mathbf{L}_h, \mathbf{G}\right)_{\mathcal{T}_h} + \langle \mathbf{S}\boldsymbol{u}_h, \boldsymbol{v}\rangle_{\partial\Omega_D} \\ &\quad + \left\langle \mathbf{S}\left(\boldsymbol{u}_h - \widehat{\boldsymbol{u}}_h^i\right), \boldsymbol{v} - \widehat{\boldsymbol{v}}\right\rangle_{\partial\mathcal{T}_h \setminus \partial\Omega_D}, \end{aligned} \tag{2.29}$$

$$\begin{aligned} a_{skew}\left(\left(\mathbf{L}_h, \boldsymbol{u}_h, p_h, \widehat{\boldsymbol{u}}_h^i\right), (\mathbf{G}, \boldsymbol{v}, q, \widehat{\boldsymbol{v}})\right) &= \left(\boldsymbol{u}_h, \nabla \cdot \mathbf{G}\right)_{\mathcal{T}_h} - \left(\nabla \cdot \mathbf{L}_h, \boldsymbol{v}\right)_{\mathcal{T}_h} \\ &\quad + \left(\nabla p_h, \boldsymbol{v}\right)_{\mathcal{T}_h} - \left(\boldsymbol{u}_h, \nabla q\right)_{\mathcal{T}_h} - \left\langle \widehat{\boldsymbol{u}}_h^i, \mathbf{G}\boldsymbol{n}\right\rangle_{\partial\mathcal{T}_h \setminus \partial\Omega_D} + \left\langle \mathbf{L}_h\boldsymbol{n}, \widehat{\boldsymbol{v}}\right\rangle_{\partial\mathcal{T}_h \setminus \partial\Omega_D} \\ &\quad + \left\langle \widehat{\boldsymbol{u}}_h^i \cdot \boldsymbol{n}, q\right\rangle_{\partial\mathcal{T}_h \setminus \partial\Omega_D} - \left\langle p_h, \widehat{\boldsymbol{v}} \cdot \boldsymbol{n}\right\rangle_{\partial\mathcal{T}_h \setminus \partial\Omega_D}, \end{aligned} \tag{2.30}$$

and

$$\ell\left(\mathbf{G},\boldsymbol{v},q,\widehat{\boldsymbol{v}}\right)=\left\langle\widehat{\boldsymbol{u}}_h^D,\mathbf{G}\boldsymbol{n}\right\rangle_{\partial\Omega_D}+\left(\boldsymbol{f},\boldsymbol{v}\right)_{\mathcal{T}_h}$$
$$+\left\langle\mathbf{S}\widehat{\boldsymbol{u}}_h^D,\boldsymbol{v}\right\rangle_{\partial\Omega_D}-\left\langle\widehat{\boldsymbol{u}}_h^D\cdot\boldsymbol{n},q\right\rangle_{\partial\Omega_D}-\left\langle\boldsymbol{f}_N,\widehat{\boldsymbol{v}}\right\rangle_{\partial\Omega_N}. \tag{2.31}$$

Setting $\boldsymbol{f}=\mathbf{0}$, $\boldsymbol{u}_D=\mathbf{0}$ (and therefore $\widehat{\boldsymbol{u}}_h^D=\mathbf{0}$), and $\boldsymbol{f}_N=\mathbf{0}$ gives $\ell=0$. Setting $\left(\mathbf{G},\boldsymbol{v},q,\widehat{\boldsymbol{v}}\right)=\left(\mathbf{L}_h,\boldsymbol{u}_h,p_h,\widehat{\boldsymbol{u}}_h^i\right)$ gives $a_{skew}=0$ leaving only the symmetric terms,

$$\mathrm{Re}\left(\mathbf{L}_h,\mathbf{L}_h\right)_{\mathcal{T}_h}+\left\langle\mathbf{S}\left(\boldsymbol{u}_h-\widehat{\boldsymbol{u}}_h^i\right),\boldsymbol{u}_h-\widehat{\boldsymbol{u}}_h^i\right\rangle_{\partial\mathcal{T}_h\backslash\partial\Omega_D}+\left\langle\mathbf{S}\boldsymbol{u}_h,\boldsymbol{u}_h\right\rangle_{\partial\Omega_D}=0. \tag{2.32}$$

All of the terms in the previous expression are nonnegative and as a consequence must be zero. Thus $\mathbf{L}_h=\mathbf{0}$ in $\mathcal{T}_h$, $\boldsymbol{u}_h=\widehat{\boldsymbol{u}}_h$ on $\mathcal{E}_h\backslash\partial\Omega_D$, and $\boldsymbol{u}_h=\mathbf{0}$ on $\partial\Omega_D$.

Integration by parts reveals that equation (2.25a) reduces to $\left(\nabla u_h,\mathbf{G}\right)_{\mathcal{T}_h}=0$ and since $\nabla\boldsymbol{V}_h\subset\mathbf{G}_h$, we set $\mathbf{G}=\nabla u_h$ to conclude that u_h is elementwise constant. But since $\boldsymbol{u}_h=\widehat{\boldsymbol{u}}_h$ on $\mathcal{E}_h^o$ and $\widehat{\boldsymbol{u}}_h$ is single valued on $\mathcal{E}_h^o$, $\boldsymbol{u}_h$ is continuous across each internal interface, and therefore $\boldsymbol{u}_h$ is globally constant. Since $\widehat{\boldsymbol{u}}_h$ is zero on $\partial\Omega_D$ we conclude $\boldsymbol{u}_h=\mathbf{0}$ and $\widehat{\boldsymbol{u}}_h=\mathbf{0}$.

Then (2.25b) reduces to $\left(\nabla p_h,\boldsymbol{v}\right)_{\mathcal{T}_h}=0$, and since $\nabla Q_h\subset\boldsymbol{V}_h$, we can conclude p_h is elementwise constant. Since (2.25d) reduces to $\left\langle p_h\boldsymbol{n},\widehat{\boldsymbol{v}}\right\rangle_{\partial\mathcal{T}_h\backslash\partial\Omega}$ for $\widehat{\boldsymbol{v}}$ with support on $\mathcal{E}_h^o$, then p_h is globally continuous and globally constant. In the case that $\partial\Omega_N\neq\emptyset$, we have $\left\langle p_h\boldsymbol{n},\widehat{\boldsymbol{v}}\right\rangle_{\partial\Omega_N}=0$ implies that $p_h=0$ on $\partial\Omega_N$ and therefore that $p_h=0$ everywhere. Otherwise the zero mean discrete pressure condition (2.27) implies p_h is zero. □

We next prove that the local solver, (2.25a) – (2.25c), in Formulation 2.1 determines the local pressure p_h only up to an elementwise constant.

Theorem 2.3. *(well-posedness of the local solver of Formulation 2.1)*
Suppose that $\tau_t>0$ and $\tau_n>0$. Given $\boldsymbol{f}$ and $\widehat{\boldsymbol{u}}_h$, there exists a unique solution $\left(\mathbf{L}_h,\boldsymbol{u}_h,p_h\right)$ in $\mathbf{G}_h\times\boldsymbol{V}_h\times Q_h/\mathcal{P}_0\left(\mathcal{T}_h\right)$ to the local equations (2.25a) – (2.25c).

Proof. It is sufficient to restrict our attention to a single element, and prove that if $\boldsymbol{f}$ and $\widehat{\boldsymbol{u}}_h$ are zero, then the solution $(\mathbf{L}_h, \boldsymbol{u}_h, p_h)$ is zero. We can rewrite the local solver defined by (2.25a) – (2.25c) restricted to one element as find $(\mathbf{L}_h, \boldsymbol{u}_h, p_h)$ in $\mathbf{G}_h(K) \times \boldsymbol{V}_h(K) \times Q_h(K)$ such that

$$\begin{aligned} &\operatorname{Re}(\mathbf{L}_h, \mathbf{G})_K + \langle \mathbf{S}\boldsymbol{u}_h, \boldsymbol{v}\rangle_{\partial K} \\ &\quad + (\boldsymbol{u}_h, \nabla \cdot \mathbf{G})_K - (\nabla \cdot \mathbf{L}_h, \boldsymbol{v})_K + (\nabla p_h, \boldsymbol{v})_K - (\boldsymbol{u}_h, \nabla q)_K \\ &\quad = (\boldsymbol{f}, \boldsymbol{v})_K + \langle \mathbf{S}\widehat{\boldsymbol{u}}_h, \boldsymbol{v}\rangle_{\partial K} + \langle \widehat{\boldsymbol{u}}_h, \mathbf{G}\boldsymbol{n}\rangle_{\partial K} - \langle \widehat{\boldsymbol{u}}_h \cdot \boldsymbol{n}, q\rangle_{\partial K} \end{aligned} \tag{2.33}$$

for all $(\mathbf{G}, \boldsymbol{v}, q)$ in $\mathbf{G}_h(K) \times \boldsymbol{V}_h(K) \times Q_h(K)$. Setting $\boldsymbol{f}$ and $\widehat{\boldsymbol{u}}_h$ to zero, and setting $(\mathbf{G}, \boldsymbol{v}, q) = (\mathbf{L}_h, \boldsymbol{u}_h, p_h)$, we have

$$\operatorname{Re}(\mathbf{L}_h, \mathbf{L}_h)_K + \langle \mathbf{S}\boldsymbol{u}_h, \boldsymbol{u}_h\rangle_{\partial K} = 0. \tag{2.34}$$

Thus $\mathbf{L}_h = \mathbf{0}$ in K and $\boldsymbol{u}_h = \mathbf{0}$ on ∂K.

Integrating by parts what remains of (2.25a) gives that $\boldsymbol{u}_h$ is constant in K, and since $\boldsymbol{u}_h = \mathbf{0}$ on ∂K, that $\boldsymbol{u}_h = \mathbf{0}$ in K. Integrating (2.25b) by parts gives that p_h is constant in K. □

2.2.1 Modifications for Local Solver Invertibility

As we saw in the previous section, given $\boldsymbol{f}$ and $\widehat{\boldsymbol{u}}_h$, the local solver (2.25a) – (2.25c) of the HDG Formulation 2.1 does not uniquely define the pressure p_h in Q_h. The reason for this can be seen as follows. It is known that the Stokes equations with only Dirichlet boundary conditions must be equipped with an additional condition on the pressure, usually the zero mean pressure condition, in order to be well-posed. The local solver of Formulation 2.1 can be interpreted as solving the Dirichlet problem on each element with $\widehat{\boldsymbol{u}}_h$ as the boundary data. From what we know about the Dirichlet problem for the Stokes equations, we could not have expected that this

local problem would be well-posed. An HDG scheme whose local (element) problem is not well-posed is not particularly useful, as it loses one of the main advantages of HDG methods as compared to DG methods – the ability to condense the volume (DG) unknowns out of the global linear system to have a resulting global system with a reduced number of unknowns. Therefore, Formulation 2.1 must be modified in order to be useful.

There are two methods in the literature for addressing this issue [53]. One method is a direct method that involves the introduction of additional global unknowns. The other method is an iterative method, involving pseudotime, that does not change the number of unknowns. We review those methods here before introducing a new method in the next section that uses a different form of the HDG flux to avoid this issue all together.

2.2.1.1 The Augmented Lagrangian Approach

The Augmented Lagrangian approach for Stokes HDG schemes introduced in [53]. It is described by adding a pseudotime derivative to (2.3c) as

$$\frac{\partial p}{\partial \tau} + \nabla \cdot \boldsymbol{u} = 0, \tag{2.35}$$

providing an initial condition $p(\tau = 0) = p_0$, then solving for the steady state solution with an HDG spatial discretization of (2.3a), (2.3b), and (2.35), with an implicit Euler temporal discretization, and with the choice of $p_0 = 0$. Altering Formulation 2.1 in such a manner, we have the following formulation describing a single pseudotime step.

Formulation 2.2. *Find* $(\mathbf{L}_h^k, \boldsymbol{u}_h^k, p_h^k, \widehat{\boldsymbol{u}}_h^{i,k})$ *in* $\mathbf{G}_h \times \boldsymbol{V}_h \times Q_h \times \widehat{\boldsymbol{V}}_h^i$ *such that the local*

equations

$$\mathrm{Re}\left(\mathbf{L}_h^k, \mathbf{G}\right)_{\mathcal{T}_h} + \left(\boldsymbol{u}_h^k, \nabla\cdot\mathbf{G}\right)_{\mathcal{T}_h} - \left\langle \widehat{\boldsymbol{u}}_h^{i,k}, \mathbf{G}\boldsymbol{n}\right\rangle_{\partial\mathcal{T}_h\setminus\partial\Omega_D} = \left\langle \widehat{\boldsymbol{u}}_h^{D}, \mathbf{G}\boldsymbol{n}\right\rangle_{\partial\Omega_D}, \tag{2.36a}$$

$$-\left(\nabla\cdot\mathbf{L}_h^k, \boldsymbol{v}\right)_{\mathcal{T}_h} + \left(\nabla p_h^k, \boldsymbol{v}\right)_{\mathcal{T}_h} + \left\langle \mathbf{S}\boldsymbol{u}_h^k, \boldsymbol{v}\right\rangle_{\partial\Omega_D} + \left\langle \mathbf{S}\left(\boldsymbol{u}_h^k - \widehat{\boldsymbol{u}}_h^{i,k}\right), \boldsymbol{v}\right\rangle_{\partial\mathcal{T}_h\setminus\partial\Omega_D} = \left(\boldsymbol{f}, \boldsymbol{v}\right)_{\mathcal{T}_h} + \left\langle \mathbf{S}\widehat{\boldsymbol{u}}_h^{D}, \boldsymbol{v}\right\rangle_{\partial\Omega_D}, \tag{2.36b}$$

$$\frac{1}{\Delta\tau}\left(p_h^k, q\right)_{\mathcal{T}_h} - \left(\boldsymbol{u}_h^k, \nabla q\right)_{\mathcal{T}_h} + \left\langle \widehat{\boldsymbol{u}}_h^{i,k}\cdot\boldsymbol{n}, q\right\rangle_{\partial\mathcal{T}_h\setminus\partial\Omega_D} = -\left\langle \widehat{\boldsymbol{u}}_h^{D}\cdot\boldsymbol{n}, q\right\rangle_{\partial\Omega_D}, + \frac{1}{\Delta\tau}\left(p_h^{k-1}, q\right)_{\mathcal{T}_h}, \tag{2.36c}$$

and the conservation equation and Neumann boundary condition

$$-\left\langle -\mathbf{L}_h^k\boldsymbol{n} + p_h^k\boldsymbol{n} + \mathbf{S}\left(\boldsymbol{u}_h^k - \widehat{\boldsymbol{u}}_h^{i,k}\right), \widehat{\boldsymbol{v}}\right\rangle_{\partial\mathcal{T}_h\setminus\partial\Omega_D} = -\left\langle \boldsymbol{f}_N, \widehat{\boldsymbol{v}}\right\rangle_{\partial\Omega_N} \tag{2.36d}$$

hold for all $(\mathbf{G}, \boldsymbol{v}, q, \widehat{\boldsymbol{v}})$ *in* $\mathbf{G}_h \times \boldsymbol{V}_h \times Q_h \times \widehat{\boldsymbol{V}}_h^i$*, where* $\widehat{\boldsymbol{u}}_h^D$ *is defined by* (2.23) *and* $\mathbf{S}$ *is defined by* (2.26)*.*

In the above, k represents the pseudotime step number. Finally, [53] describes a stopping criterion for the pseudotime iterations,

$$\frac{\left\|p_h^k - p_h^{k-1}\right\|}{\left\|p_h^k\right\|} < \epsilon. \tag{2.37}$$

Algorithm 1 describes the solution procedure. We emphasize here that $\Delta\tau$ and ϵ must

Algorithm 1 Augmented Lagrangian solution procedure.

```
choose Δτ and ϵ
set p_h^0 = 0, k = 1
while true do
  solve for (L_h^k, u_h^k, p_h^k, û_h^k) using Formulation 2.2
  if (2.37) is true then
    break
  end if
  k ← k + 1
end while
```

be chosen. We also remark that the stopping criterion (2.37) will not be useful as it

is written if the exact pressure is zero. To handle such cases, it may be useful to add a small positive parameter (whose magnitude must be chosen) to the denominator of (2.37).

Some remarks are in order. First, it can be seen that the local solver associated with Formulation 2.2 is well-posed. Indeed, repeating the arguments in the proof for Theorem 2.3, now with p_h^{k-1} as an additional forcing function, instead of (2.34) we will have

$$\mathrm{Re}\left(\mathbf{L}_h^k, \mathbf{L}_h^k\right)_K + \left\langle \mathbf{S}\boldsymbol{u}_h^k, \boldsymbol{u}_h^k \right\rangle_{\partial K} + \frac{1}{\Delta\tau}\left(p_h^k, p_h^k\right)_K = 0, \tag{2.38}$$

which allows us to conclude $p_h^k = 0$. Second, forming the condensed global system (in terms of $\widehat{\boldsymbol{u}}_h$ only) gives a global system

$$A\widehat{U}^k = F^{k-1}, \tag{2.39}$$

where the matrix A is symmetric and positive definite. See Appendix B for details.

2.2.1.2 The Average Edge Pressure Approach

A direct (as opposed to iterative) approach to modifying Formulation 2.1 to obtain a well-posed local solver is given in [53]. The method involves introducing a global unknown representing an elementwise average edge-pressure. We give a slightly different presentation here with implementation using a Lagrange polynomial basis in mind. We do so by altering Formulation 2.1 to read as follows.

Formulation 2.3. *Find* $(\mathbf{L}_h, \boldsymbol{u}_h, p_h, \widehat{\boldsymbol{u}}_h^i, \rho_h)$ *in* $\mathbf{G}_h \times \boldsymbol{V}_h \times Q_h \times \widehat{\boldsymbol{V}}_h^i \times \mathcal{P}_0(\partial\mathcal{T}_h)$ *such*

that the local equations

$$\mathrm{Re}\,(\mathbf{L}_h, \mathbf{G})_{\mathcal{T}_h} + (\boldsymbol{u}_h, \nabla \cdot \mathbf{G})_{\mathcal{T}_h} - \left\langle \widehat{\boldsymbol{u}}_h^i, \mathbf{G}\boldsymbol{n} \right\rangle_{\partial \mathcal{T}_h \setminus \partial\Omega_D} = \left\langle \widehat{\boldsymbol{u}}_h^D, \mathbf{G}\boldsymbol{n} \right\rangle_{\partial\Omega_D}, \tag{2.40a}$$

$$-(\nabla \cdot \mathbf{L}_h, \boldsymbol{v})_{\mathcal{T}_h} + (\nabla p_h, \boldsymbol{v})_{\mathcal{T}_h} + \langle \mathbf{S}\boldsymbol{u}_h, \boldsymbol{v} \rangle_{\partial\Omega_D} + \left\langle \mathbf{S}\left(\boldsymbol{u}_h - \widehat{\boldsymbol{u}}_h^i\right), \boldsymbol{v} \right\rangle_{\partial \mathcal{T}_h \setminus \partial\Omega_D} = (\boldsymbol{f}, \boldsymbol{v})_{\mathcal{T}_h} + \left\langle \mathbf{S}\widehat{\boldsymbol{u}}_h^D, \boldsymbol{v} \right\rangle_{\partial\Omega_D}, \tag{2.40b}$$

$$-(\boldsymbol{u}_h, \nabla q)_{\mathcal{T}_h} + \left\langle \widehat{\boldsymbol{u}}_h^i \cdot \boldsymbol{n}, q - \overline{q} \right\rangle_{\partial \mathcal{T}_h \setminus \partial\Omega_D} + \langle p_h - \rho_h, \overline{q} \rangle_{\partial \mathcal{T}_h} = -\left\langle \widehat{\boldsymbol{u}}_h^D \cdot \boldsymbol{n}, q - \overline{q} \right\rangle_{\partial\Omega_D}, \tag{2.40c}$$

the conservation equation and Neumann boundary condition

$$-\left\langle -\mathbf{L}_h\boldsymbol{n} + p_h\boldsymbol{n} + \mathbf{S}\left(\boldsymbol{u}_h - \widehat{\boldsymbol{u}}_h^i\right), \widehat{\boldsymbol{v}} \right\rangle_{\partial \mathcal{T}_h \setminus \partial\Omega_D} = -\langle \boldsymbol{f}_N, \widehat{\boldsymbol{v}} \rangle_{\partial\Omega_N}, \tag{2.40d}$$

and the constraint

$$\left\langle \widehat{\boldsymbol{u}}_h^i \cdot \boldsymbol{n}, \psi \right\rangle_{\partial \mathcal{T}_h \setminus \partial\Omega_D} = -\left\langle \widehat{\boldsymbol{u}}_h^D \cdot \boldsymbol{n}, \psi \right\rangle_{\partial\Omega_D} \tag{2.40e}$$

hold for all $(\mathbf{G}, \boldsymbol{v}, q, \widehat{\boldsymbol{v}}, \psi)$ *in* $\mathbf{G}_h \times \boldsymbol{V}_h \times Q_h \times \widehat{\boldsymbol{V}}_h^i \times \mathcal{P}_0(\partial \mathcal{T}_h)$*, where* $\widehat{\boldsymbol{u}}_h^D$ *is defined by* (2.23) *and* $\mathbf{S}$ *is defined by* (2.26)*. If* $\partial\Omega_N = \emptyset$*, we additionally require the zero mean pressure conditions for the uniqueness of the pressure,* (2.27)*.*

In the above, the notation $\overline{q}$ is defined by $\overline{q} := |\partial K|^{-1} \langle q, 1 \rangle_{\partial K}$ as the ∂K-wise average of q, and $|\partial K|$ is the length of the perimeter of element K. The new unknowns ρ_h which are sought in $\mathcal{P}_0(\partial \mathcal{T}_h)$ represent the ∂K-wise average pressure. Indeed, taking q to be an elementwise constant in (2.40c), we recover $\overline{p}_h = \rho_h$.

We observe that Formulation 2.1 and Formulation 2.3 give the same solution. Indeed, we can show that (2.40c) and (2.40e) are equivalent to (2.25c). Given that we've already shown $\overline{p}_h = \rho_h$, we have $-(\boldsymbol{u}_h, \nabla q)_{\mathcal{T}_h} + \langle \widehat{\boldsymbol{u}}_h \cdot \boldsymbol{n}, q - \overline{q} \rangle_{\partial \mathcal{T}_h} = 0$. Setting ψ in (2.40e) equal to $\overline{q}$ and adding the result to the previous expression, we recover (2.25c). Conversely, setting $\boldsymbol{q}$ in (2.25c) equal to any elementwise constant ψ, we

recover (2.40e). Then setting $\psi = \overline{q}$ and subtracting (2.40e) from (2.25c), and *defining* $\rho_h := \overline{p}_h$ and therefore that $\langle \overline{p}_h, \overline{q} \rangle_{\partial K} = \langle p_h, \overline{q} \rangle_{\partial K} = \langle \rho_h, \overline{q} \rangle_{\partial K}$ for any q, we recover (2.40c).

As with the Augmented Lagrangian iterative approach, we can see that the modifications result in a well-posed local solver. Indeed, repeating the arguments in the proof for Theorem 2.3, now with ρ_h as a forcing function, instead of (2.34) we will have

$$\mathrm{Re}\,(\mathbf{L}_h, \mathbf{L}_h)_K + \langle \mathbf{S}\boldsymbol{u}_h, \boldsymbol{u}_h \rangle_{\partial K} + \langle \overline{p}_h, \overline{p}_h \rangle_K = 0, \tag{2.41}$$

which allows us to conclude $p_h = 0$ on ∂K. Then, following the same arguments as before, we conclude that p_h is elementwise constant, and therefore zero.

As shown in [53], the condensed global system takes the form of a saddle point problem,

$$\begin{bmatrix} A & B^\top \\ -B & 0 \end{bmatrix} \begin{Bmatrix} \widehat{U} \\ \rho \end{Bmatrix} = \begin{Bmatrix} F_1 \\ F_2 \end{Bmatrix}, \tag{2.42}$$

where A is symmetric and positive definite. See Appendix B for details.

2.3 HDG Schemes Using the $(\widehat{\boldsymbol{u}}_h^t, \widehat{f}_h)$ Flux

In this section, we define new HDG schemes for the Stokes equations. We do this by using the flux (2.18) on all skeleton faces $\mathcal{E}_h^o$. The justification of this choice will become evident when we analyze the well-posedness of the local solver associated with this scheme, where we verify that no special treatment is required for the uniqueness of the local pressure. Recall that for trace unknowns, this flux has the tangent velocity $\widehat{\boldsymbol{u}}_h^t$ and a scalar $\widehat{f}_h$ which approximates $-\frac{1}{\mathrm{Re}}\boldsymbol{n} \cdot [\nabla \boldsymbol{u} \cdot \boldsymbol{n}] + p$. The volume unknowns will still be sought from the discontinuous polynomial spaces

(2.20). The discontinuous polynomial space in which we seek $\widehat{f}_h$ and $\widehat{\boldsymbol{u}}_h^t$, respectively, are

$$\widehat{F}_h := \left\{ \widehat{g} \in L^2(\mathcal{E}_h) \ : \ \widehat{g}|_e \in \widehat{F}_h(e) \right\}, \tag{2.43}$$

$$\widehat{\boldsymbol{V}}_h^t := \left\{ \widehat{\boldsymbol{v}}^t \in \left[L^2(\mathcal{E}_h) \right]^d \ : \ \widehat{\boldsymbol{v}}^t|_e \in \widehat{\boldsymbol{V}}_h^t(e) \right\}, \tag{2.44}$$

where $\widehat{F}_h(e)$ is a scalar polynomial space, and $\widehat{\boldsymbol{V}}_h^t(e)$ is a vector valued polynomial space with no normal component, defined by

$$\widehat{\boldsymbol{V}}_h^t(e) = \left\{ \sum_{i=1}^{d-1} \boldsymbol{t}^i \widehat{v}_{h,i} \ : \ \widehat{v}_{h,i} \in \widehat{V}_h(e) \right\}, \tag{2.45}$$

where $\widehat{V}_h(e)$ is a scalar polynomial space defined on e, and $\left\{ \boldsymbol{t}^1, \ldots, \boldsymbol{t}^{d-1} \right\}$ is a basis of the tangent space of e.

Realize that (2.18) defines $\boldsymbol{u}_h^*$ as

$$\boldsymbol{u}_h^* = \widehat{\boldsymbol{u}}_h^t + \mathbf{N}\boldsymbol{u}_h + \frac{1}{\tau_n} \left(-\boldsymbol{n} \cdot \mathbf{L}_h \boldsymbol{n} + p_h - \widehat{f}_h \right) \boldsymbol{n}. \tag{2.46}$$

The enforcement of the tangent component of the Dirichlet boundary condition (2.4g) then simplifies to an L^2 projection of the tangent part of the Dirichlet boundary data $\boldsymbol{u}_D$ to the trace unknown $\widehat{\boldsymbol{u}}_h^t$ on $\partial\Omega_D$, thereby decoupling $\widehat{\boldsymbol{u}}_h^t$ on $\partial\Omega_D$ from the rest of the unknowns. The normal part of the Dirichlet condition is enforced weakly as will be shown below.

Similarly, (2.18) defines

$$-\mathbf{L}_h^* \boldsymbol{n} + p_h^* \boldsymbol{n} = \widehat{f}_h \boldsymbol{n} + \mathbf{T} \left(-\mathbf{L}_h \boldsymbol{n} \right) + \tau_t \left(\boldsymbol{u}_h^t - \widehat{\boldsymbol{u}}_h^t \right), \tag{2.47}$$

so the enforcement of the normal component of the Neumann boundary condition (2.4h) simplifies to an L^2 projection of the normal part of the Neumann boundary data $\boldsymbol{f}_N$ to the trace unknown $\widehat{f}_h$ on $\partial\Omega_N$, thereby decoupling $\widehat{f}_h$ on $\partial\Omega_N$ from the

rest of the unknowns. The tangent part of the Neumann condition is enforced weakly as will be shown below.

As before, we decompose the trace unknowns into the decoupled parts and the coupled parts of the trace unknowns. We decompose $\widehat{f}_h$ by

$$\widehat{f}_h = \widehat{f}_h^i + \widehat{f}_h^N \tag{2.48}$$

where $\widehat{f}_h^N$ is defined on $\partial\Omega_N$ as the L^2 projection of the normal component of the Neumann boundary data,

$$\left\langle \widehat{f}_h^N, \widehat{g} \right\rangle_{\partial\Omega_N} = \langle \boldsymbol{f}_N \cdot \boldsymbol{n}, \widehat{g} \rangle_{\partial\Omega_N} \quad \text{for all } \widehat{g} \in \widehat{F}_h(e) \text{ for all } e \in \partial\Omega_N, \tag{2.49}$$

and $\widehat{f}_h^i$ is the trace unknown $\widehat{f}_h$ restricted to $\mathcal{E}_h \backslash \partial\Omega_N$. Similarly, we decompose $\widehat{\boldsymbol{u}}_h^t$ by

$$\widehat{\boldsymbol{u}}_h^t = \widehat{\boldsymbol{u}}_h^{t,i} + \widehat{\boldsymbol{u}}_h^{t,D} \tag{2.50}$$

where $\widehat{\boldsymbol{u}}_h^{t,D}$ is defined on $\partial\Omega_D$ as the L^2 projection of the tangential component of the Dirichlet boundary data,

$$\left\langle \widehat{\boldsymbol{u}}_h^{t,D}, \widehat{\boldsymbol{v}}^t \right\rangle_{\partial\Omega_D} = \left\langle \boldsymbol{u}_D^t, \widehat{\boldsymbol{v}}^t \right\rangle_{\partial\Omega_D} \quad \text{for all } \widehat{\boldsymbol{v}}^t \in \widehat{\boldsymbol{V}}_h^t(e) \text{ for all } e \in \partial\Omega_D, \tag{2.51}$$

and $\widehat{\boldsymbol{u}}_h^{t,i}$ is the trace unknown $\widehat{\boldsymbol{u}}_h^t$ restricted to $\mathcal{E}_h \backslash \partial\Omega_D$. Again, in writing (2.48) and (2.50) we identify $\widehat{f}_h^i$, $\widehat{f}_h^N$, $\widehat{\boldsymbol{u}}_h^{t,i}$, and $\widehat{\boldsymbol{u}}_h^{t,D}$ with their extensions by zero to $\mathcal{E}_h$. We assume that all discrete spaces are of equal polynomial order. We also note that we have made a slight abuse of notation as the superscript "i" (for "interior") has a different meaning for $\widehat{f}_h^i$ and $\widehat{\boldsymbol{u}}_h^{t,i}$. Finally, we define the polynomial spaces

$$\widehat{F}_h^i := \left\{ \widehat{g} \in L^2(\mathcal{E}_h \backslash \partial\Omega_N) \ : \ \widehat{g}|_e \in \widehat{F}_h(e) \right\}, \tag{2.52}$$

$$\widehat{\boldsymbol{V}}_h^{t,i} := \left\{ \widehat{\boldsymbol{v}}^t \in \left[L^2(\mathcal{E}_h \backslash \partial\Omega_D) \right]^d \ : \ \widehat{\boldsymbol{v}}^t|_e \in \widehat{\boldsymbol{V}}_h^t(e) \right\}, \tag{2.53}$$

in which $\widehat{f}_h^i$ and $\widehat{\boldsymbol{u}}_h^{t,i}$, respectively, lie. With this in place, we write the HDG scheme as follows.

Formulation 2.4. *Find* $(\mathbf{L}_h, \boldsymbol{u}_h, p_h, \widehat{\boldsymbol{u}}_h^{t,i}, \widehat{f}_h^i)$ *in* $\mathbf{G}_h \times \boldsymbol{V}_h \times Q_h \times \widehat{\boldsymbol{V}}_h^{t,i} \times \widehat{F}_h^i$ *such that the local equations*

$$\begin{aligned}
&\operatorname{Re}(\mathbf{L}_h, \mathbf{G})_{\mathcal{T}_h} - (\nabla \boldsymbol{u}_h, \mathbf{G})_{\mathcal{T}_h} + \left\langle \boldsymbol{u}_h^t, \mathbf{G}\boldsymbol{n} \right\rangle_{\partial \mathcal{T}_h} - \left\langle \widehat{\boldsymbol{u}}_h^{t,i}, \mathbf{G}\boldsymbol{n} \right\rangle_{\partial \mathcal{T}_h \backslash \partial \Omega_D} \\
&\quad + \left\langle \frac{1}{\tau_n} f_h, -\boldsymbol{n} \cdot \mathbf{G}\boldsymbol{n} \right\rangle_{\partial \Omega_N} + \left\langle \frac{1}{\tau_n} \left(f_h - \widehat{f}_h^i \right), -\boldsymbol{n} \cdot \mathbf{G}\boldsymbol{n} \right\rangle_{\partial \mathcal{T}_h \backslash \partial \Omega_N} \\
&\quad = \left\langle \widehat{\boldsymbol{u}}_h^{t,D}, \mathbf{G}\boldsymbol{n} \right\rangle_{\partial \Omega_D} + \left\langle \frac{1}{\tau_n} \widehat{f}_h^N, -\boldsymbol{n} \cdot \mathbf{G}\boldsymbol{n} \right\rangle_{\partial \Omega_N}, \qquad (2.54a) \\
&(\mathbf{L}_h, \nabla \boldsymbol{v})_{\mathcal{T}_h} - (p_h, \nabla \cdot \boldsymbol{v})_{\mathcal{T}_h} + \left\langle \widehat{f}_h^i, \boldsymbol{v} \cdot \boldsymbol{n} \right\rangle_{\partial \mathcal{T}_h \backslash \partial \Omega_N} - \left\langle \mathbf{L}_h \boldsymbol{n}, \boldsymbol{v}^t \right\rangle_{\partial \mathcal{T}_h} \\
&\quad + \left\langle \tau_t \boldsymbol{u}_h^t, \boldsymbol{v}^t \right\rangle_{\partial \Omega_D} + \left\langle \tau_t \left(\boldsymbol{u}_h^t - \widehat{\boldsymbol{u}}_h^{t,i} \right), \boldsymbol{v}^t \right\rangle_{\partial \mathcal{T}_h \backslash \partial \Omega_D} \\
&\quad = (\boldsymbol{f}, \boldsymbol{v})_{\mathcal{T}_h} + \left\langle \tau_t \widehat{\boldsymbol{u}}_h^{t,D}, \boldsymbol{v}^t \right\rangle_{\partial \Omega_D} + \left\langle \widehat{f}_h^N, \boldsymbol{v} \cdot \boldsymbol{n} \right\rangle_{\partial \Omega_N}, \qquad (2.54b) \\
&(\nabla \cdot \boldsymbol{u}_h, q)_{\mathcal{T}_h} + \left\langle \frac{1}{\tau_n} f_h, q \right\rangle_{\partial \Omega_N} + \left\langle \frac{1}{\tau_n} \left(f_h - \widehat{f}_h^i \right), q \right\rangle_{\partial \mathcal{T}_h \backslash \partial \Omega_N} \\
&\quad = \left\langle \frac{1}{\tau_n} \widehat{f}_h^N, q \right\rangle_{\partial \Omega_N}, \qquad (2.54c)
\end{aligned}$$

and the conservation equations combined with the tangential part of the Neumann boundary condition and the normal part of the Dirichlet boundary condition

$$\begin{aligned}
&- \left\langle -\mathbf{L}_h \boldsymbol{n} + \tau_t \left(\boldsymbol{u}_h^t - \widehat{\boldsymbol{u}}_h^{t,i} \right), \widehat{\boldsymbol{v}}^t \right\rangle_{\partial \mathcal{T}_h \backslash \partial \Omega_D} = - \left\langle \boldsymbol{f}_N^t, \widehat{\boldsymbol{v}}^t \right\rangle_{\partial \Omega_N}, \qquad (2.54d) \\
&- \left\langle \boldsymbol{u}_h \cdot \boldsymbol{n} + \frac{1}{\tau_n} \left(f_h - \widehat{f}_h^i \right), \widehat{g} \right\rangle_{\partial \mathcal{T}_h \backslash \partial \Omega_N} = - \left\langle \boldsymbol{u}_D \cdot \boldsymbol{n}, \widehat{g} \right\rangle_{\partial \Omega_D} \qquad (2.54e)
\end{aligned}$$

hold for all $(\mathbf{G}, \boldsymbol{v}, q, \widehat{\boldsymbol{v}}^t, \widehat{g})$ *in* $\mathbf{G}_h \times \boldsymbol{V}_h \times Q_h \times \widehat{\boldsymbol{V}}_h^{t,i} \times \widehat{F}_h^i$*, where* $f_h := -\boldsymbol{n} \cdot \mathbf{L}_h \boldsymbol{n} + p_h$*. In the case that* $\partial \Omega_N = \emptyset$*, we require the zero mean pressure condition for uniqueness of the pressure,* (2.27)*.*

Note that we have identified the scalar test function $\widehat{g}$ with $-\boldsymbol{n} \cdot \widehat{\mathbf{G}}\boldsymbol{n} + \widehat{q}$ on $\partial \mathcal{T}_h \backslash \partial \Omega$ and with $\widehat{\boldsymbol{w}} \cdot \boldsymbol{n}$ on $\partial \Omega_D$ in order to write (2.4d), (2.4f), and the normal part of (2.4g) in a combined manner as (2.54e). Similarly, the normal part of (2.4e) is automatically satisfied, and we identify $\mathbf{T}\widehat{\boldsymbol{w}}$ with $\widehat{\boldsymbol{v}}^t$ to write (2.4e) and the tangent

part of (2.4h) in a combined manner as (2.54d). We are now ready to prove well-posedness of Formulation 2.4 and its local solver.

Theorem 2.4. *(well-posedness of Formulation 2.4)*
Suppose that $\tau_t > 0$ and $\tau_n > 0$. Then Formulation 2.4 is well-posed in the sense that given $\boldsymbol{f}$, $\boldsymbol{u}_D$, and $\boldsymbol{f}_N$, there exists a unique solution $\left(\mathbf{L}_h, \boldsymbol{u}_h, p_h, \widehat{\boldsymbol{u}}_h^t, \widehat{f}_h\right)$ in $\mathbf{G}_h \times \boldsymbol{V}_h \times Q_h \times \widehat{\boldsymbol{V}}_h^t \times \widehat{F}_h$.

Proof. It is sufficient to prove that if $\boldsymbol{f} = \mathbf{0}$, $\boldsymbol{u}_D = \mathbf{0}$ and $\boldsymbol{f}_N = \mathbf{0}$, then the solution $\left(\mathbf{L}_h, \boldsymbol{u}_h, p_h, \widehat{\boldsymbol{u}}_h^t, \widehat{f}_h\right)$ is zero. We can rewrite (2.54) as

$$\begin{aligned} &a_{sym}\left(\left(\mathbf{L}_h, \boldsymbol{u}_h, p_h, \widehat{\boldsymbol{u}}_h^{t,i}, \widehat{f}_h^i\right), \left(\mathbf{G}, \boldsymbol{v}, q, \widehat{\boldsymbol{v}}^t, \widehat{g}\right)\right) \\ &\quad + a_{skew}\left(\left(\mathbf{L}_h, \boldsymbol{u}_h, p_h, \widehat{\boldsymbol{u}}_h^{t,i}, \widehat{f}_h^i\right), \left(\mathbf{G}, \boldsymbol{v}, q, \widehat{\boldsymbol{v}}^t, \widehat{g}\right)\right) = \ell\left(\mathbf{G}, \boldsymbol{v}, q, \widehat{\boldsymbol{v}}^t, \widehat{g}\right) \end{aligned} \tag{2.55}$$

where, using for simplicity $g := -\boldsymbol{n} \cdot \mathbf{G}\boldsymbol{n} + q$,

$$\begin{aligned} &a_{sym}\left(\left(\mathbf{L}_h, \boldsymbol{u}_h, p_h, \widehat{\boldsymbol{u}}_h^{t,i}, \widehat{f}_h^i\right), \left(\mathbf{G}, \boldsymbol{v}, q, \widehat{\boldsymbol{v}}^t, \widehat{g}\right)\right) := \\ &\quad \mathrm{Re}\left(\mathbf{L}_h, \mathbf{G}\right)_{\mathcal{T}_h} + \left\langle \frac{1}{\tau_n} f_h, g \right\rangle_{\partial\Omega_N} + \left\langle \frac{1}{\tau_n}\left(f_h - \widehat{f}_h^i\right), g - \widehat{g} \right\rangle_{\partial\mathcal{T}_h \setminus \partial\Omega_N} \\ &\quad + \left\langle \tau_t \boldsymbol{u}_h^t, \boldsymbol{v}^t \right\rangle_{\partial\Omega_D} + \left\langle \tau_t\left(\boldsymbol{u}_h^t - \widehat{\boldsymbol{u}}_h^{t,i}\right), \boldsymbol{v}^t - \widehat{\boldsymbol{v}}^t \right\rangle_{\partial\mathcal{T}_h \setminus \partial\Omega_D}, \end{aligned} \tag{2.56}$$

$$\begin{aligned} &a_{skew}\left(\left(\mathbf{L}_h, \boldsymbol{u}_h, p_h, \widehat{\boldsymbol{u}}_h^{t,i}, \widehat{f}_h^i\right), \left(\mathbf{G}, \boldsymbol{v}, q, \widehat{\boldsymbol{v}}^t, \widehat{g}\right)\right) := -\left(\nabla \boldsymbol{u}_h, \mathbf{G}\right)_{\mathcal{T}_h} + \left(\mathbf{L}_h, \nabla \boldsymbol{v}\right)_{\mathcal{T}_h} \\ &\quad - \left(p_h, \nabla \cdot \boldsymbol{v}\right)_{\mathcal{T}_h} + \left(\nabla \cdot \boldsymbol{u}_h, q\right)_{\mathcal{T}_h} + \left\langle \widehat{f}_h^i, \boldsymbol{v} \cdot \boldsymbol{n} \right\rangle_{\partial\mathcal{T}_h \setminus \partial\Omega_N} - \left\langle \boldsymbol{u}_h \cdot \boldsymbol{n}, \widehat{g} \right\rangle_{\partial\mathcal{T}_h \setminus \partial\Omega_N} \\ &\quad - \left\langle \widehat{\boldsymbol{u}}_h^{t,i}, \mathbf{G}\boldsymbol{n} \right\rangle_{\partial\mathcal{T}_h \setminus \partial\Omega_D} + \left\langle \mathbf{L}_h \boldsymbol{n}, \widehat{\boldsymbol{v}}^t \right\rangle_{\partial\mathcal{T}_h \setminus \partial\Omega_D} + \left\langle \boldsymbol{u}_h^t, \mathbf{G}\boldsymbol{n} \right\rangle_{\partial\mathcal{T}_h} - \left\langle \mathbf{L}_h \boldsymbol{n}, \boldsymbol{v}^t \right\rangle_{\partial\mathcal{T}_h}, \end{aligned} \tag{2.57}$$

$$\begin{aligned} &\ell\left(\mathbf{G}, \boldsymbol{v}, q, \widehat{\boldsymbol{v}}^t, \widehat{g}\right) := \left(\boldsymbol{f}, \boldsymbol{v}\right)_{\mathcal{T}_h} - \left\langle \boldsymbol{f}_N^t, \widehat{\boldsymbol{v}}^t \right\rangle_{\partial\Omega_N} - \left\langle \boldsymbol{u}_D \cdot \boldsymbol{n}, \widehat{g} \right\rangle_{\partial\Omega_D} + \left\langle \frac{1}{\tau_n} \widehat{f}_h^N, g \right\rangle_{\partial\Omega_N} \\ &\quad + \left\langle \tau_t \widehat{\boldsymbol{u}}_h^{t,D}, \boldsymbol{v}^t \right\rangle_{\partial\Omega_D} - \left\langle \widehat{f}_h^N, \boldsymbol{v} \cdot \boldsymbol{n} \right\rangle_{\partial\Omega_N} + \left\langle \widehat{\boldsymbol{u}}_h^{t,D}, \mathbf{G}\boldsymbol{n} \right\rangle_{\partial\Omega_D}. \end{aligned} \tag{2.58}$$

Setting $\boldsymbol{f} = \mathbf{0}$, $\boldsymbol{u}_D = \mathbf{0}$ (and therefore $\widehat{\boldsymbol{u}}_h^{t,D} = 0$), and $\boldsymbol{f}_N = \mathbf{0}$ (and therefore $\widehat{f}_h^N = 0$), we have $\ell = 0$. Setting $\left(\mathbf{G}, \boldsymbol{v}, q, \widehat{\boldsymbol{v}}^t, \widehat{g}\right) = \left(\mathbf{L}_h, \boldsymbol{u}_h, p_h, \widehat{\boldsymbol{u}}_h^{t,i}, \widehat{f}_h^i\right)$, we have $a_{skew} = 0$.

What remains are the symmetric terms a_{sym}, giving

$$\mathrm{Re}\,(\mathbf{L}_h,\mathbf{L}_h)_{\mathcal{T}_h}+\left\langle\frac{1}{\tau_n}\left(f_h-\widehat{f}_h^i\right),f_h-\widehat{f}_h^i\right\rangle_{\partial\mathcal{T}_h\backslash\partial\Omega_N}+\left\langle\frac{1}{\tau_n}f_h,f_h\right\rangle_{\partial\Omega_N}$$
$$+\left\langle\tau_t\left(\boldsymbol{u}_h^t-\widehat{\boldsymbol{u}}_h^{t,i}\right),\boldsymbol{u}_h^t-\widehat{\boldsymbol{u}}_h^{t,i}\right\rangle_{\partial\mathcal{T}_h\backslash\partial\Omega_D}+\left\langle\tau_t\boldsymbol{u}_h^t,\boldsymbol{u}_h^t\right\rangle_{\partial\Omega_D}=0. \quad (2.59)$$

All the terms in the previous expression are nonnegative and therefore must be zero. Thus $\mathbf{L}_h=\mathbf{0}$ in $\mathcal{T}_h$, $\boldsymbol{u}_h^t=\widehat{\boldsymbol{u}}_h^{t,i}$ on $\mathcal{E}_h\backslash\partial\Omega_D$, $\boldsymbol{u}_h^t=0$ on $\partial\Omega_D$, $p_h=\widehat{f}_h$ on $\mathcal{E}_h\backslash\partial\Omega_N$, and $p_h=0$ on $\partial\Omega_N$.

Equation (2.54a) reduces to $(\nabla u_h,\mathbf{G})_{\mathcal{T}_h}=0$, and since $\nabla\boldsymbol{V}_h\subset\mathbf{G}_h$ we can set $\mathbf{G}=\nabla u_h$ to conclude that u_h is elementwise constant. But since $\boldsymbol{u}_h^t=\widehat{\boldsymbol{u}}_h^{t,i}$ on $\mathcal{E}_h^o$ and $\widehat{\boldsymbol{u}}_h^t$ is single valued on $\mathcal{E}_h^o$, and since the remainder (2.54e) implies $\langle\boldsymbol{u}_h\cdot\boldsymbol{n},\widehat{g}\rangle_{\partial\mathcal{T}_h\backslash\partial\Omega}=0$, the tangential and normal components of $\boldsymbol{u}_h$ are continuous across each internal interface, and therefore $\boldsymbol{u}_h$ is globally constant. Equation (2.54e) also implies the normal component of $\boldsymbol{u}_h$ is zero on $\partial\Omega_D$, and we already have that $\boldsymbol{u}_h^t$ is zero on $\partial\Omega_D$, we conclude that $\boldsymbol{u}_h$ and $\widehat{\boldsymbol{u}}_h^{t,i}$ are zero.

Integrating (2.54b) by parts gives $(\nabla p_h,\boldsymbol{v})_{\mathcal{T}_h}=0$, and since $\nabla Q_h\subset\boldsymbol{V}_h$ we have p_h is elementwise constant. And since $p_h=\widehat{f}_h$ on $\mathcal{E}_h^o$, p_h is globally constant. In the case that $\partial\Omega_N\neq\emptyset$, since $p_h=0$ on $\partial\Omega_N$ we can conclude $p_h=0$ and $\widehat{f}_h=0$. Otherwise, if $\partial\Omega_N=\emptyset$, then (2.27) implies p_h and $\widehat{f}_h$ are zero. □

Theorem 2.5. *(well-posedness of the local solver of Formulation 2.4)*
Suppose that $\tau_t>0$ and $\tau_n>0$. Given $\boldsymbol{f}$, $\widehat{\boldsymbol{u}}_h^t$, and $\widehat{f}_h$, there exists a unique solution $(\mathbf{L}_h,\boldsymbol{u}_h,p_h)$ in $\mathbf{G}_h\times\boldsymbol{V}_h\times Q_h$ to the local equations (2.54a) – (2.54c) .

Proof. It is sufficient to restrict our attention to a single element, and prove that if $\boldsymbol{f}$, $\widehat{\boldsymbol{u}}_h^t$, and $\widehat{f}_h$ are zero, then the solution $(\mathbf{L}_h,\boldsymbol{u}_h,p_h)$ is zero. We can rewrite the local problem associated with Formulation 2.4 as: seek $(\mathbf{L}_h,\boldsymbol{u}_h,p_h)$ in $\mathbf{G}_h(K)\times\boldsymbol{V}_h(K)\times$

$Q_h(K)$ such that

$$\begin{aligned}
&\mathrm{Re}\,(\mathbf{L}_h, \mathbf{G})_K + \left\langle \frac{1}{\tau_n} f_h, g \right\rangle_{\partial K} + \left\langle \tau_t \boldsymbol{u}_h^t, \boldsymbol{v}^t \right\rangle_{\partial K} - (\nabla \boldsymbol{u}_h, \mathbf{G})_K + (\mathbf{L}_h, \nabla \boldsymbol{v})_K \\
&\quad - (p_h, \nabla \cdot \boldsymbol{v})_K + (\nabla \cdot \boldsymbol{u}_h, q)_K + \left\langle \boldsymbol{u}_h^t, \mathbf{G}\boldsymbol{n} \right\rangle_{\partial K} - \left\langle \mathbf{L}_h \boldsymbol{n}, \boldsymbol{v}^t \right\rangle_{\partial K} \\
&\quad = (\boldsymbol{f}, \boldsymbol{v})_K + \left\langle \frac{1}{\tau_n} \widehat{f}_h, g \right\rangle_{\partial K} + \left\langle \tau_t \widehat{\boldsymbol{u}}_h^t, \boldsymbol{v}^t \right\rangle_{\partial K} + \left\langle \widehat{\boldsymbol{u}}_h^t, \mathbf{G}\boldsymbol{n} \right\rangle_{\partial K} - \left\langle \widehat{f}_h, \boldsymbol{v} \cdot \boldsymbol{n} \right\rangle_{\partial K} \quad (2.60)
\end{aligned}$$

for all $(\mathbf{G}, \boldsymbol{v}, q)$ in $\mathbf{G}_h(K) \times \boldsymbol{V}_h(K) \times Q_h(K)$. Setting $\boldsymbol{f}$, $\widehat{\boldsymbol{u}}_h^t$, and $\widehat{f}_h$ to zero, and setting $(\mathbf{G}, \boldsymbol{v}, q) = (\mathbf{L}_h, \boldsymbol{u}_h, p_h)$, we have

$$\mathrm{Re}\,(\mathbf{L}_h, \mathbf{L}_h)_K + \left\langle \tau_t \boldsymbol{u}_h^t, \boldsymbol{u}_h^t \right\rangle_{\partial K} + \left\langle \frac{1}{\tau_n} f_h, f_h \right\rangle_{\partial K} = 0. \quad (2.61)$$

Thus $\mathbf{L}_h = \mathbf{0}$ in K, and $\boldsymbol{u}_h^t = \mathbf{0}$ and $p_h = 0$ on ∂K.

Integrating (2.54b) by parts gives that p_h is constant in K, and since $p_h = 0$ on ∂K, that $p_h = 0$ in K. What remains of (2.54a) gives that $\boldsymbol{u}_h$ is constant in K, and since $\boldsymbol{u}_h^t = \mathbf{0}$ on ∂K, that $\boldsymbol{u}_h = \mathbf{0}$ in K. □

Finally, we note that the condensed global system associated with Formulation 2.4 takes the form

$$\begin{bmatrix} A & B^\top \\ -B & D \end{bmatrix} \begin{bmatrix} \widehat{U}^t \\ \widehat{F} \end{bmatrix} = \begin{bmatrix} F_1 \\ F_2 \end{bmatrix}, \quad (2.62)$$

where A and D are symmetric and positive semi-definite. If $\partial\Omega_N$ is nonempty, then D is positive definite. Otherwise, constraining one degree of freedom associated with $\widehat{f}_h$ renders D positive definite (see the Discussion section at the end of this chapter). Details are in Appendix B.

2.4 Numerical Results

We consider as a numerical test problem an analytical solution by Kovasznay [45] to the two dimensional incompressible Navier-Stokes equations. The solution is

given by

$$u_1 = 1 - \exp \lambda x_1 \cos 2\pi x_2, \tag{2.63}$$

$$u_2 = \frac{\lambda}{2\pi} \exp \lambda x_1 \sin 2\pi x_2, \tag{2.64}$$

$$p = -\frac{1}{2} \exp 2\lambda x_1, \tag{2.65}$$

where $\lambda = \frac{\mathrm{Re}}{2} - \sqrt{\frac{\mathrm{Re}^2}{4} + 4\pi^2}$. For the Stokes equations, we apply the advection term of the exact solution as a forcing term, i.e., we set

$$\boldsymbol{f} = -\boldsymbol{u} \cdot \nabla \boldsymbol{u}. \tag{2.66}$$

A domain of $[0, 2] \times [-0.5, 1.5]$ is considered, with the exact velocity solution prescribed as Dirichlet boundary conditions on all parts of the domain boundary. We set $\mathrm{Re} = 10$ and compute on a mesh of $N \times N$ tensor product square elements, defining the element size $h := \frac{2}{N}$.

In Figure 2.1, the numerical solution $\boldsymbol{u}_h$ and p_h are plotted. In Figure 2.2, the $L^2(\Omega)$ error of the volume unknowns $(\mathbf{L}_h, \boldsymbol{u}_h, p_h)$ are plotted along with their convergence rates. The left column of plots shows the L^2 error obtained using the $\widehat{\boldsymbol{u}}_h$ flux (2.16) on all skeleton faces with the average edge-pressure modification (i.e., Formulation 2.3), while the right column shows the L^2 error obtained using the $(\widehat{\boldsymbol{u}}_h^t, \widehat{f}_h)$ flux (2.18) on the interior skeleton faces and the $\widehat{\boldsymbol{u}}_h$ flux (2.16) on the boundary skeleton faces. In both cases τ_t and τ_n are chosen as the upwind parameters τ_t^S and τ_n^S, respectively, which are defined in (2.7). As expected, the errors using the two versions of the Godunov flux are virtually identical. In both cases, the observed convergence rates are $k+1$ for $\boldsymbol{u}_h$, and close to $k+1$ for $\mathbf{L}_h$ and p_h.

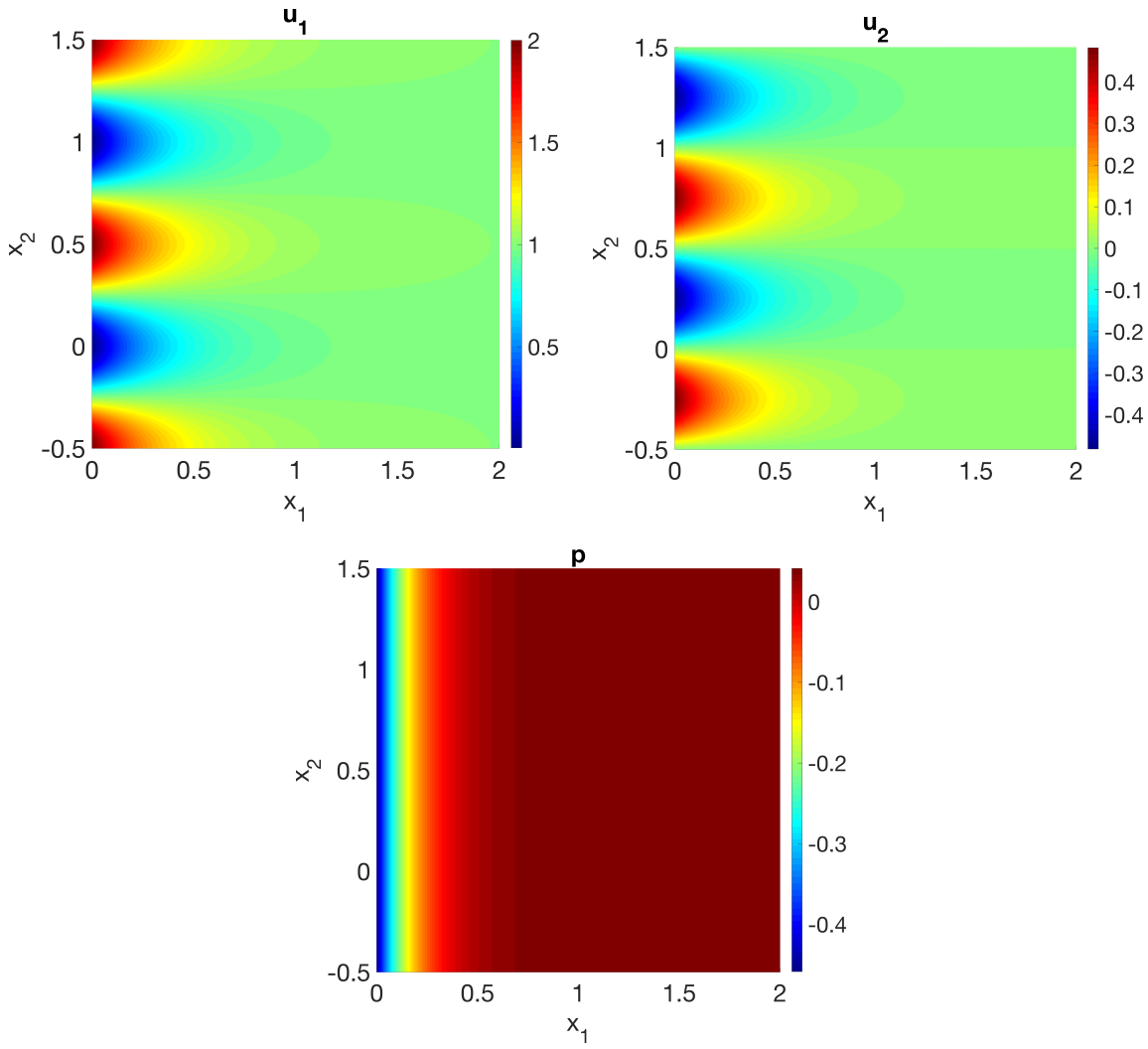

Figure 2.1: Stokes HDG schemes: Kovasznay flow problem solution - $\boldsymbol{u}_{h1}$ (top left), $\boldsymbol{u}_{h2}$ (top right), and p_h (bottom).

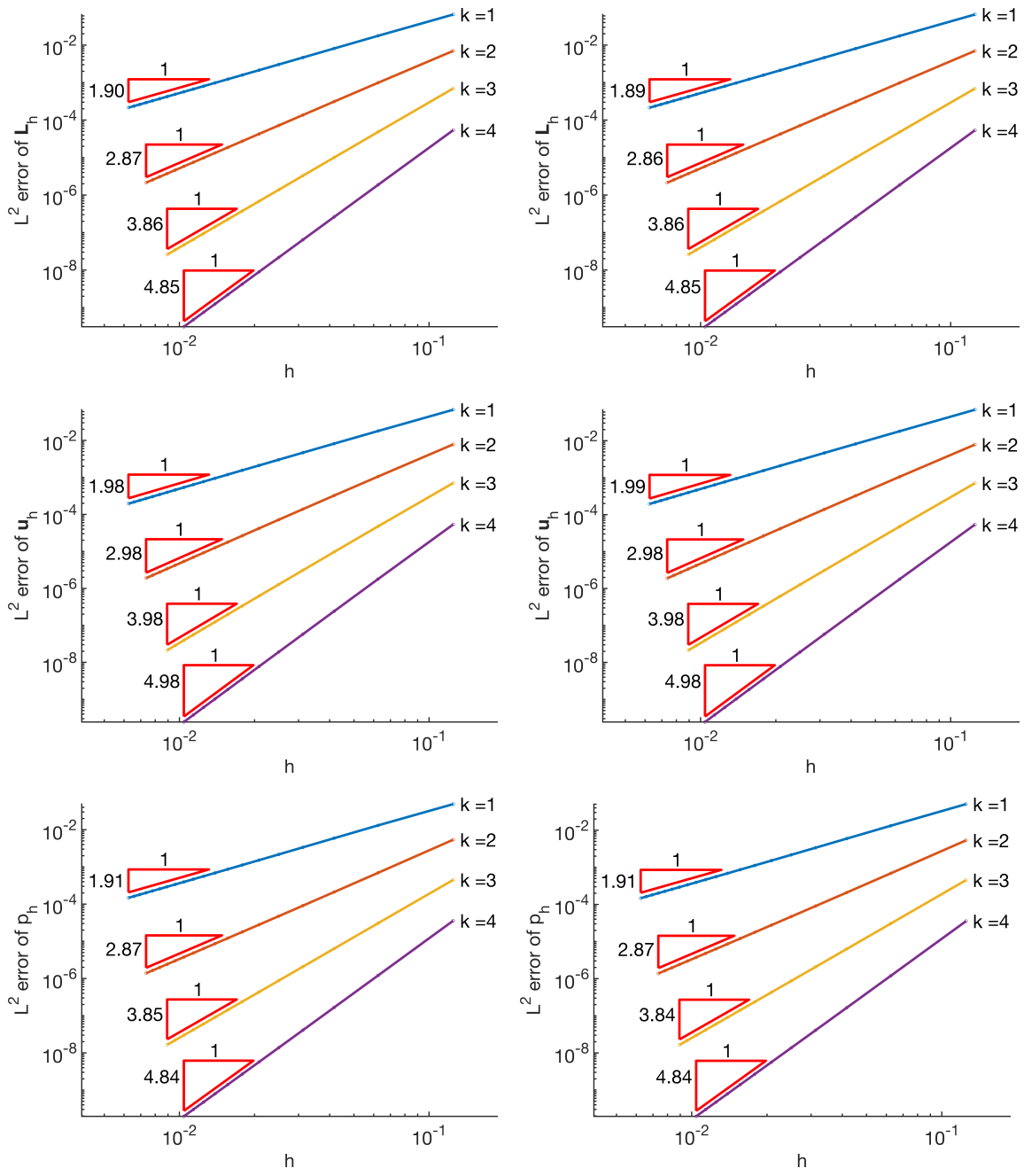

Figure 2.2: Stokes HDG schemes: Kovasznay flow problem L^2 convergence of volume unknowns using $\widehat{\boldsymbol{u}}_h$ flux (2.16) (left), using $(\widehat{\boldsymbol{u}}_h^t, \widehat{f}_h)$ flux (2.18) (right).

2.5 Discussion

We used the upwind HDG framework in [9] to derive an HDG scheme based on the $\widehat{\boldsymbol{u}}_h$ flux (2.16), rediscovering the existing HDG scheme in [53], and relating specific values for the stabilization tensor that result in the upwind flux. Additionally, through manipulation of the upwind flux, we have developed a new HDG scheme based on the $(\widehat{\boldsymbol{u}}_h^t, \widehat{f}_h)$ flux (2.18). The schemes based on the $\widehat{\boldsymbol{u}}_h$ flux require modifications in order for the HDG local solver to be well-posed. One modification involves solving a trace system iteratively (in addition to any iterative linear solver), while introducing multiple parameters related to the iterations. Another modification involves introducing an elementwise constant *global* unknown, rendering the global system a saddle point system. The global unknowns in the latter modified system are of a different nature; the $\widehat{\boldsymbol{u}}_h$ unknowns are discontinuous polynomials on the mesh skeleton, whereas the ρ_h unknowns are elementwise discontinuous constants. This presents challenges in the design of linear solvers and preconditioners. The new scheme based on the $(\widehat{\boldsymbol{u}}_h^t, \widehat{f}_h)$ flux offers some advantages from both of these schemes. No iterations are needed, and all unknowns in the condensed global system are of the same nature: discontinuous polynomials on the mesh skeleton. Additionally, the trace system does not result in a traditional saddle point system; there are no zero blocks on the diagonal, which allows more flexibility in the types of preconditioners we can apply, including allowing for the application of the simple Jacobi/block Jacobi preconditioners.

When using the $(\widehat{\boldsymbol{u}}_h^t, \widehat{f}_h)$ flux (2.18), it can be convenient to use that flux on the interior skeleton face only, and to use a different flux on the domain boundary. In addition to being potentially easier to implement, applying the boundary conditions in this way minimizes the number of globally coupled unknowns, since all of the boundary unknowns are decoupled from the interior ones. For example, if all of the boundary conditions are Dirichlet boundary conditions (2.2a), then we can use the $\widehat{\boldsymbol{u}}_h$

flux (2.16) on the domain boundary so that the application of the boundary conditions are simply the projection of the boundary data to the trace unknown, rather than the "mixed" way of applying them described in Formulation 2.4. It can be shown that the global system and the local solver remain well-posed, and that the condensed global matrix structure (2.62) does not change.

As pointed out in the definitions of the HDG schemes, an additional constraint is required when we have $\partial\Omega_N = \emptyset$ in order to uniquely define the pressure. Even though the zero mean pressure constraint (2.27) appears to be a global equation that couples volume variables across elements, the implementation can be handled in a way that does not break the locality of the local problems. In the case of Formulation 2.1, the analysis reveals that we must only constrain one degree of freedom associated with ρ_h in order to uniquely define ρ_h and therefore p_h. Depending on the linear solver, it may or may not be necessary to explicitly constrain that degree of freedom. Similarly for Formulation 2.4, we must only constrain one degree of freedom associated with $\widehat{f}_h$. Then we must only shift p_h in a postprocessing step in order to satisfy (2.27) (if desired).

Chapter 3

Oseen Equations

In this chapter, we employ the upwind HDG framework proposed in [9] in order to derive HDG schemes for the Oseen equations. Similar to the the previous chapter on the Stokes equations, we manipulate the upwind flux in order to express it in four different ways, each of which can be shown to lead to a well-posed HDG scheme. One of the schemes is related to the scheme in [11], whereas the other three are new contributions in this work. We present two of these schemes in detail and prove the aforementioned well-posedness. The two schemes are employed in numerical tests and their convergence is demonstrated. Additionally we define a Picard-type iterative method that can be used to solve the (nonlinear) incompressible Navier-Stokes equations, and we demonstrate the convergence of the scheme.

3.1 Construction of Upwind HDG Schemes

For notation used in this chapter and throughout this work, see Appendix A. The incompressible Navier-Stokes equations read

$$\rho\frac{\partial \boldsymbol{u}}{\partial t} + \rho\boldsymbol{u}\cdot\nabla\boldsymbol{u} - \mu\Delta\boldsymbol{u} + \nabla p = \boldsymbol{f}, \tag{3.1a}$$

$$\nabla\cdot\boldsymbol{u} = 0. \tag{3.1b}$$

Here, $\boldsymbol{u}$ is the fluid velocity, p is the pressure, μ is the dynamic viscosity of the fluid, and ρ is the fluid density. We assume that we can infer from the problem we are solving a characteristic velocity u_0 and a characteristic length l_0 through which we

can define a characteristic time scale $t_0 := \frac{l_0}{u_0}$, a characteristic (dynamic) pressure $p_0 := \rho u_0^2$, and a scaling for the forcing function $f_0 := \frac{\rho u_0^2}{l_0}$. Then we commit a slight abuse in notation by using the same symbols for the dimensionless variables as we did in the previous expression for the fully dimensional variables; that is, we make the substitutions $\frac{\boldsymbol{u}}{u_0} \to \boldsymbol{u}$, $l_0\nabla \to \nabla$, etc., in order to nondimensionalize the incompressible Navier-Stokes equations as

$$\frac{\partial \boldsymbol{u}}{\partial t} + \boldsymbol{u}\cdot\nabla\boldsymbol{u} - \frac{1}{\mathrm{Re}}\Delta\boldsymbol{u} + \nabla p = \boldsymbol{f}, \tag{3.2a}$$

$$\nabla\cdot\boldsymbol{u} = 0, \tag{3.2b}$$

where the Reynolds number $\mathrm{Re} := \frac{\rho l_0 u_0}{\mu}$ is an indication of the ratio of inertial forces to viscous forces on the fluid. In the limit that $\mathrm{Re} \to 0$, the nonlinear advection is negligible and we recover the Stokes equations. As $\mathrm{Re} \to \infty$, viscosity become negligible and we recover the incompressible Euler equations. By assuming steady flow, and linearizing about a known advection field $\boldsymbol{w}$, we arrive at the Oseen equations

$$-\frac{1}{\mathrm{Re}}\Delta\boldsymbol{u} + \boldsymbol{w}\cdot\nabla\boldsymbol{u} + \nabla p = \boldsymbol{f}, \tag{3.3a}$$

$$\nabla\cdot\boldsymbol{u} = 0, \tag{3.3b}$$

where $\boldsymbol{w}$ is assumed to be divergence free and is assumed to reside in $H(div, \Omega)$. For simplicity, we consider only Dirichlet boundary conditions,

$$\boldsymbol{u} = \boldsymbol{u}_D \quad \text{on } \partial\Omega. \tag{3.4}$$

A compatibility condition on the Dirichlet boundary data $\int\limits_{\partial\Omega} \boldsymbol{u}_D\cdot\boldsymbol{n} = 0$ should be satisfied, and we have to impose an additional constraint on the pressure. We choose this constraint to be $\int\limits_{\Omega} p = 0$. Comments will be made later on generalizations to different types of boundary conditions.

Toward applying the upwind HDG framework [9], we first put (3.3) into first order form through the definition of an auxiliary variable. We define the auxiliary variable $\mathbf{L}$ through the velocity gradient, resulting in the first order system

$$\mathrm{Re}\mathbf{L} - \nabla \boldsymbol{u} = 0, \tag{3.5a}$$

$$-\nabla \cdot \mathbf{L} + \nabla p + \nabla \cdot (\boldsymbol{u} \otimes \boldsymbol{w}) = \boldsymbol{f}, \tag{3.5b}$$

$$\nabla \cdot \boldsymbol{u} = 0. \tag{3.5c}$$

In the above, we have used the divergence-free assumption on $\boldsymbol{w}$ to put the system into divergence form. To define a general HDG scheme for the Oseen equations, we multiply (3.5) by test functions, integrate over the computational domain, integrate by parts, and replace the boundary terms with yet-to-be-defined numerical flux terms, which we then enforce to be weakly continuous across element interfaces. HDG schemes derived in this manner for (3.5) will take a general form consisting of the local equations

$$\mathrm{Re}\left(\mathbf{L}_h, \mathbf{G}\right)_{\mathcal{T}_h} + \left(\boldsymbol{u}_h, \nabla \cdot \mathbf{G}\right)_{\mathcal{T}_h} - \left\langle \boldsymbol{u}_h^* \otimes \boldsymbol{n}, \mathbf{G} \right\rangle_{\partial \mathcal{T}_h} = 0, \tag{3.6a}$$

$$\begin{aligned} &\left(\mathbf{L}_h, \nabla \boldsymbol{v}\right)_{\mathcal{T}_h} - \left(p_h, \nabla \cdot \boldsymbol{v}\right)_{\mathcal{T}_h} - \left(\boldsymbol{u}_h \otimes \boldsymbol{w}, \nabla \boldsymbol{v}\right)_{\mathcal{T}_h} \\ &\qquad + \left\langle -\mathbf{L}_h^* \boldsymbol{n} + p_h^* \boldsymbol{n} + (\boldsymbol{w} \cdot \boldsymbol{n}) \boldsymbol{u}_h^*, \boldsymbol{v} \right\rangle_{\partial \mathcal{T}_h} = \left(\boldsymbol{f}, \boldsymbol{v}\right)_{\mathcal{T}_h}, \end{aligned} \tag{3.6b}$$

$$-\left(\boldsymbol{u}_h, \nabla q\right)_{\mathcal{T}_h} + \left\langle \boldsymbol{u}_h^* \cdot \boldsymbol{n}, q \right\rangle_{\partial \mathcal{T}_h} = 0, \tag{3.6c}$$

the conservation equations

$$\left\langle \boldsymbol{u}_h^* \otimes \boldsymbol{n}, \widehat{\mathbf{G}} \right\rangle_{\partial \mathcal{T}_h \setminus \partial \Omega} = 0, \tag{3.6d}$$

$$-\left\langle -\mathbf{L}_h^* \boldsymbol{n} + p_h^* \boldsymbol{n} + (\boldsymbol{w} \cdot \boldsymbol{n}) \boldsymbol{u}_h^*, \widehat{\boldsymbol{v}} \right\rangle_{\partial \mathcal{T}_h \setminus \partial \Omega} = 0, \tag{3.6e}$$

$$-\left\langle \boldsymbol{u}_h^* \cdot \boldsymbol{n}, \widehat{q} \right\rangle_{\partial \mathcal{T}_h \setminus \partial \Omega} = 0, \tag{3.6f}$$

and the Dirichlet boundary condition

$$\left\langle \boldsymbol{u}_h^*, \widehat{\boldsymbol{w}} \right\rangle_{\partial \Omega} = \left\langle \boldsymbol{u}_D, \widehat{\boldsymbol{w}} \right\rangle_{\partial \Omega}. \tag{3.6g}$$

In the above, $(\mathbf{L}_h, \boldsymbol{u}_h, p_h)$ will be sought in some discontinuous polynomial spaces on the volume of the domain, and $(\mathbf{G}, \boldsymbol{v}, q)$ are test functions in those same spaces. The quantities $\boldsymbol{u}_h^*$ and $-\mathbf{L}_h^*\boldsymbol{n}+p_h^*\boldsymbol{n}+(\boldsymbol{w}\cdot\boldsymbol{n})\boldsymbol{u}_h^*$ are yet-to-be-defined, not-necessarily-single-valued numerical fluxes, which are function of the volume unknowns $(\mathbf{L}_h, \boldsymbol{u}_h, p_h)$ and trace variables $\left(\widehat{\mathbf{L}}_h, \widehat{\boldsymbol{u}}_h, \widehat{p}_h\right)$. The trace variables reside in discontinuous polynomial spaces defined on the mesh skeleton, as do the interior test functions $\left(\widehat{\mathbf{G}}, \widehat{\boldsymbol{v}}, \widehat{q}\right)$, and boundary test function $\widehat{\boldsymbol{w}}$. In what follows, we derive different choices for the starred quantities and analyze schemes that result from some specific choices. The fluxes we derive will have a minimal number of trace unknowns (d scalar unknowns) so that not all of the trace unknowns $\left(\widehat{\mathbf{L}}_h, \widehat{\boldsymbol{u}}_h, \widehat{p}_h\right)$ (and their corresponding test functions) will exist as unknowns (and test functions). Related to this is the fact that not all of the conservation equations (3.6d) – (3.6f) must be explicitly enforced, as some will be automatically satisfied depending on the choice of the numerical flux. Additionally, the boundary test function $\widehat{\boldsymbol{w}}$ will have a natural association with the interior skeleton test functions among $\left(\widehat{\mathbf{G}}, \widehat{\boldsymbol{v}}, \widehat{q}\right)$ that do exist in the scheme. These points will be made clearer after we derive the HDG numerical fluxes.

To derive the numerical fluxes, we observe that the first order system (3.5) fits into the framework of (1.1) and is, in fact, a symmetric hyperbolic system. Choosing the ordering of unknowns as the column vector $\boldsymbol{U} := (\mathrm{vec}\,(\mathbf{L})\,;\boldsymbol{u};p)$, and defining $m := \boldsymbol{w}\cdot\boldsymbol{n}$, we have

$$\mathbf{A} = \begin{bmatrix} \mathbf{0} & -\boldsymbol{n}\otimes_K\mathbf{I} & \mathbf{0} \\ -\boldsymbol{n}^\top\otimes_K\mathbf{I} & m\mathbf{I} & \boldsymbol{n} \\ \mathbf{0} & \boldsymbol{n}^\top & 0 \end{bmatrix}. \tag{3.7}$$

We perform the eigendecomposition $\mathbf{A} = \mathbf{R}\mathbf{D}\mathbf{R}^{-1}$, where $\mathbf{D}$ is a diagonal matrix comprising the eigenvalues of $\mathbf{A}$, and $\mathbf{R}$ is a matrix whose columns are the eigenvectors corresponding those eigenvalues. Defining $|\mathbf{D}|$ by taking the absolute value of each

eigenvalue in $\mathbf{D}$, we can define $|\mathbf{A}| := \mathbf{R}\,|\mathbf{D}|\,\mathbf{R}^{-1}$. It can be shown that for the Oseen system we have

$$|\mathbf{A}| = \begin{bmatrix} \mathbf{N}\otimes_K \left(\frac{1}{\tau_t^O}\mathbf{T} + \frac{1}{\tau_n^O}\mathbf{N}\right) & -\frac{m}{2}\boldsymbol{n}\otimes_K \left(\frac{1}{\tau_t^O}\mathbf{T} + \frac{1}{\tau_n^O}\mathbf{N}\right) & -\frac{1}{\tau_n^O}\boldsymbol{n}\otimes_K \boldsymbol{n} \\ -\frac{m}{2}\boldsymbol{n}^\top\otimes_K \left(\frac{1}{\tau_t^O}\mathbf{T} + \frac{1}{\tau_n^O}\mathbf{N}\right) & \begin{pmatrix} \left(\frac{m}{2}\right)^2 \left(\frac{1}{\tau_t^O}\mathbf{T} + \frac{1}{\tau_n^O}\mathbf{N}\right) \\ + \left(\tau_t^O\mathbf{T} + \tau_n^O\mathbf{N}\right) \end{pmatrix} & \frac{m}{2}\frac{1}{\tau_n^O}\boldsymbol{n} \\ -\frac{1}{\tau_n^O}\boldsymbol{n}^\top\otimes_K \boldsymbol{n}^\top & \frac{m}{2}\frac{1}{\tau_n^O}\boldsymbol{n}^\top & \frac{1}{\tau_n^O} \end{bmatrix}, \tag{3.8}$$

where

$$\tau_t^O := \frac{1}{2}\sqrt{4+m^2} \quad \text{and} \quad \tau_n^O := \frac{1}{2}\sqrt{8+m^2}. \tag{3.9}$$

Later we will allow for the generalization $\tau_t^O \to \tau_t$, $\tau_n^O \to \tau_n$, where τ_t and τ_n are freely chosen positive parameters, allowing us to define simpler fluxes and relate the upwind schemes to existing schemes. We define the normal upwind flux $\boldsymbol{F}_n^*$ as a column vector $\boldsymbol{F}_n^* := (\mathrm{vec}\,(-\boldsymbol{u}^*\otimes\boldsymbol{n})\,; -\mathbf{L}^*\boldsymbol{n} + p^*\boldsymbol{n} + m\boldsymbol{u}^*; \boldsymbol{u}^*\cdot\boldsymbol{n})$. Since there is a one-to-one correspondence between $\mathrm{vec}\,(-\boldsymbol{u}^*\otimes\boldsymbol{n})$ and $-\boldsymbol{u}^*\otimes\boldsymbol{n}$, we also identify $\boldsymbol{F}_n^*$ with the triple

$$\boldsymbol{F}_n^* = \begin{pmatrix} -\boldsymbol{u}^*\otimes\boldsymbol{n}, \\ -\mathbf{L}^*\boldsymbol{n} + p^*\boldsymbol{n} + m\boldsymbol{u}^*, \\ \boldsymbol{u}^*\cdot\boldsymbol{n} \end{pmatrix}. \tag{3.10}$$

In this way, we can write the exact upwind flux $\boldsymbol{F}_n^* = \mathbf{A}\boldsymbol{U} + |\mathbf{A}|\,(\boldsymbol{U}-\boldsymbol{U}^*)$ as

$$\boldsymbol{F}_n^* = \begin{pmatrix} -\left(\boldsymbol{u} + \mathbf{S}_O^{-1}\left(-\left(\mathbf{L}-\mathbf{L}^*\right)\boldsymbol{n} + \left(p-p^*\right)\boldsymbol{n} + \frac{m}{2}\left(\boldsymbol{u}-\boldsymbol{u}^*\right)\right)\right)\otimes\boldsymbol{n}, \\ -\mathbf{L}\boldsymbol{n} + p\boldsymbol{n} + m\boldsymbol{u} + \mathbf{S}_O\left(\boldsymbol{u}-\boldsymbol{u}^*\right) \\ +\frac{m}{2}\mathbf{S}_O^{-1}\left(-\left(\mathbf{L}-\mathbf{L}^*\right)\boldsymbol{n} + \left(p-p^*\right)\boldsymbol{n} + \frac{m}{2}\left(\boldsymbol{u}-\boldsymbol{u}^*\right)\right), \\ \boldsymbol{u}\cdot\boldsymbol{n} + \frac{1}{\tau_n^O}\left(-\boldsymbol{n}\cdot\left(\mathbf{L}-\mathbf{L}^*\right)\boldsymbol{n} + \left(p-p^*\right) + \frac{m}{2}\left(\boldsymbol{u}-\boldsymbol{u}^*\right)\cdot\boldsymbol{n}\right) \end{pmatrix}, \tag{3.11}$$

where

$$\mathbf{S}_O := \tau_t^O\mathbf{T} + \tau_n^O\mathbf{N}, \qquad \mathbf{S}_O^{-1} = \frac{1}{\tau_t^O}\mathbf{T} + \frac{1}{\tau_n^O}\mathbf{N}. \tag{3.12}$$

At this point, we can eliminate "starred quantities" with the aim of defining an HDG flux with minimal trace unknowns. As we did the Stokes equations, we manipulate

the flux (3.11) in several different ways leading to fluxes that are suitable for use in HDG schemes. We begin with a lemma that gives key relationship between the upwind states.

Lemma 3.1. *The following relationships between the upwind states hold:*

$$\tau_t^O \mathbf{T}\left(\boldsymbol{u}-\boldsymbol{u}^*\right) = -\mathbf{T}\left[-\left(\mathbf{L}-\mathbf{L}^*\right)\boldsymbol{n} + \frac{m}{2}\left(\boldsymbol{u}-\boldsymbol{u}^*\right)\right], \tag{3.13a}$$

$$\tau_n^O \mathbf{N}\left(\boldsymbol{u}-\boldsymbol{u}^*\right) = -\mathbf{N}\left[-\left(\mathbf{L}-\mathbf{L}^*\right)\boldsymbol{n} + \left(p-p^*\right)\boldsymbol{n} + \frac{m}{2}\left(\boldsymbol{u}-\boldsymbol{u}^*\right)\right]. \tag{3.13b}$$

Proof. We arrive at the result by equating the normal components of the left and right side of the first component of flux (3.11), and doing the same for the tangent components. □

Note that (3.13) can be arrived at by equating the second component of (3.11), and (3.13b) can be arrived at by equating the third component of (3.11). That is to say that (3.13b) and (3.13a) are the only two relations we can discover from (3.11).

Next, we use (3.13) to reduce the number of upwind quantities on the right hand side of (3.11) to d scalar unknowns in different ways. The presence of the advection term in the Navier-Stokes momentum equations opens up the possibility of expressing the upwind flux in more ways than we could for the Stokes equations. First, we explore different forms of the flux based on choosing the normal component of either $\boldsymbol{u}^*$ or $-\mathbf{L}^*\boldsymbol{n} + p^*\boldsymbol{n} + \frac{1}{2}(\boldsymbol{w}\cdot\boldsymbol{n})\boldsymbol{u}^*$, and choosing the tangential component of either $\boldsymbol{u}^*$ or $-\mathbf{L}^*\boldsymbol{n} + p^*\boldsymbol{n} + \frac{1}{2}(\boldsymbol{w}\cdot\boldsymbol{n})\boldsymbol{u}^*$. Essentially, we can choose either the left or right side of (3.13a) and either the left or right side of (3.13b). It turns out that these fluxes, when discretized, lead to well-posed HDG schemes. These fluxes are listed below.

The $\boldsymbol{u}_h^*$ flux: The quantities $-\mathbf{L}^*\boldsymbol{n} + p^*\boldsymbol{n}$ can be eliminated from (3.11) so that (3.11) can be written as

$$\boldsymbol{F}_n^* = \begin{pmatrix} -\boldsymbol{u}^* \otimes \boldsymbol{n}, \\ -\mathbf{L}\boldsymbol{n} + p\boldsymbol{n} + \frac{m}{2}\boldsymbol{u} + \frac{m}{2}\boldsymbol{u}^* + \left(\tau_t^O \mathbf{T} + \tau_n^O \mathbf{N}\right)(\boldsymbol{u} - \boldsymbol{u}^*), \\ \boldsymbol{u}^* \cdot \boldsymbol{n} \end{pmatrix}. \tag{3.14}$$

The $-\mathbf{L}^*\boldsymbol{n}+p^*\boldsymbol{n}+\frac{m}{2}\boldsymbol{u}^*$ flux: The flux (3.11) can be written with $-\mathbf{L}^*\boldsymbol{n}+p^*\boldsymbol{n}+\frac{m}{2}\boldsymbol{u}^*$ as the only starred quantities,

$$\boldsymbol{F}_n^* = \begin{pmatrix} -\left(\boldsymbol{u} + \mathbf{S}_O^{-1}\left(-\left[\mathbf{L} - \mathbf{L}^*\right]\boldsymbol{n} + \left[p - p^*\right]\boldsymbol{n} + \frac{m}{2}\left[\boldsymbol{u} - \boldsymbol{u}^*\right]\right)\right) \otimes \boldsymbol{n}, \\ -\mathbf{L}^*\boldsymbol{n} + p^*\boldsymbol{n} + \frac{m}{2}\boldsymbol{u}^* + \frac{m}{2}\boldsymbol{u} \\ +\frac{m}{2}\mathbf{S}_O^{-1}\left(-\left[\mathbf{L} - \mathbf{L}^*\right]\boldsymbol{n} + \left[p - p^*\right]\boldsymbol{n} + \frac{m}{2}\left[\boldsymbol{u} - \boldsymbol{u}^*\right]\right), \\ \boldsymbol{u}\cdot\boldsymbol{n} + \frac{1}{\tau_n^O}\left(-\boldsymbol{n}\cdot\left(\left[\mathbf{L} - \mathbf{L}^*\right]\boldsymbol{n}\right) + \left[p - p^*\right] + \frac{m}{2}\left[\boldsymbol{u} - \boldsymbol{u}^*\right]\cdot\boldsymbol{n}\right) \end{pmatrix}. \tag{3.15}$$

The $(\mathbf{T}\boldsymbol{u}^*, f^*)$ flux: The flux (3.11) can be written with f^* and $\mathbf{T}\boldsymbol{u}^*$ as the only starred quantities,

$$\boldsymbol{F}_n^* = \begin{pmatrix} -\left(\mathbf{T}\boldsymbol{u}^* + \mathbf{N}\boldsymbol{u} + \frac{1}{\tau_n^O}\left(-\boldsymbol{n}\cdot\mathbf{L}\boldsymbol{n} + p + \frac{m}{2}\boldsymbol{u}\cdot\boldsymbol{n} - f^*\right)\boldsymbol{n}\right) \otimes \boldsymbol{n}, \\ f^*\boldsymbol{n} + \frac{m}{2}\mathbf{T}\boldsymbol{u}^* + \frac{m}{2}\boldsymbol{u} - \mathbf{T}\mathbf{L}\boldsymbol{n} \\ +\frac{m}{2}\frac{1}{\tau_n^O}\left(-\boldsymbol{n}\cdot\mathbf{L}\boldsymbol{n} + p + \frac{m}{2}\boldsymbol{u}\cdot\boldsymbol{n} - f^*\right)\boldsymbol{n} + \tau_t^O\mathbf{T}\left(\boldsymbol{u} - \boldsymbol{u}^*\right), \\ \boldsymbol{u}\cdot\boldsymbol{n} + \frac{1}{\tau_n^O}\left(-\boldsymbol{n}\cdot\mathbf{L}\boldsymbol{n} + p + \frac{m}{2}\boldsymbol{u}\cdot\boldsymbol{n} - f^*\right) \end{pmatrix}, \tag{3.16}$$

where $f^* := -\boldsymbol{n}\cdot\mathbf{L}^*\boldsymbol{n} + p^* + \frac{m}{2}\boldsymbol{u}^*\cdot\boldsymbol{n}$.

The $\left(\mathbf{N}\boldsymbol{u}^*, \mathbf{T}\left(-\mathbf{L}^*\boldsymbol{n} + \frac{m}{2}\boldsymbol{u}^*\right)\right)$ flux: The flux (3.11) can be written with $\mathbf{N}\boldsymbol{u}^*$ and $\mathbf{T}\left(-\mathbf{L}^*\boldsymbol{n} + \frac{m}{2}\boldsymbol{u}^*\right)$ as the only starred quantities,

$$\boldsymbol{F}_n^* = \begin{pmatrix} -\left(\mathbf{N}\boldsymbol{u}^* + \mathbf{T}\boldsymbol{u} + \frac{1}{\tau_t^O}\mathbf{T}\left(-\left[\mathbf{L} - \mathbf{L}^*\right]\boldsymbol{n} + \frac{m}{2}\left[\boldsymbol{u} - \boldsymbol{u}^*\right]\right)\right) \otimes \boldsymbol{n}, \\ \mathbf{T}\left(-\mathbf{L}^*\boldsymbol{n} + \frac{m}{2}\boldsymbol{u}^*\right) + \mathbf{N}\left(-\mathbf{L}\boldsymbol{n} + p\boldsymbol{n} + \frac{m}{2}\boldsymbol{u}\right) + \frac{m}{2}\mathbf{N}\boldsymbol{u}^* + \frac{m}{2}\mathbf{T}\boldsymbol{u} \\ +\frac{m}{2}\frac{1}{\tau_t^O}\mathbf{T}\left(-\left[\mathbf{L} - \mathbf{L}^*\right]\boldsymbol{n} + \frac{m}{2}\left[\boldsymbol{u} - \boldsymbol{u}^*\right]\right) + \tau_n^O\mathbf{N}\left(\boldsymbol{u} - \boldsymbol{u}^*\right), \\ \boldsymbol{u}^*\cdot\boldsymbol{n} \end{pmatrix}. \tag{3.17}$$

It is not obvious that the above forms of the upwind flux will lead to well-posed HDG schemes, and they are in fact not the only ways that we can express the upwind flux. The relations (3.13) between the upwind states can be re-expressed as

$$\left(\tau_t^O + \frac{m}{2}\right)\mathbf{T}\left(\boldsymbol{u} - \boldsymbol{u}^*\right) = -\mathbf{T}\left[-\left(\mathbf{L} - \mathbf{L}^*\right)\boldsymbol{n}\right], \tag{3.18a}$$

$$\left(\tau_n^O + \frac{m}{2}\right)\mathbf{N}\left(\boldsymbol{u} - \boldsymbol{u}^*\right) = -\mathbf{N}\left[-\left(\mathbf{L} - \mathbf{L}^*\right)\boldsymbol{n} + \left(p - p^*\right)\boldsymbol{n}\right]. \tag{3.18b}$$

Then, we can write the upwind flux in terms of the normal component of either $\boldsymbol{u}^*$ and $-\mathbf{L}^*\boldsymbol{n} + p^*\boldsymbol{n}$ and the tangential component of either $\boldsymbol{u}^*$ and $-\mathbf{L}^*\boldsymbol{n} + p^*\boldsymbol{n}$. That is, we can choose either the left or right side of (3.18a) and either the left or right side of (3.18b). We have already considered the case where we write the upwind flux in terms of $\boldsymbol{u}^*$ only, giving (3.14). The three remaining forms, as it turns out, do not lead to well-posed HDG schemes when used on all skeleton faces, but it is possible that they could serve a purpose by being used on the domain boundary in order to decouple as many unknowns as possible. For the sake of readability, these additional forms of the flux, and their discrete counterparts, are given in Appendix C.

In order to define numerical fluxes

$$\boldsymbol{F}^*_{n,h} = \begin{pmatrix} -\boldsymbol{u}^*_h \otimes \boldsymbol{n}, \\ -\mathbf{L}^*_h\boldsymbol{n} + p^*_h\boldsymbol{n} + (\boldsymbol{w}\cdot\boldsymbol{n})\boldsymbol{u}^*_h, \\ \boldsymbol{u}^*_h \cdot \boldsymbol{n} \end{pmatrix} \tag{3.19}$$

to be used in the HDG scheme (3.6), we append a subscript h to the terms in (3.14) – (3.17) and replace the starred quantities on the right side of the different forms of the upwind flux with hatted unknown quantities residing on the mesh skeleton. Additionally we replace τ_t^O and τ_n^O with τ_t and τ_n, which, from the well-posedness analysis, can be freely chosen positive values. It is sometimes convenient to use the following notation for the normal and tangential stabilization terms,

$$\mathbf{S} := \tau_t\mathbf{T} + \tau_n\mathbf{N}, \qquad \mathbf{S}^{-1} = \frac{1}{\tau_t}\mathbf{T} + \frac{1}{\tau_n}\mathbf{N}. \tag{3.20}$$

This gives the following numerical fluxes.

The $\widehat{\boldsymbol{u}}_h$ flux:

$$\boldsymbol{F}^*_{n,h} := \begin{pmatrix} -\widehat{\boldsymbol{u}}_h \otimes \boldsymbol{n}, \\ -\mathbf{L}_h\boldsymbol{n} + p_h\boldsymbol{n} + \frac{m}{2}\boldsymbol{u}_h + \frac{m}{2}\widehat{\boldsymbol{u}}_h + (\tau_t\mathbf{T} + \tau_n\mathbf{N})\left(\boldsymbol{u}_h - \widehat{\boldsymbol{u}}_h\right), \\ \widehat{\boldsymbol{u}}_h \cdot \boldsymbol{n} \end{pmatrix}. \tag{3.21}$$

The $\widehat{\boldsymbol{f}}_h$ flux (where $\widehat{\boldsymbol{f}}_h$ approximates $-\mathbf{L}^*\tilde{\boldsymbol{n}} + p^*\tilde{\boldsymbol{n}} + \mathrm{sgn}\frac{m}{2}\boldsymbol{u}^*$):

$$\boldsymbol{F}^*_{n,h} = \begin{pmatrix} -\left(\boldsymbol{u}_h + \mathbf{S}^{-1}\left(-\mathbf{L}_h\boldsymbol{n} + p_h\boldsymbol{n} + \frac{m}{2}\boldsymbol{u}_h - \mathrm{sgn}\widehat{\boldsymbol{f}}_h\right)\right)\otimes\boldsymbol{n}, \\ \mathrm{sgn}\widehat{\boldsymbol{f}}_h + \frac{m}{2}\boldsymbol{u}_h \\ +\frac{m}{2}\mathbf{S}^{-1}\left(-\mathbf{L}_h\boldsymbol{n} + p_h\boldsymbol{n} + \frac{m}{2}\boldsymbol{u}_h - \mathrm{sgn}\widehat{\boldsymbol{f}}_h\right), \\ \boldsymbol{u}_h\cdot\boldsymbol{n} + \frac{1}{\tau_n}\left(-\boldsymbol{n}\cdot(\mathbf{L}_h\boldsymbol{n}) + p_h + \frac{m}{2}\boldsymbol{u}_h\cdot\boldsymbol{n} - \widehat{\boldsymbol{f}}_h\cdot\tilde{\boldsymbol{n}}\right) \end{pmatrix}. \tag{3.22}$$

The $(\widehat{\boldsymbol{u}}^t_h, \widehat{f}_h)$ flux (where $\widehat{f}_h$ approximates $-\boldsymbol{n}\cdot\mathbf{L}^*\boldsymbol{n} + p^* + \frac{1}{2}(\boldsymbol{w}\cdot\boldsymbol{n})(\boldsymbol{u}^*\cdot\boldsymbol{n})$):

$$\boldsymbol{F}^*_{n,h} := \begin{pmatrix} -\left(\widehat{\boldsymbol{u}}^t_h + \mathbf{N}\boldsymbol{u}_h\right)\otimes\boldsymbol{n} \\ -\frac{1}{\tau_n}\left(-\boldsymbol{n}\cdot\mathbf{L}_h\boldsymbol{n} + p_h + \frac{m}{2}\boldsymbol{u}_h\cdot\boldsymbol{n} - \widehat{f}_h\right)\mathbf{N}, \\ \widehat{f}_h\boldsymbol{n} + \frac{m}{2}\widehat{\boldsymbol{u}}^t_h + \frac{m}{2}\boldsymbol{u}_h - \mathbf{T}\mathbf{L}_h\boldsymbol{n} \\ +\frac{m}{2}\frac{1}{\tau_n}\left(-\boldsymbol{n}\cdot\mathbf{L}_h\boldsymbol{n} + p_h + \frac{m}{2}\boldsymbol{u}_h\cdot\boldsymbol{n} - \widehat{f}_h\right)\boldsymbol{n} + \tau_t\left(\boldsymbol{u}^t_h - \widehat{\boldsymbol{u}}^t_h\right), \\ \boldsymbol{u}_h\cdot\boldsymbol{n} + \frac{1}{\tau_n}\left(-\boldsymbol{n}\cdot\mathbf{L}_h\boldsymbol{n} + p_h + \frac{m}{2}\boldsymbol{u}_h\cdot\boldsymbol{n} - \widehat{f}_h\right) \end{pmatrix}. \tag{3.23}$$

The $\left(\widehat{u}^{\tilde{n}}_h, \widehat{\boldsymbol{f}}^t_h\right)$ flux (where $\widehat{\boldsymbol{f}}^t_h$ approximates $\mathbf{T}\left(-\mathbf{L}^*\tilde{\boldsymbol{n}} + \mathrm{sgn}\frac{m}{2}\boldsymbol{u}^*\right)$ and $\widehat{u}^{\tilde{n}}_h$ approximates $\boldsymbol{u}^*\cdot\tilde{\boldsymbol{n}}$):

$$\boldsymbol{F}^*_n = \begin{pmatrix} -\left(\widehat{u}^{\tilde{n}}_h\tilde{\boldsymbol{n}} + \boldsymbol{u}^t_h + \frac{1}{\tau_t}\mathbf{T}\left(-\mathbf{L}_h\boldsymbol{n} + \frac{m}{2}\boldsymbol{u}_h - \mathrm{sgn}\widehat{\boldsymbol{f}}^t_h\right)\right)\otimes\boldsymbol{n}, \\ \mathrm{sgn}\widehat{\boldsymbol{f}}^t_h - \mathbf{N}\mathbf{L}_h\boldsymbol{n} + p_h\boldsymbol{n} + \frac{m}{2}\widehat{u}^{\tilde{n}}_h\tilde{\boldsymbol{n}} + \frac{m}{2}\boldsymbol{u}_h \\ +\frac{m}{2}\frac{1}{\tau_t}\mathbf{T}\left(-\mathbf{L}_h\boldsymbol{n} + \frac{m}{2}\boldsymbol{u}_h - \mathrm{sgn}\widehat{\boldsymbol{f}}^t_h\right) + \tau_n\left(\mathbf{N}\boldsymbol{u} - \widehat{u}^{\tilde{n}}_h\tilde{\boldsymbol{n}}\right), \\ \mathrm{sgn}\widehat{u}^{\tilde{n}}_h \end{pmatrix}. \tag{3.24}$$

In (3.22) and (3.24), we rely on an arbitrarily chosen normal direction $\tilde{\boldsymbol{n}}$ associated with a skeleton face e, and

$$\mathrm{sgn} := \mathrm{sgn}(\boldsymbol{n}) = \begin{cases} 1, & \text{if } \boldsymbol{n} = \tilde{\boldsymbol{n}}, \\ -1, & \text{if } \boldsymbol{n} = -\tilde{\boldsymbol{n}} \end{cases}$$

associated with each face of each element K in order to allow the unknowns on the mesh skeleton to be single-valued.

It can be shown that the use of fluxes (3.21) through (3.24) lead to well-posed HDG schemes, but some of the fluxes are more practical than others. Using (3.21) or (3.24) results in a scheme that requires modifications in order to uniquely define the

pressure p_h in the local solver, similar to some of the fluxes discussed in Chapter 2 for the Stokes equations. The flux (3.22) results in a scheme where the velocity $\widehat{\boldsymbol{u}}_h$ is not uniquely defined by the local solver if $\boldsymbol{w} \cdot \boldsymbol{n} = 0$ on a set of nonzero measure on $\partial\mathcal{T}_h$ (unless we consider the time-dependent version of the Oseen equations with implicit time stepping, in which case it is well-posed without modifications). The flux (3.23) results in a scheme that is in any case well-posed without modifications. In what follows, we concretely define and prove the well-posedness of HDG schemes based on the fluxes (3.21) and (3.23).

3.2 HDG Schemes Using the $\widehat{\boldsymbol{u}}_h$ Flux

In this section, we define an HDG scheme based on (3.14), which is the "familiar" form that can be related to the scheme proposed in the work by Cesmelioglu et al. [11], and can be related to the fluid subsystem of the incompressible MHD scheme [46]. As before, we consider polynomial spaces of equal order $k \geq 1$ for all volume and trace unknowns. The discontinuous polynomial spaces in which we seek the volume unknowns $(\mathbf{L}_h, \boldsymbol{u}_h, p_h)$ are as follows:

$$\mathbf{G}_h := \left\{ \mathbf{G} \in \left[L^2(\Omega)\right]^{d\times d} \ : \ \mathbf{G}|_K \in \mathbf{G}_h(K) \right\}, \tag{3.25a}$$

$$\boldsymbol{V}_h := \left\{ \boldsymbol{v} \in \left[L^2(\Omega)\right]^{d} \ : \ \boldsymbol{v}|_K \in \boldsymbol{V}_h(K) \right\}, \tag{3.25b}$$

$$Q_h := \left\{ q \in L^2(\Omega) \ : \ q|_K \in Q_h(K) \right\}, \tag{3.25c}$$

where $\mathbf{G}_h(K)$, $\boldsymbol{V}_h(K)$, $Q_h(K)$ are polynomial spaces defined on K. The discontinuous polynomial space in which we seek the trace unknowns $\widehat{\boldsymbol{u}}_h$ is

$$\widehat{\boldsymbol{V}}_h := \left\{ \widehat{\boldsymbol{v}} \in \left[L^2(\mathcal{E}_h)\right]^{d} \ : \ \widehat{\boldsymbol{v}}|_e \in \widehat{\boldsymbol{V}}_h(e) \right\}, \tag{3.26}$$

where $\widehat{\boldsymbol{V}}_h(e)$ is a polynomial space defined on e.

With the numerical flux (3.21), the enforcement of the Dirichlet boundary condition (3.6g) simplifies to an L^2 projection of the Dirichlet boundary data to the trace unknown on $\partial\Omega$, thereby decoupling the trace unknowns on $\partial\Omega$ from the rest of the unknowns. Then we can decompose the trace unknown

$$\widehat{\boldsymbol{u}}_h = \widehat{\boldsymbol{u}}_h^i + \widehat{\boldsymbol{u}}_h^D \tag{3.27}$$

where $\widehat{\boldsymbol{u}}_h^D$ is defined on $\partial\Omega$ as the L^2 projection of the boundary data,

$$\left\langle \widehat{\boldsymbol{u}}_h^D, \widehat{\boldsymbol{v}} \right\rangle_{\partial\Omega} = \langle \boldsymbol{u}_D, \widehat{\boldsymbol{v}} \rangle_{\partial\Omega} \quad \text{for all } \widehat{\boldsymbol{v}} \in \widehat{\boldsymbol{V}}_h(e) \text{ for all } e \in \partial\Omega, \tag{3.28}$$

and $\widehat{\boldsymbol{u}}_h^i$ is the trace unknown $\widehat{\boldsymbol{u}}_h$ restricted to the interior skeleton faces $\mathcal{E}_h^o$. Note that in writing (3.27) we identify $\widehat{\boldsymbol{u}}_h^i$ and $\widehat{\boldsymbol{u}}_h^D$ with their extensions by zero to the whole skeleton $\mathcal{E}_h$. Then $\widehat{\boldsymbol{u}}_h^i$ resides in the polynomial space

$$\widehat{\boldsymbol{V}}_h^i := \left\{ \widehat{\boldsymbol{v}} \in \left[L^2(\mathcal{E}_h^o) \right]^d \,:\, \widehat{\boldsymbol{v}}|_e \in \widehat{\boldsymbol{V}}_h(e) \right\}. \tag{3.29}$$

With this in place, we write the HDG scheme as follows.

Formulation 3.1. *Find* $(\mathbf{L}_h, \boldsymbol{u}_h, p_h, \widehat{\boldsymbol{u}}_h^i)$ *in* $\mathbf{G}_h \times \boldsymbol{V}_h \times Q_h \times \widehat{\boldsymbol{V}}_h^i$ *such that the local equations*

$$\operatorname{Re}\left(\mathbf{L}_h, \mathbf{G}\right)_{\mathcal{T}_h} + \left(\boldsymbol{u}_h, \nabla\cdot\mathbf{G}\right)_{\mathcal{T}_h} - \left\langle \widehat{\boldsymbol{u}}_h^i, \mathbf{G}\boldsymbol{n} \right\rangle_{\partial\mathcal{T}_h\setminus\partial\Omega} = \left\langle \widehat{\boldsymbol{u}}_h^D, \mathbf{G}\boldsymbol{n} \right\rangle_{\partial\Omega}, \tag{3.30a}$$

$$\begin{aligned} &-\left(\nabla\cdot\mathbf{L}_h, \boldsymbol{v}\right)_{\mathcal{T}_h} + \left(\nabla p_h, \boldsymbol{v}\right)_{\mathcal{T}_h} - \frac{1}{2}\left(\boldsymbol{u}_h\otimes\boldsymbol{w}, \nabla\boldsymbol{v}\right)_{\mathcal{T}_h} + \frac{1}{2}\left(\nabla\boldsymbol{u}_h, \boldsymbol{v}\otimes\boldsymbol{w}\right)_{\mathcal{T}_h} \\ &\quad + \left\langle \frac{1}{2}\left(\boldsymbol{w}\cdot\boldsymbol{n}\right)\widehat{\boldsymbol{u}}_h^i + \mathbf{S}\left(\boldsymbol{u}_h - \widehat{\boldsymbol{u}}_h^i\right), \boldsymbol{v} \right\rangle_{\partial\mathcal{T}_h\setminus\partial\Omega} + \left\langle \mathbf{S}\boldsymbol{u}_h, \boldsymbol{v} \right\rangle_{\partial\Omega} \\ &\quad = \left(\boldsymbol{f}, \boldsymbol{v}\right)_{\mathcal{T}_h} - \left\langle \frac{1}{2}\left(\boldsymbol{w}\cdot\boldsymbol{n}\right)\widehat{\boldsymbol{u}}_h^D - \mathbf{S}\widehat{\boldsymbol{u}}_h^D, \boldsymbol{v} \right\rangle_{\partial\Omega}, \end{aligned} \tag{3.30b}$$

$$-\left(\boldsymbol{u}_h, \nabla q\right)_{\mathcal{T}_h} + \left\langle \widehat{\boldsymbol{u}}_h^i\cdot\boldsymbol{n}, q \right\rangle_{\partial\mathcal{T}_h\setminus\partial\Omega} = -\left\langle \widehat{\boldsymbol{u}}_h^D\cdot\boldsymbol{n}, q \right\rangle_{\partial\Omega}, \tag{3.30c}$$

and the conservation equation

$$-\left\langle -\mathbf{L}_h\boldsymbol{n} + p_h\boldsymbol{n} + \frac{1}{2}\left(\boldsymbol{w}\cdot\boldsymbol{n}\right)\boldsymbol{u}_h + \mathbf{S}\left(\boldsymbol{u}_h - \widehat{\boldsymbol{u}}_h^i\right), \widehat{\boldsymbol{v}} \right\rangle_{\partial\mathcal{T}_h\setminus\partial\Omega} = 0 \tag{3.30d}$$

hold for all $(\mathbf{G}, \boldsymbol{v}, q, \widehat{\boldsymbol{v}})$ *in* $\mathbf{G}_h \times \boldsymbol{V}_h \times Q_h \times \widehat{\boldsymbol{V}}_h^i$*, where* $\mathbf{S}$ *is defined as in* (3.20)*,* $\widehat{\boldsymbol{u}}_h^D$ *is defined as in* (3.28)*, and with the zero mean pressure conditions for the uniqueness of the pressure,*

$$(p_h, 1)_{\partial \mathcal{T}_h} = 0. \tag{3.31}$$

To come to the above formulation from (3.6), realize that use of the flux (3.21) implies that the conservation conditions (3.6d) and (3.6f) are automatically satisfied, and so we do not need to explicitly include these equations in the formulation. We have integrated by parts terms in (2.4e) in order to write the scheme in a concise manner that reveals the symmetric and skew symmetric terms, and have used the divergence-free assumption on $\boldsymbol{w}$. Also, we have used the fact that $\boldsymbol{w} \in H(div, \Omega)$ to conclude $-\left\langle \frac{1}{2} (\boldsymbol{w} \cdot \boldsymbol{n}) \widehat{\boldsymbol{u}}_h, \widehat{\boldsymbol{v}} \right\rangle_{\partial \mathcal{T}_h \setminus \partial \Omega} = 0$ and have removed this term from (3.30d).

In the following, we discuss the well-posedness of Formulation 3.1.

Theorem 3.2. *(well-posedness of Formulation 3.1)*
Suppose that $\tau_t > 0$ *and* $\tau_n > 0$ *(which is always true for* $\tau_t = \tau_t^O$ *and* $\tau_n = \tau_n^O$*). Then Formulation 3.1 is well-posed in the sense that given* $\boldsymbol{f}$ *and* $\boldsymbol{u}_D$*, there exists a unique solution* $(\mathbf{L}_h, \boldsymbol{u}_h, p_h, \widehat{\boldsymbol{u}}_h)$ *in* $\mathbf{G}_h \times \boldsymbol{V}_h \times Q_h \times \widehat{\boldsymbol{V}}_h$*.*

Proof. It is sufficient to prove that setting $\boldsymbol{f} = \mathbf{0}$ and $\boldsymbol{u}_D = \mathbf{0}$ implies that the solution $(\mathbf{L}_h, \boldsymbol{u}_h, p_h, \widehat{\boldsymbol{u}}_h)$ is zero. We can rewrite (3.30) as

$$\begin{aligned} & a_{sym}\left(\left(\mathbf{L}_h, \boldsymbol{u}_h, \widehat{\boldsymbol{u}}_h^i\right), (\mathbf{G}, \boldsymbol{v}, \widehat{\boldsymbol{v}})\right) \\ & \quad + a_{skew}\left(\left(\mathbf{L}_h, \boldsymbol{u}_h, p_h, \widehat{\boldsymbol{u}}_h^i\right), (\mathbf{G}, \boldsymbol{v}, q, \widehat{\boldsymbol{v}})\right) = \ell\left(\mathbf{G}, \boldsymbol{v}, q, \widehat{\boldsymbol{v}}\right), \end{aligned} \tag{3.32}$$

where

$$
\begin{aligned}
a_{sym}\left(\left(\mathbf{L}_h, \boldsymbol{u}_h, \widehat{\boldsymbol{u}}_h^i\right), (\mathbf{G}, \boldsymbol{v}, \widehat{\boldsymbol{v}})\right) &= \mathrm{Re}\,(\mathbf{L}_h, \mathbf{G})_{\mathcal{T}_h} + \langle \mathbf{S}\boldsymbol{u}_h, \boldsymbol{v}\rangle_{\partial\Omega} \\
&+ \left\langle \mathbf{S}\left(\boldsymbol{u}_h - \widehat{\boldsymbol{u}}_h^i\right), \boldsymbol{v} - \widehat{\boldsymbol{v}}\right\rangle_{\partial\mathcal{T}_h\setminus\partial\Omega}, \qquad a_{skew}\left(\left(\mathbf{L}_h, \boldsymbol{u}_h, p_h, \widehat{\boldsymbol{u}}_h^i\right)\right. \\
&+ (\nabla p_h, \boldsymbol{v})_{\mathcal{T}_h} - (\boldsymbol{u}_h, \nabla q)_{\mathcal{T}_h} - \frac{1}{2}(\boldsymbol{u}_h \otimes \boldsymbol{w}, \nabla \boldsymbol{v})_{\mathcal{T}_h} + \frac{1}{2}(\nabla \boldsymbol{u}_h, \boldsymbol{v} \otimes \boldsymbol{w})_{\mathcal{T}_h} \\
&- \left\langle \widehat{\boldsymbol{u}}_h^i, \mathbf{G}\boldsymbol{n}\right\rangle_{\partial\mathcal{T}_h\setminus\partial\Omega} + \langle \mathbf{L}_h\boldsymbol{n}, \widehat{\boldsymbol{v}}\rangle_{\partial\mathcal{T}_h\setminus\partial\Omega} + \left\langle \widehat{\boldsymbol{u}}_h^i \cdot \boldsymbol{n}, q\right\rangle_{\partial\mathcal{T}_h\setminus\partial\Omega} - \langle p_h, \widehat{\boldsymbol{v}}\cdot\boldsymbol{n}\rangle_{\partial\mathcal{T}_h\setminus\partial\Omega} \\
&+ \frac{1}{2}\left\langle (\boldsymbol{w}\cdot\boldsymbol{n})\widehat{\boldsymbol{u}}_h^i, v\right\rangle_{\partial\mathcal{T}_h\setminus\partial\Omega} - \frac{1}{2}\langle (\boldsymbol{w}\cdot\boldsymbol{n})\boldsymbol{u}_h, \widehat{\boldsymbol{v}}\rangle_{\partial\mathcal{T}_h\setminus\partial\Omega}, \qquad (3.33)
\end{aligned}
$$

$$
\ell(\mathbf{G}, \boldsymbol{v}, q, \widehat{\boldsymbol{v}}) = (\boldsymbol{f}, \boldsymbol{v})_{\mathcal{T}_h} - \left\langle \widehat{\boldsymbol{u}}_h^D, -\mathbf{G}\boldsymbol{n} + q\boldsymbol{n} + \frac{1}{2}(\boldsymbol{w}\cdot\boldsymbol{n})\boldsymbol{v} - \mathbf{S}\boldsymbol{v}\right\rangle_{\partial\Omega}. \qquad (3.34)
$$

Setting $\boldsymbol{f} = \mathbf{0}$ and $\boldsymbol{u}_D = \mathbf{0}$ (and therefore $\widehat{\boldsymbol{u}}_h^D = \mathbf{0}$ on $\partial\Omega$), we have $\ell = 0$. Setting $(\mathbf{G}, \boldsymbol{v}, q, \widehat{\boldsymbol{v}}) = \left(\mathbf{L}_h, \boldsymbol{u}_h, p_h, \widehat{\boldsymbol{u}}_h^i\right)$, then $a_{skew} = 0$, and the only remaining terms are a_{sym}, giving

$$
\mathrm{Re}\,(\mathbf{L}_h, \mathbf{L}_h)_{\mathcal{T}_h} + \left\langle \mathbf{S}\left(\boldsymbol{u}_h - \widehat{\boldsymbol{u}}_h^i\right), \boldsymbol{u}_h - \widehat{\boldsymbol{u}}_h^i\right\rangle_{\partial\mathcal{T}_h\setminus\partial\Omega} + \langle \mathbf{S}\boldsymbol{u}_h, \boldsymbol{u}_h\rangle_{\partial\Omega} = 0. \qquad (3.35)
$$

Thus $\mathbf{L}_h = \mathbf{0}$ in $\mathcal{T}_h$, $\boldsymbol{u}_h = \widehat{\boldsymbol{u}}_h^i$ on $\mathcal{E}_h^o$, and $\boldsymbol{u}_h = \mathbf{0}$ on $\partial\Omega$.

Equation (3.30a) reduces to $(\nabla u_h, \mathbf{G})_{\mathcal{T}_h} = 0$, and since $\nabla \boldsymbol{V}_h \subset \mathbf{G}_h$, we set $\mathbf{G} = \nabla u_h$ to conclude that u_h is elementwise constant. But since $\boldsymbol{u}_h = \widehat{\boldsymbol{u}}_h$ on $\mathcal{E}_h^o$ and $\widehat{\boldsymbol{u}}_h$ is single valued on $\mathcal{E}_h^o$, $\boldsymbol{u}_h$ is continuous across each internal interface, and therefore $\boldsymbol{u}_h$ is globally constant. With the zero boundary condition we conclude $\boldsymbol{u}_h = \mathbf{0}$ and $\widehat{\boldsymbol{u}}_h = \mathbf{0}$.

Integrating what remains of (3.30b) by parts gives $(\nabla p_h, \boldsymbol{v})_{\mathcal{T}_h} = 0$, and since $\nabla Q_h \subset \boldsymbol{V}_h$ we conclude that p_h is elementwise constant. Since (3.30d) reduces to $\langle p_h\boldsymbol{n}, \widehat{\boldsymbol{v}}\rangle_{\partial\mathcal{T}_h\setminus\partial\Omega}$, then p_h is globally continuous and globally constant. Then (3.31) implies p_h is zero. □

We next prove that the local solver, (3.30a) – (3.30c), in Formulation 3.1 determines the local pressure p_h only up to an elementwise constant.

Theorem 3.3. *(well-posedness of the local solver of Formulation 3.1)*
Suppose that $\tau_t > 0$ *and* $\tau_n > 0$. *Given* $\boldsymbol{f}$ *and* $\widehat{\boldsymbol{u}}_h$, *there exists a unique solution* $(\mathbf{L}_h, \boldsymbol{u}_h, p_h)$ *in* $\mathbf{G}_h \times \boldsymbol{V}_h \times Q_h/\mathcal{P}_0(\mathcal{T}_h)$ *to the local equations* (2.25a) – (2.25c).

Proof. It is sufficient to restrict our attention to a single element, and prove that if $\boldsymbol{f}$ and $\widehat{\boldsymbol{u}}_h$ are zero, then the solution $(\mathbf{L}_h, \boldsymbol{u}_h, p_h)$ is zero. We can rewrite the local problem associated with Formulation 3.1 as find $(\mathbf{L}_h, \boldsymbol{u}_h, p_h)$ in $\mathbf{G}_h(K) \times \boldsymbol{V}_h(K) \times Q_h(K)$ such that

$$\begin{aligned}
&\operatorname{Re}(\mathbf{L}_h, \mathbf{G})_K + \langle \mathbf{S}\boldsymbol{u}_h, \boldsymbol{v}\rangle_{\partial K} + (\boldsymbol{u}_h, \nabla\cdot\mathbf{G})_K - (\nabla\cdot\mathbf{L}_h, \boldsymbol{v})_K \\
&\quad + (\nabla p_h, \boldsymbol{v})_K - (\boldsymbol{u}_h, \nabla q)_K - \frac{1}{2}(\boldsymbol{u}_h\otimes\boldsymbol{w}, \nabla\boldsymbol{v})_K + \frac{1}{2}(\nabla\boldsymbol{u}_h, \boldsymbol{v}\otimes\boldsymbol{w})_K \\
&\quad = (\boldsymbol{f}, \boldsymbol{v})_K - \left\langle \widehat{\boldsymbol{u}}_h, -\mathbf{G}\boldsymbol{n} + q\boldsymbol{n} + \frac{1}{2}(\boldsymbol{w}\cdot\boldsymbol{n})\boldsymbol{v} - \mathbf{S}\boldsymbol{v}\right\rangle_{\partial K}
\end{aligned} \tag{3.36}$$

for all $(\mathbf{G}, \boldsymbol{v}, q)$ in $\mathbf{G}_h(K) \times \boldsymbol{V}_h(K) \times Q_h(K)$. Setting $\boldsymbol{f}$ and $\widehat{\boldsymbol{u}}_h$ to zero, and setting $(\mathbf{G}, \boldsymbol{v}, q) = (\mathbf{L}_h, \boldsymbol{u}_h, p_h)$, we have

$$\operatorname{Re}(\mathbf{L}_h, \mathbf{L}_h)_K + \langle \mathbf{S}\boldsymbol{u}_h, \boldsymbol{u}_h\rangle_{\partial K} = 0. \tag{3.37}$$

Thus $\mathbf{L}_h = \mathbf{0}$ in K and $\boldsymbol{u}_h = \mathbf{0}$ on ∂K.

What remains of (3.30a) gives that $\boldsymbol{u}_h$ is constant in K, and since $\boldsymbol{u}_h = \mathbf{0}$ on ∂K, that $\boldsymbol{u}_h = \mathbf{0}$ in K. Integrating (3.30b) by parts gives that p_h is constant in K. □

Formulation 3.1 can be modified in the same way that Formulation 2.1 that the Stokes equations can be modified in order to attain a unique pressure p_h in Q_h, and therefore well-posedness of the local solver. See Chapter 2.2.1.1 for a discussion on the augmented Lagrangian (iterative) method of modifying Formulation 3.1. The matrix

system (which must be solved multiple times) associated with the Formulation 3.1 altered by the augmented Lagrangian method looks like

$$A\widehat{U}^k = F^{k-1}, \tag{3.38}$$

where A^k is positive definite. See Chapter 2.2.1.2 for a discussion on a direct method involving an elementwise edge-average pressure as a global variable. The matrix system associated with the Formulation 3.1 altered by the average edge-pressure method looks like

$$\begin{bmatrix} A & B^\top \\ -B & 0 \end{bmatrix} \begin{bmatrix} \widehat{U} \\ \rho \end{bmatrix} = \begin{bmatrix} F_1 \\ F_2 \end{bmatrix}, \tag{3.39}$$

where A is positive definite.

3.3 HDG Schemes Using the $(\widehat{\boldsymbol{u}}_h^t, \widehat{f}_h)$ Flux

In this section, we define new HDG schemes for the Oseen equations. We do this by using the $(\widehat{\boldsymbol{u}}_h^t, \widehat{f}_h)$ flux (3.23) on all skeleton faces $\mathcal{E}_h^o$. The justification of this choice will become evident when we analyze the well-posedness of the local solver associated with this scheme, where we verify that no special treatment is required for uniqueness of the local pressure. Recall that for trace unknowns, this flux has the tangent velocity $\widehat{\boldsymbol{u}}_h^t$ and a scalar $\widehat{f}_h$ which approximates $-\frac{1}{\mathrm{Re}}\boldsymbol{n}\cdot[\nabla\boldsymbol{u}\cdot\boldsymbol{n}] + p + \frac{1}{2}(\boldsymbol{w}\cdot\boldsymbol{n})(\boldsymbol{u}\cdot\boldsymbol{n})$. The volume unknowns will still be sought from the discontinuous polynomial spaces (3.25). The discontinuous polynomial space in which we seek $\widehat{f}_h$ and $\widehat{\boldsymbol{u}}_h^t$, respectively, are

$$\widehat{F}_h := \left\{ \widehat{g} \in L^2(\mathcal{E}_h) \ : \ \widehat{g}|_e \in \widehat{F}_h(e) \right\}, \tag{3.40}$$

$$\widehat{\boldsymbol{V}}_h^t := \left\{ \widehat{\boldsymbol{v}}^t \in \left[L^2(\mathcal{E}_h)\right]^d \ : \ \widehat{\boldsymbol{v}}^t|_e \in \widehat{\boldsymbol{V}}_h^t(e) \right\}, \tag{3.41}$$

where $\widehat{F}_h(e)$ is a scalar polynomial space, and $\widehat{\boldsymbol{V}}_h^t(e)$ is a vector valued polynomial space with no normal component, defined by

$$\widehat{\boldsymbol{V}}_h^t(e) = \left\{ \sum_{i=1}^{d-1} \boldsymbol{t}^i \widehat{v}_{h,i} \ : \ \widehat{v}_{h,i} \in \widehat{V}_h(e) \right\}, \tag{3.42}$$

where $\widehat{V}_h(e)$ is a scalar polynomial space defined on e, and $\left\{\boldsymbol{t}^1, \ldots, \boldsymbol{t}^{d-1}\right\}$ is a basis of the tangent space of e.

Realize that (3.23) defines $\boldsymbol{u}_h^*$ as

$$\boldsymbol{u}_h^* = \widehat{\boldsymbol{u}}_h^t + \mathbf{N}\boldsymbol{u}_h + \frac{1}{\tau_n}\left(-\boldsymbol{n}\cdot\mathbf{L}_h\boldsymbol{n} + p_h + \frac{1}{2}(\boldsymbol{w}\cdot\boldsymbol{n})(\boldsymbol{u}_h\cdot\boldsymbol{n}) - \widehat{f}_h \right)\boldsymbol{n}. \tag{3.43}$$

The enforcement of the tangent component of the Dirichlet boundary condition (3.6g) then simplifies to an L^2 projection of the tangent part of the Dirichlet boundary data $\boldsymbol{u}_D$ to the trace unknown $\widehat{\boldsymbol{u}}_h^t$ on $\partial\Omega$, thereby decoupling $\widehat{\boldsymbol{u}}_h^t$ on $\partial\Omega$ from the rest of the unknowns. The normal part of the Dirichlet condition is enforced weakly as will be shown below.

Also (3.23) defines

$$-\mathbf{L}_h^*\boldsymbol{n} + p_h^*\boldsymbol{n} + \frac{m}{2}\boldsymbol{u}_h^* = \widehat{f}_h\boldsymbol{n} + \mathbf{T}\left(-\mathbf{L}_h\boldsymbol{n} + \frac{1}{2}(\boldsymbol{w}\cdot\boldsymbol{n})\boldsymbol{u}_h \right) + \tau_t\left(\boldsymbol{u}_h^t - \widehat{\boldsymbol{u}}_h^t\right). \tag{3.44}$$

Since we consider only Dirichlet boundary conditions in this development, the $\widehat{f}_h$ unknowns on $\partial\Omega$ will remain coupled to the rest of the unknowns.

As before, we decompose the velocity trace unknowns into the decoupled parts and the coupled parts of the trace unknowns,

$$\widehat{\boldsymbol{u}}_h^t = \widehat{\boldsymbol{u}}_h^{t,i} + \widehat{\boldsymbol{u}}_h^{t,D}, \tag{3.45}$$

where $\widehat{\boldsymbol{u}}_h^{t,D}$ is defined on $\partial\Omega$ as the L^2 projection of the tangential components of the boundary data,

$$\left\langle \widehat{\boldsymbol{u}}_h^{t,D}, \widehat{\boldsymbol{v}}^t \right\rangle_{\partial\Omega} = \left\langle \boldsymbol{u}_D^t, \widehat{\boldsymbol{v}}^t \right\rangle_{\partial\Omega} \quad \text{for all } \widehat{\boldsymbol{v}}^t \in \widehat{\boldsymbol{V}}_h^t(e) \text{ for all } e \in \partial\Omega, \tag{3.46}$$

and $\widehat{\boldsymbol{u}}_h^{t,i}$ is the trace unknown $\widehat{\boldsymbol{u}}_h^t$ restricted to $\mathcal{E}_h^o$. Again, in writing (3.45) we identify $\widehat{\boldsymbol{u}}_h^{t,i}$, and $\widehat{\boldsymbol{u}}_h^{t,D}$ with their extensions by zero to $\mathcal{E}_h$. We assume that all discrete spaces are of equal polynomial order. Finally, we define the polynomial space

$$\widehat{\boldsymbol{V}}_h^{t,i} := \left\{ \widehat{\boldsymbol{v}}^t \in \left[L^2(\mathcal{E}_h^o)\right]^d \ : \ \widehat{\boldsymbol{v}}^t|_e \in \widehat{\boldsymbol{V}}_h^t(e) \right\}, \tag{3.47}$$

in which $\widehat{\boldsymbol{u}}_h^{t,i}$ lies. With this in place, we write the HDG scheme as follows.

Formulation 3.2. *Find* $(\mathbf{L}_h, \boldsymbol{u}_h, p_h, \widehat{\boldsymbol{u}}_h^{t,i}, \widehat{f}_h)$ *in* $\mathbf{G}_h \times \boldsymbol{V}_h \times Q_h \times \widehat{\boldsymbol{V}}_h^{t,i} \times \widehat{F}_h$ *such that the local equations*

$$\begin{aligned}
&\mathrm{Re}\,(\mathbf{L}_h, \mathbf{G})_{\mathcal{T}_h} - (\nabla \boldsymbol{u}_h, \mathbf{G})_{\mathcal{T}_h} + \left\langle \boldsymbol{u}_h^t, \mathbf{G}\boldsymbol{n} \right\rangle_{\partial\mathcal{T}_h} - \left\langle \widehat{\boldsymbol{u}}_h^{t,i}, \mathbf{G}\boldsymbol{n} \right\rangle_{\partial\mathcal{T}_h \setminus \partial\Omega} \\
&\quad + \left\langle \frac{1}{\tau_n}\left(f_h - \widehat{f}_h\right), -\boldsymbol{n}\cdot\mathbf{G}\boldsymbol{n} \right\rangle_{\partial\mathcal{T}_h} = \left\langle \widehat{\boldsymbol{u}}_h^{t,D}, \mathbf{G}\boldsymbol{n} \right\rangle_{\partial\Omega}, \qquad (3.48a) \\
&(\mathbf{L}_h, \nabla \boldsymbol{v})_{\mathcal{T}_h} - (p_h, \nabla\cdot\boldsymbol{v})_{\mathcal{T}_h} - \frac{1}{2}\left(\boldsymbol{u}_h \otimes \boldsymbol{w}, \nabla \boldsymbol{v}\right)_{\mathcal{T}_h} + \frac{1}{2}\left(\nabla \boldsymbol{u}_h, \boldsymbol{v}\otimes\boldsymbol{w}\right)_{\mathcal{T}_h} \\
&\quad + \left\langle \widehat{f}_h, \boldsymbol{v}\cdot\boldsymbol{n} \right\rangle_{\partial\mathcal{T}_h} - \left\langle \mathbf{L}_h\boldsymbol{n}, \boldsymbol{v}^t \right\rangle_{\partial\mathcal{T}_h} + \left\langle \frac{1}{2}\left(\boldsymbol{w}\cdot\boldsymbol{n}\right)\widehat{\boldsymbol{u}}_h^{t,i} + \tau_t\left(\boldsymbol{u}_h^t - \widehat{\boldsymbol{u}}_h^{t,i}\right), \boldsymbol{v}^t \right\rangle_{\partial\mathcal{T}_h\setminus\partial\Omega} \\
&\quad + \left\langle \tau_t \boldsymbol{u}_h^t, \boldsymbol{v}^t \right\rangle_{\partial\Omega} + \left\langle \frac{1}{\tau_n}\left(f_h - \widehat{f}_h\right), \frac{1}{2}\left(\boldsymbol{w}\cdot\boldsymbol{n}\right)\boldsymbol{v}\cdot\boldsymbol{n} \right\rangle_{\partial\mathcal{T}_h} \\
&\quad = (\boldsymbol{f}, \boldsymbol{v})_{\mathcal{T}_h} - \left\langle \frac{1}{2}\left(\boldsymbol{w}\cdot\boldsymbol{n}\right)\widehat{\boldsymbol{u}}_h^{t,D} - \tau_t\widehat{\boldsymbol{u}}_h^{t,D}, \boldsymbol{v}^t \right\rangle_{\partial\Omega}, \qquad (3.48b) \\
&(\nabla\cdot\boldsymbol{u}_h, q)_{\mathcal{T}_h} + \left\langle \frac{1}{\tau_n}\left(f_h - \widehat{f}_h\right), q \right\rangle_{\partial\mathcal{T}_h} = 0, \qquad (3.48c)
\end{aligned}$$

and the conservation equations combined with the normal part of the boundary condition

$$\begin{aligned}
&-\left\langle -\mathbf{L}_h\boldsymbol{n} + \frac{1}{2}\left(\boldsymbol{w}\cdot\boldsymbol{n}\right)\boldsymbol{u}_h^t + \tau_t\left(\boldsymbol{u}_h^t - \widehat{\boldsymbol{u}}_h^t\right), \widehat{\boldsymbol{v}}^t \right\rangle_{\partial\mathcal{T}_h\setminus\partial\Omega} = 0, \qquad (3.48d) \\
&-\left\langle \boldsymbol{u}_h\cdot\boldsymbol{n} + \frac{1}{\tau_n}\left(f_h - \widehat{f}_h\right), \widehat{g} \right\rangle_{\partial\mathcal{T}_h} = -\left\langle \boldsymbol{u}_D\cdot\boldsymbol{n}, \widehat{g} \right\rangle_{\partial\Omega} \qquad (3.48e)
\end{aligned}$$

hold for all $(\mathbf{G}, \boldsymbol{v}, q, \widehat{\boldsymbol{v}}^t, \widehat{g})$ *in* $\mathbf{G}_h \times \boldsymbol{V}_h \times Q_h \times \widehat{\boldsymbol{V}}_h^{t,i} \times \widehat{F}_h$*, where*

$$f_h := -\boldsymbol{n}\cdot\mathbf{L}_h\boldsymbol{n} + p_h + \frac{1}{2}(\boldsymbol{w}\cdot\boldsymbol{n})(\boldsymbol{u}_h\cdot\boldsymbol{n}), \tag{3.49}$$

and with the zero mean pressure conditions for the uniqueness of the pressure, (3.31)*.*

Note that we have identified the scalar test function $\widehat{g}$ with $-\boldsymbol{n}\cdot\widehat{\mathbf{G}}\boldsymbol{n}+\widehat{q}+\frac{1}{2}(\boldsymbol{w}\cdot\boldsymbol{n})(\widehat{\boldsymbol{v}}\cdot\boldsymbol{n})$ on $\partial\mathcal{T}_h\backslash\partial\Omega$ and with $\widehat{\boldsymbol{w}}\cdot\boldsymbol{n}$ on $\partial\Omega$ in order to write (3.6d), (3.6f), the normal part of (3.6e), and the normal part of (3.6g) in a combined manner as (3.48e). Similarly, we identify $\mathbf{T}\widehat{\boldsymbol{w}}$ with $\widehat{\boldsymbol{v}}^t$ to write the tangent part of (3.6e) as (3.48d). Also note that we have integrated by parts the terms in (3.48a) and (3.48c) and half of the advection term in (3.48b) in order to put the scheme into the form as the above formulation, which readily reveals the symmetric and skew-symmetric terms. Also, we have used the fact that $\boldsymbol{w}\in H(div,\Omega)$ to conclude $-\left\langle\frac{1}{2}\left(\boldsymbol{w}\cdot\boldsymbol{n}\right)\widehat{\boldsymbol{u}}_h^{t,i},\widehat{\boldsymbol{v}}^t\right\rangle_{\partial\mathcal{T}_h\backslash\partial\Omega}=0$ and have removed this term from (3.48d). We are now ready to prove well-posedness of Formulation 3.2 and its local solver.

Theorem 3.4. *(well-posedness of Formulation 3.2)*
Suppose that $\tau_t>0$ and $\tau_n>0$ (which is always true for $\tau_t=\tau_t^O$ and $\tau_n=\tau_n^O$). Then Formulation 3.2 is well-posed in the sense that given $\boldsymbol{f}$ and $\boldsymbol{u}_D$, there exists a unique solution $\left(\mathbf{L}_h,\boldsymbol{u}_h,p_h,\widehat{\boldsymbol{u}}_h^t,\widehat{f}_h\right)$ in $\mathbf{G}_h\times\boldsymbol{V}_h\times Q_h\times\widehat{\boldsymbol{V}}_h^t\times\widehat{F}_h$.

Proof. It is sufficient to prove that if $\boldsymbol{f}=\mathbf{0}$ and $\boldsymbol{u}_D=\mathbf{0}$, then $\left(\mathbf{L}_h,\boldsymbol{u}_h,p_h,\widehat{\boldsymbol{u}}_h^t,\widehat{f}_h\right)$ is zero. We can rewrite (3.48) as

$$\begin{aligned}&a_{sym}\left(\left(\mathbf{L}_h,\boldsymbol{u}_h,p_h,\widehat{\boldsymbol{u}}_h^{t,i},\widehat{f}_h\right),\left(\mathbf{G},\boldsymbol{v},q,\widehat{\boldsymbol{v}}^t,\widehat{g}\right)\right)\\&\quad+a_{skew}\left(\left(\mathbf{L}_h,\boldsymbol{u}_h,p_h,\widehat{\boldsymbol{u}}_h^{t,i},\widehat{f}_h\right),\left(\mathbf{G},\boldsymbol{v},q,\widehat{\boldsymbol{v}}^t,\widehat{g}\right)\right)=\ell\left(\mathbf{G},\boldsymbol{v},q,\widehat{\boldsymbol{v}}^t,\widehat{g}\right)\end{aligned}\tag{3.50}$$

where

$$a_{sym}\left(\left(\mathbf{L}_h,\boldsymbol{u}_h,p_h,\widehat{\boldsymbol{u}}_h^{t,i},\widehat{f}_h\right),\left(\mathbf{G},\boldsymbol{v},q,\widehat{\boldsymbol{v}}^t,\widehat{g}\right)\right) := \mathrm{Re}\left(\mathbf{L}_h,\mathbf{G}\right)_{\mathcal{T}_h} + \left\langle \tau_t \boldsymbol{u}_h^t, \boldsymbol{v}^t\right\rangle_{\partial\Omega}$$
$$+ \left\langle \tau_t\left(\boldsymbol{u}_h^t - \widehat{\boldsymbol{u}}_h^{t,i}\right), \boldsymbol{v}^t - \widehat{\boldsymbol{v}}^t\right\rangle_{\partial\mathcal{T}_h\backslash\partial\Omega} + \left\langle \frac{1}{\tau_n}\left(f_h - \widehat{f}_h^i\right), g - \widehat{g}\right\rangle_{\partial\mathcal{T}_h}, \tag{3.51}$$

$$a_{skew}\left(\left(\mathbf{L}_h,\boldsymbol{u}_h,p_h,\widehat{\boldsymbol{u}}_h^{t,i},\widehat{f}_h\right),\left(\mathbf{G},\boldsymbol{v},q,\widehat{\boldsymbol{v}}^t,\widehat{g}\right)\right) := -\left(\nabla\boldsymbol{u}_h,\mathbf{G}\right)_{\mathcal{T}_h} + \left(\mathbf{L}_h,\nabla\boldsymbol{v}\right)_{\mathcal{T}_h}$$
$$- \left(p_h,\nabla\cdot\boldsymbol{v}\right)_{\mathcal{T}_h} + \left(\nabla\cdot\boldsymbol{u}_h,q\right)_{\mathcal{T}_h} + \left\langle \widehat{f}_h^i, \boldsymbol{v}\cdot\boldsymbol{n}\right\rangle_{\partial\mathcal{T}_h} - \left\langle \boldsymbol{u}_h\cdot\boldsymbol{n},\widehat{g}\right\rangle_{\partial\mathcal{T}_h} + \left\langle \boldsymbol{u}_h^t, \mathbf{G}\boldsymbol{n}\right\rangle_{\partial\mathcal{T}_h}$$
$$- \left\langle \mathbf{L}_h\boldsymbol{n}, \boldsymbol{v}^t\right\rangle_{\partial\mathcal{T}_h} - \left\langle \widehat{\boldsymbol{u}}_h^{t,i}, \mathbf{G}\boldsymbol{n}\right\rangle_{\partial\mathcal{T}_h\backslash\partial\Omega} + \left\langle \mathbf{L}_h\boldsymbol{n}, \widehat{\boldsymbol{v}}^t\right\rangle_{\partial\mathcal{T}_h\backslash\partial\Omega} - \frac{1}{2}\left(\boldsymbol{u}_h\otimes\boldsymbol{w},\nabla\boldsymbol{v}\right)_{\mathcal{T}_h}$$
$$+ \frac{1}{2}\left(\nabla\boldsymbol{u}_h,\boldsymbol{v}\otimes\boldsymbol{w}\right)_{\mathcal{T}_h} + \frac{1}{2}\left\langle(\boldsymbol{w}\cdot\boldsymbol{n})\widehat{\boldsymbol{u}}_h^{t,i}, \boldsymbol{v}^t\right\rangle_{\partial\mathcal{T}_h\backslash\partial\Omega} - \frac{1}{2}\left\langle(\boldsymbol{w}\cdot\boldsymbol{n})\boldsymbol{u}_h^t, \widehat{\boldsymbol{v}}^t\right\rangle_{\partial\mathcal{T}_h\backslash\partial\Omega}, \tag{3.52}$$

$$\ell\left(\mathbf{G},\boldsymbol{v},q,\widehat{\boldsymbol{v}}^t,\widehat{g}\right) := \left(\boldsymbol{f},\boldsymbol{v}\right)_{\mathcal{T}_h} - \left\langle \boldsymbol{u}_D\cdot\boldsymbol{n},\widehat{g}\right\rangle_{\partial\Omega}$$
$$- \left\langle \frac{1}{2}(\boldsymbol{w}\cdot\boldsymbol{n})\widehat{\boldsymbol{u}}_h^{t,i} - \tau_t\widehat{\boldsymbol{u}}_h^{t,D}, \boldsymbol{v}^t\right\rangle_{\partial\Omega} + \left\langle \widehat{\boldsymbol{u}}_h^{t,D}, \mathbf{G}\boldsymbol{n}\right\rangle_{\partial\Omega}, \tag{3.53}$$

where we have have written for simplicity the combination of test functions

$$g := -\boldsymbol{n}\cdot\mathbf{G}\boldsymbol{n} + q + \frac{1}{2}(\boldsymbol{w}\cdot\boldsymbol{n})(\boldsymbol{v}\cdot\boldsymbol{n}). \tag{3.54}$$

Setting $\boldsymbol{f} = \mathbf{0}$ and $\boldsymbol{u}_D = \mathbf{0}$ (and therefore $\widehat{\boldsymbol{u}}_h^{t,D} = 0$) gives $\ell = 0$, and setting $\left(\mathbf{G},\boldsymbol{v},q,\widehat{\boldsymbol{v}}^t,\widehat{g}\right) = \left(\mathbf{L}_h,\boldsymbol{u}_h,p_h,\widehat{\boldsymbol{u}}_h^{t,i},\widehat{f}_h\right)$ gives $a_{skew} = 0$. All that remains is the a_{sym} terms, giving

$$\mathrm{Re}\left(\mathbf{L}_h,\mathbf{L}_h\right)_{\mathcal{T}_h} + \left\langle \tau_t\boldsymbol{u}_h^t,\boldsymbol{u}_h^t\right\rangle_{\partial\Omega} + \left\langle \tau_t\left(\boldsymbol{u}_h^t - \widehat{\boldsymbol{u}}_h^{t,i}\right), \boldsymbol{u}_h^t - \widehat{\boldsymbol{u}}_h^{t,i}\right\rangle_{\partial\mathcal{T}_h\backslash\partial\Omega}$$
$$+ \left\langle \frac{1}{\tau_n}\left(f_h - \widehat{f}_h\right), f_h - \widehat{f}_h\right\rangle_{\partial\mathcal{T}_h} = 0. \tag{3.55}$$

All the terms on the left side of the preceding expression are nonnegative and therefore must each be zero. Thus $\mathbf{L}_h = \mathbf{0}$ in $\mathcal{T}_h$, $\boldsymbol{u}_h^t = \widehat{\boldsymbol{u}}_h^{t,i}$ on $\mathcal{E}_h^o$, $\boldsymbol{u}_h^t = 0$ on $\partial\Omega$, and $p_h + \frac{1}{2}\left(\boldsymbol{w}\cdot\boldsymbol{n}\right)\left(\boldsymbol{u}_h\cdot\boldsymbol{n}\right) = \widehat{f}_h$ on $\mathcal{E}_h$.

Equation (3.48a) reduces to $\left(\nabla u_h,\mathbf{G}\right)_{\mathcal{T}_h} = 0$, and since $\nabla\boldsymbol{V}_h \subset \mathbf{G}_h$ we can set $\mathbf{G} = \nabla u_h$ to conclude that u_h is elementwise constant. But since $\boldsymbol{u}_h^t = \widehat{\boldsymbol{u}}_h^{t,i}$ on $\mathcal{E}_h^o$ and $\widehat{\boldsymbol{u}}_h^t$ is single valued on $\mathcal{E}_h^o$, and since (3.48e) reduces to $\left\langle \boldsymbol{u}_h\cdot\boldsymbol{n},\widehat{g}\right\rangle_{\partial\mathcal{T}_h} = 0$, the

tangential and normal components of $\boldsymbol{u}_h$ are continuous across each internal interface, and therefore $\boldsymbol{u}_h$ and is globally constant. Since we already have concluded that $\boldsymbol{u}_h^t$ is zero on $\partial\Omega$ (and additionally (3.48e) implies the normal component of $\boldsymbol{u}_h$ is zero on $\partial\Omega$), we can conclude that $\boldsymbol{u}_h$ and $\widehat{\boldsymbol{u}}_h^t$ are zero.

Integrating (3.48b) by parts gives $(\nabla p_h, \boldsymbol{v})_{\mathcal{T}_h} = 0$, and since $\nabla Q_h \subset \boldsymbol{V}_h$ we can set $\boldsymbol{v}$ to ∇p_h to conclude that p_h is elementwise constant. Because $p_h = \widehat{f}_h$ on $\mathcal{E}_h$, p_h is globally constant. Then (3.31) implies p_h and $\widehat{f}_h$ are zero. □

Theorem 3.5. *(well-posedness of the local solver of Formulation 3.2)*
Suppose that $\tau_t > 0$ and $\tau_n > 0$. Given $\boldsymbol{f}$, $\widehat{\boldsymbol{u}}_h^t$, and $\widehat{f}_h$, there exists a unique solution $(\mathbf{L}_h, \boldsymbol{u}_h, p_h)$ in $\mathbf{G}_h \times \boldsymbol{V}_h \times Q_h$ to the local equations (3.48a) – (3.48c).

Proof. It is sufficient to restrict our attention to a single element, and prove that if $\boldsymbol{f}$, $\widehat{\boldsymbol{u}}_h^t$, and $\widehat{f}_h$ are zero, then the solution $(\mathbf{L}_h, \boldsymbol{u}_h, p_h)$ is zero. We can rewrite the local problem associated with Formulation 3.2 as find $(\mathbf{L}_h, \boldsymbol{u}_h, p_h)$ in $\mathbf{G}_h(K) \times \boldsymbol{V}_h(K) \times Q_h(K)$ such that

$$\begin{aligned}
&\operatorname{Re}(\mathbf{L}_h, \mathbf{G})_K + \left\langle \tau_t \boldsymbol{u}_h^t, \boldsymbol{v}^t \right\rangle_{\partial K} + \left\langle \frac{1}{\tau_n} f_h, g \right\rangle_{\partial K} \\
&\quad - (\nabla \boldsymbol{u}_h, \mathbf{G})_K + (\mathbf{L}_h, \nabla \boldsymbol{v})_K - (p_h, \nabla \cdot \boldsymbol{v})_K + (\nabla \cdot \boldsymbol{u}_h, q)_K \\
&\quad - \frac{1}{2}(\boldsymbol{u}_h \otimes \boldsymbol{w}, \nabla \boldsymbol{v})_K + \frac{1}{2}(\nabla \boldsymbol{u}_h, \boldsymbol{v} \otimes \boldsymbol{w})_K + \left\langle \boldsymbol{u}_h^t, \mathbf{G}\boldsymbol{n} \right\rangle_{\partial K} - \left\langle \mathbf{L}_h \boldsymbol{n}, \boldsymbol{v}^t \right\rangle_{\partial K} \\
&\quad = (\boldsymbol{f}, \boldsymbol{v})_K + \left\langle \widehat{\boldsymbol{u}}_h^t, \mathbf{G}\boldsymbol{n} \right\rangle_{\partial K} - \left\langle \frac{1}{2}(\boldsymbol{w} \cdot \boldsymbol{n})\, \widehat{\boldsymbol{u}}_h^t - \tau_t \widehat{\boldsymbol{u}}_h^t, \boldsymbol{v}^t \right\rangle_{\partial K} \\
&\quad - \left\langle \widehat{f}_h, \boldsymbol{v} \cdot \boldsymbol{n} \right\rangle_{\partial K} + \left\langle \frac{1}{\tau_n} \widehat{f}_h, g \right\rangle_{\partial K}
\end{aligned} \tag{3.56}$$

for all $(\mathbf{G}, \boldsymbol{v}, q)$ in $\mathbf{G}_h(K) \times \boldsymbol{V}_h(K) \times Q_h(K)$, where f_h is defined as in (3.49) and g is defined as in (3.54). Setting $\boldsymbol{f}$, $\widehat{\boldsymbol{u}}_h^t$, and $\widehat{f}_h$ to zero, and setting $(\mathbf{G}, \boldsymbol{v}, q) = (\mathbf{L}_h, \boldsymbol{u}_h, p_h)$, we have

$$\operatorname{Re}(\mathbf{L}_h, \mathbf{L}_h)_K + \left\langle \tau_t \boldsymbol{u}_h^t, \boldsymbol{u}_h^t \right\rangle_{\partial K} + \left\langle \frac{1}{\tau_n} f_h, f_h \right\rangle_{\partial K} = 0. \tag{3.57}$$

Thus $\mathbf{L}_h = \mathbf{0}$ in K, and $\boldsymbol{u}_h^t = \mathbf{0}$ and $p_h + \frac{1}{2}(\boldsymbol{w} \cdot \boldsymbol{n})(\boldsymbol{u}_h \cdot \boldsymbol{n}) = 0$ on ∂K.

What remains of (3.48a) gives that $\boldsymbol{u}_h$ is constant in K, and since $\boldsymbol{u}_h^t = \mathbf{0}$ on ∂K, that $\boldsymbol{u}_h = \mathbf{0}$ in K. Integrating (3.48b) by parts gives that p_h is constant in K, and since $p_h + \frac{1}{2}(\boldsymbol{w} \cdot \boldsymbol{n})(\boldsymbol{u}_h \cdot \boldsymbol{n}) = p_h = 0$ on ∂K, that $p_h = 0$ in K. □

Finally, we note that the condensed global system associated with Formulation 3.2 takes the form

$$\begin{bmatrix} A & B \\ C & D \end{bmatrix} \begin{bmatrix} \widehat{U}^t \\ \widehat{F} \end{bmatrix} = \begin{bmatrix} F_1 \\ F_2 \end{bmatrix}, \tag{3.58}$$

where A and D are positive semi-definite and constraining one degree of freedom associated with $\widehat{f}_h$ (which is done to enforce (3.31)) renders D positive definite.

3.4 Numerical Results

We consider as a numerical test problem the same problems as considered in the previous chapter on the Stokes equations. The problem is an analytical solution by Kovasznay [45] to the two dimensional incompressible Navier-Stokes equations. The solution is given by

$$u_1 = 1 - \exp \lambda x_1 \cos 2\pi x_2, \tag{3.59}$$

$$u_2 = \frac{\lambda}{2\pi} \exp \lambda x_1 \sin 2\pi x_2, \tag{3.60}$$

$$p = -\frac{1}{2} \exp 2\lambda x_1. \tag{3.61}$$

A domain of $[0, 2] \times [-0.5, 1.5]$ is considered, with the exact velocity solution prescribed as Dirichlet boundary conditions on all parts of the domain boundary. Setting $\boldsymbol{f} = 0$, $\boldsymbol{w} = \boldsymbol{u}$, and $\boldsymbol{u}_D = \boldsymbol{u}$, we compute on a mesh of $N \times N$ tensor product square elements, defining the element size $h := \frac{2}{N}$.

In Figure 3.1, the numerical solution $\boldsymbol{u}_h$ and p_h are plotted. In Figure 3.2, the $L^2(\Omega)$ error of the volume unknowns $(\mathbf{L}_h, \boldsymbol{u}_h, p_h)$ are plotted along with their convergence rates. The left column of plots shows the L^2 error obtained using the $\widehat{\boldsymbol{u}}_h$ flux (3.21) on all skeleton faces (i.e., Formulation 3.1), while the right column shows the L^2 error obtained using the $(\widehat{\boldsymbol{u}}_h^t, \widehat{f}_h)$ flux (3.23) on the interior skeleton faces and the $\widehat{\boldsymbol{u}}_h$ flux (3.21) on the boundary skeleton faces. In both cases τ_t and τ_n are chosen as the upwind parameters τ_t^O and τ_n^O, respectively, which are defined in (3.9). As expected, the errors using the two versions of the Godunov flux are virtually identical. In both cases, the observed convergence rates are $k+1$ for $\boldsymbol{u}_h$, and close to $k+1$ for $\mathbf{L}_h$ and p_h.

Next we demonstrate the utility of the HDG schemes for the Oseen equations for solving the (nonlinear) incompressible Navier-Stokes equations (3.2). If we consider the Oseen equations (3.3) to be a linear map $\boldsymbol{w} \mapsto \boldsymbol{u}$, then any fixed point of that mapping is a solution to the steady state incompressible Navier-Stokes equations (3.2). With this in mind, we can use the general Oseen HDG scheme (3.6) in an iterative manner to numerically solve the incompressible Navier-Stokes equations. Omitting the specification of trial/test spaces for simplicity, we can express the Oseen HDG schemes as solving

$$a\left(\boldsymbol{w}; \mathbf{L}_h, \boldsymbol{u}_h, p_h, \widehat{\boldsymbol{U}}_h; \mathbf{G}, \boldsymbol{v}, q, \widehat{\boldsymbol{V}}\right) = \ell\left(\mathbf{G}, \boldsymbol{v}, q, \widehat{\boldsymbol{V}}\right), \tag{3.62}$$

where $\widehat{\boldsymbol{U}}_h$ and $\widehat{\boldsymbol{V}}$ represent the global unknowns and test functions, respectively. For example, for Formulation 3.1 with the average edge-pressure modification, $\widehat{\boldsymbol{U}}_h$ represents $(\widehat{\boldsymbol{u}}_h^i, \rho_h)$ and $\widehat{\boldsymbol{V}}$ represents $(\widehat{\boldsymbol{v}}, \psi)$, and for Formulation 3.2, $\widehat{\boldsymbol{U}}_h$ represents $(\widehat{\boldsymbol{u}}_h^{t,i}, \widehat{f}_h^i)$ and $\widehat{\boldsymbol{V}}$ represents $(\widehat{\boldsymbol{v}}^t, \widehat{g})$. Then, we can define one step of the Picard iteration as solving for $\left(\mathbf{L}_h^m, \boldsymbol{u}_h^m, p_h^m, \widehat{\boldsymbol{U}}_h^m\right)$ using

$$a\left(\boldsymbol{u}_h^{m-1}; \mathbf{L}_h^m, \boldsymbol{u}_h^m, p_h^m, \widehat{\boldsymbol{U}}_h^m; \mathbf{G}, \boldsymbol{v}, q, \widehat{\boldsymbol{V}}\right) = \ell\left(\mathbf{G}, \boldsymbol{v}, q, \widehat{\boldsymbol{V}}\right). \tag{3.63}$$

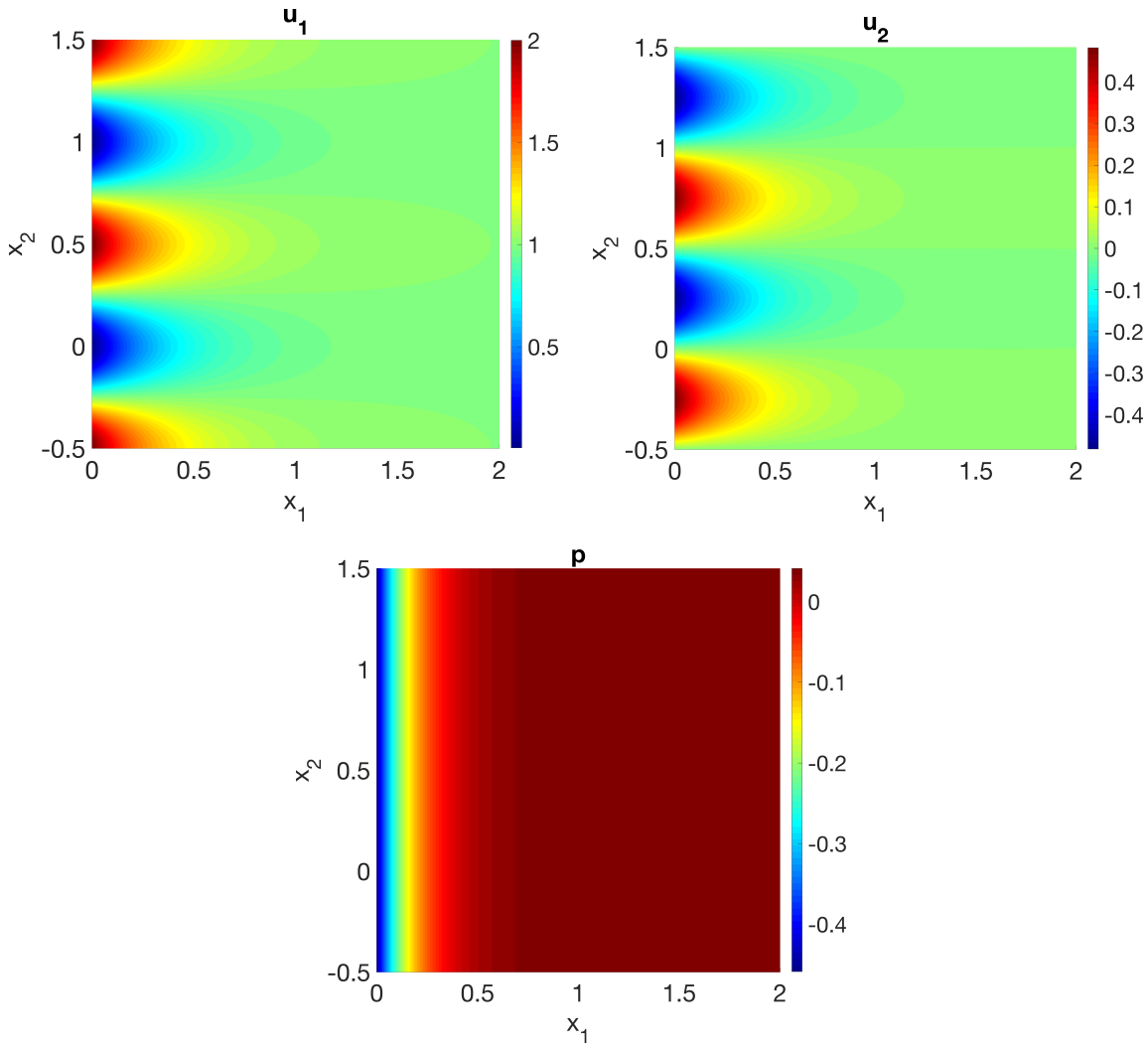

Figure 3.1: Oseen HDG schemes: Kovasznay flow problem solution - $\boldsymbol{u}_{h1}$ (top left), $\boldsymbol{u}_{h2}$ (top right), and p_h (bottom).

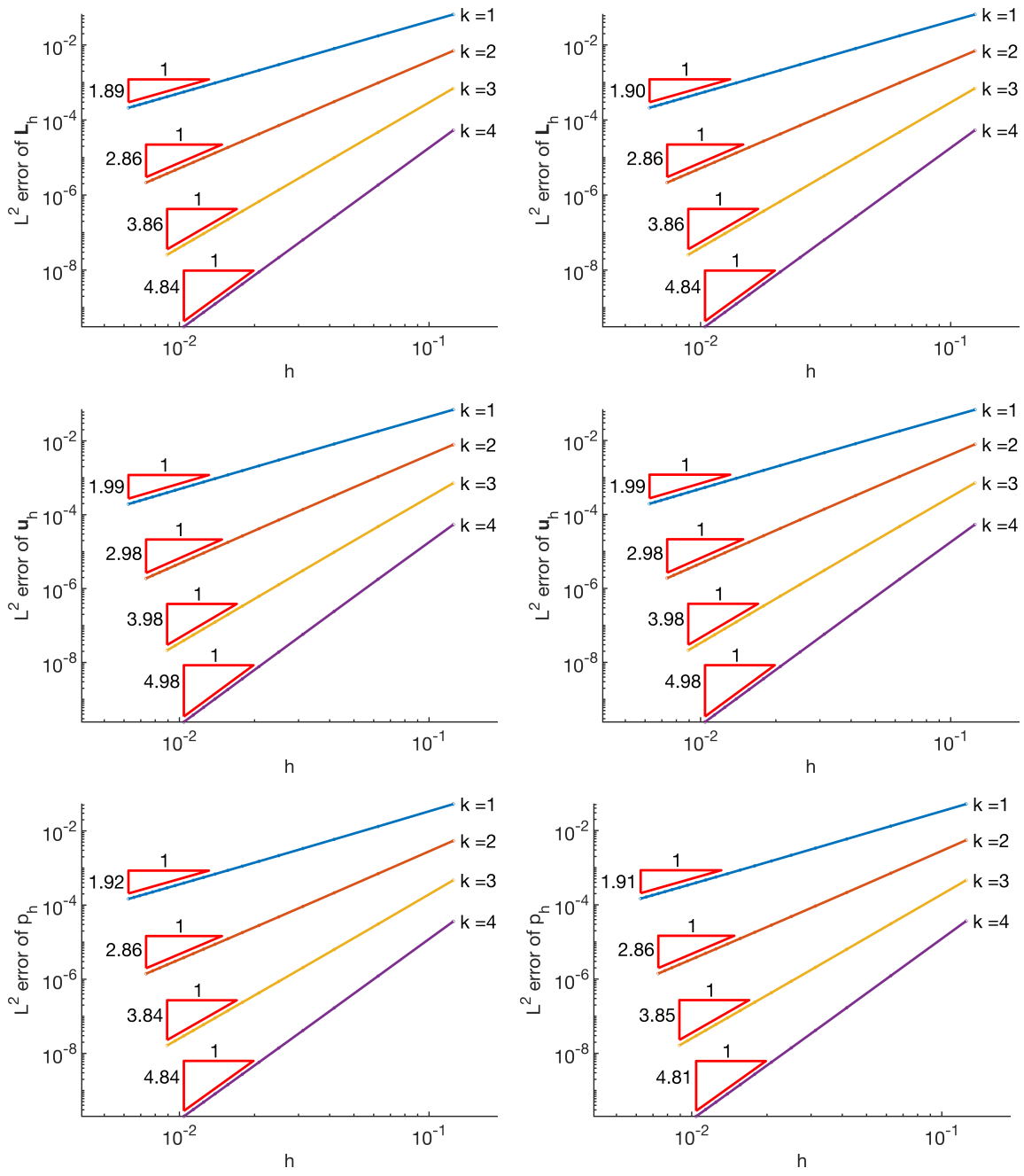

Figure 3.2: Oseen HDG schemes: Kovasznay flow problem L^2 convergence of volume unknowns using $\widehat{\boldsymbol{u}}_h$ flux (3.21) (left), using $(\widehat{\boldsymbol{u}}_h^t, \widehat{f}_h)$ flux (3.23) (right).

It remains to define stopping criteria for the nonlinear iteration. One possible stopping criterion involves using a nonlinear residual $\boldsymbol{r}^m \in \boldsymbol{V}_h$ to the discretized momentum equation that we define by

$$(\boldsymbol{r}^m, \boldsymbol{v})_{\mathcal{T}_h} = a\left(\boldsymbol{u}_h^m; \mathbf{L}_h^m, \boldsymbol{u}_h^m, p_h^m, \widehat{\boldsymbol{U}}_h^m; \mathbf{0}, \boldsymbol{v}, 0, \mathbf{0}\right) - \ell\left(\mathbf{0}, \boldsymbol{v}, 0, \mathbf{0}\right) \tag{3.64}$$

for all $\boldsymbol{v}$ in $\boldsymbol{V}_h$ and stopping when

$$\|\boldsymbol{r}^m\|_{L^2(\Omega)} < \delta \tag{3.65}$$

for some $\delta > 0$. The Picard iteration is outlined in Algorithm 2.

Algorithm 2 Picard Iteration for Steady Incompressible Navier-Stokes HDG Schemes.

set initial guess $\boldsymbol{u}_h^0$, choose stopping tolerance δ, and set $m = 1$
while true **do**
  solve for $\left(\mathbf{L}_h^m, \boldsymbol{u}_h^m, p_h^m, \widehat{\boldsymbol{U}}_h^m\right)$ using (3.63)
  if (3.65) is true **then**
    break
  end if
  $m \leftarrow m + 1$
end while

Using the Picard iteration, we can solve the Kovasznay problem by applying the boundary conditions $\boldsymbol{u}_D$ as the exact solution $\boldsymbol{u}$ and applying zero forcing. In Figure 3.3, the $L^2(\Omega)$ error of the volume unknowns $(\mathbf{L}_h, \boldsymbol{u}_h, p_h)$ are plotted along with their convergence rates. The left column of plots shows the L^2 error obtained using the $\widehat{\boldsymbol{u}}_h$ flux (3.21) on all skeleton faces (i.e., Formulation 3.1), while the right column shows the L^2 error obtained using the $(\widehat{\boldsymbol{u}}_h^t, \widehat{f}_h)$ flux (3.23) on the interior skeleton faces and the $\widehat{\boldsymbol{u}}_h$ flux (3.21) on the boundary skeleton faces. In both cases τ_t and τ_n are chosen as the upwind parameters τ_t^O and τ_n^O, respectively. In both cases, the tolerance for the stopping criterion (3.65) was taken as $\delta = 10^{-10}$ in order to avoid that the error plots level out. For the $\widehat{\boldsymbol{u}}_h$ flux, 10-11 iterations were needed in order to

reach the stopping criterion regardless of polynomial order or mesh refinement level. For the $(\widehat{\boldsymbol{u}}_h^t, \widehat{f}_h)$ flux, it took 11-12 iterations regardless of polynomial order or mesh refinement level. In both cases, an initial guess of zero was used. Again, the errors using the two versions of the Godunov flux are virtually identical. In both cases, the observed convergence rates are $k+1$ for $\boldsymbol{u}_h$, and close to $k+1$ for $\mathbf{L}_h$ and p_h, which are the same convergence rates as for the linear Oseen scheme.

3.5 Discussion

Through the upwind HDG methodology [9], we have derived two families of HDG schemes for the Oseen equations. One scheme is based on the $\widehat{\boldsymbol{u}}_h$ flux, and can be related to the scheme analyzed by Cesmelioglu et. al [11]. Rearranging the second term of (3.21), we can write

$$\begin{aligned}-\mathbf{L}_h^*\boldsymbol{n} + p_h^*\boldsymbol{n} + (\boldsymbol{w}\cdot\boldsymbol{n})\boldsymbol{u}_h^* = &-\mathbf{L}_h\boldsymbol{n} + p_h\boldsymbol{n} + (\boldsymbol{w}\cdot\boldsymbol{n})\widehat{\boldsymbol{u}}_h \\ &+ \left(\left[\tau_t + \frac{1}{2}\boldsymbol{w}\cdot\boldsymbol{n}\right]\mathbf{T} + \left[\tau_n + \frac{1}{2}\boldsymbol{w}\cdot\boldsymbol{n}\right]\mathbf{N}\right)(\boldsymbol{u}_h - \widehat{\boldsymbol{u}}_h)\,.\end{aligned}$$

If we denote the stabilization tensor used in [11] by $\mathbf{S}^C := \frac{1}{\mathrm{Re}}\tau_n^C\mathbf{N} + \frac{1}{\mathrm{Re}}\tau_t^C\mathbf{T}$, then we can recover the scheme from [11] by choosing $\tau_n = \frac{1}{\mathrm{Re}}\tau_n^C - \frac{1}{2}\boldsymbol{w}\cdot\boldsymbol{n}$ and $\tau_t = \frac{1}{\mathrm{Re}}\tau_t^C - \frac{1}{2}\boldsymbol{w}\cdot\boldsymbol{n}$ in Formulation 3.1.

Some comments are in order regarding the difference between these similar fluxes. First, we have already shown in the well-posedness for Formulation 3.1 that we must only choose $\tau_t > 0$ and $\tau_n > 0$ for well-posedness, which is always true in particular for the upwind flux parameters τ_t^O and τ_n^O. So, if we would like to define a scheme with ∂K-wise constant, skeleton face-wise constant, or globally constant stability parameters τ_t and τ_n, the only restriction on those stability parameters is that they are positive. On the other hand, using the scheme analyzed in [11], if we would like to define a scheme with ∂K-wise constant, skeleton face-wise constant, or globally

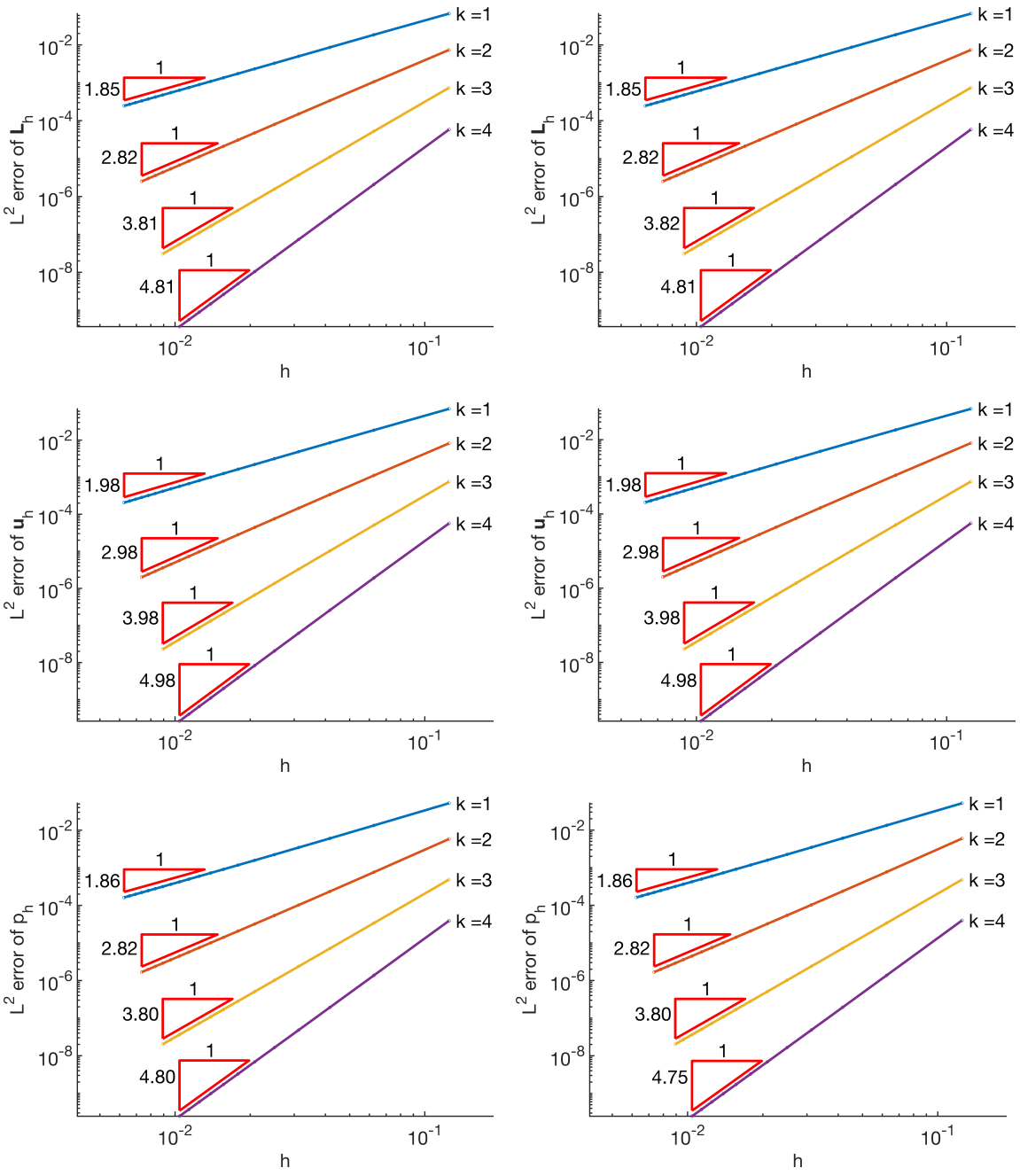

Figure 3.3: Oseen HDG schemes: Kovasznay flow problem nonlinear solution with Picard iteration - L^2 convergence of volume unknowns using $\widehat{\boldsymbol{u}}_h$ flux (3.21) (left), using $(\widehat{\boldsymbol{u}}_h^t, \widehat{f}_h)$ flux (3.23) (right).

constant stability parameters τ_t^C and τ_n^C, we must ensure that $\min\left(\frac{1}{\mathrm{Re}}\tau_t^C - \frac{1}{2}\boldsymbol{w}\cdot\boldsymbol{n}\right) > 0$ ∂K-wise, skeleton face-wise, or globally.

Second, it may appear that the form of the flux in [11] with $(\boldsymbol{w}\cdot\boldsymbol{n})\widehat{\boldsymbol{u}}_h$ is a simpler form of the flux than the one in (3.21) which has the terms $\frac{1}{2}(\boldsymbol{w}\cdot\boldsymbol{n})\widehat{\boldsymbol{u}}_h + \frac{1}{2}(\boldsymbol{w}\cdot\boldsymbol{n})\boldsymbol{u}_h$. But as we put the advection term in Formulation 3.1 into a form which ensures the skew symmetry of the volume terms upon discretization,

$$-\left(\boldsymbol{u}_h\otimes\boldsymbol{w},\nabla\boldsymbol{v}\right)_{\mathcal{T}_h} = -\frac{1}{2}\left(\boldsymbol{u}_h\otimes\boldsymbol{w},\nabla\boldsymbol{v}\right)_{\mathcal{T}_h} + \frac{1}{2}\left(\nabla\boldsymbol{u}_h,\boldsymbol{v}\otimes\boldsymbol{w}\right)_{\mathcal{T}_h} - \frac{1}{2}\left\langle(\boldsymbol{w}\cdot\boldsymbol{n})\boldsymbol{u}_h,\boldsymbol{v}\right\rangle_{\partial\mathcal{T}_h},$$

the only advection boundary term remaining in Formulation 3.1 is $\frac{1}{2}\left\langle(\boldsymbol{w}\cdot\boldsymbol{n})\widehat{\boldsymbol{u}}_h,\boldsymbol{v}\right\rangle_{\partial\mathcal{T}_h}$, whereas putting the formulation analyzed in [11] into a similar form gives advection boundary terms as $\left\langle(\boldsymbol{w}\cdot\boldsymbol{n})\widehat{\boldsymbol{u}}_h - \frac{1}{2}(\boldsymbol{w}\cdot\boldsymbol{n})\boldsymbol{u}_h,\boldsymbol{v}\right\rangle_{\partial\mathcal{T}_h}$. Because of this and the discussion in the previous paragraph, we favor defining the stabilization parameters as in Formulation 3.1 for the Oseen HDG scheme based on the $\widehat{\boldsymbol{u}}_h$ flux.

Third, the formulation in [11] with constant stability parameters (satisfying the conditions already discussed) was proven to converge at order $k+1$ for equal order total degree (simplicial) elements for sufficiently smooth solutions. Here, we have numerically demonstrated the convergence of Formulation 3.1 for 2D tensor product elements, but have made no theoretical claims. This is reserved for future work.

The second family of schemes that we have derived is based on the $(\widehat{\boldsymbol{u}}_h^t,\widehat{f}_h)$ flux. These schemes are new schemes that are published only in this work (at the time of writing). As opposed to the HDG schemes based on the $\widehat{\boldsymbol{u}}_h$ flux, these HDG schemes do not require special modifications to achieve well-posedness of the local solver. Thus we avoid the iterative nature of the augmented Lagrangian method, and we avoid the introduction additional unknowns of a different nature and the saddle point system that arises from the average edge-pressure method.

It should be reiterated that we have assumed $\nabla \cdot \boldsymbol{w} = 0$ throughout this chapter by setting $((\nabla \cdot \boldsymbol{w})\boldsymbol{u}_h, \boldsymbol{v}) = 0$ upon integration by parts of half the advection term in (3.6b) to write (3.30b) and (3.48b). When using these schemes iteratively to solve the incompressible Navier-Stokes equations using the Picard iteration outlined in the previous section, we take $\boldsymbol{w}$ to be $\boldsymbol{u}_h^{m-1}$ when solving the mth iterate. It can be seen from (3.30c) and (3.48c) that $\boldsymbol{u}_h$ is only weakly divergence free, and not exactly divergence free. It is an option to perform a postprocessing on the velocity in order to obtain a postprocessed velocity which is exactly divergence free and lies in $H(div, \Omega)$ [24], and then to use the postprocessed velocity as $\boldsymbol{w}$ in the next iteration. Postprocessing is not explored in this work, however, and we simply use the previous iterate of $\boldsymbol{u}_h$. However, we still use Formulations 3.1 and 3.2 as they are written. With this in mind, it can be interpreted that we have added $-\frac{1}{2}(\nabla \cdot \boldsymbol{w})\boldsymbol{u}$ to the left side of the momentum equation (3.3a) and therefore have *added the source term* $-\frac{1}{2}\left((\nabla \cdot \boldsymbol{w})\boldsymbol{u}_h, \boldsymbol{v}\right)_{\mathcal{T}_h}$ to the left side of (3.6b). This term will then cancel the term of opposite sign arising from integration by parts that we have up to this point assumed to be zero on the basis of $\boldsymbol{w}$ being divergence free.

A similar idea applies to the conservation conditions (3.30d) and (3.48d), where we have assumed $\boldsymbol{w} \in H(div, \Omega)$ in order to exclude the $-\frac{1}{2}\left\langle (\boldsymbol{w} \cdot \boldsymbol{n})\widehat{\boldsymbol{u}}_h, \widehat{\boldsymbol{v}} \right\rangle_{\partial \mathcal{T}_h \setminus \partial\Omega}$ and $-\frac{1}{2}\left\langle (\boldsymbol{w} \cdot \boldsymbol{n})\widehat{\boldsymbol{u}}_h^{t,i}, \widehat{\boldsymbol{v}}^t \right\rangle_{\partial \mathcal{T}_h \setminus \partial\Omega}$ terms in Formulation 3.1 and Formulation 3.2, respectively. When $\boldsymbol{w}$ is taken as the previous iterate of $\boldsymbol{u}_h$, these terms would no longer be exactly zero, so their omission is interpreted as an approximate enforcement of conservation, or as *adding the stabilization terms* $\frac{1}{2}\left\langle (\boldsymbol{w} \cdot \boldsymbol{n})\widehat{\boldsymbol{u}}_h, \widehat{\boldsymbol{v}} \right\rangle_{\partial \mathcal{T}_h \setminus \partial\Omega}$ and $\frac{1}{2}\left\langle (\boldsymbol{w} \cdot \boldsymbol{n})\widehat{\boldsymbol{u}}_h^{t,i}, \widehat{\boldsymbol{v}}^t \right\rangle_{\partial \mathcal{T}_h \setminus \partial\Omega}$ to the conservation conditions of Formulation 3.1 and Formulation 3.2, respectively. It is interesting to note that using the $\widehat{\boldsymbol{f}}_h$ flux (3.22) avoids this issue altogether.

Chapter 4

Induction Equation

In this chapter, we explore HDG schemes for the induction equation, which is a subset of the MHD equations. Through the upwind framework [9], we derive HDG schemes for the induction equation in the limit of zero velocity. We do so for the saddle point system that arises from the introduction of a scalar Lagrange multiplier, which is used to facilitate the enforcement of the solenoidal constraint on the magnetic field. The schemes and their corresponding numerical fluxes derived here prove useful in defining HDG schemes for the resistive MHD equations, which is shown in the next chapter. This chapter is a brief exposition when compared to the previous chapters on the Stokes and Oseen equations, as we do not discover any new schemes here, but rather rediscover the schemes of [16] for the velocity-vorticity-pressure form of the Stokes equations, which take the same form as the induction equation in the limit of zero velocity.

4.1 Construction of Upwind HDG Schemes

For notation used in this chapter and throughout this work, see Appendix A. Recall the Maxwell's equations,

$$\nabla \cdot \boldsymbol{E} = \frac{\rho}{\epsilon_0}, \qquad \text{(Gauss)} \tag{4.1a}$$

$$\nabla \times \boldsymbol{E} = -\frac{\partial \boldsymbol{b}}{\partial t}, \qquad \text{(Faraday)} \tag{4.1b}$$

$$\nabla \times \boldsymbol{b} = \mu_0 \left(\boldsymbol{J} + \epsilon_0 \frac{\partial \boldsymbol{E}}{\partial t} \right), \quad \text{(Ampere-Maxwell)} \tag{4.1c}$$

$$\nabla \cdot \boldsymbol{b} = 0. \qquad \text{(no magn. monopole)} \tag{4.1d}$$

Here, $\boldsymbol{E}$ is an electric field, $\boldsymbol{b}$ is a magnetic induction, from here on termed the magnetic field, $\boldsymbol{J}$ is a current, ρ is a charge density, ϵ_0 is the permittivity of free space, and μ_0 is the permeability of free space. Maxwell's contribution to the Ampere-Maxwell law is the the term $\mu_0 \epsilon_0 \frac{\partial \boldsymbol{E}}{\partial t} = \frac{1}{c^2} \frac{\partial \boldsymbol{E}}{\partial t}$, known as the "displacement current", where $c := \sqrt{\epsilon_0 \mu_0}$ is the speed of light in a vacuum. One of the assumptions under which the MHD equations are valid is an ordering assumption in which the displacement current is negligible; that is, we are interested in the low-frequency, long-time limit of Maxwell's equations. With this assumption the Ampere-Maxwell law becomes Ampere's Law again,

$$\nabla \times \boldsymbol{b} = \mu_0 \boldsymbol{J}. \tag{4.2}$$

Toward application of an induction equation HDG scheme to resistive MHD, we close the system with a generalized Ohm's law for a moving conducting fluid,

$$\boldsymbol{E} + \boldsymbol{u} \times \boldsymbol{b} = \eta \boldsymbol{J}, \tag{4.3}$$

where η is the resistivity of the fluid, and $\boldsymbol{u}$ is the fluid velocity. With these assumptions, we can eliminate $\boldsymbol{E}$ and $\boldsymbol{J}$ to derive an evolution equation for $\boldsymbol{b}$. Indeed, from

Faraday's Law (4.1b), Ampere's Law (4.2), and the generalized Ohm's Law (4.3), we arrive at the "induction equation",

$$\frac{\partial \boldsymbol{b}}{\partial t} + \nabla \times \left(\frac{\eta}{\mu_0} \nabla \times \boldsymbol{b} \right) - \nabla \times (\boldsymbol{u} \times \boldsymbol{b}) = 0. \tag{4.4}$$

Then (4.4) and (4.1d) determine $\boldsymbol{b}$, $\boldsymbol{J}$ is recovered from (4.2), and $\boldsymbol{E}$ is recovered from (4.3).

Considering the induction equation (4.4) with the solenoidal constraint on the magnetic field (4.1d), it appears that the system is over-constrained, as we have more equations than unknowns. However, if we have an initial condition on $\boldsymbol{b}$ that is divergence free, we can see that $\boldsymbol{b}$ will remain divergence free for all time. Indeed, taking the divergence of (4.1b), we have $\frac{\partial \nabla \cdot \boldsymbol{b}}{\partial t} = 0$. Thus, it is clear that (4.1d) is an involution that is satisfied for all times by the mathematical structure of this system, and that the system is not overdetermined. However, this approach is in general not applicable to numerical methods for solving the induction equation, and is not applicable to the steady state version ($\frac{\partial}{\partial t} = 0$) of (4.4) and (4.1d). Approaches to enforcing the solenoidal constraint (4.1d) for finite element methods include exact penalty [33, 28] and weighted exact penalty methods [34], methods involving saddle-point systems with the introduction of a magnetic Lagrange multiplier, [61, 25, 37, 5, 64] and methods derived from a vector potential form of the PDE [62].

We choose the Lagrange multiplier method here, which amounts to modifying (4.4) to read

$$\frac{\partial \boldsymbol{b}}{\partial t} + \nabla \times \left(\frac{\eta}{\mu_0} \nabla \times \boldsymbol{b} \right) - \nabla \times (\boldsymbol{u} \times \boldsymbol{b}) + \nabla r = 0, \tag{4.5}$$

and equipping r with a homogeneous Dirichlet boundary condition. Now, considering (4.1d) as not just an initial condition, taking the divergence of (4.5) gives $\Delta r = 0$ and with the homogeneous Dirichlet boundary condition, we have the $r = 0$. Thus,

r can be considered a "dummy variable" introduced to facilitate enforcement of the solenoidal constraint in the otherwise overdetermined system.

When considering variational formulations for the induction equation, it is possible to seek $\boldsymbol{b}$ in a divergence-free space, in which case it is not necessary to include the Lagrange multiplier r. When the Lagrange multiplier is included in the formulation, we seek $\boldsymbol{b}$ in a larger space and then enforce that $\boldsymbol{b}$ is orthogonal to the orthogonal complement of divergence-free functions in L^2. When discretizing, the latter allows one to use familiar finite element spaces. See [61] for details.

We will define HDG schemes for a nondimensionalized version of the induction equation (4.5) and the solenoidal constraint (4.1d). For simplicity here and applicability later, we assume the limit of $\boldsymbol{u} = \boldsymbol{0}$. We assume that we can infer from the problem we are solving a characteristic magnetic field strength, b_0, and a characteristic length, l_0. From this, we can define a characteristic time scale by $t_0 = \frac{\mu_0 l_0^2}{\eta}$ to write the induction equation in nondimensional form, where all quantities are to be interpreted as dimensionless,

$$\frac{\partial \boldsymbol{b}}{\partial t} + \nabla \times (\nabla \times \boldsymbol{b}) + \nabla r = \boldsymbol{g}, \tag{4.6}$$

where we have incorporated a forcing term $\boldsymbol{g}$ that we assume to be divergence free. We have also implicitly chosen a characteristic value for r as $r_0 = \frac{\mu_0 l_0}{\eta b_0}$. Defining a characteristic current density by $J_0 = \frac{b_0}{\mu_0 l_0}$, we can define the "auxiliary" dimensionless variable $\boldsymbol{J}$ (in the spirit of Ampere's law) and write the first order induction equation system as

$$\boldsymbol{J} - \nabla \times \boldsymbol{b} = 0, \tag{4.7a}$$

$$\frac{\partial \boldsymbol{b}}{\partial t} + \nabla \times \boldsymbol{J} + \nabla r = \boldsymbol{g}, \tag{4.7b}$$

$$\nabla \cdot \boldsymbol{b} = 0. \tag{4.7c}$$

The equations can be equipped with two different sets of boundary conditions [29], but for this chapter we consider the following boundary conditions on $\partial\Omega$:

$$\boldsymbol{n} \times \boldsymbol{b} = \boldsymbol{n} \times \boldsymbol{b}_D, \tag{4.8a}$$

$$r = r_D = 0. \tag{4.8b}$$

To define a general semidiscrete HDG scheme for the system (4.7), we multiply (4.7) by test functions, integrate over the computational domain, integrate by parts, and replace the boundary terms with yet-to-be-defined numerical flux terms, which we then enforce to be weakly continuous across element interfaces. HDG schemes derived in this manner for (4.7) will take a general form consisting of the local equations

$$(\boldsymbol{J}_h, \boldsymbol{H})_{\mathcal{T}_h} - (\boldsymbol{b}_h, \nabla \times \boldsymbol{H})_{\mathcal{T}_h} - \langle \boldsymbol{n} \times \boldsymbol{b}_h^*, \boldsymbol{H} \rangle_{\partial\mathcal{T}_h} = 0, \tag{4.9a}$$

$$\left(\frac{\partial \boldsymbol{b}_h}{\partial t}, \boldsymbol{c}\right)_{\mathcal{T}_h} + (\boldsymbol{J}_h, \nabla \times \boldsymbol{c})_{\mathcal{T}_h} - (r_h, \nabla \cdot \boldsymbol{c})_{\mathcal{T}_h} + \langle \boldsymbol{n} \times \boldsymbol{J}_h^* + r_h^* \boldsymbol{n}, \boldsymbol{c} \rangle_{\partial\mathcal{T}_h} = (\boldsymbol{g}, \boldsymbol{c})_{\mathcal{T}_h}, \tag{4.9b}$$

$$-(\boldsymbol{b}_h, \nabla s)_{\mathcal{T}_h} + \langle \boldsymbol{b}_h^* \cdot \boldsymbol{n}, s \rangle_{\partial\mathcal{T}_h} = 0, \tag{4.9c}$$

the conservation equations

$$-\left\langle -\boldsymbol{n} \times \boldsymbol{b}_h^{t\,*}, \widehat{\boldsymbol{H}}^t \right\rangle_{\partial\mathcal{T}_h \setminus \partial\Omega} = 0, \tag{4.9d}$$

$$-\langle \boldsymbol{n} \times \boldsymbol{J}_h^* + r_h^* \boldsymbol{n}, \widehat{\boldsymbol{c}} \rangle_{\partial\mathcal{T}_h \setminus \partial\Omega} = 0, \tag{4.9e}$$

$$-\langle \boldsymbol{b}_h^* \cdot \boldsymbol{n}, \widehat{s} \rangle_{\partial\mathcal{T}_h \setminus \partial\Omega} = 0, \tag{4.9f}$$

and the boundary conditions

$$\left\langle \mathbf{T}\boldsymbol{b}_h^*, \widehat{\boldsymbol{z}}^t \right\rangle_{\partial\Omega} = \left\langle \boldsymbol{b}_D^t, \widehat{\boldsymbol{z}}^t \right\rangle_{\partial\Omega}, \tag{4.9g}$$

$$\langle r_h^*, \widehat{z} \rangle_{\partial\Omega} = \langle r_D, \widehat{z} \rangle_{\partial\Omega}. \tag{4.9h}$$

In the above, $(\boldsymbol{J}_h, \boldsymbol{b}_h, r_h)$ will be sought in some discontinuous polynomial spaces on the volume of the domain, and $(\boldsymbol{H}, \boldsymbol{c}, s)$ are test functions in those same spaces. The

starred quantities $\boldsymbol{J}_h^*$, $\boldsymbol{u}_h^*$ and r_h^* are yet-to-be-defined not-necessarily-single-valued functions of the volume unknowns $(\boldsymbol{J}_h, \boldsymbol{b}_h, r_h)$ and trace variables $\left(\widehat{\boldsymbol{J}}_h, \widehat{\boldsymbol{b}}_h, \widehat{r}_h\right)$. The trace variables reside in discontinuous polynomial spaces defined on the mesh skeleton, as do the interior test functions $\left(\widehat{\boldsymbol{H}}, \widehat{\boldsymbol{c}}, \widehat{s}\right)$ and boundary test functions $\left(\widehat{\boldsymbol{z}}^t, \widehat{z}\right)$. In what follows, we derive different choices for the numerical flux $\boldsymbol{F}_{n,h}^*$ and thus different choices for the starred quantities. The fluxes we derive will have a minimal number of trace unknowns (d scalar unknowns) so that not all of the trace unknowns $\left(\widehat{\boldsymbol{J}}_h, \widehat{\boldsymbol{b}}_h, \widehat{r}_h\right)$ (and their corresponding test functions) will exist as unknowns (and test functions). Related to this is the fact that not all of (4.9d) – (4.9f) must be explicitly enforced. The choice of the numerical flux will dictate which among (4.9d) – (4.9f) must be explicitly enforced. Additionally, the boundary test functions $\left(\widehat{\boldsymbol{z}}^t, \widehat{z}\right)$ will have a natural association with the interior skeleton test functions among $\left(\widehat{\boldsymbol{H}}, \widehat{\boldsymbol{c}}, \widehat{s}\right)$ that do exist in the scheme. These points will be made clearer after we derive the HDG numerical fluxes.

We will now derive the upwind HDG flux, but first we point out that the induction equation first order system (4.7) is identical to a velocity-vorticity-pressure first order Stokes system. Cockburn and Gopalakrishnan [16] propose four different HDG schemes for the velocity-vorticity-pressure form of the Stokes equations. Here, we will rediscover these schemes through the upwind framework [9].

The first order system (4.7) fits into the general framework (1.1), and is symmetric hyperbolic. Indeed, choosing the ordering of unknowns in a column vector as $\boldsymbol{U} := (\boldsymbol{J}; \boldsymbol{b}; r)$, we have

$$\mathbf{A} = \begin{bmatrix} \mathbf{0} & \mathbf{B}^\top & \mathbf{0} \\ \mathbf{B} & \mathbf{0} & \boldsymbol{n} \\ \mathbf{0} & \boldsymbol{n}^\top & 0 \end{bmatrix}, \tag{4.10}$$

where

$$\mathbf{B} := \begin{bmatrix} n_2 \\ -n_1 \end{bmatrix} \text{ if } d = 2, \quad \mathbf{B} := \begin{bmatrix} 0 & -n_3 & n_2 \\ n_3 & 0 & -n_1 \\ -n_2 & n_1 & 0 \end{bmatrix} \text{ if } d = 3.$$

In 3D, the tensor $\mathbf{B}$ applies the cross product with the normal vector, i.e., $\mathbf{B}\boldsymbol{b} = \boldsymbol{n} \times \boldsymbol{b}$ and $\mathbf{B}^\top = -\mathbf{B}$ applies the same with the opposite sign. In 2D, $\mathbf{B}$ acts on a scalar as $\mathbf{B}a = \boldsymbol{n} \times a$, and its transpose acts on a vector as $\mathbf{B}^\top \boldsymbol{b} = -\boldsymbol{n} \times \boldsymbol{b}$. We perform the eigendecomposition $\mathbf{A} = \mathbf{R}\mathbf{D}\mathbf{R}^{-1}$, where $\mathbf{D}$ is a diagonal matrix comprising the eigenvalues of $\mathbf{A}$, and $\mathbf{R}$ is a matrix whose columns are the eigenvectors corresponding those eigenvalues. Defining $|\mathbf{D}|$ by taking the absolute value of each eigenvalue in $\mathbf{D}$, we can define $|\mathbf{A}| := \mathbf{R}\,|\mathbf{D}|\,\mathbf{R}^{-1}$. It can be shown that for the induction equation system we have

$$|\mathbf{A}| = \begin{bmatrix} \frac{1}{\beta_t^M}\mathbf{T} & \mathbf{0} & \mathbf{0} \\ \mathbf{0} & \beta_t^M \mathbf{T} + \beta_n^M \mathbf{N} & \mathbf{0} \\ \mathbf{0} & \mathbf{0} & \frac{1}{\beta_n^M} \end{bmatrix}, \tag{4.11}$$

where

$$\beta_t^M := 1 \quad \text{and} \quad \beta_n^M := 1. \tag{4.12}$$

Later, we will consider more general parameters β_t and β_n than β_t^M and β_n^M which give the upwind flux. This allows us to generalize the upwind scheme and to make connections to existing HDG methods. We define the normal upwind flux $\boldsymbol{F}_n^*$ as a column vector $\boldsymbol{F}_n^* := (-\boldsymbol{n} \times \boldsymbol{b}^*; \boldsymbol{n} \times \boldsymbol{J}^* + r^*\boldsymbol{n}; \boldsymbol{b}^* \cdot \boldsymbol{n})$. We can then write the exact upwind flux in its one-sided form as

$$\boldsymbol{F}_n^* = \mathbf{A}\boldsymbol{U} + |\mathbf{A}|\,(\boldsymbol{U} - \boldsymbol{U}^*) = \begin{pmatrix} -\boldsymbol{n} \times \boldsymbol{b} + \frac{1}{\beta_t^M}\mathbf{T}\,(\boldsymbol{J} - \boldsymbol{J}^*) \\ \boldsymbol{n} \times \boldsymbol{J} + r\boldsymbol{n} + \left(\beta_t^M \mathbf{T} + \beta_n^M \mathbf{N}\right)(\boldsymbol{b} - \boldsymbol{b}^*) \\ \boldsymbol{b} \cdot \boldsymbol{n} + \frac{1}{\beta_n^M}\,(r - r^*) \end{pmatrix}. \tag{4.13}$$

At this point, we can eliminate "starred quantities" on the right side of (4.13) with the aim of defining an HDG flux with minimal trace unknowns. It turns out that

we can reduce the number of trace unknowns in (at least) four different ways that lead to viable HDG schemes with minimal trace unknowns. The key to reducing the number of trace unknowns is the following relations between the upwind states.

Lemma 4.1. *The following relationships between the upwind states hold:*

$$\beta_t^M \boldsymbol{n} \times (\boldsymbol{b} - \boldsymbol{b}^*) = \mathbf{T}\left(\boldsymbol{J} - \boldsymbol{J}^*\right), \tag{4.14a}$$

$$-\beta_n^M \mathbf{N}\left(\boldsymbol{b} - \boldsymbol{b}^*\right) = \left(r - r^*\right). \tag{4.14b}$$

Proof. The claims follow directly from equating the tangential components of the left and right sides of the second term of (4.13), and doing the same for the normal components. □

Note that the same expressions come as a result of equating the left and right sides of the first and third terms of (4.13). Using (4.14a) to eliminate either $\mathbf{T}\boldsymbol{J}^*$ or $\mathbf{T}\boldsymbol{b}^*$, and using (4.14b) to eliminate either $\mathbf{N}\boldsymbol{b}^*$ or r^*, we arrive at the following four forms of the upwind flux.

The $\boldsymbol{b}^*$ flux: The quantities r^* and $\mathbf{T}\boldsymbol{J}^*$ can be eliminated from (4.13) so that (4.13) can be written in terms of $\boldsymbol{b}^*$ only, as

$$\boldsymbol{F}_n^* = \begin{pmatrix} -\boldsymbol{n} \times \boldsymbol{b}^*, \\ \boldsymbol{n} \times \boldsymbol{J} + r\boldsymbol{n} + \left(\beta_t^M \mathbf{T} + \beta_n^M \mathbf{N}\right)\left(\boldsymbol{b} - \boldsymbol{b}^*\right), \\ \boldsymbol{b}^* \cdot \boldsymbol{n} \end{pmatrix}. \tag{4.15}$$

The $(\mathbf{T}\boldsymbol{b}^*, r^*)$ flux: The quantities $\mathbf{N}\boldsymbol{b}^*$ and $\mathbf{T}\boldsymbol{J}^*$ can be eliminated from (4.13) so that (4.13) can be written in terms of $\mathbf{T}\boldsymbol{b}^*$ and r^* only, as

$$\boldsymbol{F}_n^* = \begin{pmatrix} -\boldsymbol{n} \times \boldsymbol{b}^*, \\ \boldsymbol{n} \times \boldsymbol{J} + r^*\boldsymbol{n} + \beta_t^M \mathbf{T}\left(\boldsymbol{b} - \boldsymbol{b}^*\right), \\ \boldsymbol{b} \cdot \boldsymbol{n} + \frac{1}{\beta_n^M}\left(r - r^*\right) \end{pmatrix}. \tag{4.16}$$

The $(\mathbf{T}\boldsymbol{J}^*, \mathbf{N}\boldsymbol{b}^*)$ flux: The quantities $\mathbf{T}\boldsymbol{b}^*$ and r^* can be eliminated from (4.13) so that (4.13) can be written in terms of $\mathbf{T}\boldsymbol{J}^*$ and $\mathbf{N}\boldsymbol{b}^*$ only, as

$$\boldsymbol{F}_n^* = \begin{pmatrix} -\boldsymbol{n}\times\boldsymbol{b} + \frac{1}{\beta_t^M}\mathbf{T}\left(\boldsymbol{J}-\boldsymbol{J}^*\right), \\ \boldsymbol{n}\times\boldsymbol{J}^* + r\boldsymbol{n} + \beta_n^M\mathbf{N}\left(\boldsymbol{b}-\boldsymbol{b}^*\right), \\ \boldsymbol{b}^*\cdot\boldsymbol{n} \end{pmatrix}. \tag{4.17}$$

The $(\mathbf{T}\boldsymbol{J}^*, r^*)$ flux: The quantities $\boldsymbol{b}^*$ can be eliminated from (4.13) so that (4.13) can be written in terms of $\boldsymbol{J}^*$ and r^* only, as

$$\boldsymbol{F}_n^* = \begin{pmatrix} -\boldsymbol{n}\times\boldsymbol{b} + \frac{1}{\beta_t^M}\mathbf{T}\left(\boldsymbol{J}-\boldsymbol{J}^*\right), \\ \boldsymbol{n}\times\boldsymbol{J}^* + r^*\boldsymbol{n}, \\ \boldsymbol{b}\cdot\boldsymbol{n} + \frac{1}{\beta_n^M}\left(r-r^*\right) \end{pmatrix}. \tag{4.18}$$

Finally, in order to define numerical fluxes

$$\boldsymbol{F}_{n,h}^* := \begin{pmatrix} -\boldsymbol{n}\times\boldsymbol{b}_h^*, \\ \boldsymbol{n}\times\boldsymbol{J}_h^* + r_h^*\boldsymbol{n}, \\ \boldsymbol{b}_h^*\cdot\boldsymbol{n} \end{pmatrix} \tag{4.19}$$

to be used in the HDG scheme (4.9), we append a subscript h to the terms in (4.20) – (4.23) and replace the starred quantities on the right side of (4.20) – (4.23) with hatted unknown quantities residing on the mesh skeleton. Additionally we replace β_t^M and β_n^M with β_t and β_n, which, from the well-posedness analysis, can be freely chosen positive values. This gives the following numerical fluxes.

The $\widehat{\boldsymbol{b}}_h$ flux:

$$\boldsymbol{F}_{n,h}^* = \begin{pmatrix} -\boldsymbol{n}\times\widehat{\boldsymbol{b}}_h, \\ \boldsymbol{n}\times\boldsymbol{J}_h + r_h\boldsymbol{n} + \left(\beta_t\mathbf{T} + \beta_n\mathbf{N}\right)\left(\boldsymbol{b}_h - \widehat{\boldsymbol{b}}_h\right), \\ \widehat{\boldsymbol{b}}_h\cdot\boldsymbol{n} \end{pmatrix}. \tag{4.20}$$

The $(\widehat{\boldsymbol{b}}_h^t, \widehat{r}_h)$ flux:

$$\boldsymbol{F}_{n,h}^* = \begin{pmatrix} -\boldsymbol{n}\times\widehat{\boldsymbol{b}}_h^t, \\ \boldsymbol{n}\times\boldsymbol{J}_h + \widehat{r}_h\boldsymbol{n} + \beta_t\left(\boldsymbol{b}_h^t - \widehat{\boldsymbol{b}}_h^t\right), \\ \boldsymbol{b}_h\cdot\boldsymbol{n} + \frac{1}{\beta_n}\left(r_h - \widehat{r}_h\right) \end{pmatrix}. \tag{4.21}$$

The $(\widehat{\boldsymbol{J}}_h^t, \widehat{b}_h^{\tilde{n}})$ flux, (where $\widehat{b}_h^{\tilde{n}}$ approximates $\boldsymbol{b}^* \cdot \tilde{\boldsymbol{n}}$):

$$\boldsymbol{F}_{n,h}^* = \begin{pmatrix} -\boldsymbol{n} \times \boldsymbol{b}_h^t + \frac{1}{\beta_t}\left(\boldsymbol{J}_h^t - \widehat{\boldsymbol{J}}_h^t\right), \\ \boldsymbol{n} \times \widehat{\boldsymbol{J}}_h^t + r_h \boldsymbol{n} + \beta_n \left(\mathbf{N}\boldsymbol{b}_h - \widehat{b}_h^{\tilde{n}} \tilde{\boldsymbol{n}}\right), \\ \mathrm{sgn}\widehat{b}_h^{\tilde{n}} \end{pmatrix}. \tag{4.22}$$

The $(\widehat{\boldsymbol{J}}_h^t, \widehat{r}_h)$ flux:

$$\boldsymbol{F}_{n,h}^* = \begin{pmatrix} -\boldsymbol{n} \times \boldsymbol{b}_h^t + \frac{1}{\beta_t}\left(\boldsymbol{J}_h^t - \widehat{\boldsymbol{J}}_h^t\right), \\ \boldsymbol{n} \times \widehat{\boldsymbol{J}}_h^t + \widehat{r}_h \boldsymbol{n}, \\ \boldsymbol{b}_h \cdot \boldsymbol{n} + \frac{1}{\beta_n}\left(r_h - \widehat{r}_h\right) \end{pmatrix}. \tag{4.23}$$

In (4.22), we rely on an arbitrarily chosen normal direction $\tilde{\boldsymbol{n}}$ associated with a skeleton face e, and

$$\mathrm{sgn} := \mathrm{sgn}(\boldsymbol{n}) = \begin{cases} 1, & \text{if } \boldsymbol{n} = \tilde{\boldsymbol{n}}, \\ -1, & \text{if } \boldsymbol{n} = -\tilde{\boldsymbol{n}} \end{cases}$$

associated with each face of each element K in order to allow the unknowns on the mesh skeleton to be single-valued.

Using the fluxes (4.20) – (4.23) in the general HDG scheme gives the four (steady state) schemes proposed in [16], so we do not explicitly define them here. But in order to explicitly define the schemes, we must only realize a few points. First, not all of the conservation equations (4.9d) – (4.9f) must be explicitly enforced, as some of them will be automatically satisfied. Which of them will be automatically satisfied depends on choice of the numerical flux, and which trace unknowns exist in those fluxes. For example, choosing the $\widehat{\boldsymbol{b}}_h$ flux (4.20), the conservation equations (4.9d) and (4.9f) are automatically satisfied as a consequence of the single valuedness of $\widehat{\boldsymbol{b}}_h$ on the mesh skeleton, and so we do not have $\widehat{\mathbf{G}}$ or $\widehat{q}$ in the formulation. We are left with the only trace test function as $\widehat{\boldsymbol{c}}$, corresponding to the only trace variable $\widehat{\boldsymbol{b}}_h$. Second, we can associate the test functions $\widehat{\boldsymbol{z}}^t$ and $\widehat{z}$ on the domain boundary with the same tangential and normal trace test functions that exist on the interior of the

domain. For the same example of the $\widehat{\boldsymbol{b}}_h$ flux (4.20), $\widehat{\boldsymbol{z}}^t$ is replaced by $\widehat{\boldsymbol{c}}^t$, and $\widehat{z}$ is replaced by the scalar test function $\widehat{c}_h^n$. Lastly (and optionally), we observe that all, part, or none of the boundary conditions (4.9g) – (4.9h) simplify to L^2 projections of the boundary data to the trace unknowns on the boundary. Returning to the example of the $\widehat{\boldsymbol{b}}_h$ flux (4.20), the boundary condition on the magnetic field (4.9g) simply becomes an L^2 projection of $\boldsymbol{b}_D^t$ to the tangential components of $\widehat{\boldsymbol{b}}_h$. Thus, in the local equations (4.9a) – (4.9c), the tangential components of the trace unknown $\widehat{\boldsymbol{b}}_h$ can be treated as known quantities contributing to the right hand side of the equations. This treatment does not affect the well-posedness of the scheme, but it does affect the matrix structure.

It can be shown that *semidiscrete (or fully implicit)* and *steady state* global HDG scheme (4.9) with any of the fluxes (4.20) – (4.23) is well-posed. Well posedness for the local solver (4.9a) – (4.9c) differs between the four fluxes. The $(\widehat{\boldsymbol{b}}_h^t, \widehat{r}_h)$ flux (4.21) leads to a well-posed local solver without modification. The $\widehat{\boldsymbol{b}}_h$ flux (4.20) and the $(\widehat{\boldsymbol{J}}_h^t, \widehat{\boldsymbol{b}}_h^n)$ flux (4.22) run into the same issues that we encountered for HDG schemes for the Stokes equations using the $\widehat{\boldsymbol{u}}_h$ flux (2.11); that is, the local solver defines the pressure (in this case Lagrange multiplier r_h) only up to a constant, and therefore we cannot eliminate the volume unknowns from the global system without modifications to the scheme. Thankfully, we can modify the scheme using the same direct or iterative methods described in Section 2.2.1 to deal with this issue. Finally, the flux (4.23) leads to a well-posed *semidiscrete (or fully discrete with implicit time discretization)* local solver without modifications. But the *steady state* local solver does not define $\boldsymbol{b}_h$ uniquely in $[\mathcal{P}_k(K)]^d$. The remedy for this situation is more complicated than the remedy for fluxes (4.20) and (4.22), where r_h was defined uniquely up to a constant by the local solver. Thus, for direct-to-steady-state simulations, we deem the flux (4.23) impractical. Details are found in [16] and are not discussed here.

4.2 Discussion

Through the upwind HDG framework, we have derived four different forms of the HDG flux that can be used in the general upwind HDG scheme (4.9). Generalizing the schemes by allowing positive stability parameters β_t and β_n, we have recovered the schemes developed in [16] for the velocity-vorticity-pressure form of the Stokes equations. Indeed, the "type I hybridization" in [16] corresponds to the $(\widehat{\boldsymbol{b}}_h^t, \widehat{r}_h)$ flux (4.21), the "type II hybridization" in [16] corresponds to the $\widehat{\boldsymbol{b}}_h$ flux (4.20), the "type III hybridization" in [16] corresponds to the $(\widehat{\boldsymbol{J}}_h^t, \widehat{b}_h^{\tilde{n}})$ flux (4.22), and the "type IV hybridization" in [16] corresponds to the $(\widehat{\boldsymbol{J}}_h^t, \widehat{r}_h)$ flux (4.23). In doing so, we have revealed that setting the stabilization parameters in [16] to one, we recover the Godunov flux.

We reiterate that through these definitions of the numerical flux, one or more of the conservation conditions (4.9d)–(4.9f) is satisfied automatically by construction, and only the remaining conditions are explicitly enforced. For example, if we choose to use the $\widehat{\boldsymbol{b}}_h$ flux (4.20), then (4.9d) and (4.9f) are automatically satisfied due to the single-valuedness of $\widehat{\boldsymbol{b}}_h$ on the mesh skeleton, and we only need to enforce (4.9e). If, however, we have a material interface with a transmission condition rather than a conservation, we can handle this "naturally". For example, if we have a material interface Γ at which $[\![\boldsymbol{n} \times \boldsymbol{b}]\!] = \boldsymbol{j}$ for some known $\boldsymbol{j}$, we can treat it by modifying (4.9d) by

$$-\left\langle -\boldsymbol{n} \times \boldsymbol{b}_h^{t\,*}, \widehat{\boldsymbol{H}}^t \right\rangle_{\partial \mathcal{T}_h \setminus \partial\Omega} = \left\langle \boldsymbol{j}, \widehat{\boldsymbol{H}}^t \right\rangle_{\Gamma} \tag{4.24}$$

and defining the HDG flux as one that does not automatically enforce $[\![\boldsymbol{n} \times \boldsymbol{b}_h^*]\!] = \boldsymbol{0}$ on skeleton faces that intersect Γ. That is, we can use a flux on those skeleton faces

that does not have $\widehat{\boldsymbol{b}}_h^t$ as a trace unknown. Using (4.22) or (4.23), this reads

$$-\left\langle -\boldsymbol{n}\times\boldsymbol{b}_h^t+\left(\boldsymbol{J}_h^t-\widehat{\boldsymbol{J}}_h^t\right),\widehat{\boldsymbol{H}}^t\right\rangle_{\partial\mathcal{T}_h\setminus\partial\Omega}=\left\langle \boldsymbol{j},\widehat{\boldsymbol{H}}^t\right\rangle_{\Gamma}. \tag{4.25}$$

This treatment assumes that the interface Γ is represented by a union of skeleton faces. Again, it is not necessary to use the same flux on every skeleton face.

Chapter 5

Incompressible Magnetohydrodynamics

In this chapter, we present the first known HDG schemes for magnetohydrodynamics, in particular a linearization of the visco-resistive incompressible magnetohydrodynamics equations. We construct HDG schemes by using numerical fluxes that are a combination of the fluxes for the Oseen equations and the induction equation. For a particular choice of the HDG flux, we prove well-posedness of the scheme and we perform a rigorous projection-based error analysis to obtain L^2 estimates for the volume unknowns. Numerical convergence tests for the linear scheme are performed for smooth and singular solutions. A Picard iteration is used in numerical studies using the linear HDG solver to solve the nonlinear MHD equations for both steady-state and time dependent problems.

5.1 Construction of Upwind HDG Schemes

For notation used in this chapter and throughout this work, see Appendix A. The visco-resistive, incompressible magnetohydrodynamics equations are given by

$$\rho\frac{\partial \boldsymbol{u}}{\partial t} - \mu\Delta\boldsymbol{u} + \rho\boldsymbol{u}\cdot\nabla\boldsymbol{u} + \nabla p - \frac{1}{\mu_0}(\nabla\times\boldsymbol{b})\times\boldsymbol{b} = \boldsymbol{f}, \qquad \text{(momentum)} \tag{5.1a}$$

$$\nabla\cdot\boldsymbol{u} = 0, \qquad \text{(mass)} \tag{5.1b}$$

$$\frac{\partial \boldsymbol{b}}{\partial t} + \nabla\times(\frac{\eta}{\mu_0}\nabla\times\boldsymbol{b}) - \nabla\times(\boldsymbol{u}\times\boldsymbol{b}) + \nabla r = \boldsymbol{g}, \qquad \text{(induction)} \tag{5.1c}$$

$$\nabla\cdot\boldsymbol{b} = 0. \qquad \text{(involution)} \tag{5.1d}$$

combining the induction equation (4.5) and the incompressible Navier-Stokes equations (3.2) with the additional contribution to the momentum equation of the Lorentz force $-\boldsymbol{J} \times \boldsymbol{b}$, which describes the electromagnetic forces on the fluid. The primal variables in (5.1) are the the fluid velocity, $\boldsymbol{u}$, the mechanical pressure, p, the magnetic field, $\boldsymbol{b}$, and a scalar Lagrange multiplier, r, which is introduced to facilitate the enforcement of the solenoidal constraint, (5.1d), on the magnetic field. Recall that in order to arrive at the induction equation (5.1c) we have assumed that the displacement current of the Maxwell-Faraday equation is negligible so that

$$\nabla \times \boldsymbol{b} = \mu_0 \boldsymbol{J}, \tag{5.2}$$

and we have assumed a generalized Ohm's law of the form

$$\boldsymbol{E} + \boldsymbol{u} \times \boldsymbol{b} = \eta \boldsymbol{J}. \tag{5.3}$$

For a more detailed discussion of this and of the role of the Lagrange multiplier r, see the chapter on the induction equation (Chapter 4) and the discussions in [60, 61, 25]. In (5.1a), we have used Ampere's Law (5.2) in order to eliminate $\boldsymbol{J}$ and express the Lorentz force as a function of $\boldsymbol{b}$ only. The fluid density, ρ, viscosity, μ, and resistivity, η, are assumed to be constant. The permeability of free space is denoted by μ_0 and the source term $\boldsymbol{g}$ is assumed to be divergence-free.

We non-dimensionalize (5.1) by introducing a characteristic length scale, l_0, a characteristic velocity scale, u_0, and a characteristic magnetic field scale, b_0. We then define a characteristic time scale by $t_0 := \frac{l_0}{u_0}$, a characteristic dynamic pressure by $p_0 := \rho u_0^2$, a scaling for r by $r_0 := \frac{\rho u_0^3 \mu_0}{b_0}$, a scaling for $\boldsymbol{f}$ by $f_0 := \frac{\rho u_0^2}{l_0}$, and a scaling for $\boldsymbol{g}$ by $g_0 := \frac{\rho u_0^3 \mu_0}{l_0 b_0}$. With some manipulation, (5.1) can then be written in non-dimensional form. In the following, in an abuse of notation, we make the substitutions $\frac{\boldsymbol{u}}{u_0} \to \boldsymbol{u}$, $\frac{p}{p_0} \to p$, $\frac{\boldsymbol{f}}{f_0} \to \boldsymbol{f}$, $\frac{\boldsymbol{b}}{b_0} \to \boldsymbol{b}$, $\frac{r}{r_0} \to r$, $\frac{\boldsymbol{g}}{g_0} \to \boldsymbol{g}$, $\frac{t}{t_0} \to t$, and

$l_0\nabla \to \nabla$, and write the nondimensionalized viscous, resistive, incompressible MHD equations as

$$\frac{\partial \boldsymbol{u}}{\partial t} + \boldsymbol{u}\cdot\nabla\boldsymbol{u} + \nabla p - \frac{1}{\mathrm{Re}}\Delta\boldsymbol{u} - \kappa(\nabla\times\boldsymbol{b})\times\boldsymbol{b} = \boldsymbol{f}, \qquad \text{(momentum)} \tag{5.4a}$$

$$\nabla\cdot\boldsymbol{u} = 0, \qquad \text{(mass)} \tag{5.4b}$$

$$\kappa\frac{\partial \boldsymbol{b}}{\partial t} + \frac{\kappa}{\mathrm{Rm}}\nabla\times(\nabla\times\boldsymbol{b}) - \kappa\nabla\times(\boldsymbol{u}\times\boldsymbol{b}) + \nabla r = \boldsymbol{g}, \qquad \text{(induction)} \tag{5.4c}$$

$$\nabla\cdot\boldsymbol{b} = 0. \qquad \text{(no monopole)} \tag{5.4d}$$

Here, the Reynolds number $\mathrm{Re} := \frac{\rho l_0 u_0}{\mu}$ is the ratio of inertial forces to viscous forces on the fluid, the magnetic Reynolds number $\mathrm{Rm} := \frac{\mu_0 u_0 l_0}{\eta}$ is the ratio of magnetic advection to magnetic diffusion, and the coupling parameter $\kappa := \frac{b_0^2}{\rho\mu_0 u_0^2}$ is the ratio of electromagnetic forces to inertial forces. We can also write $\kappa = \frac{\mathrm{Ha}^2}{\mathrm{ReRm}}$, where $\mathrm{Ha} := \frac{b_0 l_0}{\sqrt{\mu\eta}}$ is the Hartmann number, or we can write $\kappa = \frac{u_A^2}{u_0^2}$, where $u_A := \frac{b_0}{\sqrt{\rho\mu_0}}$ is the Alfvén speed. See [31, 49] for more details on dimensionless parameters related to MHD. Notice that our nondimensionalization of the induction equation is slightly different from that in Chapter 4, where we considered the small velocity limit of the induction equation in our upwind HDG scheme construction. Here, we do not make this assumption, and we define the characteristic time scale through a characteristic velocity rather than through the resistivity, leading to the dimensionless parameter Rm.

Toward applying the upwind HDG framework [9], we first put (5.4) into first order form through the definition of auxiliary variables $\mathbf{L}$ and $\boldsymbol{J}$, defined through the velocity gradient and the curl of the magnetic field, respectively. This leads to the

first order system

$$\mathrm{Re}\mathbf{L} - \nabla \boldsymbol{u} = \mathbf{0}, \tag{5.5a}$$

$$\frac{\partial \boldsymbol{u}}{\partial t} + \nabla \cdot (\boldsymbol{u} \otimes \boldsymbol{u}) + \nabla p - \nabla \cdot \mathbf{L} - \kappa(\nabla \times \boldsymbol{b}) \times \boldsymbol{b} = \boldsymbol{f}, \tag{5.5b}$$

$$\nabla \cdot \boldsymbol{u} = 0, \tag{5.5c}$$

$$\frac{\mathrm{Rm}}{\kappa}\boldsymbol{J} - \nabla \times \boldsymbol{b} = \mathbf{0}, \tag{5.5d}$$

$$\kappa \frac{\partial \boldsymbol{b}}{\partial t} + \nabla r - \kappa \nabla \times (\boldsymbol{u} \times \boldsymbol{b}) + \nabla \times \boldsymbol{J} = \boldsymbol{g}, \tag{5.5e}$$

$$\nabla \cdot \boldsymbol{b} = 0. \tag{5.5f}$$

Throughout this chapter, we may refer to $\boldsymbol{J}$ as the current density or as simply the current. This should be understood in a nondimensional sense, where the characteristic current is defined by $J_0 = \frac{Rm}{\kappa}\frac{b_0}{\mu_0 l_0} = \frac{\rho u_0^3 \mu_0}{\eta b_0}$.

We consider both the transient MHD equations, (5.5), and the steady state MHD equations (which can be derived by setting $\frac{\partial \boldsymbol{u}}{\partial t} = \mathbf{0}$ and $\frac{\partial \boldsymbol{b}}{\partial t} = \mathbf{0}$ in the time dependent equations). When considering the transient MHD equations, (5.5) is equipped with the initial conditions

$$\boldsymbol{u}(t=0) = \boldsymbol{u}_0, \qquad \boldsymbol{b}(t=0) = \boldsymbol{b}_0. \tag{5.6}$$

We next discuss the fluid boundary conditions and magnetic boundary conditions separately. For simplicity, we consider Dirichlet boundary conditions on the fluid velocity,

$$\boldsymbol{u} = \boldsymbol{u}_D \quad \text{on } \partial\Omega. \tag{5.7}$$

A compatibility condition on the Dirichlet boundary data $\int\limits_{\partial\Omega} \boldsymbol{u}_D \cdot \boldsymbol{n} = 0$ should be satisfied. For uniqueness, an additional constraint must be imposed on the pressure. We choose this constraint to be $\int\limits_{\Omega} p = 0$.

For the magnetic boundary conditions, the equations can be equipped with two different sets of boundary conditions [29], but for this chapter we consider the boundary conditions

$$\boldsymbol{n} \times \boldsymbol{b} = \boldsymbol{n} \times \boldsymbol{b}_D \quad \text{on } \partial\Omega, \tag{5.8a}$$

$$r = r_D = 0 \quad \text{on } \partial\Omega. \tag{5.8b}$$

Toward solving the resistive, incompressible MHD equations, (5.4), or equivalently (5.5), with boundary conditions (5.7) – (5.8) using an HDG formulation, we linearize (5.5) about a prescribed velocity $\boldsymbol{w}$ and a prescribed magnetic field $\boldsymbol{d}$ [25]:

$$\mathrm{Re}\mathbf{L} - \nabla \boldsymbol{u} = \mathbf{0}, \tag{5.9a}$$

$$\frac{\partial \boldsymbol{u}}{\partial t} + \nabla \cdot (\boldsymbol{u} \otimes \boldsymbol{w}) + \nabla p - \nabla \cdot \mathbf{L} - \kappa(\nabla \times \boldsymbol{b}) \times \boldsymbol{d} = \boldsymbol{f}, \tag{5.9b}$$

$$\nabla \cdot \boldsymbol{u} = 0, \tag{5.9c}$$

$$\frac{\mathrm{Rm}}{\kappa}\boldsymbol{J} - \nabla \times \boldsymbol{b} = \mathbf{0}, \tag{5.9d}$$

$$\kappa\frac{\partial \boldsymbol{b}}{\partial t} + \nabla r - \kappa\nabla \times (\boldsymbol{u} \times \boldsymbol{d}) + \nabla \times \boldsymbol{J} = \boldsymbol{g}, \tag{5.9e}$$

$$\nabla \cdot \boldsymbol{b} = 0. \tag{5.9f}$$

Here $\boldsymbol{w}$ is assumed to reside in $H(div, \Omega)$ and be divergence-free, while $\boldsymbol{d}$ is assumed to reside in $H(div, \Omega) \cap H(curl, \Omega)$.

Formally, multiplying (5.9) by a test function, integrating by parts, replacing the boundary terms with a not-necessarily-single-valued HDG flux, the local equations of the HDG schemes for the linearized MHD equations will take the form

$$\mathrm{Re}\,(\mathbf{L}_h, \mathbf{G})_{\mathcal{T}_h} + (\boldsymbol{u}_h, \nabla \cdot \mathbf{G})_{\mathcal{T}_h} + \left\langle \left(\boldsymbol{F}^*_{n,h}\right)_1, \mathbf{G} \right\rangle_{\partial\mathcal{T}_h} = 0, \tag{5.10a}$$

$$\left(\frac{\partial \boldsymbol{u}_h}{\partial t}, \boldsymbol{v}\right)_{\mathcal{T}_h} + (\mathbf{L}_h, \nabla \boldsymbol{v})_{\mathcal{T}_h} - (p_h, \nabla \cdot \boldsymbol{v})_{\mathcal{T}_h} - (\boldsymbol{u}_h \otimes \boldsymbol{w}, \nabla \boldsymbol{v})_{\mathcal{T}_h}$$
$$+\kappa\,(\boldsymbol{b}_h, \nabla \times (\boldsymbol{v} \times \boldsymbol{d}))_{\mathcal{T}_h} + \left\langle \left(\boldsymbol{F}^*_{n,h}\right)_2, \boldsymbol{v} \right\rangle_{\partial\mathcal{T}_h} = (\boldsymbol{f}, \boldsymbol{v})_{\mathcal{T}_h}, \tag{5.10b}$$

$$-(\boldsymbol{u}_h, \nabla q)_{\mathcal{T}_h} + \left\langle \left(\boldsymbol{F}^*_{n,h}\right)_3, q \right\rangle_{\partial\mathcal{T}_h} = 0, \tag{5.10c}$$

$$\frac{\mathrm{Rm}}{\kappa}\left(\boldsymbol{J}_h, \boldsymbol{H}\right)_{\mathcal{T}_h} - \left(\boldsymbol{b}_h, \nabla \times \boldsymbol{H}\right)_{\mathcal{T}_h} + \left\langle \left(\boldsymbol{F}^*_{n,h}\right)_4, \boldsymbol{H} \right\rangle_{\partial\mathcal{T}_h} = 0, \tag{5.10d}$$

$$\kappa\left(\frac{\partial \boldsymbol{b}_h}{\partial t}, \boldsymbol{c}\right)_{\mathcal{T}_h} + \left(\boldsymbol{J}_h, \nabla \times \boldsymbol{c}\right)_{\mathcal{T}_h} - \left(r_h, \nabla \cdot \boldsymbol{c}\right)_{\mathcal{T}_h}$$

$$-\kappa\left(\boldsymbol{u}_h, \boldsymbol{d} \times (\nabla \times \boldsymbol{c})\right)_{\mathcal{T}_h} + \left\langle \left(\boldsymbol{F}^*_{n,h}\right)_5, \boldsymbol{c} \right\rangle_{\partial\mathcal{T}_h} = \left(\boldsymbol{g}, \boldsymbol{c}\right)_{\mathcal{T}_h}, \tag{5.10e}$$

$$-\left(\boldsymbol{b}_h, \nabla s\right)_{\mathcal{T}_h} + \left\langle \left(\boldsymbol{F}^*_{n,h}\right)_6, s \right\rangle_{\partial\mathcal{T}_h} = 0. \tag{5.10f}$$

By weakly enforcing the single valuedness of the HDG flux, the conservation conditions take the form

$$\left\langle \left(\boldsymbol{F}^*_{n,h}\right)_1, \widehat{\mathbf{G}} \right\rangle_{\partial\mathcal{T}_h \setminus \partial\Omega} = 0, \tag{5.11a}$$

$$\left\langle \left(\boldsymbol{F}^*_{n,h}\right)_2, \widehat{\boldsymbol{v}} \right\rangle_{\partial\mathcal{T}_h \setminus \partial\Omega} = 0, \tag{5.11b}$$

$$\left\langle \left(\boldsymbol{F}^*_{n,h}\right)_3, \widehat{q} \right\rangle_{\partial\mathcal{T}_h \setminus \partial\Omega} = 0, \tag{5.11c}$$

$$\left\langle \left(\boldsymbol{F}^*_{n,h}\right)_4, \widehat{\boldsymbol{H}} \right\rangle_{\partial\mathcal{T}_h \setminus \partial\Omega} = 0, \tag{5.11d}$$

$$\left\langle \left(\boldsymbol{F}^*_{n,h}\right)_5, \widehat{\boldsymbol{c}} \right\rangle_{\partial\mathcal{T}_h \setminus \partial\Omega} = 0, \tag{5.11e}$$

$$\left\langle \left(\boldsymbol{F}^*_{n,h}\right)_6, \widehat{s} \right\rangle_{\partial\mathcal{T}_h \setminus \partial\Omega} = 0, \tag{5.11f}$$

where some of these equations will be automatically satisfied depending on the form of numerical flux. The system is closed by the boundary conditions

$$\left\langle \boldsymbol{u}^*_h, \widehat{\boldsymbol{w}} \right\rangle_{\partial\Omega} = \left\langle \boldsymbol{u}_D, \widehat{\boldsymbol{w}} \right\rangle_{\partial\Omega}, \tag{5.12a}$$

$$\left\langle \mathbf{T}\boldsymbol{b}^*_h, \widehat{\boldsymbol{z}}^t \right\rangle_{\partial\Omega} = \left\langle \boldsymbol{b}^t_D, \widehat{\boldsymbol{z}}^t \right\rangle_{\partial\Omega}, \tag{5.12b}$$

$$\left\langle r^*_h, \widehat{z} \right\rangle_{\partial\Omega} = \left\langle r_D, \widehat{z} \right\rangle_{\partial\Omega}. \tag{5.12c}$$

In the above, we define the six components $\left(\boldsymbol{F}^*_{n,h}\right)_i$ – tensor, vector, or scalar valued

– of the normal ("n") numerical ("h") flux by the tuple

$$\boldsymbol{F}^*_{n,h} = \begin{pmatrix} -\boldsymbol{u}^*_h \otimes \boldsymbol{n}, \\ -\mathbf{L}^*_h \boldsymbol{n} + p^* \boldsymbol{n} + (\boldsymbol{w}\cdot\boldsymbol{n})\boldsymbol{u}^*_h + \kappa \boldsymbol{d} \times (\boldsymbol{n} \times \boldsymbol{b}^*_h), \\ \boldsymbol{u}^*_h \cdot \boldsymbol{n}, \\ -\boldsymbol{n} \times \boldsymbol{b}^*_h, \\ \boldsymbol{n} \times \boldsymbol{J}^*_h + r^*_h \boldsymbol{n} - \boldsymbol{n} \times (\boldsymbol{u}^*_h \times \kappa \boldsymbol{d}), \\ \boldsymbol{b}^*_h \cdot \boldsymbol{n} \end{pmatrix}. \tag{5.13}$$

As before, there is a one to one correspondence between the tuple and a column vector where each entry of the tuple appears in order, beginning with $-\vec{\boldsymbol{u}^*_h} \otimes \boldsymbol{n}$. The unknowns $(\mathbf{L}_h, \boldsymbol{u}_h, p_h, \boldsymbol{J}_h, \boldsymbol{b}_h, r_h)$ will be sought in some discontinuous polynomial spaces on the volume of the domain, and $(\mathbf{G}, \boldsymbol{v}, q, \boldsymbol{H}, \boldsymbol{c}, s)$ are test functions in those same spaces. The six components of the numerical flux $\boldsymbol{F}^*_{n,h}$ (where each component is scalar, vector, or tensor valued) are yet-to-be-defined functions of the volume unknowns $(\mathbf{L}_h, \boldsymbol{u}_h, p_h, \boldsymbol{J}_h, \boldsymbol{b}_h, r_h)$ and trace variables $\left(\widehat{\mathbf{L}}_h, \widehat{\boldsymbol{u}}_h, \widehat{p}_h, \widehat{\boldsymbol{J}}_h, \widehat{\boldsymbol{b}}_h, \widehat{r}_h\right)$. The trace variables reside in discontinuous polynomial spaces defined on the mesh skeleton, as do the interior test functions $\left(\widehat{\mathbf{G}}, \widehat{\boldsymbol{v}}, \widehat{q}, \widehat{\boldsymbol{H}}, \widehat{\boldsymbol{c}}, \widehat{s}\right)$, and boundary test functions $\left(\widehat{\boldsymbol{w}}, \widehat{\boldsymbol{z}}^t, \widehat{z}\right)$. In what follows, we derive different choices for the numerical flux and analyze schemes that result from some specific choices. The fluxes we derive will be such that not all of (5.11a) – (5.11f) must be explicitly enforced, and the boundary test functions $\left(\widehat{\boldsymbol{w}}, \widehat{\boldsymbol{z}}^t, \widehat{z}\right)$ will have a natural association with $\left(\widehat{\mathbf{G}}, \widehat{\boldsymbol{v}}, \widehat{q}, \widehat{\boldsymbol{H}}, \widehat{\boldsymbol{c}}, \widehat{s}\right)$.

To derive the upwind numerical fluxes, we observe that the first order system (5.9) fits into the framework of (1.1), and is symmetric hyperbolic. Choosing the ordering of unknowns as the column vector $\boldsymbol{U} := (\mathrm{vec}\,(\mathbf{L})\,; \boldsymbol{u}; p; \boldsymbol{J}; \boldsymbol{b}; r)$, and defining $m := \boldsymbol{w}\cdot\boldsymbol{n}$, we have

$$\mathbf{A} = \left[\begin{array}{ccc|ccc} \mathbf{0} & -\boldsymbol{n}\otimes_K \mathbf{I} & \mathbf{0} & \mathbf{0} & \mathbf{0} & \mathbf{0} \\ -\boldsymbol{n}^\top \otimes_K \mathbf{I} & (\boldsymbol{w}\cdot\boldsymbol{n})\mathbf{I} & \boldsymbol{n} & \mathbf{0} & \kappa \boldsymbol{n}\boldsymbol{d}^\top - \kappa(\boldsymbol{d}\cdot\boldsymbol{n})\mathbf{I} & \mathbf{0} \\ \mathbf{0} & \boldsymbol{n}^\top & 0 & \mathbf{0} & \mathbf{0} & 0 \\ \hline \mathbf{0} & \mathbf{0} & \mathbf{0} & \mathbf{0} & \mathbf{B}^\top & \mathbf{0} \\ \mathbf{0} & \kappa \boldsymbol{d}\boldsymbol{n}^\top - \kappa(\boldsymbol{d}\cdot\boldsymbol{n})\mathbf{I} & \mathbf{0} & \mathbf{B} & \mathbf{0} & \boldsymbol{n} \\ \mathbf{0} & \mathbf{0} & 0 & \mathbf{0} & \boldsymbol{n}^\top & 0 \end{array}\right], \tag{5.14}$$

where

$$\mathbf{B} := \begin{bmatrix} n_2 \\ -n_1 \end{bmatrix} \text{ if } d = 2, \quad \mathbf{B} := \begin{bmatrix} 0 & -n_3 & n_2 \\ n_3 & 0 & -n_1 \\ -n_2 & n_1 & 0 \end{bmatrix} \text{ if } d = 3.$$

In 3D, the tensor $\mathbf{B}$ applies the cross product with the normal vector, i.e., $\mathbf{B}\boldsymbol{b} = \boldsymbol{n} \times \boldsymbol{b}$ and $\mathbf{B}^\top = -\mathbf{B}$ applies the same with the opposite sign. In 2D, $\mathbf{B}$ acts on a scalar as $\mathbf{B}a = \boldsymbol{n} \times a$, and its transpose acts on a vector as $\mathbf{B}^\top \boldsymbol{b} = -\boldsymbol{n} \times \boldsymbol{b}$.

In order to compute the upwind flux, we must calculate $\mathbf{A} := \mathbf{R}\mathbf{D}\mathbf{R}^{-1}$, where $\mathbf{D}$ is a diagonal matrix comprising the eigenvalues of $\mathbf{A}$, and $\mathbf{R}$ is a square matrix whose columns are the corresponding eigenvectors. In the case of $\mathbf{A}$ given by (5.14), some of the eigenvalues are roots of sixth order polynomials, which cannot be found analytically, so it becomes impractical to use (5.14) to derive the explicit, closed-form expression of the upwind HDG flux.

We propose a method of deriving HDG fluxes for the general HDG formulation (5.10) – (5.12) that avoids the calculation of eigenvalues of (5.14) by using the results from the Oseen and induction equations in chapters 3 and 4, respectively. Thus, we will not derive exact upwind fluxes, but rather upwind-based fluxes. Recognize that the top left block of the $\mathbf{A}$ matrix (5.14) is the same as the $\mathbf{A}$ matrix (3.7) corresponding to the Oseen equations, and the bottom right block of (5.14) is the same as the $\mathbf{A}$ matrix (4.10) corresponding to the induction equation in the limit of zero velocity. Knowing this, we define a numerical flux for the MHD HDG scheme (5.10) – (5.12) that results in well-posedness by setting

$$\boldsymbol{F}^*_{n,h} = \begin{pmatrix} -\boldsymbol{u}_h^{*O} \otimes \boldsymbol{n}, \\ -\mathbf{L}_h^{*O}\boldsymbol{n} + p_h^{*O}\boldsymbol{n} + (\boldsymbol{w} \cdot \boldsymbol{n})\boldsymbol{u}_h^{*O} \\ +\kappa \boldsymbol{d} \times \left(\boldsymbol{n} \times \left(\xi \boldsymbol{b}_h^t + (1-\xi)\widehat{\boldsymbol{b}}_h^t \right) \right), \\ \boldsymbol{u}_h^{*O} \cdot \boldsymbol{n}, \\ -\boldsymbol{n} \times \boldsymbol{b}_h^{*M}, \\ \boldsymbol{n} \times \boldsymbol{J}_h^{*M} + r_h^{*M}\boldsymbol{n} - \boldsymbol{n} \times (((1-\xi)\boldsymbol{u}_h + \xi \widehat{\boldsymbol{u}}_h) \times \kappa \boldsymbol{d}), \\ \boldsymbol{b}_h^{*M} \cdot \boldsymbol{n} \end{pmatrix}, \tag{5.15}$$

where $\mathbf{L}_h^{*O}$, $\boldsymbol{u}_h^{*O}$, and p_h^{*O} are defined by any of the fluxes (3.21) – (3.24) for the Oseen equations, and $\boldsymbol{J}_h^{*M}$, $\boldsymbol{b}_h^{*M}$, and r_h^{*M} are defined by any of the fluxes (4.20) – (4.23) for the induction equation, and where ξ is a real number. This method of constructing HDG schemes for the MHD equations requires the existence of the trace unknowns $\widehat{\boldsymbol{u}}_h$ or $\widehat{\boldsymbol{b}}_h^t$, or both. We can prove well-posedness of these schemes using the arguments we have used in previous chapters for the Stokes, Oseen, and induction equations provided that we choose certain combinations of the Oseen flux, induction flux, and parameter ξ. The idea is to require that the terms in the HDG scheme associated with the Lorentz force $\kappa\boldsymbol{d} \times (\nabla \times \boldsymbol{b})$ and the term $\nabla \times (\boldsymbol{u} \times \kappa\boldsymbol{d})$ produce skew-symmetric contributions to the complete global system considering all trace and volume unknowns. (Note that it is these terms that are associated with the propagation of Alfvén waves in the physical system [31].) This allows the well-posedness argument to be a simple extension of the well-posedness arguments for the HDG schemes for the Oseen equations and induction equation.

It is important to note that even though with the introduction of the auxiliary variables $\mathbf{L}_h$ and $\boldsymbol{J}_h$ we have 20 scalar volume unknowns (in 3D), we can eliminate these auxiliary variables through (5.10a) and (5.10d). Doing so reveals that the first order general HDG scheme (5.10) – (5.12) can be cast as a primal scheme, with 8 volume unknowns, that cannot be derived in an obvious way without the use of the first order system. Most importantly, there are 6 scalar trace unknowns for all of the HDG fluxes defined in the manner just outlined. Thus, we have an additional 8/6 reduction of unknowns compared to conventional discontinuous Galerkin schemes beyond the geometrical argument of the ratio of trace unknowns to volume unknowns for a single scalar variable.

A list of the possible fluxes is given in Table 5.1. For uniqueness of p_h in the local solver, the first, second, third, fourth, seventh, and tenth fluxes in Table 5.1

trace variables	Oseen flux	Induction flux	value of ξ
$\left(\widehat{\boldsymbol{u}}_h, \widehat{\boldsymbol{b}}_h\right)$	(3.21)	(4.20)	anything
$\left(\widehat{\boldsymbol{u}}_h, \widehat{\boldsymbol{b}}_h^t, \widehat{r}_h\right)$	(3.21)	(4.21)	anything
$\left(\widehat{\boldsymbol{u}}_h, \widehat{\boldsymbol{J}}_h^t, \widehat{b}_h^{\tilde{n}}\right)$	(3.21)	(4.22)	1
$\left(\widehat{\boldsymbol{u}}_h, \widehat{\boldsymbol{J}}_h^t, \widehat{r}_h\right)$	(3.21)	(4.23)	1
$\left(\widehat{\boldsymbol{f}}_h, \widehat{\boldsymbol{b}}_h\right)$	(3.22)	(4.20)	0
$\left(\widehat{\boldsymbol{u}}_h^t, \widehat{f}_h, \widehat{\boldsymbol{b}}_h\right)$	(3.23)	(4.20)	0
$\left(\widehat{u}_h^{\tilde{n}}, \widehat{\boldsymbol{f}}_h^t, \widehat{\boldsymbol{b}}_h\right)$	(3.24)	(4.20)	0
$\left(\widehat{\boldsymbol{f}}_h, \widehat{\boldsymbol{b}}_h^t, \widehat{r}_h\right)$	(3.22)	(4.21)	0
$\left(\widehat{\boldsymbol{u}}_h^t, \widehat{f}_h, \widehat{\boldsymbol{b}}_h^t, \widehat{r}_h\right)$	(3.23)	(4.21)	0
$\left(\widehat{u}_h^{\tilde{n}}, \widehat{\boldsymbol{f}}_h^t, \widehat{\boldsymbol{b}}_h^t, \widehat{r}_h\right)$	(3.24)	(4.21)	0

Table 5.1: HDG fluxes for the linearized incompressible visco-resistive MHD equations.

require that (5.10c) be modified using the average edge-pressure or augmented Lagrangian methods used for the the Stokes equations in Chapter 2. For uniqueness of r_h in the local solver, the first, third, fifth, sixth, and seventh fluxes require a similar modification for (5.10f). For direct to steady state simulations, more complicated modifications are required for the fourth flux (for the uniqueness of $\boldsymbol{b}_h$ in the local solver) and for the fifth and eighth fluxes (for the uniqueness of $\boldsymbol{u}_h$ in the local solver).

In the following sections, we concretize three HDG schemes. The first scheme uses the $(\widehat{\boldsymbol{u}}_h, \widehat{\boldsymbol{b}}_h)$ flux with the average edge-pressure modification for both the fluid and magnetic subsystems. The second scheme uses the $(\widehat{\boldsymbol{u}}_h^t, \widehat{f}_h, \widehat{\boldsymbol{b}}_h^t, \widehat{r}_h)$ flux, as this is the only flux listed in Table 5.1 that requires no modification for well-posedness, even for direct to steady state simulation. The third scheme uses the $(\widehat{\boldsymbol{u}}_h, \widehat{\boldsymbol{b}}_h^t, \widehat{r}_h)$ flux with the average edge-pressure modification for the magnetic subsystem. This third scheme is analyzed rigorously and used in the numerical tests that follow.

5.2 HDG Schemes Using the $(\widehat{\boldsymbol{u}}_h, \widehat{\boldsymbol{b}}_h)$ Flux

In this section, we define an HDG scheme with trace unknowns $(\widehat{\boldsymbol{u}}_h, \widehat{\boldsymbol{b}}_h)$ that is based on the upwind fluxes (3.21) for the Oseen equations and (4.20) for the induction equation coupled together in a manner described by (5.15). We write the scheme using the average edge-pressure approach for ensuring uniqueness of the pressure p_h and of the scalar Lagrange multiplier r_h in the local solver. This method is detailed for the Stokes equations in Section 2.2.1.2.

For clarity, we will explicitly write the numerical flux here:

$$\boldsymbol{F}^*_{n,h} = \begin{pmatrix} -\widehat{\boldsymbol{u}}_h \otimes \boldsymbol{n}, \\ -\mathbf{L}_h \boldsymbol{n} + p_h \boldsymbol{n} + \frac{1}{2}(\boldsymbol{w}\cdot\boldsymbol{n})\boldsymbol{u}_h + \frac{1}{2}(\boldsymbol{w}\cdot\boldsymbol{n})\widehat{\boldsymbol{u}}_h + \mathbf{S}_u\left(\boldsymbol{u}_h - \widehat{\boldsymbol{u}}_h\right) \\ +\kappa \boldsymbol{d} \times \left(\boldsymbol{n} \times \left(\xi \boldsymbol{b}_h + (1-\xi)\widehat{\boldsymbol{b}}_h\right)\right), \\ \widehat{\boldsymbol{u}}_h \cdot \boldsymbol{n}, \\ -\boldsymbol{n} \times \widehat{\boldsymbol{b}}_h, \\ \boldsymbol{n} \times \boldsymbol{J}_h + r_h \boldsymbol{n} + \mathbf{S}_b\left(\boldsymbol{b}_h - \widehat{\boldsymbol{b}}_h\right) \\ -\boldsymbol{n} \times \left(\left((1-\xi)\boldsymbol{u}_h + \xi\widehat{\boldsymbol{u}}_h\right) \times \kappa \boldsymbol{d}\right), \\ \widehat{\boldsymbol{b}}_h \cdot \boldsymbol{n} \end{pmatrix}, \tag{5.16}$$

where

$$\mathbf{S}_u := \tau_t \mathbf{T} + \tau_n \mathbf{N}, \tag{5.17}$$

$$\mathbf{S}_b := \beta_t \mathbf{T} + \beta_n \mathbf{N} \tag{5.18}$$

for positive τ_t, τ_n, β_t, and β_n. Here, ξ can be freely chosen. Some natural choices are $\xi = 0$ (which includes $\boldsymbol{u}_h$ and $\widehat{\boldsymbol{b}}_h$ in the fluid-magnetic coupling terms), $\xi = 1$ (which includes $\widehat{\boldsymbol{u}}_h$ and $\boldsymbol{b}_h$ in the fluid-magnetic coupling terms), and $\xi = \frac{1}{2}$ (which is halfway between the previous two choices). This definition of the numerical flux is

equivalent to defining

$$\begin{aligned}
\boldsymbol{u}_h^* = \widehat{\boldsymbol{u}}_h, \quad \boldsymbol{b}_h^* = \widehat{\boldsymbol{b}}_h, \quad r_h^* = r_h + \beta_n \left(\boldsymbol{b}_h - \widehat{\boldsymbol{b}}_h\right) \cdot \boldsymbol{n}, \\
\boldsymbol{n} \times \boldsymbol{J}_h^* = \boldsymbol{n} \times \boldsymbol{J}_h + \beta_t \mathbf{T} \left(\boldsymbol{b}_h - \widehat{\boldsymbol{b}}_h\right) - (1-\xi)\boldsymbol{n} \times ((\boldsymbol{u}_h - \widehat{\boldsymbol{u}}_h) \times \kappa \boldsymbol{d}), \\
-\mathbf{L}_h^* \boldsymbol{n} + p_h^* \boldsymbol{n} = -\mathbf{L}_h \boldsymbol{n} + p_h \boldsymbol{n} + \xi \kappa \boldsymbol{d} \times \left(\boldsymbol{n} \times \left(\boldsymbol{b}_h - \widehat{\boldsymbol{b}}_h\right)\right) \\
+ \left(\mathbf{S}_u + \frac{1}{2}(\boldsymbol{w} \cdot \boldsymbol{n})\mathbf{I}\right)(\boldsymbol{u}_h - \widehat{\boldsymbol{u}}_h).
\end{aligned}$$

These expressions prove useful in enforcing types of boundary conditions, different from (5.7) and (5.8), for which it may not be immediately obvious how to express by looking at (5.16).

We consider polynomial spaces of equal order $k \geq 1$ for all volume and trace unknowns. The discontinuous polynomial spaces in which we seek the volume unknowns $(\mathbf{L}_h, \boldsymbol{u}_h, p_h, \boldsymbol{J}_h, \boldsymbol{b}_h, r_h)$ are as follows:

$$\mathbf{G}_h := \left\{\mathbf{G} \in \left[L^2(\Omega)\right]^{d\times d} \ : \ \mathbf{G}|_K \in \mathbf{G}_h(K)\right\}, \tag{5.19a}$$

$$\boldsymbol{V}_h := \left\{\boldsymbol{v} \in \left[L^2(\Omega)\right]^{d} \ : \ \boldsymbol{v}|_K \in \boldsymbol{V}_h(K)\right\}, \tag{5.19b}$$

$$Q_h := \left\{q \in L^2(\Omega) \ : \ q|_K \in Q_h(K)\right\}, \tag{5.19c}$$

$$\boldsymbol{H}_h := \left\{\boldsymbol{H} \in \left[L^2(\Omega)\right]^{\tilde{d}} \ : \ \boldsymbol{H}|_K \in \boldsymbol{H}_h(K)\right\}, \tag{5.19d}$$

$$\boldsymbol{C}_h := \left\{\boldsymbol{c} \in \left[L^2(\Omega)\right]^{d} \ : \ \boldsymbol{c}|_K \in \boldsymbol{C}_h(K)\right\}, \tag{5.19e}$$

$$S_h := \left\{s \in L^2(\Omega) \ : \ s|_K \in S_h(K)\right\}, \tag{5.19f}$$

where $\mathbf{G}_h(K)$, $\boldsymbol{V}_h(K)$, $Q_h(K)$, $\boldsymbol{H}_h(K)$, $\boldsymbol{C}_h(K)$, $S_h(K)$ are polynomial spaces defined on K.

With the numerical flux (5.16), the enforcement of the Dirichlet boundary condition on the velocity (5.12a) simplifies to an L^2 projection of the Dirichlet boundary data $\boldsymbol{u}_D$ to the trace unknown on $\partial\Omega$, thereby decoupling the trace unknowns on $\partial\Omega$

from the rest of the unknowns. We decompose the velocity trace unknown as

$$\widehat{\boldsymbol{u}}_h = \widehat{\boldsymbol{u}}_h^i + \widehat{\boldsymbol{u}}_h^D, \tag{5.20}$$

where $\widehat{\boldsymbol{u}}_h^i$ is the trace unknown $\widehat{\boldsymbol{u}}_h$ restricted to the interior skeleton faces $\mathcal{E}_h^o$, and $\widehat{\boldsymbol{u}}_h^D$ is $\widehat{\boldsymbol{u}}_h$ restricted to the domain boundary $\partial\Omega$. Note that in writing (5.20), we associate $\widehat{\boldsymbol{u}}_h^i$ and $\widehat{\boldsymbol{u}}_h^D$ with their extensions by zero to the whole skeleton $\mathcal{E}_h$. We define the polynomial space in which $\widehat{\boldsymbol{u}}_h^i$ lies by

$$\widehat{\boldsymbol{V}}_h^i := \left\{ \widehat{\boldsymbol{v}} \in \left[L^2(\mathcal{E}_h^o)\right]^d \ : \ \widehat{\boldsymbol{v}}|_e \in \widehat{\boldsymbol{V}}_h(e) \right\}, \tag{5.21}$$

where $\widehat{\boldsymbol{V}}_h(e)$ is a vector-valued polynomial space defined on e. Then $\widehat{\boldsymbol{u}}_h^D$ is the L^2 projection of the velocity boundary data,

$$\left\langle \widehat{\boldsymbol{u}}_h^D, \widehat{\boldsymbol{v}} \right\rangle_{\partial\Omega} = \langle \boldsymbol{u}_D, \widehat{\boldsymbol{v}} \rangle_{\partial\Omega} \quad \text{for all } \widehat{\boldsymbol{v}} \in \widehat{\boldsymbol{V}}_h(e) \text{ for all } e \in \partial\Omega. \tag{5.22}$$

The enforcement of the boundary condition on the tangential components of the magnetic field (5.12b) simplifies to an L^2 projection of the boundary data $\boldsymbol{b}_D^t$ to the *tangential components* of the trace unknown $\widehat{\boldsymbol{b}}_h$ on $\partial\Omega$, thereby decoupling the tangential components of $\widehat{\boldsymbol{b}}_h$ on $\partial\Omega$ from the rest of the unknowns. We decompose the magnetic field trace unknown by

$$\widehat{\boldsymbol{b}}_h = \widehat{\boldsymbol{b}}_h^i + \widehat{b}_h^{n,D}\boldsymbol{n} + \widehat{\boldsymbol{b}}_h^{t,D} \tag{5.23}$$

where $\widehat{\boldsymbol{b}}_h^i$ is the trace unknown $\widehat{\boldsymbol{b}}_h$ restricted to $\mathcal{E}_h^o$, where $\widehat{b}_h^{n,D}\boldsymbol{n}$ is the normal component of $\widehat{\boldsymbol{b}}_h$ restricted to $\partial\Omega$, and where $\widehat{\boldsymbol{b}}_h^{t,D}$ is the tangential component of $\widehat{\boldsymbol{b}}_h$ restricted to $\partial\Omega$. We define the polynomial spaces in which $\widehat{\boldsymbol{b}}_h^i$ and $\widehat{b}_h^{n,D}$, respectively, lie by

$$\widehat{\boldsymbol{C}}_h^i := \left\{ \widehat{\boldsymbol{c}} \in \left[L^2(\mathcal{E}_h^o)\right]^d \ : \ \widehat{\boldsymbol{c}}|_e \in \widehat{\boldsymbol{C}}_h(e) \right\}, \tag{5.24}$$

$$\widehat{C}_h^D := \left\{ \widehat{c} \in L^2(\partial\Omega) \ : \ \widehat{c}|_e \in \widehat{C}_h(e) \right\}, \tag{5.25}$$

where $\widehat{\boldsymbol{C}}_h(e)$ and $\widehat{C}_h(e)$ are vector valued and scalar valued polynomial spaces defined on e. Then $\widehat{\boldsymbol{b}}_h^{t,D}$ is the L^2 projection of the magnetic field boundary data,

$$\left\langle \widehat{\boldsymbol{b}}_h^{t,D}, -\boldsymbol{n}\times(\boldsymbol{n}\times\widehat{\boldsymbol{c}})\right\rangle_{\partial\Omega} = \left\langle \boldsymbol{b}_D^t, -\boldsymbol{n}\times(\boldsymbol{n}\times\widehat{\boldsymbol{c}})\right\rangle_{\partial\Omega} \quad \text{for all } \widehat{\boldsymbol{c}}\in\widehat{\boldsymbol{C}}_h(e) \text{ for all } e\in\partial\Omega. \tag{5.26}$$

With this in place, we write the HDG scheme as follows.

Formulation 5.1. *Find* $(\mathbf{L}_h, \boldsymbol{u}_h, p_h, \boldsymbol{J}_h, \boldsymbol{b}_h, r_h, \widehat{\boldsymbol{u}}_h^i, \widehat{\boldsymbol{b}}_h^i, \widehat{b}_h^{n,D}, \rho_h, \gamma_h)$ *in* $\mathbf{G}_h\times\boldsymbol{V}_h\times Q_h\times \boldsymbol{H}_h\times\boldsymbol{C}_h\times S_h\times\widehat{\boldsymbol{V}}_h^i\times\widehat{\boldsymbol{C}}_h^i\times\widehat{C}_h^D\times\mathcal{P}_0(\partial\mathcal{T}_h)\times\mathcal{P}_0(\partial\mathcal{T}_h)$ *such that the local equations*

$$\mathrm{Re}\,(\mathbf{L}_h,\mathbf{G})_{\mathcal{T}_h} + (\boldsymbol{u}_h,\nabla\cdot\mathbf{G})_{\mathcal{T}_h} - \langle\widehat{\boldsymbol{u}}_h,\mathbf{G}\boldsymbol{n}\rangle_{\partial\mathcal{T}_h} = 0, \tag{5.27a}$$

$$\begin{aligned}\left(\frac{\partial\boldsymbol{u}_h}{\partial t},\boldsymbol{v}\right)_{\mathcal{T}_h} &- (\nabla\cdot\mathbf{L}_h,\boldsymbol{v})_{\mathcal{T}_h} + (\nabla p_h,\boldsymbol{v})_{\mathcal{T}_h} - \frac{1}{2}(\boldsymbol{u}_h\otimes\boldsymbol{w},\nabla\boldsymbol{v})_{\mathcal{T}_h} + \frac{1}{2}(\nabla\boldsymbol{u}_h,\boldsymbol{v}\otimes\boldsymbol{w})_{\mathcal{T}_h}\\ &+ (\nabla\times\boldsymbol{b}_h,\boldsymbol{v}\times\kappa\boldsymbol{d})_{\mathcal{T}_h} + \left\langle\frac{1}{2}(\boldsymbol{w}\cdot\boldsymbol{n})\,\widehat{\boldsymbol{u}}_h + \mathbf{S}_u(\boldsymbol{u}_h-\widehat{\boldsymbol{u}}_h),\boldsymbol{v}\right\rangle_{\partial\mathcal{T}_h}\\ &- [1-\xi]\left\langle\boldsymbol{n}\times\left(\boldsymbol{b}_h-\widehat{\boldsymbol{b}}_h\right),\boldsymbol{v}\times\kappa\boldsymbol{d}\right\rangle_{\partial\mathcal{T}_h} = (\boldsymbol{f},\boldsymbol{v})_{\mathcal{T}_h},\end{aligned} \tag{5.27b}$$

$$-(\boldsymbol{u}_h,\nabla q)_{\mathcal{T}_h} + \langle\widehat{\boldsymbol{u}}_h\cdot\boldsymbol{n}, q-\overline{q}\rangle_{\partial\mathcal{T}_h} + \langle\overline{p}_h-\rho_h,\overline{q}\rangle_{\partial\mathcal{T}_h} = 0, \tag{5.27c}$$

$$\frac{\mathrm{Rm}}{\kappa}(\boldsymbol{J}_h,\boldsymbol{H})_{\mathcal{T}_h} - (\boldsymbol{b}_h,\nabla\times\boldsymbol{H})_{\mathcal{T}_h} - \left\langle\boldsymbol{n}\times\widehat{\boldsymbol{b}}_h,\boldsymbol{H}\right\rangle_{\partial\mathcal{T}_h} = 0, \tag{5.27d}$$

$$\begin{aligned}\kappa\left(\frac{\partial\boldsymbol{b}_h}{\partial t},\boldsymbol{c}\right)_{\mathcal{T}_h} &+ (\nabla\times\boldsymbol{J}_h,\boldsymbol{c})_{\mathcal{T}_h} + (\nabla r_h,\boldsymbol{c})_{\mathcal{T}_h} - (\boldsymbol{u}_h\times\kappa\boldsymbol{d},\nabla\times\boldsymbol{c})_{\mathcal{T}_h}\\ &+ \langle([1-\xi]\,\boldsymbol{u}_h+\xi\widehat{\boldsymbol{u}}_h)\times\kappa\boldsymbol{d},\boldsymbol{n}\times\boldsymbol{c}\rangle_{\partial\mathcal{T}_h} + \left\langle\mathbf{S}_b\left(\boldsymbol{b}_h-\widehat{\boldsymbol{b}}_h\right),\boldsymbol{c}\right\rangle_{\partial\mathcal{T}_h} = (\boldsymbol{g},\boldsymbol{c})_{\mathcal{T}_h},\end{aligned} \tag{5.27e}$$

$$-(\boldsymbol{b}_h,\nabla s)_{\mathcal{T}_h} + \left\langle\widehat{\boldsymbol{b}}_h\cdot\boldsymbol{n}, s-\overline{s}\right\rangle_{\partial\mathcal{T}_h} + \langle\overline{r}_h-\gamma_h,\overline{s}\rangle_{\partial\mathcal{T}_h} = 0, \tag{5.27f}$$

the conservation equations

$$-\left\langle -\mathbf{L}_h\boldsymbol{n} + p_h\boldsymbol{n} + \frac{1}{2}(\boldsymbol{w}\cdot\boldsymbol{n})\,\boldsymbol{u}_h + \mathbf{S}_u(\boldsymbol{u}_h-\widehat{\boldsymbol{u}}_h) + \kappa\boldsymbol{d}\times(\boldsymbol{n}\times\xi\boldsymbol{b}_h),\widehat{\boldsymbol{v}}\right\rangle_{\partial\mathcal{T}_h\setminus\partial\Omega} = 0, \tag{5.27g}$$

$$-\left\langle\boldsymbol{n}\times\boldsymbol{J}_h + r_h\boldsymbol{n} + \mathbf{S}_b\left(\boldsymbol{b}_h-\widehat{\boldsymbol{b}}_h\right) - \boldsymbol{n}\times([1-\xi]\,\boldsymbol{u}_h\times\kappa\boldsymbol{d}),\widehat{\boldsymbol{c}}\right\rangle_{\partial\mathcal{T}_h\setminus\partial\Omega} = 0, \tag{5.27h}$$

the boundary condition

$$-\left\langle r_h + \beta_n \left(\boldsymbol{b}_h \cdot \boldsymbol{n} - \widehat{b}_h^{n,D} \right), \widehat{c} \right\rangle_{\partial\Omega} = -\left\langle r_D, \widehat{c} \right\rangle_{\partial\Omega}, \tag{5.27i}$$

and the additional constraints

$$\langle \widehat{\boldsymbol{u}}_h \cdot \boldsymbol{n}, \psi \rangle_{\partial\mathcal{T}_h} = 0, \tag{5.27j}$$

$$\left\langle \widehat{\boldsymbol{b}}_h \cdot \boldsymbol{n}, \phi \right\rangle_{\partial\mathcal{T}_h} = 0 \tag{5.27k}$$

hold for all $(\mathbf{G}, \boldsymbol{v}, q, \boldsymbol{H}, \boldsymbol{c}, s, \widehat{\boldsymbol{v}}, \widehat{\boldsymbol{c}}, \widehat{c}, \psi, \phi)$ *in* $\mathbf{G}_h \times \boldsymbol{V}_h \times Q_h \times \boldsymbol{H}_h \times \boldsymbol{C}_h \times S_h \times \widehat{\boldsymbol{V}}_h^i \times \widehat{\boldsymbol{C}}_h^i \times \widehat{C}_h^D \times \mathcal{P}_0(\partial\mathcal{T}_h) \times \mathcal{P}_0(\partial\mathcal{T}_h)$*, where* $\widehat{\boldsymbol{u}}_h$ *and* $\widehat{\boldsymbol{b}}_h$ *are as defined in* (5.20) *and* (5.23)*, and where* $\mathbf{S}_u$ *and* $\mathbf{S}_b$ *are defined as in* (5.17) *and* (5.18)*, respectively. Additionally, the pressure is subject to the zero mean pressure constraint,*

$$(p_h, 1)_{\partial\mathcal{T}_h} = 0. \tag{5.28}$$

For simplicity in writing the above, we have written $\widehat{\boldsymbol{u}}_h$ instead of $\widehat{\boldsymbol{u}}_h^i$ and $\widehat{\boldsymbol{u}}_h^D$. Note that we seek only $\widehat{\boldsymbol{u}}_h^i$ in the formulation, so $\widehat{\boldsymbol{u}}_h^D$ should be interpreted as a known quantity defined by (5.22) that contributes to the right hand side. Of course, it is not necessary to do this. We can seek the entire $\widehat{\boldsymbol{u}}_h$ by keeping (5.22) in the formulation and keeping $\widehat{\boldsymbol{u}}_h^D$ as unknowns in (5.27a) – (5.27c), (5.27e), and (5.27j). A similar statement applies to $\widehat{\boldsymbol{b}}_h$. These interpretations are mathematically equivalent, however the former ensures that the expected matrix structure is realized in the implementation. We have integrated by parts some terms in (5.10) in order to reveal the symmetric and skew-symmetric terms and to write the scheme in a concise manner. Also, we have used the assumption that $\boldsymbol{w} \in H(div, \Omega)$ and that $\boldsymbol{d} \in H(div, \Omega) \cap H(curl, \Omega)$ to conclude

$$-\left\langle \frac{1}{2} (\boldsymbol{w} \cdot \boldsymbol{n}) \widehat{\boldsymbol{u}}_h, \widehat{\boldsymbol{v}} \right\rangle_{\partial\mathcal{T}_h \setminus \partial\Omega} = 0 \text{ and } -\left\langle \kappa \boldsymbol{d} \times \left(\boldsymbol{n} \times \widehat{\boldsymbol{b}}_h^t \right), \widehat{\boldsymbol{v}}^t \right\rangle_{\partial\mathcal{T}_h \setminus \partial\Omega} = 0,$$

so we have not considered these terms in the conservation equations.

It can be shown that the formulation is well-posed and that its local solver is also well-posed. This is true for the semidiscrete, fully discrete with implicit time stepping, and steady-state schemes. This can be shown using similar arguments as we use to show well-posedness for the HDG scheme with the $(\widehat{\boldsymbol{u}}_h, \widehat{\boldsymbol{b}}_h^t, \widehat{r}_h)$ flux shown in Section 5.4, so we omit the proofs here. It can also be shown that the condensed (volume unknowns eliminated) matrix system associated with Formulation 5.1 takes the form

$$\begin{bmatrix} A & B & E & 0 \\ -B^\top & 0 & 0 & 0 \\ F & 0 & C & D \\ 0 & 0 & -D^\top & 0 \end{bmatrix} \begin{bmatrix} \widehat{U} \\ \rho \\ \widehat{B} \\ \gamma \end{bmatrix} = \begin{bmatrix} F_1 \\ F_2 \\ F_3 \\ F_4 \end{bmatrix}, \tag{5.29}$$

where A and C are positive definite. The matrix form and the positive definiteness can be revealed in a similar manner as was done for the HDG schemes for the Stokes equations in Chapter 2 and in Appendix B. The details for this MHD scheme are omitted.

5.3 HDG Schemes Using the $(\widehat{\boldsymbol{u}}_h^t, \widehat{f}_h, \widehat{\boldsymbol{b}}_h^t, \widehat{r}_h)$ Flux

In this section, we define an HDG scheme with trace unknowns $(\widehat{\boldsymbol{u}}_h^t, \widehat{f}_h, \widehat{\boldsymbol{b}}_h^t, \widehat{r}_h)$ that is based on the upwind fluxes (3.23) for the Oseen equations and (4.21) for the induction equation coupled together in a manner described by (5.15). For clarity, we

will explicitly write the numerical flux here:

$$\boldsymbol{F}^*_{n,h} = \begin{pmatrix} -\left(\widehat{\boldsymbol{u}}^t_h + \mathbf{N}\boldsymbol{u}_h + \frac{1}{\tau_n}\left(f_h - \widehat{f}_h\right)\right) \otimes \boldsymbol{n}, \\ \widehat{f}_h\boldsymbol{n} - \mathbf{TL}_h\boldsymbol{n} + \frac{1}{2}(\boldsymbol{w}\cdot\boldsymbol{n})\widehat{\boldsymbol{u}}^t_h + \frac{1}{2}(\boldsymbol{w}\cdot\boldsymbol{n})\boldsymbol{u}_h + \kappa\boldsymbol{d}\times\left(\boldsymbol{n}\times\widehat{\boldsymbol{b}}^t_h\right) \\ +\frac{1}{2}(\boldsymbol{w}\cdot\boldsymbol{n})\frac{1}{\tau_n}\left(f_h - \widehat{f}_h\right)\boldsymbol{n} + \tau_t\left(\boldsymbol{u}^t_h - \widehat{\boldsymbol{u}}^t_h\right), \\ \boldsymbol{u}_h\cdot\boldsymbol{n} + \frac{1}{\tau_n}\left(f_h - \widehat{f}_h\right), \\ -\boldsymbol{n}\times\widehat{\boldsymbol{b}}^t_h, \\ \boldsymbol{n}\times\boldsymbol{J}_h + \widehat{r}_h\boldsymbol{n} + \beta_t\left(\boldsymbol{b}^t_h - \widehat{\boldsymbol{b}}^t_h\right) - \boldsymbol{n}\times(\boldsymbol{u}_h\times\kappa\boldsymbol{d}), \\ \boldsymbol{b}_h\cdot\boldsymbol{n} + \frac{1}{\beta_n}(r_h - \widehat{r}_h) \end{pmatrix}, \quad (5.30)$$

where

$$f_h := -\boldsymbol{n}\cdot\mathbf{L}_h\boldsymbol{n} + p_h + \frac{1}{2}(\boldsymbol{w}\cdot\boldsymbol{n})(\boldsymbol{u}_h\cdot\boldsymbol{n}) \quad (5.31)$$

and where τ_t, τ_n, β_t, and β_n are positive parameters. This definition of the numerical flux is equivalent to defining

$$\begin{aligned} \boldsymbol{u}^*_h &= \widehat{\boldsymbol{u}}^t_h + \mathbf{N}\boldsymbol{u}_h + \frac{1}{\tau_n}\left(f_h - \widehat{f}_h\right)\boldsymbol{n}, \\ \boldsymbol{b}^*_h &= \widehat{\boldsymbol{b}}^t_h + \mathbf{N}\boldsymbol{b}_h + \frac{1}{\beta_n}(r_h - \widehat{r}_h)\,\boldsymbol{n}, \\ r^*_h &= \widehat{r}_h, \\ \boldsymbol{n}\times\boldsymbol{J}^*_h &= \boldsymbol{n}\times\boldsymbol{J}_h + \beta_t\left(\boldsymbol{b}^t_h - \widehat{\boldsymbol{b}}^t_h\right) - \boldsymbol{n}\times\left(\left[\boldsymbol{u}^t_h - \widehat{\boldsymbol{u}}^t_h - \frac{1}{\tau_n}\left(f_h - \widehat{f}_h\right)\right]\times\kappa\boldsymbol{d}\right), \\ -\mathbf{L}^*_h\boldsymbol{n} + p^*_h\boldsymbol{n} &= \widehat{f}_h\boldsymbol{n} - \mathbf{TL}_h\boldsymbol{n} - \frac{1}{2}(\boldsymbol{w}\cdot\boldsymbol{n})(\boldsymbol{u}\cdot\boldsymbol{n})\boldsymbol{n} - \frac{1}{2}(\boldsymbol{w}\cdot\boldsymbol{n})\frac{1}{\tau_n}\left(f_h - \widehat{f}_h\right)\boldsymbol{n} \\ &\quad + \left(\tau_t + \frac{1}{2}\boldsymbol{w}\cdot\boldsymbol{n}\right)\left(\boldsymbol{u}^t_h - \widehat{\boldsymbol{u}}^t_h\right). \end{aligned}$$

These expressions prove useful in enforcing types of boundary conditions, different from (5.7) and (5.8), for which it may not be immediately obvious how to express by looking at (5.30).

For the volume unknowns, we consider the same equal-order polynomial spaces (5.19) as we do for the other HDG schemes for the MHD equations.

With the numerical flux (5.30), the enforcement of the Dirichlet boundary condition on the velocity (5.12a) simplifies to an L^2 projection of the *tangential component* of the Dirichlet boundary data $\boldsymbol{u}_D$ to the trace unknown $\widehat{\boldsymbol{u}}_h^t$ on $\partial\Omega$, thereby decoupling $\widehat{\boldsymbol{u}}_h^t$ on $\partial\Omega$ from the rest of the unknowns. The normal component of (5.12a) is included in the formulation below. We decompose the velocity trace unknown as

$$\widehat{\boldsymbol{u}}_h^t = \widehat{\boldsymbol{u}}_h^{t,i} + \widehat{\boldsymbol{u}}_h^{t,D}, \tag{5.32}$$

where $\widehat{\boldsymbol{u}}_h^{t,i}$ is the trace unknown $\widehat{\boldsymbol{u}}_h^t$ restricted to the interior skeleton faces $\mathcal{E}_h^o$, and $\widehat{\boldsymbol{u}}_h^{t,D}$ is $\widehat{\boldsymbol{u}}_h^t$ restricted to the domain boundary $\partial\Omega$. (In writing (5.32), we associate $\widehat{\boldsymbol{u}}_h^{t,i}$ and $\widehat{\boldsymbol{u}}_h^{t,D}$ with their extensions by zero to the whole skeleton $\mathcal{E}_h$.) We define the polynomial space in which $\widehat{\boldsymbol{u}}_h^{t,i}$ lies by

$$\widehat{\boldsymbol{V}}_h^{t,i} := \left\{ \widehat{\boldsymbol{v}}^t \in \left[L^2(\mathcal{E}_h^o)\right]^d \ : \ \widehat{\boldsymbol{v}}^t|_e \in \widehat{\boldsymbol{V}}_h^t(e) \right\}, \tag{5.33}$$

where $\widehat{\boldsymbol{V}}_h^t(e)$ is a vector valued polynomial space with no normal component, defined by

$$\widehat{\boldsymbol{V}}_h^t(e) = \left\{ \sum_{i=1}^{d-1} \boldsymbol{t}^i \widehat{v}_{h,i} \ : \ \widehat{v}_{h,i} \in \widehat{V}_h(e) \right\}, \tag{5.34}$$

where $\widehat{V}_h(e)$ is a scalar polynomial space defined on e, and $\left\{\boldsymbol{t}^1, \ldots, \boldsymbol{t}^{d-1}\right\}$ is a basis of the tangent space of e. Then $\widehat{\boldsymbol{u}}_h^{t,D}$ is the L^2 projection of the tangential component of the velocity boundary data,

$$\left\langle \widehat{\boldsymbol{u}}_h^{t,D}, \widehat{\boldsymbol{v}}^t \right\rangle_{\partial\Omega} = \left\langle \boldsymbol{u}_D^t, \widehat{\boldsymbol{v}}^t \right\rangle_{\partial\Omega} \quad \text{for all } \widehat{\boldsymbol{v}}^t \in \widehat{\boldsymbol{V}}_h^t(e) \text{ for all } e \in \partial\Omega. \tag{5.35}$$

The enforcement of the boundary condition on the tangential components of the magnetic field (5.12b) simplifies to an L^2 projection of the boundary data $\boldsymbol{b}_D^t$ to the trace unknown $\widehat{\boldsymbol{b}}_h^t$ on $\partial\Omega$, thereby decoupling $\widehat{\boldsymbol{b}}_h^t$ on $\partial\Omega$ from the rest of the unknowns. We decompose the magnetic field trace unknown by

$$\widehat{\boldsymbol{b}}_h^t = \widehat{\boldsymbol{b}}_h^{t,i} + \widehat{\boldsymbol{b}}_h^{t,D} \tag{5.36}$$

where $\widehat{\boldsymbol{b}}_h^{t,i}$ is the trace unknown $\widehat{\boldsymbol{b}}_h^t$ restricted to $\mathcal{E}_h^o$, and where $\widehat{\boldsymbol{b}}_h^{t,D}$ is $\widehat{\boldsymbol{b}}_h^t$ restricted to $\partial\Omega$. We define the polynomial space in which $\widehat{\boldsymbol{b}}_h^{t,i}$ lies by

$$\widehat{\boldsymbol{C}}_h^{t,i} := \left\{ \widehat{\boldsymbol{c}}^t \in \left[L^2(\mathcal{E}_h^o)\right]^d \ : \ \widehat{\boldsymbol{c}}^t|_e \in \widehat{\boldsymbol{C}}_h^t(e) \right\}, \tag{5.37}$$

where $\widehat{\boldsymbol{C}}_h^t(e)$ is a vector valued polynomial space with no normal component, defined by

$$\widehat{\boldsymbol{C}}_h^t(e) = \left\{ \sum_{i=1}^{d-1} \boldsymbol{t}^i \widehat{c}_{h,i} \ : \ \widehat{c}_{h,i} \in \widehat{C}_h(e) \right\}, \tag{5.38}$$

where $\widehat{C}_h(e)$ is a scalar polynomial space defined on e. Then $\widehat{\boldsymbol{b}}_h^{t,D}$ is the L^2 projection of the magnetic field boundary data,

$$\left\langle \widehat{\boldsymbol{b}}_h^{t,D}, \widehat{\boldsymbol{c}}^t \right\rangle_{\partial\Omega} = \left\langle \boldsymbol{b}_D^t, \widehat{\boldsymbol{c}}^t \right\rangle_{\partial\Omega} \quad \text{for all } \widehat{\boldsymbol{c}}^t \in \widehat{\boldsymbol{C}}_h^t(e) \text{ for all } e \in \partial\Omega. \tag{5.39}$$

The enforcement of the boundary condition on the magnetic scalar Lagrange multiplier (5.12b) simplifies to an L^2 projection of the boundary data r_D to the trace unknown $\widehat{r}_h$ on $\partial\Omega$, thereby decoupling $\widehat{r}_h$ on $\partial\Omega$ from the rest of the unknowns. We decompose $\widehat{r}_h$ by

$$\widehat{r}_h = \widehat{r}_h^i + \widehat{r}_h^D \tag{5.40}$$

where $\widehat{r}_h^i$ is the trace unknown $\widehat{r}_h$ restricted to $\mathcal{E}_h^o$, and where $\widehat{r}_h^D$ is $\widehat{r}_h$ restricted to $\partial\Omega$. We define the polynomial space in which $\widehat{r}_h^i$ lies by

$$\widehat{S}_h^i := \left\{ \widehat{s} \in L^2(\mathcal{E}_h^o) \ : \ \widehat{s}|_e \in \widehat{S}_h(e) \right\}, \tag{5.41}$$

where $\widehat{S}_h(e)$ is a polynomial defined on e. Then $\widehat{r}_h^D$ is the L^2 projection of the scalar Lagrange multiplier boundary data r_D (which is zero for real applications),

$$\left\langle \widehat{r}_h^D, \widehat{s} \right\rangle_{\partial\Omega} = \left\langle r_D, \widehat{s} \right\rangle_{\partial\Omega} \quad \text{for all } \widehat{s} \in \widehat{S}_h(e) \text{ for all } e \in \partial\Omega. \tag{5.42}$$

Finally, we define the polynomial space for $\widehat{f}_h$ (which corresponds to no boundary condition) by

$$\widehat{F}_h := \left\{ \widehat{g} \in L^2(\mathcal{E}_h) \ : \ \widehat{g}|_e \in \widehat{F}_h(e) \right\}, \tag{5.43}$$

where $\widehat{F}_h(e)$ is a polynomial defined on e.

With this in place, we write the HDG scheme as follows.

Formulation 5.2. *Find* $(\mathbf{L}_h, \boldsymbol{u}_h, p_h, \boldsymbol{J}_h, \boldsymbol{b}_h, r_h, \widehat{\boldsymbol{u}}_h^{t,i}, \widehat{f}_h, \widehat{\boldsymbol{b}}_h^{t,i}, \widehat{r}_h^i)$ *in* $\mathbf{G}_h \times \boldsymbol{V}_h \times Q_h \times \boldsymbol{H}_h \times \boldsymbol{C}_h \times S_h \times \widehat{\boldsymbol{V}}_h^{t,i} \times \widehat{F}_h \times \widehat{\boldsymbol{C}}_h^{t,i} \times \widehat{S}_h^i$ *such that the local equations*

$$\begin{aligned}
&\mathrm{Re}\,(\mathbf{L}_h, \mathbf{G})_{\mathcal{T}_h} - (\nabla \boldsymbol{u}_h, \mathbf{G})_{\mathcal{T}_h} + \left\langle \boldsymbol{u}_h^t - \widehat{\boldsymbol{u}}_h^t, \mathbf{G}\boldsymbol{n} \right\rangle_{\partial\mathcal{T}_h} \\
&\qquad - \left\langle \frac{1}{\tau_n}\left(f_h - \widehat{f}_h\right), \boldsymbol{n}\cdot\mathbf{G}\boldsymbol{n} \right\rangle_{\partial\mathcal{T}_h} = 0, && (5.44a)\\
&\left(\frac{\partial \boldsymbol{u}_h}{\partial t}, \boldsymbol{v}\right)_{\mathcal{T}_h} + (\mathbf{L}_h, \nabla \boldsymbol{v})_{\mathcal{T}_h} - (p_h, \nabla\cdot\boldsymbol{v})_{\mathcal{T}_h} - \frac{1}{2}(\boldsymbol{u}_h \otimes \boldsymbol{w}, \nabla \boldsymbol{v})_{\mathcal{T}_h} + \frac{1}{2}(\nabla \boldsymbol{u}_h, \boldsymbol{v}\otimes\boldsymbol{w})_{\mathcal{T}_h} \\
&\qquad + (\nabla\times\boldsymbol{b}_h, \boldsymbol{v}\times\kappa\boldsymbol{d})_{\mathcal{T}_h} + \left\langle \widehat{f}_h, \boldsymbol{v}\cdot\boldsymbol{n} \right\rangle_{\partial\mathcal{T}_h} + \left\langle -\mathbf{L}_h\boldsymbol{n} + \frac{1}{2}(\boldsymbol{w}\cdot\boldsymbol{n})\widehat{\boldsymbol{u}}_h^t, \boldsymbol{v}^t \right\rangle_{\partial\mathcal{T}_h} \\
&\qquad + \left\langle \frac{1}{\tau_n}\left(f_h - \widehat{f}_h\right), \frac{1}{2}(\boldsymbol{w}\cdot\boldsymbol{n})\boldsymbol{v}\cdot\boldsymbol{n} \right\rangle_{\partial\mathcal{T}_h} + \left\langle \tau_t\left(\boldsymbol{u}_h^t - \widehat{\boldsymbol{u}}_h^t\right), \boldsymbol{v}^t \right\rangle_{\partial\mathcal{T}_h} \\
&\qquad - \left\langle \boldsymbol{n}\times\left(\boldsymbol{b}_h^t - \widehat{\boldsymbol{b}}_h^t\right), \boldsymbol{v}\times\kappa\boldsymbol{d} \right\rangle_{\partial\mathcal{T}_h} = (\boldsymbol{f}, \boldsymbol{v})_{\mathcal{T}_h}, && (5.44b)\\
&(\nabla\cdot\boldsymbol{u}_h, q)_{\mathcal{T}_h} + \left\langle \frac{1}{\tau_n}\left(f_h - \widehat{f}_h\right), q \right\rangle_{\partial\mathcal{T}_h} = 0, && (5.44c)\\
&\frac{\mathrm{Rm}}{\kappa}(\boldsymbol{J}_h, \boldsymbol{H})_{\mathcal{T}_h} - (\boldsymbol{b}_h, \nabla\times\boldsymbol{H})_{\mathcal{T}_h} - \left\langle \boldsymbol{n}\times\widehat{\boldsymbol{b}}_h^t, \boldsymbol{H} \right\rangle_{\partial\mathcal{T}_h} = 0, && (5.44d)\\
&\kappa\left(\frac{\partial \boldsymbol{b}_h}{\partial t}, \boldsymbol{c}\right)_{\mathcal{T}_h} + (\nabla\times\boldsymbol{J}_h, \boldsymbol{c})_{\mathcal{T}_h} - (r_h, \nabla\cdot\boldsymbol{c})_{\mathcal{T}_h} - (\boldsymbol{u}_h\times\kappa\boldsymbol{d}, \nabla\times\boldsymbol{c})_{\mathcal{T}_h} + \langle \widehat{r}_h, \boldsymbol{c}\cdot\boldsymbol{n}\rangle_{\partial\mathcal{T}_h} \\
&\qquad + \left\langle \beta_t\left(\boldsymbol{b}_h^t - \widehat{\boldsymbol{b}}_h^t\right), \boldsymbol{c}^t \right\rangle_{\partial\mathcal{T}_h} + \left\langle \boldsymbol{u}_h\times\kappa\boldsymbol{d}, \boldsymbol{n}\times\boldsymbol{c}^t \right\rangle_{\partial\mathcal{T}_h} = (\boldsymbol{g}, \boldsymbol{c})_{\mathcal{T}_h}, && (5.44e)\\
&(\nabla\cdot\boldsymbol{b}_h, s)_{\mathcal{T}_h} + \left\langle \frac{1}{\beta_n}(r_h - \widehat{r}_h), s \right\rangle_{\partial\mathcal{T}_h} = 0, && (5.44f)
\end{aligned}$$

and the conservation equations and normal component of the velocity boundary con-

dition

$$-\left\langle -\mathbf{L}_h\boldsymbol{n}+\frac{1}{2}(\boldsymbol{w}\cdot\boldsymbol{n})\boldsymbol{u}_h^t+\tau_t\left(\boldsymbol{u}_h^t-\widehat{\boldsymbol{u}}_h^t\right),\widehat{\boldsymbol{v}}^t\right\rangle_{\partial\mathcal{T}_h\backslash\partial\Omega}=0, \tag{5.44g}$$

$$-\left\langle \boldsymbol{u}_h\cdot\boldsymbol{n}+\frac{1}{\tau_n}\left(f_h-\widehat{f}_h\right),\widehat{g}\right\rangle_{\partial\mathcal{T}_h}=-\left\langle \boldsymbol{u}_D\cdot\boldsymbol{n},\widehat{g}\right\rangle_{\partial\Omega}, \tag{5.44h}$$

$$-\left\langle \boldsymbol{n}\times\boldsymbol{J}_h+\beta_t\left(\boldsymbol{b}_h^t-\widehat{\boldsymbol{b}}_h^t\right)-\boldsymbol{n}\times(\boldsymbol{u}_h\times\kappa\boldsymbol{d}),\widehat{\boldsymbol{c}}^t\right\rangle_{\partial\mathcal{T}_h\backslash\partial\Omega}=0, \tag{5.44i}$$

$$-\left\langle \boldsymbol{b}_h\cdot\boldsymbol{n}+\frac{1}{\tau_n}\left(f_h-\widehat{f}_h\right),\widehat{s}\right\rangle_{\partial\mathcal{T}_h\backslash\partial\Omega}=0 \tag{5.44j}$$

hold for all $(\mathbf{G},\boldsymbol{v},q,\boldsymbol{H},\boldsymbol{c},s,\widehat{\boldsymbol{v}}^t,\widehat{g},\widehat{\boldsymbol{c}}^t,\widehat{s})$ *in* $\mathbf{G}_h\times\boldsymbol{V}_h\times Q_h\times\boldsymbol{H}_h\times\boldsymbol{C}_h\times S_h\times\widehat{\boldsymbol{V}}_h^{t,i}\times\widehat{F}_h\times\widehat{\boldsymbol{C}}_h^{t,i}\times\widehat{S}_h^i$ *where* $\widehat{\boldsymbol{u}}_h^t$, $\widehat{\boldsymbol{b}}_h^t$, *and* $\widehat{r}_h$ *are as defined in* (5.32), (5.36), *and* (5.40), *respectively. Additionally, the pressure is subject to the zero mean pressure constraint,* (5.28).

For simplicity in writing the above, we have written $\widehat{\boldsymbol{u}}_h^t$ instead of $\widehat{\boldsymbol{u}}_h^{t,i}$ and $\widehat{\boldsymbol{u}}_h^{t,D}$. Note that we seek only $\widehat{\boldsymbol{u}}_h^{t,i}$ in the formulation, so $\widehat{\boldsymbol{u}}_h^{t,D}$ should be interpreted as a known quantity defined by (5.35) that contributes to the right hand side. A similar statement applies to $\widehat{\boldsymbol{b}}_h^t$ and $\widehat{r}_h$.

Similar to Formulation 3.2 for the Oseen equations, we have identified the scalar test function $\widehat{g}$ with $-\boldsymbol{n}\cdot\widehat{\mathbf{G}}\boldsymbol{n}+\widehat{q}+\frac{1}{2}(\boldsymbol{w}\cdot\boldsymbol{n})(\widehat{\boldsymbol{v}}\cdot\boldsymbol{n})$ on $\partial\mathcal{T}_h\backslash\partial\Omega$ and with $\widehat{\boldsymbol{w}}\cdot\boldsymbol{n}$ on $\partial\Omega$ in order to write (5.11a), (5.11c), the normal part of (5.11b), and the normal part of (5.12a) in a combined manner as (5.44h). Similarly, we identify $\widehat{\boldsymbol{v}}^t$ with $\mathbf{T}\widehat{\boldsymbol{w}}$ to write the tangent part of (5.11b) as (5.44g).

We have integrated by parts some terms in (5.10) in order to reveal the symmetric and skew-symmetric terms and to write the scheme in a more concise manner. Also, we have used the assumption that $\boldsymbol{w}\in H(div,\Omega)$ and that $\boldsymbol{d}\in H(div,\Omega)\cap H(curl,\Omega)$ to conclude

$$-\left\langle\frac{1}{2}(\boldsymbol{w}\cdot\boldsymbol{n})\,\widehat{\boldsymbol{u}}_h^t,\widehat{\boldsymbol{v}}^t\right\rangle_{\partial\mathcal{T}_h\backslash\partial\Omega}=0 \text{ and } -\left\langle\kappa\boldsymbol{d}\times\left(\boldsymbol{n}\times\widehat{\boldsymbol{b}}_h^t\right),\widehat{\boldsymbol{v}}^t\right\rangle_{\partial\mathcal{T}_h\backslash\partial\Omega}=0,$$

so we have not considered these terms in the conservation equations.

It can be shown that the formulation is well-posed and that its local solver is also well-posed. This is true for the semidiscrete, fully discrete with implicit time stepping, and steady-state schemes. This can be shown using similar arguments as we use to show well-posedness for the HDG scheme with the $(\widehat{\boldsymbol{u}}_h, \widehat{\boldsymbol{b}}_h^t, \widehat{r}_h)$ flux shown in Section 5.4, so we omit the proofs here. It can also be shown that the condensed (volume unknowns eliminated) matrix system associated with Formulation 5.2 takes a general form

$$\begin{bmatrix} A & B & C & D \\ E & F & G & H \\ J & K & L & M \\ N & P & Q & R \end{bmatrix} \begin{bmatrix} \widehat{U}^t \\ \widehat{F} \\ \widehat{B}^t \\ \widehat{R} \end{bmatrix} = \begin{bmatrix} F_1 \\ F_2 \\ F_3 \\ F_4 \end{bmatrix}, \tag{5.45}$$

where A, F, L, and R are positive semi-definite. Additionally, R is positive definite, and F is positive definite when one degree of freedom associated with $\widehat{f}_h$ is constrained. The matrix form and the positive definiteness can be revealed in a similar manner as was done for the HDG schemes for the Stokes equations in Chapter 2 and in Appendix B. The details for this MHD scheme are omitted.

5.4 HDG Schemes Using the $(\widehat{\boldsymbol{u}}_h, \widehat{\boldsymbol{b}}_h^t, \widehat{r}_h)$ Flux

In this section, we define an HDG scheme with trace unknowns $(\widehat{\boldsymbol{u}}_h, \widehat{\boldsymbol{b}}_h^t, \widehat{r}_h)$ that is based on the upwind fluxes (3.21) for the Oseen equations and (4.21) for the induction equation coupled together in a manner described by (5.15). To ensure uniqueness of the pressure p_h in the local solver, we have several choices, among which are the augmented Lagrangian method (see Section 2.2.1.1) and the average edge-pressure technique (see Section 2.2.1.2). Traditionally, the global unknown represents an elementwise average edge-pressure [53, 56]. In our work on an MHD scheme for

the incompressible MHD equations [46], we define a method based on an elementwise pressure volume integral. Here, we choose to write the scheme using the average edge-pressure approach.

For clarity, we will explicitly write the numerical flux here:

$$\boldsymbol{F}^*_{n,h} = \begin{pmatrix} -\widehat{\boldsymbol{u}}_h \otimes \boldsymbol{n}, \\ -\mathbf{L}_h\boldsymbol{n} + p_h\boldsymbol{n} + \frac{1}{2}(\boldsymbol{w}\cdot\boldsymbol{n})\boldsymbol{u}_h + \frac{1}{2}(\boldsymbol{w}\cdot\boldsymbol{n})\widehat{\boldsymbol{u}}_h + \mathbf{S}_u\left(\boldsymbol{u}_h - \widehat{\boldsymbol{u}}_h\right) \\ +\kappa\boldsymbol{d}\times\left(\boldsymbol{n}\times\left(\xi\boldsymbol{b}_h^t + (1-\xi)\widehat{\boldsymbol{b}}_h^t\right)\right), \\ \widehat{\boldsymbol{u}}_h\cdot\boldsymbol{n}, \\ -\boldsymbol{n}\times\widehat{\boldsymbol{b}}_h^t, \\ \boldsymbol{n}\times\boldsymbol{J}_h + \widehat{r}_h\boldsymbol{n} + \beta_t\left(\boldsymbol{b}_h^t - \widehat{\boldsymbol{b}}_h^t\right) \\ -\boldsymbol{n}\times\left(\left((1-\xi)\boldsymbol{u}_h + \xi\widehat{\boldsymbol{u}}_h\right)\times\kappa\boldsymbol{d}\right), \\ \boldsymbol{b}_h\cdot\boldsymbol{n} + \frac{1}{\beta_n}\left(r_h - \widehat{r}_h\right) \end{pmatrix}, \tag{5.46}$$

where β_t and β_n are positive parameters, and where $\mathbf{S}_u$ is defined by (5.17) for positive τ_t and τ_n. Here, ξ can be freely chosen. This definition of the numerical flux is equivalent to defining

$$\begin{aligned} \boldsymbol{u}_h^* = \widehat{\boldsymbol{u}}_h, \quad \boldsymbol{b}_h^* = \widehat{\boldsymbol{b}}_h^t + \mathbf{N}\boldsymbol{b}_h + \frac{1}{\beta_n}\left(r_h - \widehat{r}_h\right), \quad r_h^* = \widehat{r}_h, \\ \boldsymbol{n}\times\boldsymbol{J}_h^* = \boldsymbol{n}\times\boldsymbol{J}_h + \beta_t\left(\boldsymbol{b}_h^t - \widehat{\boldsymbol{b}}_h^t\right) - (1-\xi)\boldsymbol{n}\times\left(\left(\boldsymbol{u}_h - \widehat{\boldsymbol{u}}_h\right)\times\kappa\boldsymbol{d}\right), \\ -\mathbf{L}_h^*\boldsymbol{n} + p_h^*\boldsymbol{n} = -\mathbf{L}_h\boldsymbol{n} + p_h\boldsymbol{n} + \xi\kappa\boldsymbol{d}\times\left(\boldsymbol{n}\times\left(\boldsymbol{b}_h - \widehat{\boldsymbol{b}}_h\right)\right) \\ + \left(\mathbf{S}_u + \frac{1}{2}(\boldsymbol{w}\cdot\boldsymbol{n})\mathbf{I}\right)\left(\boldsymbol{u}_h - \widehat{\boldsymbol{u}}_h\right). \end{aligned}$$

These expressions prove useful in enforcing types of boundary conditions, different from (5.7) and (5.8), for which it may not be immediately obvious how to express by looking at (5.46).

For the volume unknowns, we consider the same equal-order polynomial spaces (5.19) as we do for the other HDG schemes for the MHD equations. The decomposition of the velocity trace unknown $\widehat{\boldsymbol{u}}_h$ into interior and boundary components, and the definition of the polynomial space to which $\widehat{\boldsymbol{u}}_h$ belongs, is the same as for the

$\left(\widehat{\boldsymbol{u}}_h, \widehat{\boldsymbol{b}}_h\right)$ flux in Section 5.2. Similarly, the treatment of the magnetic trace unknowns $\widehat{\boldsymbol{b}}_h^t$ and $\widehat{r}_h$ is the same as for the $\left(\widehat{\boldsymbol{u}}_h^t, \widehat{f}_h, \widehat{\boldsymbol{b}}_h^t, \widehat{r}_h\right)$ flux in Section 5.3. Thus, we are ready to write the HDG scheme.

Formulation 5.3. *Find* $(\mathbf{L}_h, \boldsymbol{u}_h, p_h, \boldsymbol{J}_h, \boldsymbol{b}_h, r_h, \widehat{\boldsymbol{u}}_h^i, \widehat{\boldsymbol{b}}_h^{t,i}, \widehat{r}_h^i, \rho_h)$ *in* $\mathbf{G}_h \times \boldsymbol{V}_h \times Q_h \times \boldsymbol{H}_h \times \boldsymbol{C}_h \times S_h \times \widehat{\boldsymbol{V}}_h^i \times \widehat{\boldsymbol{C}}_h^{t,i} \times \widehat{S}_h \times \mathcal{P}_0(\partial\mathcal{T}_h)$ *such that the local equations*

$$\mathrm{Re}\left(\mathbf{L}_h, \mathbf{G}\right)_{\mathcal{T}_h} + \left(\boldsymbol{u}_h, \nabla\cdot\mathbf{G}\right)_{\mathcal{T}_h} - \left\langle\widehat{\boldsymbol{u}}_h, \mathbf{G}\boldsymbol{n}\right\rangle_{\partial\mathcal{T}_h} = 0, \tag{5.47a}$$

$$\begin{aligned}\left(\frac{\partial \boldsymbol{u}_h}{\partial t}, \boldsymbol{v}\right)_{\mathcal{T}_h} &- \left(\nabla\cdot\mathbf{L}_h, \boldsymbol{v}\right)_{\mathcal{T}_h} + \left(\nabla p_h, \boldsymbol{v}\right)_{\mathcal{T}_h} - \frac{1}{2}\left(\boldsymbol{u}_h\otimes\boldsymbol{w}, \nabla\boldsymbol{v}\right)_{\mathcal{T}_h} + \frac{1}{2}\left(\nabla\boldsymbol{u}_h, \boldsymbol{v}\otimes\boldsymbol{w}\right)_{\mathcal{T}_h}\\ &+ \left(\nabla\times\boldsymbol{b}_h, \boldsymbol{v}\times\kappa\boldsymbol{d}\right)_{\mathcal{T}_h} + \left\langle\frac{1}{2}\left(\boldsymbol{w}\cdot\boldsymbol{n}\right)\widehat{\boldsymbol{u}}_h + \mathbf{S}_u\left(\boldsymbol{u}_h - \widehat{\boldsymbol{u}}_h\right), \boldsymbol{v}\right\rangle_{\partial\mathcal{T}_h}\\ &- \left[1-\xi\right]\left\langle\boldsymbol{n}\times\left(\boldsymbol{b}_h^t - \widehat{\boldsymbol{b}}_h^t\right), \boldsymbol{v}\times\kappa\boldsymbol{d}\right\rangle_{\partial\mathcal{T}_h} = \left(\boldsymbol{f}, \boldsymbol{v}\right)_{\mathcal{T}_h},\end{aligned} \tag{5.47b}$$

$$-\left(\boldsymbol{u}_h, \nabla q\right)_{\mathcal{T}_h} + \left\langle\widehat{\boldsymbol{u}}_h\cdot\boldsymbol{n}, q-\overline{q}\right\rangle_{\partial\mathcal{T}_h} + \left\langle\overline{p}_h - \rho_h, \overline{q}\right\rangle_{\partial\mathcal{T}_h} = 0, \tag{5.47c}$$

$$\frac{\mathrm{Rm}}{\kappa}\left(\boldsymbol{J}_h, \boldsymbol{H}\right)_{\mathcal{T}_h} - \left(\boldsymbol{b}_h, \nabla\times\boldsymbol{H}\right)_{\mathcal{T}_h} - \left\langle\boldsymbol{n}\times\widehat{\boldsymbol{b}}_h^t, \boldsymbol{H}\right\rangle_{\partial\mathcal{T}_h} = 0, \tag{5.47d}$$

$$\begin{aligned}\kappa\left(\frac{\partial\boldsymbol{b}_h}{\partial t}, \boldsymbol{c}\right)_{\mathcal{T}_h} &+ \left(\nabla\times\boldsymbol{J}_h, \boldsymbol{c}\right)_{\mathcal{T}_h} - \left(r_h, \nabla\cdot\boldsymbol{c}\right)_{\mathcal{T}_h} - \left(\boldsymbol{u}_h\times\kappa\boldsymbol{d}, \nabla\times\boldsymbol{c}\right)_{\mathcal{T}_h} + \left\langle\widehat{r}_h, \boldsymbol{c}\cdot\boldsymbol{n}\right\rangle_{\partial\mathcal{T}_h}\\ &+ \left\langle\left(\left[1-\xi\right]\boldsymbol{u}_h + \xi\widehat{\boldsymbol{u}}_h\right)\times\kappa\boldsymbol{d}, \boldsymbol{n}\times\boldsymbol{c}\right\rangle_{\partial\mathcal{T}_h} + \left\langle\beta_t\left(\boldsymbol{b}_h^t - \widehat{\boldsymbol{b}}_h^t\right), \boldsymbol{c}\right\rangle_{\partial\mathcal{T}_h} = \left(\boldsymbol{g}, \boldsymbol{c}\right)_{\mathcal{T}_h},\end{aligned} \tag{5.47e}$$

$$\left(\nabla\cdot\boldsymbol{b}_h, s\right)_{\mathcal{T}_h} + \left\langle\frac{1}{\beta_n}\left(r_h - \widehat{r}_h\right), s\right\rangle_{\partial\mathcal{T}_h} = 0, \tag{5.47f}$$

the conservation equations

$$-\left\langle-\mathbf{L}_h\boldsymbol{n} + p_h\boldsymbol{n} + \frac{1}{2}\left(\boldsymbol{w}\cdot\boldsymbol{n}\right)\boldsymbol{u}_h + \mathbf{S}_u\left(\boldsymbol{u}_h - \widehat{\boldsymbol{u}}_h\right) + \kappa\boldsymbol{d}\times\left(\boldsymbol{n}\times\xi\boldsymbol{b}_h\right), \widehat{\boldsymbol{v}}\right\rangle_{\partial\mathcal{T}_h\setminus\partial\Omega} = 0, \tag{5.47g}$$

$$-\left\langle\boldsymbol{n}\times\boldsymbol{J}_h + \beta_t\left(\boldsymbol{b}_h^t - \widehat{\boldsymbol{b}}_h^t\right) - \boldsymbol{n}\times\left(\left[1-\xi\right]\boldsymbol{u}_h\times\kappa\boldsymbol{d}\right), \widehat{\boldsymbol{c}}^t\right\rangle_{\partial\mathcal{T}_h\setminus\partial\Omega} = 0, \tag{5.47h}$$

$$-\left\langle\boldsymbol{b}_h\cdot\boldsymbol{n} + \frac{1}{\beta_n}\left(r_h - \widehat{r}_h\right), \widehat{s}\right\rangle_{\partial\mathcal{T}_h\setminus\partial\Omega} = 0, \tag{5.47i}$$

and the additional constraint

$$\left\langle\widehat{\boldsymbol{u}}_h\cdot\boldsymbol{n}, \psi\right\rangle_{\partial\mathcal{T}_h} = 0 \tag{5.47j}$$

hold for all $(\mathbf{G}, \boldsymbol{v}, q, \boldsymbol{H}, \boldsymbol{c}, s, \widehat{\boldsymbol{v}}, \widehat{\boldsymbol{c}}^t, \widehat{s}, \psi)$ *in* $\mathbf{G}_h \times \boldsymbol{V}_h \times Q_h \times \boldsymbol{H}_h \times \boldsymbol{C}_h \times S_h \times \widehat{\boldsymbol{V}}_h^i \times \widehat{\boldsymbol{C}}_h^{t,i} \times \widehat{S}_h \times \mathcal{P}_0(\partial\mathcal{T}_h)$*, where* $\widehat{\boldsymbol{u}}_h$*,* $\widehat{\boldsymbol{b}}_h^t$*, and* $\widehat{r}_h$ *are as defined in* (5.20)*,* (5.36)*, and* (5.40)*, respectively, and where* $\mathbf{S}_u$ *is defined as in* (5.17)*. Additionally, the pressure is subject to the zero mean pressure constraint* (5.28)*.*

Similar comments as those in the previous sections apply regarding the separation of the trace variables into their boundary and interior components, regarding integrating terms by parts, and regarding using the assumptions on $\boldsymbol{w}$ and $\boldsymbol{d}$ in order to omit terms from the conservation equations..

In the following, we discuss the well-posedness of Formulation 5.3.

Theorem 5.1. *(well-posedness of Formulation 5.3 - steady state)*
Let Ω *be simply connected, let* $\partial\Omega$ *be connected, and let* τ_t*,* τ_n*,* β_t*, and* β_n *be positive. Then the steady state HDG Formulation 5.3 (with* $\frac{\partial}{\partial t} = 0$*) is well-posed in the sense that given* $\boldsymbol{f}$*,* $\boldsymbol{u}_D$*,* $\boldsymbol{b}_D^t$*, and* r_D*, there exists a unique solution* $\left(\mathbf{L}_h, \boldsymbol{u}_h, p_h, \boldsymbol{J}_h, \boldsymbol{b}_h, r_h, \widehat{\boldsymbol{u}}_h, \widehat{\boldsymbol{b}}_h^t, \widehat{r}_h, \rho_h\right)$ *to Formulation 5.3.*

Proof. It is sufficient to prove that if $\boldsymbol{f} = \mathbf{0}$, $\boldsymbol{u}_D = \mathbf{0}$, $\boldsymbol{b}_D^t = \mathbf{0}$, and $r_D = 0$, then the solution $\left(\mathbf{L}_h, \boldsymbol{u}_h, p_h, \boldsymbol{J}_h, \boldsymbol{b}_h, r_h, \widehat{\boldsymbol{u}}_h, \widehat{\boldsymbol{b}}_h^t, \widehat{r}_h, \rho_h\right)$ is zero.

By taking the test function q as an elementwise (nonzero) constant, it is revealed that (5.47c) is equivalent to $-\left(\boldsymbol{u}_h, \nabla q\right)_{\mathcal{T}_h} + \left\langle \widehat{\boldsymbol{u}}_h \cdot \boldsymbol{n}, q - \overline{q} \right\rangle_{\partial\mathcal{T}_h} = 0$ and $\rho_h = \overline{p}_h$. By adding $0 = -\left\langle \rho_h - \overline{p}_h, \widehat{\boldsymbol{v}} \cdot \boldsymbol{n} \right\rangle_{\partial\mathcal{T}_h \setminus \partial\Omega}$ to (5.47g), we can rewrite (5.47) as

$$\begin{aligned} & a_{sym}\left(\left(\mathbf{L}_h, \boldsymbol{u}_h, \boldsymbol{J}_h, \boldsymbol{b}_h, r_h, \widehat{\boldsymbol{u}}_h^i, \widehat{\boldsymbol{b}}_h^{t,i}, \widehat{r}_h^i\right), \left(\mathbf{G}, \boldsymbol{v}, \boldsymbol{H}, \boldsymbol{c}, s, \widehat{\boldsymbol{v}}, \widehat{\boldsymbol{c}}^t, \widehat{s}\right)\right) \\ & \quad + a_{skew}\left(\left(\mathbf{L}_h, \boldsymbol{u}_h, p_h, \boldsymbol{J}_h, \boldsymbol{b}_h, r_h, \widehat{\boldsymbol{u}}_h^i, \widehat{\boldsymbol{b}}_h^t, \widehat{r}_h\right), \left(\mathbf{G}, \boldsymbol{v}, q, \boldsymbol{H}, \boldsymbol{c}, s, \widehat{\boldsymbol{v}}, \widehat{\boldsymbol{c}}^t, \widehat{s}\right)\right) \\ & \quad = \ell\left(\mathbf{G}, \boldsymbol{v}, q, \boldsymbol{H}, \boldsymbol{c}, s, \widehat{\boldsymbol{v}}, \widehat{\boldsymbol{c}}^t, \widehat{s}\right), \end{aligned} \tag{5.48}$$

where

$$
\begin{aligned}
&a_{sym}\left(\left(\mathbf{L}_h,\boldsymbol{u}_h,\boldsymbol{J}_h,\boldsymbol{b}_h,r_h,\widehat{\boldsymbol{u}}_h^i,\widehat{\boldsymbol{b}}_h^{t,i},\widehat{r}_h^i\right),\left(\mathbf{G},\boldsymbol{v},\boldsymbol{H},\boldsymbol{c},s,\widehat{\boldsymbol{v}},\widehat{\boldsymbol{c}}^t,\widehat{s}\right)\right)\\
&\quad=\mathrm{Re}\left(\mathbf{L}_h,\mathbf{G}\right)_{\mathcal{T}_h}+\left\langle\mathbf{S}_u\left(\boldsymbol{u}_h-\widehat{\boldsymbol{u}}_h^i\right),\boldsymbol{v}-\widehat{\boldsymbol{v}}\right\rangle_{\partial\mathcal{T}_h\setminus\partial\Omega}+\left\langle\mathbf{S}_u\boldsymbol{u}_h,\boldsymbol{v}\right\rangle_{\partial\Omega}\\
&\quad+\frac{\mathrm{Rm}}{\kappa}\left(\boldsymbol{J}_h,\boldsymbol{H}\right)_{\mathcal{T}_h}+\left\langle\beta_t\left(\boldsymbol{b}_h^t-\widehat{\boldsymbol{b}}_h^{t,i}\right),\boldsymbol{c}^t-\widehat{\boldsymbol{c}}^t\right\rangle_{\partial\mathcal{T}_h\setminus\partial\Omega}+\left\langle\beta_t\boldsymbol{b}_h^t,\boldsymbol{c}^t\right\rangle_{\partial\Omega}\\
&\quad+\left\langle\frac{1}{\beta_n}\left(r_h-\widehat{r}_h^i\right),s-\widehat{s}\right\rangle_{\partial\mathcal{T}_h\setminus\partial\Omega}+\left\langle\frac{1}{\beta_n}r_h,s\right\rangle_{\partial\Omega},
\end{aligned}
\tag{5.49}
$$

$$
\begin{aligned}
&a_{skew}\left(\left(\mathbf{L}_h,\boldsymbol{u}_h,p_h,\boldsymbol{J}_h,\boldsymbol{b}_h,r_h,\widehat{\boldsymbol{u}}_h^i,\widehat{\boldsymbol{b}}_h^t,\widehat{r}_h,\rho_h\right),\left(\mathbf{G},\boldsymbol{v},q,\boldsymbol{H},\boldsymbol{c},s,\widehat{\boldsymbol{v}},\widehat{\boldsymbol{c}}^t,\widehat{s},\psi\right)\right)=\\
&\quad\left(\boldsymbol{u}_h,\nabla\cdot\mathbf{G}\right)_{\mathcal{T}_h}-\left(\nabla\cdot\mathbf{L}_h,\boldsymbol{v}\right)_{\mathcal{T}_h}+\left(\nabla p_h,\boldsymbol{v}\right)_{\mathcal{T}_h}-\left(\boldsymbol{u}_h,\nabla q\right)_{\mathcal{T}_h}-\frac{1}{2}\left(\boldsymbol{u}_h\otimes\boldsymbol{w},\nabla\boldsymbol{v}\right)_{\mathcal{T}_h}\\
&\quad+\frac{1}{2}\left(\nabla\boldsymbol{u}_h,\boldsymbol{v}\otimes\boldsymbol{w}\right)_{\mathcal{T}_h}-\left(\boldsymbol{b}_h,\nabla\times\boldsymbol{H}\right)_{\mathcal{T}_h}+\left(\nabla\times\boldsymbol{J}_h,\boldsymbol{c}\right)_{\mathcal{T}_h}-\left(r_h,\nabla\cdot\boldsymbol{c}\right)_{\mathcal{T}_h}\\
&\quad+\left(\nabla\cdot\boldsymbol{b}_h,s\right)_{\mathcal{T}_h}-\left\langle\widehat{\boldsymbol{u}}_h^i,\mathbf{G}\boldsymbol{n}\right\rangle_{\partial\mathcal{T}_h\setminus\partial\Omega}+\left\langle\mathbf{L}_h\boldsymbol{n},\widehat{\boldsymbol{v}}\right\rangle_{\partial\mathcal{T}_h\setminus\partial\Omega}+\left\langle\widehat{\boldsymbol{u}}_h^i\cdot\boldsymbol{n},q-\overline{q}\right\rangle_{\partial\mathcal{T}_h\setminus\partial\Omega}\\
&\quad-\left\langle p_h-\overline{p}_h,\widehat{\boldsymbol{v}}\cdot\boldsymbol{n}\right\rangle_{\partial\mathcal{T}_h\setminus\partial\Omega}+\frac{1}{2}\left\langle(\boldsymbol{w}\cdot\boldsymbol{n})\widehat{\boldsymbol{u}}_h^i,v\right\rangle_{\partial\mathcal{T}_h\setminus\partial\Omega}-\frac{1}{2}\left\langle(\boldsymbol{w}\cdot\boldsymbol{n})\boldsymbol{u}_h,\widehat{\boldsymbol{v}}\right\rangle_{\partial\mathcal{T}_h\setminus\partial\Omega}\\
&\quad-\left\langle\boldsymbol{n}\times\widehat{\boldsymbol{b}}_h^{t,i},\boldsymbol{H}\right\rangle_{\partial\mathcal{T}_h\setminus\partial\Omega}+\left\langle\boldsymbol{J}_h,\boldsymbol{n}\times\widehat{\boldsymbol{c}}^t\right\rangle_{\partial\mathcal{T}_h\setminus\partial\Omega}+\left\langle\widehat{r}_h^i,\boldsymbol{c}\cdot\boldsymbol{n}\right\rangle_{\partial\mathcal{T}_h\setminus\partial\Omega}\\
&\quad-\left\langle\boldsymbol{b}_h\cdot\boldsymbol{n},\widehat{s}\right\rangle_{\partial\mathcal{T}_h\setminus\partial\Omega}+\left(\nabla\times\boldsymbol{b}_h,\boldsymbol{v}\times\kappa\boldsymbol{d}\right)_{\mathcal{T}_h}-\left(\boldsymbol{u}_h\times\kappa\boldsymbol{d},\nabla\times\boldsymbol{c}\right)_{\mathcal{T}_h}\\
&\quad-[1-\xi]\left\langle\boldsymbol{n}\times\boldsymbol{b}_h^t,\boldsymbol{v}\times\kappa\boldsymbol{d}\right\rangle_{\partial\mathcal{T}_h}+[1-\xi]\left\langle\boldsymbol{u}_h\times\kappa\boldsymbol{d},\boldsymbol{n}\times\boldsymbol{c}^t\right\rangle_{\partial\mathcal{T}_h}\\
&\quad+[1-\xi]\left\langle\boldsymbol{n}\times\widehat{\boldsymbol{b}}_h^{t,i},\boldsymbol{v}\times\kappa\boldsymbol{d}\right\rangle_{\partial\mathcal{T}_h\setminus\partial\Omega}-[1-\xi]\left\langle\boldsymbol{u}_h\times\kappa\boldsymbol{d},\boldsymbol{n}\times\widehat{\boldsymbol{c}}^t\right\rangle_{\partial\mathcal{T}_h\setminus\partial\Omega}\\
&\quad+\xi\left\langle\widehat{\boldsymbol{u}}_h^i\times\kappa\boldsymbol{d},\boldsymbol{n}\times\boldsymbol{c}\right\rangle_{\partial\mathcal{T}_h\setminus\partial\Omega}-\xi\left\langle\boldsymbol{n}\times\boldsymbol{b}_h,\widehat{\boldsymbol{v}}\times\kappa\boldsymbol{d}\right\rangle_{\partial\mathcal{T}_h\setminus\partial\Omega}\\
&\quad-\left\langle\rho_h,\widehat{\boldsymbol{v}}\cdot\boldsymbol{n}\right\rangle_{\partial\mathcal{T}_h\setminus\partial\Omega}+\left\langle\widehat{\boldsymbol{u}}_h^i\cdot\boldsymbol{n},\psi\right\rangle_{\partial\mathcal{T}_h\setminus\partial\Omega},
\end{aligned}
\tag{5.50}
$$

$$
\begin{aligned}
&\ell\left(\mathbf{G},\boldsymbol{v},q,\boldsymbol{H},\boldsymbol{c},s,\widehat{\boldsymbol{v}},\widehat{\boldsymbol{c}}^t,\widehat{s}\right)=\left(\boldsymbol{f},\boldsymbol{v}\right)_{\mathcal{T}_h}+\left(\boldsymbol{g},\boldsymbol{c}\right)_{\mathcal{T}_h}-\xi\left\langle\widehat{\boldsymbol{u}}_h^D\times\kappa\boldsymbol{d},\boldsymbol{n}\times\boldsymbol{c}\right\rangle_{\partial\Omega}\\
&\quad-\left\langle\widehat{\boldsymbol{u}}_h^D,-\mathbf{G}\boldsymbol{n}+(q-\overline{q})\,\boldsymbol{n}+\frac{1}{2}(\boldsymbol{w}\cdot\boldsymbol{n})\boldsymbol{v}-\mathbf{S}_u\boldsymbol{v}\right\rangle_{\partial\Omega}+\left\langle\boldsymbol{n}\times\widehat{\boldsymbol{b}}_h^{t,D},\boldsymbol{H}\right\rangle_{\partial\Omega}\\
&\quad+\left\langle\beta_t\widehat{\boldsymbol{b}}_h^{t,D},\boldsymbol{c}\right\rangle_{\partial\Omega}-[1-\xi]\left\langle\boldsymbol{n}\times\widehat{\boldsymbol{b}}_h^{t,D},\boldsymbol{v}\times\kappa\boldsymbol{d}\right\rangle_{\partial\Omega}\\
&\quad-\left\langle\widehat{r}_h^D,\boldsymbol{c}\cdot\boldsymbol{n}-\frac{1}{\beta_n}s\right\rangle_{\partial\Omega}-\left\langle\widehat{\boldsymbol{u}}_h^D\cdot\boldsymbol{n},\psi\right\rangle_{\partial\Omega}
\end{aligned}
\tag{5.51}
$$

Setting $\boldsymbol{f}=\mathbf{0}$, $\boldsymbol{g}=\mathbf{0}$, $\boldsymbol{u}_D=\mathbf{0}$, $\boldsymbol{b}_D^t=0$, and $r_D=0$ (and therefore $\widehat{\boldsymbol{u}}_h=\mathbf{0}$, $\widehat{\boldsymbol{b}}_h^t=\mathbf{0}$, and $\widehat{r}_h=0$ on $\partial\Omega$), we have $\ell=0$. Setting $\left(\mathbf{G},\boldsymbol{v},q,\boldsymbol{H},\boldsymbol{c},s,\widehat{\boldsymbol{v}},\widehat{\boldsymbol{c}}^t,\widehat{s},\psi\right)=$

$\left(\mathbf{L}_h, \boldsymbol{u}_h, p_h, \boldsymbol{J}_h, \boldsymbol{b}_h, r_h, \widehat{\boldsymbol{u}}_h^i, \widehat{\boldsymbol{b}}_h^{t,i}, \widehat{r}_h^i, \rho_h\right)$, then $a_{skew} = 0$, and the only remaining terms are a_{sym}, giving

$$\begin{aligned}
&\mathrm{Re}\left(\mathbf{L}_h, \mathbf{L}_h\right)_{\mathcal{T}_h} + \left\langle \mathbf{S}_u\left(\boldsymbol{u}_h - \widehat{\boldsymbol{u}}_h^i\right), \boldsymbol{u}_h - \widehat{\boldsymbol{u}}_h^i\right\rangle_{\partial\mathcal{T}_h\setminus\partial\Omega} + \left\langle \mathbf{S}_u \boldsymbol{u}_h, \boldsymbol{u}_h\right\rangle_{\partial\Omega} \\
&\quad + \frac{\mathrm{Rm}}{\kappa}\left(\boldsymbol{J}_h, \boldsymbol{J}_h\right)_{\mathcal{T}_h} + \left\langle \beta_t\left(\boldsymbol{b}_h^t - \widehat{\boldsymbol{b}}_h^{t,i}\right), \boldsymbol{b}_h^t - \widehat{\boldsymbol{b}}_h^{t,i}\right\rangle_{\partial\mathcal{T}_h\setminus\partial\Omega} + \left\langle \beta_t \boldsymbol{b}_h^t, \boldsymbol{b}_h^t\right\rangle_{\partial\Omega} \\
&\quad + \left\langle \frac{1}{\beta_n}\left(r_h - \widehat{r}_h^i\right), r_h - \widehat{r}_h^i\right\rangle_{\partial\mathcal{T}_h\setminus\partial\Omega} + \left\langle \frac{1}{\beta_n} r_h, r_h\right\rangle_{\partial\Omega} = 0. \qquad (5.52)
\end{aligned}$$

Thus in $\mathcal{T}_h$ we have $\mathbf{L}_h = \mathbf{0}$ and $\boldsymbol{J}_h = \mathbf{0}$, on $\mathcal{E}_h^o$ we have $\boldsymbol{u}_h = \widehat{\boldsymbol{u}}_h^i$, $\boldsymbol{b}_h^t = \widehat{\boldsymbol{b}}_h^{t,i}$, and $r_h = \widehat{r}_h^i$, and on $\partial\Omega$ we have $\boldsymbol{u}_h = \mathbf{0}$, $\boldsymbol{b}_h^t = \mathbf{0}$, and $r_h = 0$.

Equation (5.47a) reduces to $\left(\nabla u_h, \mathbf{G}\right)_{\mathcal{T}_h} = 0$, and since $\nabla \boldsymbol{V}_h \subset \mathbf{G}_h$, we set $\mathbf{G} = \nabla u_h$ to conclude that u_h is elementwise constant. But since $\boldsymbol{u}_h = \widehat{\boldsymbol{u}}_h$ on $\mathcal{E}_h^o$ and $\widehat{\boldsymbol{u}}_h$ is single valued on $\mathcal{E}_h^o$, $\boldsymbol{u}_h$ is continuous across each internal interface, and therefore $\boldsymbol{u}_h$ is globally constant. With the zero boundary condition we conclude $\boldsymbol{u}_h = \mathbf{0}$ and $\widehat{\boldsymbol{u}}_h^i = \mathbf{0}$.

Equation (5.47i) reduces to $\left\langle \boldsymbol{b}_h \cdot \boldsymbol{n}, \widehat{s}\right\rangle_{\partial\mathcal{T}_h\setminus\partial\Omega} = 0$, which implies that the normal component of $\boldsymbol{b}_h$ is continuous across each interior edge, and therefore $\boldsymbol{b}_h \in H(div, \Omega)$. Also, since $\widehat{\boldsymbol{b}}_h^t$ is single valued on $\mathcal{E}_h^o$ and $\boldsymbol{b}_h^t = \widehat{\boldsymbol{b}}_h^t$ on $\mathcal{E}_h^o$, the tangential component of $\boldsymbol{b}_h$ is continuous across each interior edge, and therefore $\boldsymbol{b}_h \in H(curl, \Omega)$. Equation (5.47f) reduces to $\left(\nabla \cdot \boldsymbol{b}_h, s\right)_{\mathcal{T}_h} = 0$, and integration by parts of (5.47d) reduces to $\left(\nabla \times \boldsymbol{b}_h, \boldsymbol{H}\right)_{\mathcal{T}_h} = 0$. Since $\nabla \cdot \boldsymbol{C}_h \subset S_h$ and $\nabla \times \boldsymbol{C}_h \subset \boldsymbol{H}_h$, we set $s = \nabla \cdot \boldsymbol{b}_h$ and $\boldsymbol{H} = \nabla \times \boldsymbol{b}_h$ to conclude that $\nabla \cdot \boldsymbol{b}_h = 0$ and $\nabla \times \boldsymbol{b}_h = \mathbf{0}$ in $\mathcal{T}_h$. It can be shown that when $\boldsymbol{b}_h \in H(div, \Omega) \cap H(curl, \Omega)$ and $\boldsymbol{b}_h^t = \mathbf{0}$ on $\partial\Omega$, and when Ω is simply-connected with one component of the boundary, there is a constant $C > 0$ such that $\left\|\boldsymbol{b}_h\right\|_{L^2(\Omega)} \leq C\left(\left\|\nabla \cdot \boldsymbol{b}_h\right\|_{L^2(\Omega)} + \left\|\nabla \times \boldsymbol{b}_h\right\|_{L^2(\Omega)}\right)$ (see, e.g., [30, Lemma 3.4]). This implies that $\boldsymbol{b}_h = \mathbf{0}$, and hence $\widehat{\boldsymbol{b}}_h^{t,i} = \mathbf{0}$.

Equation (5.47e) reduces to $\left(\nabla r_h, \boldsymbol{c}\right)_{\mathcal{T}_h} = 0$, and since $\nabla S_h \subset \boldsymbol{C}_h$ we can set

$\boldsymbol{c} = \nabla r_h$ to conclude that r_h is elementwise constant. Since $\widehat{r}_h$ is single valued on $\mathcal{E}_h^o$ and $r_h = \widehat{r}_h$ on $\mathcal{E}_h^o$, r_h is continuous and constant over Ω. With the zero boundary condition, we conclude $r_h = 0$ and $\widehat{r}_h^i = 0$.

Equation (5.47e) reduces to $(\nabla p_h, \boldsymbol{v})_{\mathcal{T}_h} = 0$, and since $\nabla Q_h \subset \boldsymbol{V}_h$ we can set $\boldsymbol{v} = \nabla p_h$ to conclude that p_h is elementwise constant. Equation (5.47g) reduces to $\langle p_h, \widehat{\boldsymbol{v}} \cdot \boldsymbol{n} \rangle_{\partial\mathcal{T}_h \backslash \partial\Omega} = 0$, which implies that p_h is continuous across each interior edge. Finally, (5.28) implies p_h is zero, and therefore $\rho_h = 0$. □

We next prove that the local solver, (5.47a) – (5.47f), in Formulation 5.3 is well-posed.

Theorem 5.2. *(well-posedness of the local solver of Formulation 5.3 - steady state) Let τ_t, τ_n, β_t, and β_n be positive. Given $\boldsymbol{f}$, $\widehat{\boldsymbol{u}}_h$, $\widehat{\boldsymbol{b}}_h^t$, $\widehat{r}_h$, and ρ_h, there exists a unique solution $(\mathbf{L}_h, \boldsymbol{u}_h, p_h, \boldsymbol{J}_h, \boldsymbol{b}_h, r_h)$ in $\mathbf{G}_h \times \boldsymbol{V}_h \times Q_h \times \boldsymbol{H}_h \times \boldsymbol{C}_h \times S_h$ to the local equations* (5.47a) – (5.47f).

Proof. It is sufficient to restrict our attention to a single element, and prove that if $\boldsymbol{f}$, $\boldsymbol{g}$, $\widehat{\boldsymbol{u}}_h$, $\widehat{\boldsymbol{b}}_h^t$, $\widehat{r}_h$, ρ_h are zero, then the volume solution $(\mathbf{L}_h, \boldsymbol{u}_h, p_h, \boldsymbol{J}_h, \boldsymbol{b}_h, r_h)$ is zero. We can rewrite the local problem associated with Formulation 5.3 as: find $(\mathbf{L}_h, \boldsymbol{u}_h, p_h, \boldsymbol{J}_h, \boldsymbol{b}_h, r_h)$ in $\mathbf{G}_h(K) \times \boldsymbol{V}_h(K) \times Q_h(K) \times \boldsymbol{H}_h(K) \times \boldsymbol{C}_h(K) \times S_h(K)$ such that

$$
\begin{aligned}
&\mathrm{Re}\,(\mathbf{L}_h, \mathbf{G})_K + \langle \mathbf{S}_u \boldsymbol{u}_h, \boldsymbol{v} \rangle_{\partial K} + \frac{\mathrm{Rm}}{\kappa} (\boldsymbol{J}_h, \boldsymbol{H})_K + \left\langle \beta_t \boldsymbol{b}_h^t, \boldsymbol{c}^t \right\rangle_{\partial K} + \left\langle \frac{1}{\beta_n} r_h, s \right\rangle_{\partial K} \\
&\quad + \langle \overline{p}_h, \overline{q} \rangle_{\partial K} + (\boldsymbol{u}_h, \nabla \cdot \mathbf{G})_K - (\nabla \cdot \mathbf{L}_h, \boldsymbol{v})_K + (\nabla p_h, \boldsymbol{v})_K - (\boldsymbol{u}_h, \nabla q)_K \\
&\quad - \frac{1}{2} (\boldsymbol{u}_h \otimes \boldsymbol{w}, \nabla \boldsymbol{v})_K + \frac{1}{2} (\nabla \boldsymbol{u}_h, \boldsymbol{v} \otimes \boldsymbol{w})_K - (\boldsymbol{b}_h, \nabla \times \boldsymbol{H})_K + (\nabla \times \boldsymbol{J}_h, \boldsymbol{c})_K \\
&\quad - (r_h, \nabla \cdot \boldsymbol{c})_K + (\nabla \cdot \boldsymbol{b}_h, s)_K + (\nabla \times \boldsymbol{b}_h, \boldsymbol{v} \times \kappa \boldsymbol{d})_K - (\boldsymbol{u}_h \times \kappa \boldsymbol{d}, \nabla \times \boldsymbol{c})_K \\
&\quad - [1 - \xi] \left\langle \boldsymbol{n} \times \boldsymbol{b}_h^t, \boldsymbol{v} \times \kappa \boldsymbol{d} \right\rangle_{\partial K} + [1 - \xi] \left\langle \boldsymbol{u}_h \times \kappa \boldsymbol{d}, \boldsymbol{n} \times \boldsymbol{c}^t \right\rangle_{\partial K}
\end{aligned}
$$

$$
\begin{aligned}
&= (\boldsymbol{f}, \boldsymbol{v})_K + (\boldsymbol{g}, \boldsymbol{c})_K - \xi \langle \widehat{\boldsymbol{u}}_h \times \kappa \boldsymbol{d}, \boldsymbol{n} \times \boldsymbol{c} \rangle_{\partial K} + \langle \rho_h, \overline{q} \rangle_{\partial K} \\
&- \left\langle \widehat{\boldsymbol{u}}_h, -\mathbf{G}\boldsymbol{n} + (q - \overline{q})\,\boldsymbol{n} + \frac{1}{2}(\boldsymbol{w} \cdot \boldsymbol{n})\boldsymbol{v} - \mathbf{S}_u \boldsymbol{v} \right\rangle_{\partial K} + \left\langle \boldsymbol{n} \times \widehat{\boldsymbol{b}}_h^t, \boldsymbol{H} \right\rangle_{\partial K} \\
&+ \left\langle \beta_t \widehat{\boldsymbol{b}}_h^t, \boldsymbol{c} \right\rangle_{\partial K} - [1 - \xi] \left\langle \boldsymbol{n} \times \widehat{\boldsymbol{b}}_h^t, \boldsymbol{v} \times \kappa \boldsymbol{d} \right\rangle_{\partial K} - \left\langle \widehat{r}_h, \boldsymbol{c} \cdot \boldsymbol{n} - \frac{1}{\beta_n} s \right\rangle_{\partial K} \qquad (5.53)
\end{aligned}
$$

for all $(\mathbf{G}, \boldsymbol{v}, q, \boldsymbol{H}, \boldsymbol{c}, s)$ in $\mathbf{G}_h(K) \times \boldsymbol{V}_h(K) \times Q_h(K) \times \boldsymbol{H}_h(K) \times \boldsymbol{C}_h(K) \times S_h(K)$. Setting $\boldsymbol{f}$, $\widehat{\boldsymbol{u}}_h$, $\widehat{\boldsymbol{b}}_h^t$, and $\widehat{r}_h$ to zero, and setting $(\mathbf{G}, \boldsymbol{v}, q, \boldsymbol{H}, \boldsymbol{c}, s) = (\mathbf{L}_h, \boldsymbol{u}_h, p_h, \boldsymbol{J}_h, \boldsymbol{b}_h, r_h)$, we have

$$
\begin{aligned}
&\mathrm{Re}\,(\mathbf{L}_h, \mathbf{L}_h)_K + \langle \mathbf{S}_u \boldsymbol{u}_h, \boldsymbol{u}_h \rangle_{\partial K} + \langle \overline{p}_h, \overline{p}_h \rangle_{\partial K} \\
&\qquad + \frac{\mathrm{Rm}}{\kappa} (\boldsymbol{J}_h, \boldsymbol{J}_h)_K + \left\langle \beta_t \boldsymbol{b}_h^t, \boldsymbol{b}_h^t \right\rangle_{\partial K} + \left\langle \frac{1}{\beta_n} r_h, r_h \right\rangle_{\partial K} = 0. \qquad (5.54)
\end{aligned}
$$

Thus in K we have $\mathbf{L}_h = \mathbf{0}$ and $\boldsymbol{J}_h = \mathbf{0}$, and on ∂K we have $\boldsymbol{u}_h = \mathbf{0}$, $\overline{p}_h = 0$, $\boldsymbol{b}_h^t = \mathbf{0}$, and $r_h = 0$.

What remains of (5.47a) gives that $\boldsymbol{u}_h$ is constant in K, and since $\boldsymbol{u}_h = \mathbf{0}$ on ∂K, that $\boldsymbol{u}_h = \mathbf{0}$ in K. What remains of (5.47d) and (5.47f) give that $\nabla \times \boldsymbol{b}_h$ and $\nabla \cdot \boldsymbol{b}_h$ are zero. Since $\boldsymbol{b}_h \in H(div, K) \cap H(curl, K)$ and $\boldsymbol{b}_h^t = \mathbf{0}$ on ∂K, we again invoke [30, Lemma 3.4] to conclude $\boldsymbol{b}_h = \mathbf{0}$. What remains of (5.47e) gives that r_h is constant in K, and since $r_h = 0$ on ∂K, that $r_h = 0$ in K. What remains of (5.47b) gives that p_h is constant in K, and therefore $p_h = 0$ since $\overline{p}_h = 0$ on ∂K. □

It can be shown that the condensed (volume unknowns eliminated) matrix system associated with the steady state version of Formulation 5.3 takes the form

$$
\begin{bmatrix} A & B & E & G \\ -B^\top & 0 & 0 & 0 \\ F & 0 & C & J \\ H & 0 & K & L \end{bmatrix} \begin{bmatrix} \widehat{U} \\ \rho \\ \widehat{B}^t \\ \widehat{R} \end{bmatrix} = \begin{bmatrix} F_1 \\ F_2 \\ F_3 \\ F_4 \end{bmatrix}, \qquad (5.55)
$$

where C is positive semi-definite, and A and L are positive definite. The matrix form and positive definiteness can be revealed in a similar manner as was done for the

HDG schemes for the Stokes equations in Chapter 2 and in Appendix B. The details for this MHD scheme are omitted.

So far we have discussed the well-posedness and matrix formulation of the steady state version of Formulation 5.3. It turns out that the semidiscrete version and fully discrete version with implicit time stepping of Formulation 5.3 are well-posed without the assumption that Ω is simply connected and $\partial\Omega$ has one component.

Theorem 5.3. *(well-posedness of Formulation 5.3 - semidiscrete)*
Let τ_t, τ_n, β_t, and β_n be positive. The semidiscrete version of the HDG Formulation 5.3 is well-posed in the sense that given $\boldsymbol{f}$, $\boldsymbol{u}_D$, $\boldsymbol{b}_D^t$, r_D, $\boldsymbol{u}(t=0)$ and $\boldsymbol{b}(t=0)$ there exists a unique solution $\left(\mathbf{L}_h, \boldsymbol{u}_h, p_h, \boldsymbol{J}_h, \boldsymbol{b}_h, r_h, \widehat{\boldsymbol{u}}_h, \widehat{\boldsymbol{b}}_h^t, \widehat{r}_h, \rho_h\right)$ to Formulation 5.3.

Proof. Once again we take an energy approach to prove that the null space of the linear operator is empty. The proof follows the proof of Theorem 5.1 for the steady state version of Formulation 5.3. Setting all forcing (including boundary conditions and initial conditions) to zero and setting test functions to their solution counterparts, instead of (5.52), with the additional terms due to the time discretization we have

$$\begin{aligned}\frac{1}{2}\frac{\partial}{\partial t}\left(\boldsymbol{u}_h, \boldsymbol{u}_h\right)_{\mathcal{T}_h} + \frac{1}{2}\frac{\partial}{\partial t}\kappa\left(\boldsymbol{b}_h, \boldsymbol{b}_h\right)_{\mathcal{T}_h} + \mathrm{Re}\left(\mathbf{L}_h, \mathbf{L}_h\right)_{\mathcal{T}_h} + \frac{\mathrm{Rm}}{\kappa}\left(\boldsymbol{J}_h, \boldsymbol{J}_h\right)_{\mathcal{T}_h} + \left\langle \mathbf{S}_u \boldsymbol{u}_h, \boldsymbol{u}_h\right\rangle_{\partial\Omega} \\ + \left\langle \mathbf{S}_u\left(\boldsymbol{u}_h - \widehat{\boldsymbol{u}}_h^i\right), \boldsymbol{u}_h - \widehat{\boldsymbol{u}}_h^i\right\rangle_{\partial\mathcal{T}_h\setminus\partial\Omega} + \left\langle \beta_t\left(\boldsymbol{b}_h^t - \widehat{\boldsymbol{b}}_h^{t,i}\right), \boldsymbol{b}_h^t - \widehat{\boldsymbol{b}}_h^{t,i}\right\rangle_{\partial\mathcal{T}_h\setminus\partial\Omega} \\ + \left\langle \beta_t \boldsymbol{b}_h^t, \boldsymbol{b}_h^t\right\rangle_{\partial\Omega} + \left\langle \frac{1}{\beta_n}\left(r_h - \widehat{r}_h^i\right), r_h - \widehat{r}_h^i\right\rangle_{\partial\mathcal{T}_h\setminus\partial\Omega} + \left\langle \frac{1}{\beta_n} r_h, r_h\right\rangle_{\partial\Omega} = 0. \end{aligned} \tag{5.56}$$

From the nonnegativeness of the terms without time derivatives, it can be seen that

$$\frac{\partial}{\partial t}\left[\left(\boldsymbol{u}_h, \boldsymbol{u}_h\right)_{\mathcal{T}_h} + \kappa\left(\boldsymbol{b}_h, \boldsymbol{b}_h\right)_{\mathcal{T}_h}\right] \leq 0. \tag{5.57}$$

Integrating this over the time interval $[0, T]$ for an arbitrary time T and using the zero initial conditions gives

$$\left(\boldsymbol{u}_h(T), \boldsymbol{u}_h(T)\right)_{\mathcal{T}_h} + \kappa\left(\boldsymbol{b}_h(T), \boldsymbol{b}_h(T)\right)_{\mathcal{T}_h} \leq 0, \tag{5.58}$$

and therefore that $\boldsymbol{u}_h$ and $\boldsymbol{b}_h$ are zero for all time. Returning to (5.56), we can immediately conclude $\mathbf{L}_h$, $\boldsymbol{J}_h$, $\widehat{\boldsymbol{u}}_h$, and $\widehat{\boldsymbol{b}}_h^t$ are zero, and we complete the proof by showing that p_h, r_h, and $\widehat{r}_h$ are zero in an identical manner as in the proof of Theorem 5.1. $\square$

For the implicit Euler time discretization, the term $\left(\frac{\partial \boldsymbol{u}_h}{\partial t}, \boldsymbol{c}\right)_{\mathcal{T}_h}$ is replaced by $\frac{1}{\Delta t}\left(\boldsymbol{u}_h, \boldsymbol{c}\right)_{\mathcal{T}_h} - \frac{1}{\Delta t}\left(\boldsymbol{u}_h^{n-1}, \boldsymbol{c}\right)_{\mathcal{T}_h}$, and similarly the term $\left(\frac{\partial \boldsymbol{b}_h}{\partial t}, \boldsymbol{v}\right)_{\mathcal{T}_h}$ is replaced by $\frac{1}{\Delta t}\left(\boldsymbol{b}_h, \boldsymbol{c}\right)_{\mathcal{T}_h} - \frac{1}{\Delta t}\left(\boldsymbol{b}_h^{n-1}, \boldsymbol{c}\right)_{\mathcal{T}_h}$. Thus the fully discrete, implicit formulation is the same as the steady state one, with the addition of volume integrals on $\boldsymbol{u}_h$ and $\boldsymbol{b}_h$ and forcing terms, and where all variables are to be interpreted as being at the nth time step. This statement holds for other fully implicit time discretization techniques such as the backward difference formulas (BDF), and for each stage of a diagonally implicit Runge-Kutta (DIRK) method, but is most easily demonstrated for implicit Euler.

Theorem 5.4. *(well-posedness of Formulation 5.3 - fully discrete)*
Let τ_t, τ_n, β_t, and β_n be positive. The fully discrete version of the HDG Formulation 5.3 is well-posed in the sense that given $\boldsymbol{f}$, $\boldsymbol{u}_D$, $\boldsymbol{b}_D^t$, r_D, $\boldsymbol{u}_h^{n-1}$ and ${\boldsymbol{b}_h}^{n-1}$ there exists a unique solution $\left(\mathbf{L}_h, \boldsymbol{u}_h, p_h, \boldsymbol{J}_h, \boldsymbol{b}_h, r_h, \widehat{\boldsymbol{u}}_h, \widehat{\boldsymbol{b}}_h^t, \widehat{r}_h, \rho_h\right)$ for time step n to Formulation 5.3 where the time derivatives are discretized using a fully implicit method.

Proof. Once again we take an energy approach to prove that the null space of the linear operator is empty. The proof follows the proof of Theorem 5.1 for the steady state version of Formulation 5.3. Setting all forcing (including boundary conditions and previous time step solutions) to zero and setting test functions to their solution counterparts, instead of (5.52), with the additional terms due to the time derivatives

we have

$$\sigma\left(\boldsymbol{u}_h,\boldsymbol{u}_h\right)_{\mathcal{T}_h}+\kappa\sigma\left(\boldsymbol{b}_h,\boldsymbol{b}_h\right)_{\mathcal{T}_h}+\mathrm{Re}\left(\mathbf{L}_h,\mathbf{L}_h\right)_{\mathcal{T}_h}+\frac{\mathrm{Rm}}{\kappa}\left(\boldsymbol{J}_h,\boldsymbol{J}_h\right)_{\mathcal{T}_h}+\left\langle\mathbf{S}_u\boldsymbol{u}_h,\boldsymbol{u}_h\right\rangle_{\partial\Omega}$$
$$+\left\langle\mathbf{S}_u\left(\boldsymbol{u}_h-\widehat{\boldsymbol{u}}_h^i\right),\boldsymbol{u}_h-\widehat{\boldsymbol{u}}_h^i\right\rangle_{\partial\mathcal{T}_h\setminus\partial\Omega}+\left\langle\beta_t\left(\boldsymbol{b}_h^t-\widehat{\boldsymbol{b}}_h^{t,i}\right),\boldsymbol{b}_h^t-\widehat{\boldsymbol{b}}_h^{t,i}\right\rangle_{\partial\mathcal{T}_h\setminus\partial\Omega}$$
$$+\left\langle\beta_t\boldsymbol{b}_h^t,\boldsymbol{b}_h^t\right\rangle_{\partial\Omega}+\left\langle\frac{1}{\beta_n}\left(r_h-\widehat{r}_h^i\right),r_h-\widehat{r}_h^i\right\rangle_{\partial\mathcal{T}_h\setminus\partial\Omega}+\left\langle\frac{1}{\beta_n}r_h,r_h\right\rangle_{\partial\Omega}=0,\quad(5.59)$$

where σ represents time discretization of the volume term ($\frac{1}{\Delta t}$ for implicit Euler, for example). Thus we immediately conclude from the nonnegativeness of the left hand side that in $\mathcal{T}_h$ it holds that $\mathbf{L}_h$, $\boldsymbol{J}_h$, $\boldsymbol{b}_h$, and $\boldsymbol{u}_h$ are zero, and that on $\mathcal{E}_h$ it holds that $\widehat{\boldsymbol{u}}_h=\boldsymbol{u}_h=\mathbf{0}$ and $\widehat{\boldsymbol{b}}_h^t=\boldsymbol{b}_h^t=\mathbf{0}$. We complete the proof by proving that p_h, r_h, and $\widehat{r}_h$ are zero in an identical manner as in the proof of Theorem 5.1. □

Finally, we note that the well-posedness of the local solver in both the semidiscrete and fully discrete implicit formulations follows. We omit the proofs.

5.5 Error Analysis

A significant part of this work is a projection-based a priori error analysis for Formulation 5.3, which uses the $(\widehat{\boldsymbol{u}}_h,\widehat{\boldsymbol{b}}_h^t,\widehat{r}_h)$ flux (5.46). The work in this section can be found in [46].

In this section we make some additional assumptions. We assume that the Ω is simply connected with $\partial\Omega$ a Lipschitz manifold with only one component, and that $\mathcal{T}_h$ is a conforming simplicial mesh. We assume that the triangulation is shape-regular, i.e., for all d-dimensional simplices in the triangulation, the ratio of the diameter of the simplex and the radius of an inscribed d-dimensional ball is uniformly bounded. The error analysis that follows is valid for polynomial spaces $\mathbf{G}_h(K)$, $\boldsymbol{V}_h(K)$, $\widehat{\boldsymbol{V}}_h(e)$, etc., of degree at most k on volume element K and face element e. Such polynomial spaces we denote by $\mathcal{P}_k(K)$ for scalar valued polynomials on K, by $[\mathcal{P}_k(K)]^d$ for vector valued

polynomials on K, by $[\mathcal{P}_k(K)]^{d\times d}$ for tensor valued polynomials on K, and by similar notation for polynomials on e, $\mathcal{T}_h$, $\mathcal{E}_h$, etc. The well-posedness of all of the HDG schemes presented in this work up to this point are valid for more general polynomial spaces, for example, tensor product polynomial spaces. We additionally assume that $\boldsymbol{w}, \boldsymbol{d} \in W^{1,\infty}(\Omega)$. We analyze the steady state ($\frac{\partial}{\partial t} = 0$) version of Formulation 5.3 with specific choices for the parameters. We choose the flux parameters as follows,

$$\xi = \frac{1}{2}, \tag{5.60a}$$

$$\tau_t = \tau_n = \alpha_1 + \frac{1}{2}\boldsymbol{w}\cdot\boldsymbol{n} \text{ for } \alpha_1 > \frac{1}{2}\left\|\boldsymbol{w}\right\|_{L^\infty(\Omega)}, \tag{5.60b}$$

$$\beta_t = \alpha_2 > 0, \tag{5.60c}$$

$$\beta_n = \frac{1}{\alpha_3} \text{ for } \alpha_3 > 0. \tag{5.60d}$$

Note that for well-posedness it is only necessary that $\alpha_1|_{\partial K} > -\frac{1}{2}\boldsymbol{w}|_{\partial K}\cdot\boldsymbol{n}$, but we have chosen the above definition for simplicity. Writing this flux [1] explicitly gives

$$\boldsymbol{F}^*_{n,h} = \begin{pmatrix} -\widehat{\boldsymbol{u}}_h \otimes \boldsymbol{n}, \\ -\mathbf{L}_h\boldsymbol{n} + p_h\boldsymbol{n} + (\boldsymbol{w}\cdot\boldsymbol{n})\boldsymbol{u}_h + \alpha_1\left(\boldsymbol{u}_h - \widehat{\boldsymbol{u}}_h\right) \\ \quad +\kappa\boldsymbol{d}\times\left(\boldsymbol{n}\times\left(\frac{1}{2}\boldsymbol{b}_h^t + \frac{1}{2}\widehat{\boldsymbol{b}}_h^t\right)\right), \\ \widehat{\boldsymbol{u}}_h\cdot\boldsymbol{n}, \\ -\boldsymbol{n}\times\widehat{\boldsymbol{b}}_h^t, \\ \boldsymbol{n}\times\boldsymbol{J}_h + \widehat{r}_h\boldsymbol{n} + \alpha_2\left(\boldsymbol{b}_h^t - \widehat{\boldsymbol{b}}_h^t\right) \\ -\boldsymbol{n}\times\left(\left(\frac{1}{2}\boldsymbol{u}_h + \frac{1}{2}\widehat{\boldsymbol{u}}_h\right)\times\kappa\boldsymbol{d}\right), \\ \boldsymbol{b}_h\cdot\boldsymbol{n} + \alpha_3\left(r_h - \widehat{r}_h\right) \end{pmatrix}. \tag{5.61}$$

For an unknown σ we use ε_σ to denote the error between the exact solution σ and its finite element approximation σ_h. For example, $\varepsilon_{\mathbf{L}} := \mathbf{L} - \mathbf{L}_h$ and $\varepsilon_{\widehat{\boldsymbol{u}}} := \widehat{\boldsymbol{u}} - \widehat{\boldsymbol{u}}_h$, where $\widehat{\boldsymbol{u}}$ is the trace of the exact solution $\boldsymbol{u}$ on the mesh skeleton. With this definition we state the main result.

[1] The HDG scheme with this flux was first presented in September 2015 and appears in [66, 46, 47].

Theorem 5.5. *Let Ω be simply connected and $\partial\Omega$ connected. Choose α_1, α_2, and α_3 to be positive constants independent of h,* Re, Rm, *κ, $\boldsymbol{d}$, and $\boldsymbol{w}$ and to satisfy* (5.60)*. Suppose also that h is sufficiently small. Then the following error estimates hold for the numerical solution given by Formulation 5.3 to the steady state incompressible MHD equations:*

$$\begin{aligned}
\|e_{\mathbf{L}}, e_{\boldsymbol{H}}\|_{L^2(\Omega)} &\lesssim h^{k+\frac{1}{2}} \|\mathbf{L}, \boldsymbol{u}, p, \boldsymbol{J}, \boldsymbol{b}, r\|_{H^{k+1}(\Omega)}, \\
\|e_{\boldsymbol{u}}, e_{\boldsymbol{b}}\|_{L^2(\Omega)} &\lesssim h^{k+1} \|\mathbf{L}, \boldsymbol{u}, p, \boldsymbol{J}, \boldsymbol{b}, r\|_{H^{k+1}(\Omega)}, \\
\|e_p, e_r\|_{L^2(\Omega)} &\lesssim h^{k+\frac{1}{2}} \|\mathbf{L}, \boldsymbol{u}, p, \boldsymbol{J}, \boldsymbol{b}, r\|_{H^{k+1}(\Omega)}.
\end{aligned}$$

In the above error bounds, all terms independent of h are absorbed into the inequalities. As the proof for the above theorem is quite long and technical, we first describe an outline of the proof before addressing each part in detail. The analysis is a projection-based analysis. That is, we use $\Pi\sigma$ to denote some projection (will be defined later) of the unknown σ into its associated finite element space, and decompose ε_σ into $\varepsilon_\sigma^I + \varepsilon_\sigma^h$ where

$$\varepsilon_\sigma^I := \sigma - \Pi\sigma, \qquad \text{and} \qquad \varepsilon_\sigma^h := \Pi\sigma - \sigma_h. \tag{5.62}$$

We will call the ε^I and ε^h error terms as interpolation and approximation errors, respectively. We will define a collective projection $\boldsymbol{\Pi}(\mathbf{L}, \boldsymbol{u}, p, \boldsymbol{H}, \boldsymbol{b}, r, \widehat{\boldsymbol{u}}, \widehat{\boldsymbol{b}}^t, \widehat{r})$ where each component of $\boldsymbol{\Pi}$ may depend on other unknowns, i.e., the $\mathbf{L}$-component of $\boldsymbol{\Pi}(\mathbf{L}, \boldsymbol{u}, p)$ also depends on $\boldsymbol{u}$ and p. Nonetheless, for simplicity of presentation we use $\Pi\mathbf{L}$ to denote the $\mathbf{L}$-component of $\boldsymbol{\Pi}$ for example.

In the following subsections, we proceed through each step of the process.

- Define the projections and prove their optimality.
- Write the error equations and derive an energy estimate.

- Write the adjoint equations and specify a regularity assumption.
- Define the adjoint projections and prove their optimality.
- Prove an estimate for $\varepsilon_{\boldsymbol{u}}^h$ and $\varepsilon_{\boldsymbol{b}}^h$
- Put the steps together to arrive at the final error bounds.

In addition to the notation defined in Appendix A that is common in this entire work, we define here some additional notation used in this error analysis. The standard notation $W^{s,p}(D)$, $s \geq 0$, $1 \leq p \leq \infty$, is used for the Sobolev space on D based on L^p-norm with differentiability s (see, e.g., [27]) and $\|\cdot\|_{W^{s,p}(D)}$ denotes the associated norm. In particular, if $p = 2$, we use $H^s(D) := W^{s,p}(D)$ and $\|\cdot\|_{s,D}$. The symbol $W^{s,p}(\mathcal{T}_h)$ denotes the space of functions whose restrictions on K reside in $W^{s,p}(K)$ for each $K \in \mathcal{T}_h$ and its norm is $\|u\|^p_{W^{s,p}(\mathcal{T}_h)} := \sum_{K\in\mathcal{T}_h} \|u|_K\|^p_{W^{s,p}(K)}$ if $1 \leq p < \infty$ and $\|u\|_{W^{s,\infty}(\mathcal{T}_h)} := \max_{K\in\mathcal{T}_h} \|u|_K\|_{W^{s,\infty}(K)}$. For simplicity, we use $(\cdot,\cdot)$ for $(\cdot,\cdot)_{\mathcal{T}_h}$, $\langle\cdot,\cdot\rangle$ for $\langle\cdot,\cdot\rangle_{\partial\mathcal{T}_h}$, $\|\cdot\|_s$ for $\|\cdot\|_{s,\mathcal{T}_h}$, $\|\cdot\|_{\partial\mathcal{T}_h}$ for $\|\cdot\|_{0,\partial\mathcal{T}_h}$, $\|\cdot\|_{L^\infty}$ for $\|\cdot\|_{L^\infty(\mathcal{T}_h)}$, and $\|\cdot\|_{W^{s,\infty}}$ for $\|\cdot\|_{W^{s,\infty}(\mathcal{T}_h)}$. We define $\|u, v\| := \|u\| + \|v\|$. Furthermore, we denote by $A \lesssim B$ the inequality $A \leq \lambda B$ with a constant $\lambda > 0$ independent of the mesh size, and by $A \sim B$ the combination of $A \lesssim B$ and $B \lesssim A$. We will often use $\boldsymbol{\mathcal{P}}_k := \mathcal{P}_k^d$ and $\tilde{\boldsymbol{\mathcal{P}}}_k := \mathcal{P}_k^{d\times d}$ to denote vector-valued and tensor-valued polynomials of order at most k. By $\mathcal{P}_k^\perp$, $\boldsymbol{\mathcal{P}}_k^\perp$, $\tilde{\boldsymbol{\mathcal{P}}}_k^\perp$ we denote the spaces of polynomials of order at most k orthogonal to all polynomials of order at most $(k-1)$. The space $\boldsymbol{\mathcal{P}}_k^t(e)$ contains the tangential component of all polynomials in $\boldsymbol{\mathcal{P}}_k(e)$.

5.5.1 Auxiliary Lemmas

Before we proceed, we collect some technical results that are useful for our analysis.

Lemma 5.6 (Inverse Inequality. [57, Lemma 1.44]). *For $v \in \mathcal{P}_k(K)$ with $K \in \mathcal{T}_h$, there exists $C > 0$ independent of h such that*

$$\|\nabla v\|_{0,K} \leq C h_K^{-1} \|v\|_{0,K}.$$

Lemma 5.7 (Trace inequality. [57, Lemma 1.49]). *For $v \in H^1(\mathcal{T}_h)$ and for $K \in \mathcal{T}_h$ with $e \subset \partial K$, there exists $C > 0$ independent of h such that*

$$\|v\|_{0,e}^2 \leq C \left(\|\nabla v\|_{0,K} + h_K^{-1} \|v\|_{0,K} \right) \|v\|_{0,K}.$$

Applying the arithmetic-geometric mean inequality to the right side, we can derive

$$\|v\|_{0,e} \lesssim \left(h_k^{\frac{1}{2}} \|\nabla v\|_{0,K} + h_K^{-\frac{1}{2}} \|v\|_{0,K} \right). \tag{5.63}$$

If $v \in H^1(\mathcal{T}_h)$ is in piecewise polynomial spaces, we can derive the following inequality from Lemma 5.7 and the inverse inequality (Lemma 5.6):

$$\|v\|_{0,e} \lesssim h_K^{-\frac{1}{2}} \|v\|_{0,K}. \tag{5.64}$$

Lemma 5.8. *Suppose that $\Pi : H^1(K) \to \mathcal{P}_k(K)$ is a bounded interpolation which is a projection on $\mathcal{P}_k(K)$, and that $(\Pi \boldsymbol{v} - \boldsymbol{v})_{0,K} \lesssim h \|\boldsymbol{v}\|_{1,K}$. Then*

$$\|\nabla \Pi \boldsymbol{v}\|_{0,K} \lesssim \|\boldsymbol{v}\|_{1,K}.$$

Proof. For any constant c, $\nabla \Pi \boldsymbol{v} = \nabla (\Pi \boldsymbol{v} - c)$, so

$$\begin{aligned} \|\nabla \Pi \boldsymbol{v}\|_{0,K} &= \|\nabla (\Pi \boldsymbol{v} - c)\|_{0,K} \\ &\lesssim h^{-1} \|\Pi \boldsymbol{v} - c\|_{0,K} \lesssim h^{-1} \left(\|\Pi \boldsymbol{v} - \boldsymbol{v}\|_{0,K} + \|\boldsymbol{v} - c\|_{0,K} \right) \lesssim \|\boldsymbol{v}\|_{1,K}, \end{aligned}$$

where we have used the Poincaré inequality and the approximation property of Π in the last inequality. □

The following is an interpolation error bound on an element domain K. For the interpolation $\mathfrak{I} : W^{m,p}(K) \to \mathcal{P}_k(K)$ we have for $m \leq k+1$ and $1 \leq p \leq \infty$ that

$$\|v - \mathfrak{I}v\|_{W^{s,p}(K)} \leq Ch^{m-s} |v|_{W^{m,p}(K)}, \tag{5.65}$$

for $v \in W^{m,p}(K)$ and $0 \leq s \leq m$, where C is a constant independent of h. For details and generalizations, see [8, Chapter 4.4].

5.5.2 Definition of Projections and Their Properties

We desire to have error equations conform to the original equations to facilitate the error analysis. To begin, we define a collective interpolation operator $\mathbf{\Pi}\left(\mathbf{L}, \boldsymbol{u}, p, \boldsymbol{J}, \boldsymbol{b}, r, \widehat{\boldsymbol{u}}, \widehat{\boldsymbol{b}}^t, \widehat{r}\right)$ implicitly through the interpolation errors $\varepsilon_{\boldsymbol{u}}^I = \boldsymbol{u} - \Pi\boldsymbol{u}$, $\varepsilon_{\boldsymbol{b}}^I = \boldsymbol{b} - \Pi\boldsymbol{b}$, etc, where $\Pi\boldsymbol{u}$, $\Pi\boldsymbol{b}$, etc, are components of the collective projection $\mathbf{\Pi}$ on $\boldsymbol{u}, \boldsymbol{b}$, etc. Specifically:

- The L^2 projections on $e \in \mathcal{E}_h$ or on $K \in \mathcal{T}_h$ are defined as:

$$\left(\varepsilon_p^I, q\right)_K = 0, \quad q \in \mathcal{P}_k(K), \tag{5.66a}$$

$$\left(\varepsilon_{\boldsymbol{J}}^I, \boldsymbol{H}\right)_K = 0, \quad \boldsymbol{J} \in [\mathcal{P}_k(K)]^{\tilde{d}}, \tag{5.66b}$$

$$\left\langle \varepsilon_{\widehat{\boldsymbol{u}}}^I, \widehat{\boldsymbol{v}} \right\rangle_e = 0, \quad \widehat{\boldsymbol{v}} \in \boldsymbol{\mathcal{P}}_k(e), \tag{5.66c}$$

$$\left\langle \varepsilon_{\widehat{\boldsymbol{b}}^t}^I, \widehat{\boldsymbol{c}}^t \right\rangle_e = 0, \quad \widehat{\boldsymbol{c}}^t \in \boldsymbol{\mathcal{P}}_k^t(e), \tag{5.66d}$$

$$\left\langle \varepsilon_{\widehat{r}}^I, \widehat{s} \right\rangle_e = 0, \quad \widehat{s} \in \mathcal{P}_k(e). \tag{5.66e}$$

- On each $K \in \mathcal{T}_h$ and $e \in \mathcal{E}_h$ where $e \subset \partial K$, $\Pi\boldsymbol{b}$ and Πr are defined as

$$(\varepsilon_{\boldsymbol{b}}^I, \boldsymbol{c})_K = 0, \quad \boldsymbol{c} \in \boldsymbol{\mathcal{P}}_{k-1}(K), \tag{5.66f}$$

$$(\varepsilon_r^I, s)_K = 0, \quad s \in \mathcal{P}_{k-1}(K), \tag{5.66g}$$

$$\left\langle \varepsilon_{\boldsymbol{b}}^I \cdot \boldsymbol{n} + \alpha_3 \varepsilon_r^I, \widehat{s} \right\rangle_e = 0, \quad \widehat{s} \in \mathcal{P}_k(e). \tag{5.66h}$$

- On each $K \in \mathfrak{T}_h$ and $e \in \mathcal{E}_h$ where $e \subset \partial K$, $\Pi\mathbf{L}$ and $\Pi\boldsymbol{u}$ are defined as

$$-\left(\varepsilon_{\mathbf{L}}^I, \mathbf{G}\right)_K + \left(\varepsilon_{\boldsymbol{u}}^I \otimes \boldsymbol{w}, \mathbf{G}\right)_K = 0, \quad \mathbf{G} \in \tilde{\boldsymbol{\mathcal{P}}}_{k-1}(K), \tag{5.66i}$$

$$\left(\varepsilon_{\boldsymbol{u}}^I, \boldsymbol{v}\right)_K = 0, \quad \boldsymbol{v} \in \boldsymbol{\mathcal{P}}_{k-1}(K), \tag{5.66j}$$

$$\begin{aligned}&\left\langle -\varepsilon_{\mathbf{L}}^I \boldsymbol{n} + (m + \alpha_1)\,\varepsilon_{\boldsymbol{u}}^I, \widehat{\boldsymbol{v}}\right\rangle_e \\ &\quad = -\langle \varepsilon_p^I \boldsymbol{n} + \frac{1}{2}\kappa \boldsymbol{d} \times (\boldsymbol{n} \times (\varepsilon_{\boldsymbol{b}^t}^I + \varepsilon_{\widehat{\boldsymbol{b}}^t}^I)), \widehat{\boldsymbol{v}}\rangle_e, \quad \widehat{\boldsymbol{v}} \in \boldsymbol{\mathcal{P}}_k(e),\end{aligned} \tag{5.66k}$$

where $m := \boldsymbol{w} \cdot \boldsymbol{n}$ from this point forward. The well-definedness and optimality of the L^2-projections are clear. The coupled projector $\Pi(\boldsymbol{b}, r) := (\Pi\boldsymbol{b}, \Pi r)$ has been studied in [22], and in particular we have

$$\|\varepsilon_{\boldsymbol{b}}^I\|_{0,K} \lesssim h^{k+1} \|\boldsymbol{b}\|_{k+1,K} + \alpha_3 h^{k+1} \|r\|_{k+1,K}, \tag{5.67a}$$

$$\|\varepsilon_r^I\|_{0,K} \lesssim \alpha_3^{-1} h^{k+1} \|\nabla \cdot \boldsymbol{b}\|_{k,K} + h^{k+1} \|r\|_{k+1,K}, \tag{5.67b}$$

where, again, for simplicity we choose the same solution order k for all the unknowns. Here, we assume that $\boldsymbol{b}$ and r are sufficiently smooth, that is, $\boldsymbol{b} \in \left[H^{k+1}(\Omega)\right]^d$ and $r \in H^{k+1}(\Omega)$.

The following results for $\varepsilon_{\boldsymbol{u}}^I$ and $\varepsilon_{\mathbf{L}}^I$ are proven in Appendix D.

Lemma 5.9 (estimate for $\varepsilon_{\boldsymbol{u}}^I$)**.** *Suppose* $\boldsymbol{u} \in \left[H^{k+1}(\Omega)\right]^d$, $\mathbf{L} \in \left[H^{k+1}(\Omega)\right]^{d\times d}$, $r \in H^{k+1}(\Omega)$, $\boldsymbol{b} \in \left[H^{k+1}(\Omega)\right]^d$, *and* $p \in H^{k+1}(\Omega)$. *The projection* $\Pi\boldsymbol{u}$ *is well-defined and optimal, i.e.,*

$$\begin{aligned}\|\varepsilon_{\boldsymbol{u}}^I\|_0 \lesssim\ & C(\alpha_1, \boldsymbol{w})[(\alpha_1 + \|\boldsymbol{w}\|_{L^\infty} + h\,\|\boldsymbol{w}\|_{W^{1,\infty}}) h^{k+1} \|\boldsymbol{u}\|_{k+1} \\ & + h^{k+1} \|\nabla \cdot \mathbf{L} - \nabla p\|_k + \kappa h^{k+1} \|\boldsymbol{d}\|_{L^\infty} (\|\boldsymbol{b}\|_{k+1} + \alpha_3 \|r\|_{k+1})]\end{aligned}$$

where $C(\alpha_1, \boldsymbol{w}) = 1/(\alpha_1 - \frac{1}{2}\|\boldsymbol{w}\|_{L^\infty})$.

Lemma 5.10 (estimate for $\varepsilon^I_{\mathbf{L}}$)**.** *Assume* $\boldsymbol{u} \in \left[H^{k+1}(\Omega)\right]^d$, $\mathbf{L} \in \left[H^{k+1}(\Omega)\right]^{d\times d}$, $r \in H^{k+1}(\Omega), \boldsymbol{b} \in \left[H^{k+1}(\Omega)\right]^d$, *and* $p \in H^{k+1}(\Omega)$. *Furthermore, suppose the trace of the tensor* $\mathbf{L}$ *vanishes, i.e.,* $\operatorname{tr}\mathbf{L} = 0$. *There holds:*

$$\begin{aligned}\left\|\varepsilon^I_{\mathbf{L}}\right\|_0 \lesssim\ & h^{k+1}\|p\|_{k+1} + h^{k+1}\|\mathbf{L}\|_{k+1} + \kappa\|\boldsymbol{d}\|_{L^\infty}\left(h^{k+1}\|\boldsymbol{b}\|_{k+1} + \alpha_3 h^{k+1}\|r\|_{k+1}\right)\\ &+ \left(\alpha_1 + \|\boldsymbol{w}\|_{L^\infty} + h\|\boldsymbol{w}\|_{W^{1,\infty}}\right)\left\|\varepsilon^I_{\boldsymbol{u}}\right\|_0 + \left(\alpha_1 + \|\boldsymbol{w}\|_{L^\infty}\right)h^{k+1}\|\boldsymbol{u}\|_{k+1}.\end{aligned}$$

5.5.3 The Error Equations and an Energy Estimate

In this subsection, we derive an energy estimate based on the projections we have just defined.

Lemma 5.11. *Assume that the exact solution* $(\mathbf{L}, \boldsymbol{u}, p, \boldsymbol{J}, \boldsymbol{b}, r)$ *of* (5.9) *with boundary conditions* (5.7) – (5.8) *is sufficiently regular. Then the exact solution satisfies the equations of Formulation 5.3. That is, replacing* $(\mathbf{L}_h, \boldsymbol{u}_h, p_h, \boldsymbol{J}_h, \boldsymbol{b}_h, r_h, \widehat{\boldsymbol{u}}_h, \widehat{\boldsymbol{b}}^t_h, \widehat{r}_h)$ *with the exact solution* $(\mathbf{L}, \boldsymbol{u}, p, \boldsymbol{J}, \boldsymbol{b}, r, \boldsymbol{u}, \boldsymbol{b}, r)$ *in* (5.47)*, then the equations* (5.47) *hold true for all* $(\boldsymbol{G}, \boldsymbol{v}, q, \boldsymbol{J}, \boldsymbol{c}, s, \widehat{\boldsymbol{v}}, \widehat{\boldsymbol{c}}^t, \widehat{s})$ *in* $\mathbf{G}_h \times \boldsymbol{V}_h \times Q_h \times \boldsymbol{H}_h \times \boldsymbol{C}_h \times S_h \times \widehat{\boldsymbol{V}}_h \times \widehat{\boldsymbol{C}}^t_h \times \widehat{S}_h$.

Proof. The assertion follows from the sufficient regularity assumption of the exact solution and single-valuedness of $\mathbf{N}\boldsymbol{w}$ and $\boldsymbol{d}$. See [47] for details. □

Lemma 5.12 (Error equation)**.** *The approximation errors satisfy*

$$\begin{aligned}E_h^2 :=\ & \operatorname{Re}\left\|\varepsilon^h_{\mathbf{L}}\right\|_0^2 + \frac{\mathrm{Rm}}{\kappa}\left\|\varepsilon^h_{\boldsymbol{J}}\right\|_0^2 + \left\langle\left(\alpha_1 + \frac{m}{2}\right)(\varepsilon^h_{\boldsymbol{u}} - \varepsilon^h_{\widehat{\boldsymbol{u}}}), (\varepsilon^h_{\boldsymbol{u}} - \varepsilon^h_{\widehat{\boldsymbol{u}}})\right\rangle\\ &+ \alpha_2\left\|\varepsilon^h_{\boldsymbol{b}^t} - \varepsilon^h_{\widehat{\boldsymbol{b}}^t}\right\|^2_{\partial\mathcal{T}_h} + \alpha_3\left\|\varepsilon^h_r - \varepsilon^h_{\widehat{r}}\right\|^2_{\partial\mathcal{T}_h}\\ =\ & -\operatorname{Re}\left(\varepsilon^I_{\mathbf{L}}, \varepsilon^h_{\mathbf{L}}\right) - \kappa\left(\varepsilon^I_{\boldsymbol{b}}, \nabla\times\left(\varepsilon^h_{\boldsymbol{u}}\times\boldsymbol{d}\right)\right) + \kappa\left(\varepsilon^I_{\boldsymbol{u}}, \boldsymbol{d}\times\left(\nabla\times\varepsilon^h_{\boldsymbol{b}}\right)\right)\\ &- \left\langle\boldsymbol{n}\times\varepsilon^I_{\boldsymbol{J}} - \frac{1}{2}\kappa\boldsymbol{n}\times\left(\left(\varepsilon^I_{\boldsymbol{u}} + \varepsilon^I_{\widehat{\boldsymbol{u}}}\right)\times\boldsymbol{d}\right) + \alpha_2\varepsilon^I_{\boldsymbol{b}^t}, \varepsilon^h_{\boldsymbol{b}^t} - \varepsilon^h_{\widehat{\boldsymbol{b}}^t}\right\rangle. \qquad (5.68)\end{aligned}$$

Proof. Since by Lemma 5.11 the numerical and exact solutions satisfy the local equations (5.47a) – (5.47f) (equivalently (5.10) where all the derivatives are kept on the test functions), the linearity of the operators leads to the error equations:

$$\mathrm{Re}\left(\varepsilon_{\mathbf{L}}, \boldsymbol{G}\right) + \left(\varepsilon_{\boldsymbol{u}}, \nabla \cdot \boldsymbol{G}\right) - \left\langle \varepsilon_{\widehat{\boldsymbol{u}}} \otimes \boldsymbol{n}, \boldsymbol{G}\right\rangle = 0, \quad (5.69a)$$

$$\begin{aligned}&\left(\varepsilon_{\mathbf{L}}, \nabla \boldsymbol{v}\right) - \left(\varepsilon_p, \nabla \cdot \boldsymbol{v}\right) - \left(\varepsilon_{\boldsymbol{u}} \otimes \boldsymbol{w}, \nabla \boldsymbol{v}\right) + \kappa\left(\varepsilon_{\boldsymbol{b}}, \nabla \times (\boldsymbol{v} \times \boldsymbol{d})\right)\\ &+ \left\langle -\varepsilon_{\mathbf{L}}\boldsymbol{n} + m\varepsilon_{\boldsymbol{u}} + \varepsilon_p \boldsymbol{n} + \frac{1}{2}\kappa \boldsymbol{d} \times \left(\boldsymbol{n} \times \left(\varepsilon_{\boldsymbol{b}^t} + \varepsilon_{\widehat{\boldsymbol{b}}^t}\right)\right) + \alpha_1\left(\varepsilon_{\boldsymbol{u}} - \varepsilon_{\widehat{\boldsymbol{u}}}\right), \boldsymbol{v}\right\rangle = 0, \end{aligned} \quad (5.69b)$$

$$-\left(\varepsilon_{\boldsymbol{u}}, \nabla q\right) + \left\langle \varepsilon_{\widehat{\boldsymbol{u}}} \cdot \boldsymbol{n}, q\right\rangle = 0, \quad (5.69c)$$

$$\frac{\mathrm{Rm}}{\kappa}\left(\varepsilon_{\boldsymbol{J}} \boldsymbol{H}\right) - \left(\varepsilon_{\boldsymbol{b}}, \nabla \times \boldsymbol{H}\right) - \left\langle \boldsymbol{n} \times \varepsilon_{\widehat{\boldsymbol{b}}^t}, \boldsymbol{H}\right\rangle = 0, \quad (5.69d)$$

$$\begin{aligned}&\left(\varepsilon_{\boldsymbol{J}} \nabla \times \boldsymbol{c}\right) - \left(\varepsilon_r, \nabla \cdot \boldsymbol{c}\right) - \kappa\left(\varepsilon_{\boldsymbol{u}}, \boldsymbol{d} \times (\nabla \times \boldsymbol{c})\right)\\ &+ \left\langle \boldsymbol{n} \times \varepsilon_{\boldsymbol{H}} + \varepsilon_{\widehat{r}}\boldsymbol{n} - \frac{1}{2}\kappa \boldsymbol{n} \times \left(\left(\varepsilon_{\boldsymbol{u}} + \varepsilon_{\widehat{\boldsymbol{u}}}\right) \times \boldsymbol{d}\right) + \alpha_2\left(\varepsilon_{\boldsymbol{b}^t} - \varepsilon_{\widehat{\boldsymbol{b}}^t}\right), \boldsymbol{c}\right\rangle = 0, \end{aligned} \quad (5.69e)$$

$$-\left(\varepsilon_{\boldsymbol{b}}, \nabla s\right) + \left\langle \varepsilon_{\boldsymbol{b}} \cdot \boldsymbol{n} + \alpha_3\left(\varepsilon_r - \varepsilon_{\widehat{r}}\right), s\right\rangle = 0. \quad (5.69f)$$

Next, we split the error terms into their interpolation and approximation components as in (5.62) using the projections Π defined in Section 5.5.2. Due to the definitions of the projection Π in Section 5.5.2 we obtain reduced error equations (see [47] for details):

$$\mathrm{Re}\left(\varepsilon^h_{\mathbf{L}}, \boldsymbol{G}\right) + \left(\varepsilon^h_{\boldsymbol{u}}, \nabla \cdot \boldsymbol{G}\right) - \left\langle \varepsilon^h_{\widehat{\boldsymbol{u}}} \otimes \boldsymbol{n}, \boldsymbol{G}\right\rangle = -\mathrm{Re}\left(\varepsilon^I_{\boldsymbol{L}}, \boldsymbol{G}\right), \quad (5.70a)$$

$$\begin{aligned}&\left(\varepsilon^h_{\mathbf{L}}, \nabla \boldsymbol{v}\right) - \left(\varepsilon^h_p, \nabla \cdot \boldsymbol{v}\right) - \left(\varepsilon^h_{\boldsymbol{u}} \otimes \boldsymbol{w}, \nabla \boldsymbol{v}\right) + \kappa\left(\varepsilon^h_{\boldsymbol{b}}, \nabla \times (\boldsymbol{v} \times \boldsymbol{d})\right)\\ &+ \left\langle -\varepsilon^h_{\mathbf{L}}\boldsymbol{n} + m\varepsilon^h_{\boldsymbol{u}} + \varepsilon^h_p \boldsymbol{n} + \frac{1}{2}\kappa \boldsymbol{d} \times \left(\boldsymbol{n} \times \left(\varepsilon^h_{\boldsymbol{b}^t} + \varepsilon^h_{\widehat{\boldsymbol{b}}^t}\right)\right) + \alpha_1\left(\varepsilon^h_{\boldsymbol{u}} - \varepsilon^h_{\widehat{\boldsymbol{u}}}\right), \boldsymbol{v}\right\rangle\\ &\quad = -\kappa\left(\varepsilon^I_{\boldsymbol{b}}, \nabla \times (\boldsymbol{v} \times \boldsymbol{d})\right), \end{aligned} \quad (5.70b)$$

$$-\left(\varepsilon^h_{\boldsymbol{u}}, \nabla q\right) + \left\langle \varepsilon^h_{\widehat{\boldsymbol{u}}} \cdot \boldsymbol{n}, q\right\rangle = 0, \quad (5.70c)$$

$$\frac{\mathrm{Rm}}{\kappa}\left(\varepsilon_{\boldsymbol{J}}^h, \boldsymbol{H}\right) - \left(\varepsilon_{\boldsymbol{b}}^h, \nabla\times\boldsymbol{H}\right) - \left\langle \boldsymbol{n}\times\varepsilon_{\widehat{\boldsymbol{b}}^t}^h, \boldsymbol{H}\right\rangle = 0, \tag{5.70d}$$

$$\begin{aligned}&\left(\varepsilon_{\boldsymbol{J}}^h, \nabla\times\boldsymbol{c}\right) - \left(\varepsilon_r^h, \nabla\cdot\boldsymbol{c}\right) - \kappa\left(\varepsilon_{\boldsymbol{u}}^h, \boldsymbol{d}\times(\nabla\times\boldsymbol{c})\right)\\ &+\left\langle \boldsymbol{n}\times\varepsilon_{\boldsymbol{J}}^h + \varepsilon_{\widehat{r}}^h\boldsymbol{n} - \frac{1}{2}\kappa\boldsymbol{n}\times\left(\left(\varepsilon_{\boldsymbol{u}}^h + \varepsilon_{\widehat{\boldsymbol{u}}}^h\right)\times\boldsymbol{d}\right) + \alpha_2\left(\varepsilon_{\boldsymbol{b}^t}^h - \varepsilon_{\widehat{\boldsymbol{b}}^t}^h\right), \boldsymbol{c}\right\rangle =\\ &\kappa\left(\varepsilon_{\boldsymbol{u}}^I, \boldsymbol{d}\times(\nabla\times\boldsymbol{c})\right) - \left\langle \boldsymbol{n}\times\varepsilon_{\boldsymbol{J}}^I - \frac{1}{2}\kappa\boldsymbol{n}\times\left(\left(\varepsilon_{\boldsymbol{u}}^I + \varepsilon_{\widehat{\boldsymbol{u}}}^I\right)\times\boldsymbol{d}\right) + \alpha_2\varepsilon_{\boldsymbol{b}^t}^I, \boldsymbol{c}\right\rangle,\end{aligned} \tag{5.70e}$$

$$-\left(\varepsilon_{\boldsymbol{b}}^h, \nabla s\right) + \left\langle \varepsilon_{\boldsymbol{b}}^h\cdot\boldsymbol{n} + \alpha_3\left(\varepsilon_r^h - \varepsilon_{\widehat{r}}^h\right), s\right\rangle = 0. \tag{5.70f}$$

Notice that (5.70) looks like (5.10), but with the approximation error replacing the finite element solution, and with some nonzero right hand side terms. Since the approximation errors are in the finite element spaces, we can choose the test functions to be the approximation error terms. Next we take $(\boldsymbol{G}, \boldsymbol{v}, q, \boldsymbol{J}, \boldsymbol{c}, s) = (\varepsilon_{\mathbf{L}}^h, \varepsilon_{\boldsymbol{u}}^h, \varepsilon_p^h, \varepsilon_{\boldsymbol{J}}^h, \varepsilon_{\boldsymbol{b}}^h, \varepsilon_r^h)$, integrate by parts the first four terms of (5.70b) and the first term of (5.70e), and sum the resulting equations in (5.70) to arrive at

$$\begin{aligned}&\mathrm{Re}\left\|\varepsilon_{\mathbf{L}}^h\right\|_0^2 + \frac{\mathrm{Rm}}{\kappa}\left\|\varepsilon_{\boldsymbol{J}}^h\right\|_0^2 - \left\langle \varepsilon_{\widehat{\boldsymbol{u}}}^h\otimes\boldsymbol{n}, \varepsilon_{\mathbf{L}}^h\right\rangle + \left\langle \frac{m}{2}\varepsilon_{\boldsymbol{u}}^h, \varepsilon_{\boldsymbol{u}}^h\right\rangle + \left\langle \alpha_1(\varepsilon_{\boldsymbol{u}}^h - \varepsilon_{\widehat{\boldsymbol{u}}}^h), \varepsilon_{\boldsymbol{u}}^h\right\rangle\\ &+\left\langle \frac{1}{2}\kappa\boldsymbol{d}\times\left(\boldsymbol{n}\times\varepsilon_{\widehat{\boldsymbol{b}}^t}^h\right), \varepsilon_{\boldsymbol{u}}^h\right\rangle + \left\langle \varepsilon_{\widehat{\boldsymbol{u}}}^h\cdot\boldsymbol{n}, \varepsilon_p^h\right\rangle - \left\langle \boldsymbol{n}\times\varepsilon_{\widehat{\boldsymbol{b}}^t}^h, \varepsilon_{\boldsymbol{J}}^h\right\rangle + \left\langle \varepsilon_{\widehat{r}}^h\boldsymbol{n}, \varepsilon_{\boldsymbol{b}}^h\right\rangle\\ &+\left\langle \alpha_2(\varepsilon_{\boldsymbol{b}^t}^h - \varepsilon_{\widehat{\boldsymbol{b}}^t}^h), \varepsilon_{\boldsymbol{b}^t}^h\right\rangle - \left\langle \frac{1}{2}\kappa\boldsymbol{n}\times\left(\varepsilon_{\widehat{\boldsymbol{u}}}^h\times\boldsymbol{d}\right), \varepsilon_{\boldsymbol{b}}^h\right\rangle + \left\langle \alpha_3\left(\varepsilon_r^h - \varepsilon_{\widehat{r}}^h\right), \varepsilon_r^h\right\rangle\\ &= -\mathrm{Re}\left(\varepsilon_{\boldsymbol{L}}^I, \varepsilon_{\mathbf{L}}^h\right) - \kappa\left(\varepsilon_{\boldsymbol{b}}^I, \nabla\times\left(\varepsilon_{\boldsymbol{u}}^h\times\boldsymbol{d}\right)\right) + \kappa\left(\varepsilon_{\boldsymbol{u}}^I, \boldsymbol{d}\times\left(\nabla\times\varepsilon_{\boldsymbol{b}}^h\right)\right)\\ &\quad - \left\langle \boldsymbol{n}\times\varepsilon_{\boldsymbol{J}}^I - \frac{1}{2}\kappa\boldsymbol{n}\times\left(\left(\varepsilon_{\boldsymbol{u}}^I + \varepsilon_{\widehat{\boldsymbol{u}}}^I\right)\times\boldsymbol{d}\right) + \alpha_2\varepsilon_{\boldsymbol{b}^t}^I, \varepsilon_{\boldsymbol{b}}^h\right\rangle.\end{aligned} \tag{5.71}$$

Since the exact solution satisfies the conservation conditions (5.47g) – (5.47i) and

boundary conditions (5.22), (5.39), and (5.42), we have

$$\left\langle -\varepsilon_{\mathbf{L}}\boldsymbol{n} + m\varepsilon_{\boldsymbol{u}} + \varepsilon_p\boldsymbol{n} + \frac{1}{2}\kappa\boldsymbol{d}\times\left(\boldsymbol{n}\times\left(\varepsilon_{\boldsymbol{b}^t} + \varepsilon_{\widehat{\boldsymbol{b}}^t}\right)\right) + \alpha_1\left(\varepsilon_{\boldsymbol{u}} - \varepsilon_{\widehat{\boldsymbol{u}}}\right), \widehat{\boldsymbol{v}}\right\rangle_{\partial\mathcal{T}_h\setminus\partial\Omega} = 0, \tag{5.72a}$$

$$\left\langle \boldsymbol{n}\times\varepsilon_{\boldsymbol{H}} - \frac{1}{2}\kappa\boldsymbol{n}\times\left(\left(\varepsilon_{\boldsymbol{u}} + \varepsilon_{\widehat{\boldsymbol{u}}}\right)\times\boldsymbol{d}\right) + \alpha_2\left(\varepsilon_{\boldsymbol{b}^t} - \varepsilon_{\widehat{\boldsymbol{b}}^t}\right), \widehat{\boldsymbol{c}}^t\right\rangle_{\partial\mathcal{T}_h\setminus\partial\Omega} = 0, \tag{5.72b}$$

$$\left\langle \varepsilon_{\boldsymbol{b}}\cdot\boldsymbol{n} + \alpha_3\left(\varepsilon_r - \varepsilon_{\widehat{r}}\right), \widehat{s}\right\rangle_{\partial\mathcal{T}_h\setminus\partial\Omega} = 0, \tag{5.72c}$$

$$\left\langle \varepsilon_{\widehat{\boldsymbol{u}}}, \widehat{\boldsymbol{v}}\right\rangle_{\partial\Omega} = 0, \tag{5.72d}$$

$$\left\langle \varepsilon_{\widehat{\boldsymbol{b}}^t}, \widehat{\boldsymbol{c}}^t\right\rangle_{\partial\Omega} = 0, \tag{5.72e}$$

$$\left\langle \varepsilon_{\widehat{r}}, \widehat{s}\right\rangle_{\partial\Omega} = 0. \tag{5.72f}$$

We split the errors into interpolation and approximation errors as before, and use the projections defined in Section 5.5.2 to cancel terms. We refer to [47] for more details on cancellations of terms. Then we have

$$\left\langle -\varepsilon^h_{\mathbf{L}}\boldsymbol{n} + m\varepsilon^h_{\boldsymbol{u}} + \varepsilon^h_p\boldsymbol{n} + \frac{1}{2}\kappa\boldsymbol{d}\times\left(\boldsymbol{n}\times\varepsilon^h_{\boldsymbol{b}^t}\right) + \alpha_1\left(\varepsilon^h_{\boldsymbol{u}} - \varepsilon^h_{\widehat{\boldsymbol{u}}}\right), \widehat{\boldsymbol{v}}\right\rangle_{\partial\mathcal{T}_h\setminus\partial\Omega} = 0, \tag{5.73a}$$

$$\left\langle \boldsymbol{n}\times\varepsilon^h_{\boldsymbol{J}} - \frac{1}{2}\kappa\boldsymbol{n}\times\left(\varepsilon^h_{\boldsymbol{u}}\times\boldsymbol{d}\right) + \alpha_2\left(\varepsilon^h_{\boldsymbol{b}^t} - \varepsilon^h_{\widehat{\boldsymbol{b}}^t}\right), \widehat{\boldsymbol{c}}^t\right\rangle_{\partial\mathcal{T}_h\setminus\partial\Omega} \tag{5.73b}$$

$$= -\left\langle \boldsymbol{n}\times\varepsilon^I_{\boldsymbol{J}} - \frac{1}{2}\kappa\boldsymbol{n}\times\left(\left(\varepsilon^I_{\boldsymbol{u}} + \varepsilon^I_{\widehat{\boldsymbol{u}}}\right)\times\boldsymbol{d}\right) + \alpha_2\varepsilon^I_{\boldsymbol{b}^t}, \widehat{\boldsymbol{c}}^t\right\rangle_{\partial\mathcal{T}_h\setminus\partial\Omega},$$

$$\left\langle \varepsilon^h_{\boldsymbol{b}}\cdot\boldsymbol{n} + \alpha_3\left(\varepsilon^h_r - \varepsilon^h_{\widehat{r}}\right), \widehat{s}\right\rangle_{\partial\mathcal{T}_h\setminus\partial\Omega} = 0, \tag{5.73c}$$

$$\left\langle \varepsilon^h_{\widehat{\boldsymbol{u}}}, \widehat{\boldsymbol{v}}\right\rangle_{\partial\Omega} = 0, \tag{5.73d}$$

$$\left\langle \varepsilon^h_{\widehat{\boldsymbol{b}}^t}, \widehat{\boldsymbol{c}}^t\right\rangle_{\partial\Omega} = 0, \tag{5.73e}$$

$$\left\langle \varepsilon^h_{\widehat{r}}, \widehat{s}\right\rangle_{\partial\Omega} = 0. \tag{5.73f}$$

Equations (5.73d)–(5.73f) imply that on $\partial\Omega$, $\varepsilon^h_{\widehat{\boldsymbol{u}}} = \boldsymbol{0}$, $\varepsilon^h_{\widehat{\boldsymbol{b}}^t} = \boldsymbol{0}$, and $\varepsilon^h_{\widehat{r}} = 0$. With this zero contribution on $\partial\Omega$, summing of equations (5.73a)–(5.73c) with $(\widehat{\boldsymbol{v}}, \widehat{\boldsymbol{c}}^t, \widehat{s}) =$

$(\varepsilon^h_{\widehat{\boldsymbol{u}}}, \varepsilon^h_{\widehat{\boldsymbol{b}}^t}, \varepsilon^h_{\widehat{r}})$ including $\partial\Omega$ gives

$$\begin{aligned}
&\left\langle -\varepsilon^h_{\mathbf{L}}\boldsymbol{n} + m\varepsilon^h_{\boldsymbol{u}} + \varepsilon^h_p\boldsymbol{n} + \frac{1}{2}\kappa\boldsymbol{d}\times\left(\boldsymbol{n}\times\varepsilon^h_{\boldsymbol{b}^t}\right) + \alpha_1\left(\varepsilon^h_{\boldsymbol{u}} - \varepsilon^h_{\widehat{\boldsymbol{u}}}\right), \varepsilon^h_{\widehat{\boldsymbol{u}}}\right\rangle \\
&\qquad + \left\langle \boldsymbol{n}\times\varepsilon^h_{\boldsymbol{J}} - \frac{1}{2}\kappa\boldsymbol{n}\times\left(\varepsilon^h_{\boldsymbol{u}}\times\boldsymbol{d}\right) + \alpha_2\left(\varepsilon^h_{\boldsymbol{b}^t} - \varepsilon^h_{\widehat{\boldsymbol{b}}^t}\right), \varepsilon^h_{\widehat{\boldsymbol{b}}^t}\right\rangle \\
&\qquad\qquad + \left\langle \varepsilon^h_{\boldsymbol{b}}\cdot\boldsymbol{n} + \alpha_3\left(\varepsilon^h_r - \varepsilon^h_{\widehat{r}}\right), \varepsilon^h_{\widehat{r}}\right\rangle \\
&\qquad = \left\langle \boldsymbol{n}\times\varepsilon^I_{\boldsymbol{J}} - \frac{1}{2}\kappa\boldsymbol{n}\times\left(\left(\varepsilon^I_{\boldsymbol{u}} + \varepsilon^I_{\widehat{\boldsymbol{u}}}\right)\times\boldsymbol{d}\right) + \alpha_2\varepsilon^I_{\boldsymbol{b}^t}, \varepsilon^h_{\widehat{\boldsymbol{b}}^t}\right\rangle. \qquad (5.74)
\end{aligned}$$

Subtracting (5.74) from (5.71), we arrive at

$$\begin{aligned}
&\mathrm{Re}\left\|\varepsilon^h_{\mathbf{L}}\right\|_0^2 + \frac{\mathrm{Rm}}{\kappa}\left\|\varepsilon^h_{\boldsymbol{J}}\right\|_0^2 + \left\langle\alpha_1(\varepsilon^h_{\boldsymbol{u}} - \varepsilon^h_{\widehat{\boldsymbol{u}}}), (\varepsilon^h_{\boldsymbol{u}} - \varepsilon^h_{\widehat{\boldsymbol{u}}})\right\rangle + \left\langle\frac{m}{2}\varepsilon^h_{\boldsymbol{u}}, \varepsilon^h_{\boldsymbol{u}}\right\rangle \\
&\quad - \left\langle m\varepsilon^h_{\boldsymbol{u}}, \varepsilon^h_{\widehat{\boldsymbol{u}}}\right\rangle + \alpha_2\left\|\varepsilon^h_{\boldsymbol{b}^t} - \varepsilon^h_{\widehat{\boldsymbol{b}}^t}\right\|^2_{\partial\mathfrak{T}_h} + \alpha_3\left\|\varepsilon^h_r - \varepsilon^h_{\widehat{r}}\right\|^2_{\partial\mathfrak{T}_h} \\
&\quad = -\mathrm{Re}\left(\varepsilon^I_{\mathbf{L}}, \varepsilon^h_{\mathbf{L}}\right) - \kappa\left(\varepsilon^I_{\boldsymbol{b}}, \nabla\times\left(\varepsilon^h_{\boldsymbol{u}}\times\boldsymbol{d}\right)\right) + \kappa\left(\varepsilon^I_{\boldsymbol{u}}, \boldsymbol{d}\times\left(\nabla\times\varepsilon^h_{\boldsymbol{b}}\right)\right) \\
&\qquad - \left\langle \boldsymbol{n}\times\varepsilon^I_{\boldsymbol{J}} - \frac{1}{2}\kappa\boldsymbol{n}\times\left(\left(\varepsilon^I_{\boldsymbol{u}} + \varepsilon^I_{\widehat{\boldsymbol{u}}}\right)\times\boldsymbol{d}\right) + \alpha_2\varepsilon^I_{\boldsymbol{b}^t}, \varepsilon^h_{\boldsymbol{b}^t} - \varepsilon^h_{\widehat{\boldsymbol{b}}^t}\right\rangle.
\end{aligned}$$

Using the fact that $\boldsymbol{w}\in H(div,\Omega)$, and the fact that $\varepsilon^h_{\widehat{\boldsymbol{u}}} = 0$ on $\partial\Omega$ and is single-valued on $\mathcal{E}^o_h$, we can add $0 = \left\langle\frac{m}{2}\varepsilon^h_{\widehat{\boldsymbol{u}}}, \varepsilon^h_{\widehat{\boldsymbol{u}}}\right\rangle$ to the previous expression and factor the terms with m to arrive at the conclusion. □

Lemma 5.13. *There holds:*

$$\begin{aligned}
E_h^2 \lesssim\ &\mathrm{Re}\left\|\varepsilon^I_{\mathbf{L}}\right\|_0\left\|\varepsilon^h_{\mathbf{L}}\right\|_0 + \kappa\left\|\boldsymbol{d}\right\|_{W^{1,\infty}}\left(\left\|\varepsilon^I_{\boldsymbol{b}}\right\|_0\left\|\varepsilon^h_{\boldsymbol{u}}\right\|_0 + \left\|\varepsilon^I_{\boldsymbol{u}}\right\|_0\left\|\varepsilon^h_{\boldsymbol{b}}\right\|_0\right) \\
&+ \left(\left\|\varepsilon^I_{\boldsymbol{J}}\right\|_{\partial\mathfrak{T}_h} + \kappa\left\|\boldsymbol{d}\right\|_{L^\infty}\left\|\varepsilon^I_{\boldsymbol{u}}, \varepsilon^I_{\widehat{\boldsymbol{u}}}\right\|_{\partial\mathfrak{T}_h} + \alpha_2\left\|\varepsilon^I_{\boldsymbol{b}^t}\right\|_{\partial\mathfrak{T}_h}\right)\left\|\varepsilon^h_{\boldsymbol{b}^t} - \varepsilon^h_{\widehat{\boldsymbol{b}}^t}\right\|_{\partial\mathfrak{T}_h}. \qquad (5.75)
\end{aligned}$$

Proof. Bounding the energy is the same as bounding the right hand side of (5.68). The estimate of $\mathrm{Re}\left(\varepsilon^I_{\mathbf{L}}, \varepsilon^h_{\mathbf{L}}\right)$ is obtained by the Cauchy-Schwarz inequality. To estimate $\kappa\left(\varepsilon^I_{\boldsymbol{b}}, \nabla\times\left(\varepsilon^h_{\boldsymbol{u}}\times\boldsymbol{d}\right)\right)$, note that an algebraic computation gives

$$\begin{aligned}
\kappa\left(\varepsilon^I_{\boldsymbol{b}}, \nabla\times\left(\varepsilon^h_{\boldsymbol{u}}\times\boldsymbol{d}\right)\right) = \ &\kappa\left(\varepsilon^I_{\boldsymbol{b}}, \varepsilon^h_{\boldsymbol{u}}\left(\nabla\cdot\boldsymbol{d}\right) - \left(\varepsilon^h_{\boldsymbol{u}}\cdot\nabla\right)\boldsymbol{d}\right) \\
&+ \kappa\left(\varepsilon^I_{\boldsymbol{b}}, \left(\boldsymbol{d}\cdot\nabla\right)\varepsilon^h_{\boldsymbol{u}} - \boldsymbol{d}\left(\nabla\cdot\varepsilon^h_{\boldsymbol{u}}\right)\right). \qquad (5.76)
\end{aligned}$$

The boundedness of the left hand side can be obtained by

$$\begin{aligned}
&\kappa \left| \left(\varepsilon_{\boldsymbol{b}}^I, \varepsilon_{\boldsymbol{u}}^h \left(\nabla \cdot \boldsymbol{d} \right) - \left(\varepsilon_{\boldsymbol{u}}^h \cdot \nabla \right) \boldsymbol{d} \right)_K \right| \leq \kappa \| \varepsilon_{\boldsymbol{b}}^I \|_{0,K} \| \varepsilon_{\boldsymbol{u}}^h \|_{0,K} \| \boldsymbol{d} \|_{W^{1,\infty}(K)}, \\
&\kappa \left| \left(\varepsilon_{\boldsymbol{b}}^I, \left(\boldsymbol{d} \cdot \nabla \right) \varepsilon_{\boldsymbol{u}}^h - \boldsymbol{d} \left(\nabla \cdot \varepsilon_{\boldsymbol{u}}^h \right) \right)_K \right| \\
&\quad = \kappa \left| \left(\varepsilon_{\boldsymbol{b}}^I, \left(\left(\boldsymbol{d} - \mathbb{P}_0 \boldsymbol{d} \right) \cdot \nabla \right) \varepsilon_{\boldsymbol{u}}^h - \left(\boldsymbol{d} - \mathbb{P}_0 \boldsymbol{d} \right) \left(\nabla \cdot \varepsilon_{\boldsymbol{u}}^h \right) \right)_K \right| \\
&\quad \lesssim \kappa h_K \| \varepsilon_{\boldsymbol{b}}^I \|_{0,K} \| \boldsymbol{d} \|_{W^{1,\infty}(K)} \| \nabla \varepsilon_{\boldsymbol{u}}^h \|_{0,K} \lesssim \kappa \| \varepsilon_{\boldsymbol{b}}^I \|_{0,K} \| \boldsymbol{d} \|_{W^{1,\infty}(K)} \| \varepsilon_{\boldsymbol{u}}^h \|_{0,K}
\end{aligned}$$

where $\mathbb{P}_0 \boldsymbol{d}$ is the L^2 projection of $\boldsymbol{d}$ to the piecewise constant space on K, and where we used (5.66f), the Hölder inequality $\| f_1 f_2 f_3 \|_{L^1} \leq \| f_1 \|_{L^2} \| f_2 \|_{L^\infty} \| f_3 \|_{L^2}$ the interpolation error result (5.65) and the inverse estimate in the last two inequalities.

For an estimate of $\kappa \left(\varepsilon_{\boldsymbol{u}}^I, \boldsymbol{d} \times \left(\nabla \times \varepsilon_{\boldsymbol{b}}^h \right) \right)$, we first note that

$$\kappa \left(\varepsilon_{\boldsymbol{u}}^I, \boldsymbol{d} \times \left(\nabla \times \varepsilon_{\boldsymbol{b}}^h \right) \right) = \kappa \left(\varepsilon_{\boldsymbol{u}}^I, \left(\boldsymbol{d} - \mathbb{P}_0 \boldsymbol{d} \right) \times \left(\nabla \times \varepsilon_{\boldsymbol{b}}^h \right) \right)$$

due to (5.66j). A similar argument as above gives

$$\begin{aligned}
\kappa | \left(\varepsilon_{\boldsymbol{u}}^I, \boldsymbol{d} \times \left(\nabla \times \varepsilon_{\boldsymbol{b}}^h \right) \right) |_K &\leq \kappa \| \varepsilon_{\boldsymbol{u}}^I \|_{0,K} \| \boldsymbol{d} - \mathbb{P}_0 \boldsymbol{d} \|_{L^\infty(K)} \| \nabla \times \varepsilon_{\boldsymbol{b}}^h \|_{0,K} \\
&\lesssim \kappa \| \varepsilon_{\boldsymbol{u}}^I \|_{0,K} \| \boldsymbol{d} \|_{W^{1,\infty}(K)} \| \varepsilon_{\boldsymbol{b}}^h \|_{0,K}.
\end{aligned}$$

Finally, we use the Cauchy-Schwarz inequality for the last term in (5.68). □

Corollary 5.14 (Energy estimate)**.** *There holds:*

$$\begin{aligned}
E_h^2 \lesssim \operatorname{Re} \left\| \varepsilon_{\mathbf{L}}^I \right\|_0^2 &+ \kappa \left\| \boldsymbol{d} \right\|_{W^{1,\infty}} \left(\left\| \varepsilon_{\boldsymbol{b}}^I \right\|_0 \left\| \varepsilon_{\boldsymbol{u}}^h \right\|_0 + \left\| \varepsilon_{\boldsymbol{u}}^I \right\|_0 \left\| \varepsilon_{\boldsymbol{b}}^h \right\|_0 \right) \\
&+ \alpha_2^{-1} \left\| \varepsilon_{\boldsymbol{J}}^I \right\|_{\partial \mathfrak{T}_h}^2 + \kappa^2 \left\| \boldsymbol{d} \right\|_{L^\infty}^2 \left\| \varepsilon_{\boldsymbol{u}}^I \right\|_{\partial \mathfrak{T}_h}^2 + \alpha_2 \left\| \varepsilon_{\boldsymbol{b}^t}^I \right\|_{\partial \mathfrak{T}_h}^2. \qquad (5.77)
\end{aligned}$$

Proof. Apply Young's inequality to each of the terms on the right side of (5.75) involving $\left\| \varepsilon_{\mathbf{L}}^h \right\|_0$ and $\| \varepsilon_{\boldsymbol{b}^t}^h - \varepsilon_{\widehat{\boldsymbol{b}}^t}^h \|_{\partial \mathfrak{T}_h}$. Note also that $\Pi \widehat{\boldsymbol{u}}$ is the best approximation of $\boldsymbol{u}$ on $\partial \mathfrak{T}_h$, so $\left\| \varepsilon_{\widehat{\boldsymbol{u}}}^I \right\|_{\partial \mathfrak{T}_h}$ is bounded by $\left\| \varepsilon_{\boldsymbol{u}}^I \right\|_{\partial \mathfrak{T}_h}$. □

5.5.4 The Adjoint Equations and a Regularity Assumption

In the energy estimate (5.77), we do not have enough information to provide discretization error bounds, so we employ a duality argument to assist in completing the analysis. In particular, the duality argument will lead to an estimate for $\varepsilon_{\boldsymbol{u}}^h$ and $\varepsilon_{\boldsymbol{b}}^h$. A similar approach for the Oseen equation appeared in [11] but $\varepsilon_{\boldsymbol{u}}^h$ and $\varepsilon_{\boldsymbol{b}}^h$ are coupled in our MHD system, so there are nontrivial modifications to complete this duality argument.

First, we define a dual (adjoint) problem of the MHD system (5.9) as

$$\mathrm{Re}\mathbf{L}^* - \nabla \boldsymbol{u}^* = \mathbf{0}, \tag{5.78a}$$

$$-\nabla \cdot \mathbf{L}^* - \nabla p^* - (\boldsymbol{w} \cdot \nabla)\boldsymbol{u}^* - \kappa \boldsymbol{d} \times (\nabla \times \boldsymbol{b}^*) = \boldsymbol{\theta}, \tag{5.78b}$$

$$-\nabla \cdot \boldsymbol{u}^* = 0, \tag{5.78c}$$

$$\frac{\mathrm{Rm}}{\kappa}\boldsymbol{J}^* - \nabla \times \boldsymbol{b}^* = \mathbf{0}, \tag{5.78d}$$

$$\nabla \times \boldsymbol{J}^* - \nabla r^* + \kappa \nabla \times (\boldsymbol{u}^* \times \boldsymbol{d}) = \boldsymbol{\sigma}, \tag{5.78e}$$

$$-\nabla \cdot \boldsymbol{b}^* = 0 \tag{5.78f}$$

with homogeneous boundary conditions. Here, $\boldsymbol{\theta}$ and $\boldsymbol{\sigma}$ are two given functions in $L^2(\Omega)$, and the superscript "*" is used to denote the corresponding unknowns in the adjoint equation. We assume the following elliptic regularity assumption

$$\|\boldsymbol{u}^*\|_2 + \|\mathbf{L}^*, p^*, \boldsymbol{J}^*, \boldsymbol{b}^*, r^*\|_1 \lesssim \|\boldsymbol{\theta}, \boldsymbol{\sigma}\|_0, \tag{5.79}$$

where the elliptic regularity constant C_{er} may depend on Re, Rm, κ, $\boldsymbol{w}$, $\boldsymbol{d}$, and Ω.

The well-posedness of (5.78) and the conditions under which the regularity estimate (5.79) holds are discussed in Appendix C in [47].

5.5.5 Definition of Adjoint Projections and Their Properties

We now define the adjoint projection $\Pi^*(\mathbf{L}^*, \boldsymbol{u}^*, p^*, \boldsymbol{J}^*, \boldsymbol{b}^*, r^*, \widehat{\boldsymbol{u}}^*, (\widehat{\boldsymbol{b}}^*)^t, \widehat{r}^*)$ that will be used in subsequent steps. As in the splitting of errors with Π, we define

$$\varepsilon^I_{\sigma^*} = \sigma^* - \Pi^*\sigma^*$$

for an adjoint unknown σ^*. We first define $\Pi^* p^*$, $\Pi^* \boldsymbol{J}^*$, $\Pi^* \widehat{\boldsymbol{u}}^*$, $\Pi^* (\widehat{\boldsymbol{b}}^*)^t$, and $\Pi^* \widehat{r}^*$ as L^2 projections into relevant polynomials spaces, and define $\Pi^* \boldsymbol{b}^*$, $\Pi^* r^*$ to satisfy

$$(\varepsilon^I_{\boldsymbol{b}^*}, \boldsymbol{c})_K = 0, \qquad \forall \boldsymbol{c} \in \boldsymbol{\mathcal{P}}_{k-1}(K), \tag{5.80a}$$

$$(\varepsilon^I_{r^*}, s)_K = 0, \qquad \forall s \in \mathcal{P}_{k-1}(K), \tag{5.80b}$$

$$\left\langle -\varepsilon^I_{\boldsymbol{b}^*} \cdot \boldsymbol{n} + \alpha_3 \varepsilon^I_{r^*}, \widehat{s} \right\rangle_e = 0, \qquad \forall \widehat{s} \in \mathcal{P}_k(e). \tag{5.80c}$$

We then choose $\Pi^* \mathbf{L}^*$, $\Pi^* \boldsymbol{u}^*$ to satisfy

$$(\varepsilon^I_{\boldsymbol{L}^*}, \mathbf{G})_K + (\varepsilon^I_{\boldsymbol{u}^*} \otimes \boldsymbol{w}, \mathbf{G})_K = 0, \qquad \forall \mathbf{G} \in \tilde{\boldsymbol{\mathcal{P}}}_{k-1}(K), \tag{5.81a}$$

$$(\varepsilon^I_{\boldsymbol{u}^*}, \boldsymbol{v})_K = 0, \qquad \forall \boldsymbol{v} \in \boldsymbol{\mathcal{P}}_{k-1}(K), \tag{5.81b}$$

$$\left\langle -\varepsilon^I_{\boldsymbol{L}^*} \boldsymbol{n} + \alpha_1 \varepsilon^I_{\boldsymbol{u}^*}, \widehat{\boldsymbol{v}} \right\rangle_e = \left\langle \boldsymbol{f}, \widehat{\boldsymbol{v}} \right\rangle_e, \qquad \forall \widehat{\boldsymbol{v}} \in \boldsymbol{\mathcal{P}}_k(e) \tag{5.81c}$$

where

$$\boldsymbol{f} = \varepsilon^I_{p^*} \boldsymbol{n} - \frac{1}{2} \kappa \boldsymbol{d} \times \left(\boldsymbol{n} \times \left(-(\varepsilon^I_{\boldsymbol{b}^*})^t + \varepsilon^I_{(\widehat{\boldsymbol{b}}^*)^t} \right) \right).$$

Assuming that $(\mathbf{L}^*, \boldsymbol{u}^*, p^*, \boldsymbol{J}^*, \boldsymbol{b}^*, r^*, \widehat{\boldsymbol{u}}^*, (\widehat{\boldsymbol{b}}^*)^t, \widehat{r}^*)$ are sufficiently regular, we can show that the interpolation $\boldsymbol{\Pi}^*$ is well-defined and provides optimal approximations. Due to the similarity between $(\Pi \boldsymbol{b}, \Pi r)$ and $(\Pi^* \boldsymbol{b}^*, \Pi^* r^*)$, we can conclude

$$\left\| \varepsilon^I_{\boldsymbol{b}^*} \right\|_{0,K} \lesssim h^{k+1} \left\| \boldsymbol{b}^* \right\|_{k+1,K} + \alpha_3 h^{k+1} \left\| r^* \right\|_{k+1,K}, \tag{5.82a}$$

$$\left\| \varepsilon^I_{r^*} \right\|_{0,K} \lesssim \alpha_3^{-1} h^{k+1} \left\| \nabla \cdot \boldsymbol{b}^* \right\|_{k,K} + h^{k+1} \left\| r^* \right\|_{k+1,K}. \tag{5.82b}$$

It can also be shown that

$$\begin{aligned}
\|\varepsilon^I_{\boldsymbol{u}^*}\|_0 &\lesssim (\alpha_1 - \frac{1}{2}\|\boldsymbol{w}\|_{L^\infty})^{-1}\left[(\alpha_1 + h\|\boldsymbol{w}\|_{W^{1,\infty}})h^{k+1}\|\boldsymbol{u}^*\|_{k+1}\right.\\
&\qquad \left. + h^{k+1}\|\nabla\cdot\mathbf{L}^* + \nabla p^*\|_k + \kappa h^{k+1}\|\boldsymbol{d}\|_{L^\infty}\left(\|\boldsymbol{b}^*\|_{k+1} + \alpha_3\|r^*\|_{k+1}\right)\right],\\
\left\|\varepsilon^I_{\boldsymbol{L}^*}\right\|_0 &\lesssim h^{k+1}\|p^*\|_{k+1} + h^{k+1}\|\mathbf{L}^*\|_{k+1} + \kappa h^{k+1}\|\boldsymbol{d}\|_{L^\infty}\left(\|\boldsymbol{b}^*\|_{k+1} + \alpha_3\|r^*\|_{k+1}\right)\\
&\qquad + (\alpha_1 + h\|\boldsymbol{w}\|_{W^{1,\infty}})\left\|\varepsilon^I_{\boldsymbol{u}^*}\right\|_0 + \alpha_1 h^{k+1}\|\boldsymbol{u}^*\|_{k+1},
\end{aligned}$$

assuming $\operatorname{tr}\mathbf{L}^* = 0$. The proofs are analogous to those for the $\boldsymbol{\Pi}$ projections, with the only differences resulting from the absence of m from (5.81c). As a consequence, from the elliptic regularity assumption (5.79), we have

$$\max\left\{\left\|\varepsilon^I_{\boldsymbol{L}^*}\right\|_0,\ \left\|\varepsilon^I_{\boldsymbol{u}^*}\right\|_0,\ \left\|\varepsilon^I_{p^*}\right\|_0,\ \left\|\varepsilon^I_{\boldsymbol{b}^*}\right\|_0,\ \left\|\varepsilon^I_{r^*}\right\|_0\right\} \lesssim h\|\boldsymbol{\sigma},\boldsymbol{\theta}\|_0 \tag{5.83}$$

and the implicit constant depends on $\boldsymbol{d}$, $\boldsymbol{w}$, α_1, α_2, α_3 but not h.

5.5.6 An Estimate for $\varepsilon^h_{\boldsymbol{u}}$ and $\varepsilon^h_{\boldsymbol{b}}$

We use the interpolation operators Π^* defined in (5.80), (5.81) and $\varepsilon^I_{\boldsymbol{L}^*}$, $\varepsilon^I_{p^*}$, ... will denote $\mathbf{L}^* - \Pi^*\mathbf{L}^*$, $p^* - \Pi^* p^*$, etc. Testing (5.78b) with $\varepsilon^h_{\boldsymbol{u}}$ and (5.78e) with $\varepsilon^h_{\boldsymbol{b}}$ we have

$$\begin{aligned}
&\left(\varepsilon^h_{\boldsymbol{u}},\boldsymbol{\theta}\right) + \left(\varepsilon^h_{\boldsymbol{b}},\boldsymbol{\sigma}\right)\\
&\quad = \left(\varepsilon^h_{\boldsymbol{u}}, -\nabla\cdot\mathbf{L}^* - \nabla p^* - (\boldsymbol{w}\cdot\nabla)\boldsymbol{u}^* - \kappa\boldsymbol{d}\times(\nabla\times\boldsymbol{b}^*)\right)\\
&\qquad + \left(\varepsilon^h_{\boldsymbol{b}}, \nabla\times\boldsymbol{J}^* - \nabla r^* + \kappa\nabla\times(\boldsymbol{u}^*\times\boldsymbol{d})\right)\\
&\quad = \left(\nabla\varepsilon^h_{\boldsymbol{u}}, \mathbf{L}^*\right) + \left(\nabla\cdot\varepsilon^h_{\boldsymbol{u}}, p^*\right) + \left((\boldsymbol{w}\cdot\nabla)\varepsilon^h_{\boldsymbol{u}}, \boldsymbol{u}^*\right) - \kappa\left(\varepsilon^h_{\boldsymbol{u}}, \boldsymbol{d}\times(\nabla\times\boldsymbol{b}^*)\right)\\
&\qquad + \left\langle\varepsilon^h_{\boldsymbol{u}}, -\mathbf{L}^*\boldsymbol{n} - p^*\boldsymbol{n} - m\boldsymbol{u}^*\right\rangle + \left(\nabla\times\varepsilon^h_{\boldsymbol{b}}, \boldsymbol{J}^*\right) + \left(\nabla\cdot\varepsilon^h_{\boldsymbol{b}}, r^*\right)\\
&\qquad + \kappa\left(\varepsilon^h_{\boldsymbol{b}}, \nabla\times(\boldsymbol{u}^*\times\boldsymbol{d})\right) + \left\langle\varepsilon^h_{\boldsymbol{b}}, \boldsymbol{n}\times\boldsymbol{J}^* - r^*\boldsymbol{n}\right\rangle
\end{aligned}$$

$$
\begin{aligned}
&= \left(\nabla \varepsilon_{\boldsymbol{u}}^h, \Pi^* \mathbf{L}^*\right) + \left(\nabla \cdot \varepsilon_{\boldsymbol{u}}^h, \Pi^* p^*\right) + \left((\boldsymbol{w} \cdot \nabla) \varepsilon_{\boldsymbol{u}}^h, \Pi^* \boldsymbol{u}^*\right) \\
&\quad - \kappa \left(\varepsilon_{\boldsymbol{u}}^h, \boldsymbol{d} \times (\nabla \times \boldsymbol{b}^*)\right) + \left\langle \varepsilon_{\boldsymbol{u}}^h, -\mathbf{L}^* \boldsymbol{n} - p^* \boldsymbol{n} - m \boldsymbol{u}^* \right\rangle + \left(\nabla \times \varepsilon_{\boldsymbol{b}}^h, \Pi^* \boldsymbol{J}^*\right) \\
&\quad + \left(\nabla \cdot \varepsilon_{\boldsymbol{b}}^h, \Pi^* r^*\right) + \kappa \left(\nabla \times (\boldsymbol{u}^* \times \boldsymbol{d}), \varepsilon_{\boldsymbol{b}}^h\right) + \left\langle \varepsilon_{\boldsymbol{b}}^h, \boldsymbol{n} \times \boldsymbol{J}^* - r^* \boldsymbol{n} \right\rangle \\
&= \left(\varepsilon_{\boldsymbol{u}}^h, -\nabla \cdot \Pi^* \mathbf{L}^* - \nabla \Pi^* p^* - (\boldsymbol{w} \cdot \nabla) \Pi^* \boldsymbol{u}^* - \kappa \boldsymbol{d} \times (\nabla \times \boldsymbol{b}^*)\right) \\
&\quad + \left(\varepsilon_{\boldsymbol{b}}^h, \nabla \times \Pi^* \boldsymbol{J}^* - \nabla \Pi^* r^* + \kappa \nabla \times (\boldsymbol{u}^* \times \boldsymbol{d})\right) \\
&\quad + \left\langle \varepsilon_{\boldsymbol{u}}^h, -\varepsilon_{\boldsymbol{L}^*}^I \boldsymbol{n} - \varepsilon_{p^*}^I \boldsymbol{n} - m \varepsilon_{\boldsymbol{u}^*}^I \right\rangle + \left\langle \varepsilon_{\boldsymbol{b}}^h, \boldsymbol{n} \times \varepsilon_{\boldsymbol{J}^*}^I - \varepsilon_{r^*}^I \boldsymbol{n} \right\rangle
\end{aligned} \tag{5.84}
$$

where we have used integration by parts in the second equality, the properties of the Π^* operators (5.80) and (5.81) in the third equality, and integration by parts again in the last equality. This can be reduced to (see [47] for full details)

$$
\begin{aligned}
&\left(\varepsilon_{\boldsymbol{u}}^h, \boldsymbol{\theta}\right) + \left(\varepsilon_{\boldsymbol{b}}^h, \boldsymbol{\sigma}\right) \\
&= \mathrm{Re} \underbrace{\left(\varepsilon_{\mathbf{L}}^h, -\varepsilon_{\boldsymbol{L}^*}^I\right)}_{=:I_1} + \mathrm{Re} \underbrace{\left(\varepsilon_{\boldsymbol{L}}^I, \Pi^* \mathbf{L}^*\right)}_{=:I_2} + \kappa \underbrace{\left(\varepsilon_{\boldsymbol{b}}^h, \nabla \times (\varepsilon_{\boldsymbol{u}^*}^I \times \boldsymbol{d})\right)}_{=:I_3} \\
&\quad - \kappa \underbrace{\left(\varepsilon_{\boldsymbol{b}}^I, \nabla \times (\Pi^* \boldsymbol{u}^* \times \boldsymbol{d})\right)}_{=:I_4} + \kappa \underbrace{\left(\varepsilon_{\boldsymbol{u}}^I, \boldsymbol{d} \times (\nabla \times \Pi^* \boldsymbol{b}^*)\right)}_{=:I_5} - \kappa \underbrace{\left(\varepsilon_{\boldsymbol{u}}^h, \boldsymbol{d} \times (\nabla \times \varepsilon_{\boldsymbol{b}^*}^I)\right)}_{=:I_6} \\
&\quad \underbrace{- \left\langle \varepsilon_{\boldsymbol{u}}^h, m \varepsilon_{\widehat{\boldsymbol{u}}^*}^I + \kappa \boldsymbol{d} \times (\boldsymbol{n} \times (-\varepsilon_{\boldsymbol{b}^*}^I + \varepsilon_{(\widehat{\boldsymbol{b}}^*)^t}^I)) \right\rangle}_{=:I_7} \\
&\quad + \underbrace{\left\langle \varepsilon_{\widehat{\boldsymbol{b}}^t}^h, \frac{1}{2} \kappa \boldsymbol{n} \times ((-\varepsilon_{\boldsymbol{u}^*}^I + \varepsilon_{\widehat{\boldsymbol{u}}^*}^I) \times \boldsymbol{d}) + \boldsymbol{n} \times (-\varepsilon_{\boldsymbol{J}^*}^I) - \alpha_2 \varepsilon_{(\boldsymbol{b}^*)^t}^I \right\rangle}_{=:I_8} \\
&\quad + \underbrace{\left\langle \varepsilon_{\boldsymbol{b}^t}^h, \frac{1}{2} \kappa \boldsymbol{n} \times \left((-\varepsilon_{\boldsymbol{u}^*}^I + \varepsilon_{\widehat{\boldsymbol{u}}^*}^I) \times \boldsymbol{d}\right) + \boldsymbol{n} \times \varepsilon_{\boldsymbol{J}^*}^I + \alpha_2 \varepsilon_{(\boldsymbol{b}^*)^t}^I \right\rangle}_{=:I_9} \\
&\quad \underbrace{- \left\langle \boldsymbol{n} \times \varepsilon_{\boldsymbol{J}}^I - \frac{1}{2} \kappa \boldsymbol{n} \times ((\varepsilon_{\boldsymbol{u}}^I + \varepsilon_{\widehat{\boldsymbol{u}}}^I) \times \boldsymbol{d}) + \alpha_2 \varepsilon_{\boldsymbol{b}^t}^I, \Pi^* \boldsymbol{b}^* - \mathbb{P}_e \boldsymbol{b}^* \right\rangle}_{=:I_{10}}.
\end{aligned} \tag{5.85}
$$

Estimate for I_1: Combining the estimate for $\varepsilon_{\boldsymbol{L}^*}^I$ and (5.83) gives

$$
|\mathrm{Re} I_1| \leq \mathrm{Re} \left\|\varepsilon_{\mathbf{L}}^h\right\|_0 \left\|\varepsilon_{\boldsymbol{L}^*}^I\right\|_0 \lesssim h \mathrm{Re} \left\|\varepsilon_{\mathbf{L}}^h\right\|_0 \left\|\boldsymbol{\theta}, \boldsymbol{\sigma}\right\|_0. \tag{5.86}
$$

Estimate for I_2: Using (5.78a), (5.66i), (5.66j), Lemma 5.8, and the regularity of the adjoint solutions, we have

$$\begin{aligned}
|\mathrm{Re} I_2| &\leq |\mathrm{Re}\left(\varepsilon_{\boldsymbol{L}}^I, \nabla \boldsymbol{u}^*\right)| + |\mathrm{Re}\left(\varepsilon_{\boldsymbol{L}}^I, -\varepsilon_{\boldsymbol{L}^*}^I\right)| \\
&= |\mathrm{Re}\left(\varepsilon_{\boldsymbol{L}}^I, \nabla(\boldsymbol{u}^* - \mathbb{P}_1 \boldsymbol{u}^*)\right) + \left(\varepsilon_{\boldsymbol{u}}^I \otimes \boldsymbol{w}, \nabla \mathbb{P}_1 \boldsymbol{u}^*\right)| + |\mathrm{Re}\left(\varepsilon_{\boldsymbol{L}}^I, -\varepsilon_{\boldsymbol{L}^*}^I\right)| \\
&\lesssim \mathrm{Re}\left(h \left\|\varepsilon_{\boldsymbol{L}}^I\right\|_0 \|\boldsymbol{u}^*\|_2 + \|\boldsymbol{w} - \mathbb{P}_0 \boldsymbol{w}\|_{L^\infty} \left\|\varepsilon_{\boldsymbol{u}}^I\right\|_0 \|\boldsymbol{u}^*\|_1 + \left\|\varepsilon_{\boldsymbol{L}}^I\right\|_0 \left\|\varepsilon_{\boldsymbol{L}^*}^I\right\|_0\right) \\
&\lesssim h \mathrm{Re}\left(\left\|\varepsilon_{\boldsymbol{L}}^I\right\|_0 + \|\boldsymbol{w}\|_{W^{1,\infty}} \left\|\varepsilon_{\boldsymbol{u}}^I\right\|_0\right) \|\boldsymbol{\theta}, \boldsymbol{\sigma}\|_0 . \qquad (5.87)
\end{aligned}$$

Estimate for I_4: By the identity (5.76), it suffices to estimate

$$\begin{aligned}
&\left(\varepsilon_{\boldsymbol{b}}^I, \Pi^* \boldsymbol{u}^* (\nabla \cdot \boldsymbol{d}) - (\Pi^* \boldsymbol{u}^* \cdot \nabla) \boldsymbol{d}\right), \quad \text{and} \\
&\left(\varepsilon_{\boldsymbol{b}}^I, ((\boldsymbol{d} - \mathbb{P}_0 \boldsymbol{d}) \cdot \nabla) \Pi^* \boldsymbol{u}^* - (\boldsymbol{d} - \mathbb{P}_0 \boldsymbol{d}) (\nabla \cdot \Pi^* \boldsymbol{u}^*)\right).
\end{aligned}$$

By the triangle inequality, the inverse estimate, and (5.83), we have

$$\begin{aligned}
\|\nabla \Pi^* \boldsymbol{u}^*\|_0 &\leq \|\nabla(\Pi^* \boldsymbol{u}^* - \mathbb{P}_1 \boldsymbol{u}^*)\|_0 + \|\nabla \mathbb{P}_1 \boldsymbol{u}^*\|_0 \\
&\lesssim h^{-1} \|\Pi^* \boldsymbol{u}^* - \mathbb{P}_1 \boldsymbol{u}^*\|_0 + \|\boldsymbol{u}^*\|_1 \\
&\leq h^{-1} (\left\|\varepsilon_{\boldsymbol{u}^*}^I\right\|_0 + \|\boldsymbol{u}^* - \mathbb{P}_1 \boldsymbol{u}^*\|_0) + \|\boldsymbol{u}^*\|_1 \\
&\lesssim \|\boldsymbol{\theta}, \boldsymbol{\sigma}\|_0 , \\
\|\Pi^* \boldsymbol{u}^*\|_0 &\leq \left\|\varepsilon_{\boldsymbol{u}^*}^I\right\|_0 + \|\boldsymbol{u}^*\|_0 \lesssim \|\boldsymbol{\theta}, \boldsymbol{\sigma}\|_0 ,
\end{aligned}$$

thus

$$\begin{aligned}
|\kappa I_4| &\lesssim \kappa \|\boldsymbol{d}\|_{W^{1,\infty}} \left\|\varepsilon_{\boldsymbol{b}}^I\right\|_0 (\|\Pi^* \boldsymbol{u}^*\|_0 + h \|\nabla \Pi^* \boldsymbol{u}^*\|_0) \\
&\lesssim \kappa \|\boldsymbol{d}\|_{W^{1,\infty}} \left\|\varepsilon_{\boldsymbol{b}}^I\right\|_0 \|\boldsymbol{\theta}, \boldsymbol{\sigma}\|_0 . \qquad (5.88)
\end{aligned}$$

Estimate for I_5: By an argument similar to the estimate of $\|\nabla \Pi^* \boldsymbol{u}^*\|_0$ above, $\|\nabla \times \Pi^* \boldsymbol{b}^*\|_0 \lesssim \|\boldsymbol{\theta}, \boldsymbol{\sigma}\|_0$. Since $I_5 = \left(\varepsilon_{\boldsymbol{u}}^I, (\boldsymbol{d} - \mathbb{P}_0 \boldsymbol{d}) \times (\nabla \times \Pi^* \boldsymbol{b}^*)\right)$,

$$\begin{aligned}
|\kappa I_5| &\lesssim h\kappa \|\boldsymbol{d}\|_{W^{1,\infty}} \left\|\varepsilon_{\boldsymbol{u}}^I\right\|_0 \|\nabla \times \Pi^* \boldsymbol{b}^*\|_0 \\
&\lesssim h\kappa \|\boldsymbol{d}\|_{W^{1,\infty}} \left\|\varepsilon_{\boldsymbol{u}}^I\right\|_0 \|\boldsymbol{\theta}, \boldsymbol{\sigma}\|_0 . \qquad (5.89)
\end{aligned}$$

Estimate for I_6 and I_7: Integrating I_6 by parts we have

$$-\kappa I_6 = -\kappa \left(\varepsilon^I_{\boldsymbol{b}^*}, \nabla \times (\varepsilon^h_{\boldsymbol{u}} \times \boldsymbol{d})\right) - \kappa \left\langle \boldsymbol{d} \times (\boldsymbol{n} \times \varepsilon^I_{\boldsymbol{b}^*}), \varepsilon^h_{\boldsymbol{u}} \right\rangle .$$

Now we can write $-\kappa I_6 + I_7$ as

$$-\kappa I_6 + I_7 = -\kappa \left(\varepsilon^I_{\boldsymbol{b}^*}, \nabla \times (\varepsilon^h_{\boldsymbol{u}} \times \boldsymbol{d})\right) + \left\langle \varepsilon^h_{\boldsymbol{u}}, -m\varepsilon^I_{\widehat{\boldsymbol{u}}^*} - \kappa \boldsymbol{d} \times (\boldsymbol{n} \times \varepsilon^I_{(\widehat{\boldsymbol{b}}^*)^t}) \right\rangle .$$

For the first term, as in the estimate of I_4, it suffices to estimate

$$\left(\varepsilon^I_{\boldsymbol{b}^*}, \varepsilon^h_{\boldsymbol{u}} (\nabla \cdot \boldsymbol{d}) - \left(\varepsilon^h_{\boldsymbol{u}} \cdot \nabla\right) \boldsymbol{d}\right) \text{ and } \left(\varepsilon^I_{\boldsymbol{b}^*}, ((\boldsymbol{d} - \mathbb{P}_0 \boldsymbol{d}) \cdot \nabla) \varepsilon^h_{\boldsymbol{u}} - (\boldsymbol{d} - \mathbb{P}_0 \boldsymbol{d}) \left(\nabla \cdot \varepsilon^h_{\boldsymbol{u}}\right)\right) .$$

Invoking Hölder's inequality and an inverse estimate we can bound the upper bounds of the first term as

$$\left\|\varepsilon^I_{\boldsymbol{b}^*}\right\|_0 \|\boldsymbol{d}\|_{W^{1,\infty}} \left\|\varepsilon^h_{\boldsymbol{u}}\right\|_0 \lesssim h \|\boldsymbol{d}\|_{W^{1,\infty}} \left\|\varepsilon^h_{\boldsymbol{u}}\right\|_0 \|\boldsymbol{\theta}, \boldsymbol{\sigma}\|_0 .$$

For the second term, we first observe that

$$\begin{aligned} &\left\langle \varepsilon^h_{\boldsymbol{u}}, -m\varepsilon^I_{\widehat{\boldsymbol{u}}^*} - \kappa \boldsymbol{d} \times (\boldsymbol{n} \times \varepsilon^I_{(\widehat{\boldsymbol{b}}^*)^t}) \right\rangle \\ &\qquad = \left\langle \varepsilon^h_{\boldsymbol{u}}, -(\boldsymbol{w} - \mathbb{P}_0 \boldsymbol{w}) \cdot \boldsymbol{n} \varepsilon^I_{\widehat{\boldsymbol{u}}^*} - \kappa (\boldsymbol{d} - \mathbb{P}_0 \boldsymbol{d}) \times (\boldsymbol{n} \times \varepsilon^I_{(\widehat{\boldsymbol{b}}^*)^t}) \right\rangle . \end{aligned}$$

By the Hölder inequality,

$$\begin{aligned} \left| \left\langle \varepsilon^h_{\boldsymbol{u}}, -m\varepsilon^I_{\widehat{\boldsymbol{u}}^*} - \kappa \boldsymbol{d} \times (\boldsymbol{n} \times \varepsilon^I_{(\widehat{\boldsymbol{b}}^*)^t}) \right\rangle \right| \leq \left\|\varepsilon^h_{\boldsymbol{u}}\right\|_{\partial \mathfrak{T}_h} \Big(&\|\boldsymbol{w} - \mathbb{P}_0 \boldsymbol{w}\|_{L^\infty(\partial \mathfrak{T}_h)} \|\boldsymbol{u}^* - \mathbb{P}_1 \boldsymbol{u}^*\|_{\partial \mathfrak{T}_h} \\ &+ \kappa \|(\boldsymbol{d} - \mathbb{P}_0 \boldsymbol{d})\|_{L^\infty(\partial \mathfrak{T}_h)} \|\boldsymbol{b}^* - \mathbb{P}_0 \boldsymbol{b}^*\|_{\partial \mathfrak{T}_h} \Big) , \end{aligned}$$

where we used the fact that $\Pi^* \widehat{\boldsymbol{b}}^*$ and $\Pi^* \widehat{\boldsymbol{u}}^*$ are the best approximations on $\partial \mathfrak{T}_h$. By Lemma 5.7 this is estimated by $(h\kappa \|\boldsymbol{d}\|_{W^{1,\infty}} + h^2 \|\boldsymbol{w}\|_{W^{1,\infty}}) \left\|\varepsilon^h_{\boldsymbol{u}}\right\|_0 \|\boldsymbol{\theta}, \boldsymbol{\sigma}\|_0$, so

$$|-\kappa I_6 + I_7| \lesssim \left(h\kappa \|\boldsymbol{d}\|_{W^{1,\infty}} + h^2 \|\boldsymbol{w}\|_{W^{1,\infty}}\right) \left\|\varepsilon^h_{\boldsymbol{u}}\right\|_0 \|\boldsymbol{\theta}, \boldsymbol{\sigma}\|_0 . \tag{5.90}$$

Estimate for I_3, I_8, and I_9: Integrating I_3 by parts gives

$$\kappa I_3 = \kappa \left(\varepsilon^I_{\boldsymbol{u}^*}, \boldsymbol{d} \times \left(\nabla \times \varepsilon^h_{\boldsymbol{b}}\right)\right) + \kappa \left\langle \boldsymbol{n} \times \left(\varepsilon^I_{\boldsymbol{u}^*} \times \boldsymbol{d}\right), \varepsilon^h_{\boldsymbol{b}} \right\rangle .$$

Some algebraic manipulations give

$$\kappa I_3 + I_8 + I_9 = \kappa \left(\varepsilon^I_{\boldsymbol{u}^*}, \boldsymbol{d} \times \left(\nabla \times \varepsilon^h_{\boldsymbol{b}}\right)\right) + \left\langle \varepsilon^h_{\boldsymbol{b}^t}, \kappa \boldsymbol{n} \times (\varepsilon^I_{\widehat{\boldsymbol{u}}^*} \times \boldsymbol{d})\right\rangle + \left\langle \varepsilon^h_{\widehat{\boldsymbol{b}}^t} - \varepsilon^h_{\boldsymbol{b}^t}, \frac{1}{2}\kappa \boldsymbol{n} \times ((\varepsilon^I_{\widehat{\boldsymbol{u}}^*} - \varepsilon^I_{\boldsymbol{u}^*}) \times \boldsymbol{d}) - \boldsymbol{n} \times \varepsilon^I_{\boldsymbol{J}^*} - \alpha_2 \varepsilon^I_{(\boldsymbol{b}^*)^t} \right\rangle .$$

The first term is estimated by

$$\begin{aligned} \left| \left(\varepsilon^I_{\boldsymbol{u}^*}, \boldsymbol{d} \times \left(\nabla \times \varepsilon^h_{\boldsymbol{b}}\right)\right) \right| &= \left| \left(\varepsilon^I_{\boldsymbol{u}^*}, (\boldsymbol{d} - \mathbb{P}_0 \boldsymbol{d}) \times \left(\nabla \times \varepsilon^h_{\boldsymbol{b}}\right)\right) \right| \\ &\lesssim h \left\|\boldsymbol{d}\right\|_{W^{1,\infty}} \left\|\varepsilon^h_{\boldsymbol{b}}\right\|_0 \left\|\boldsymbol{\theta}, \boldsymbol{\sigma}\right\|_0 . \end{aligned}$$

For the second term we have

$$\begin{aligned} \left|\left\langle \varepsilon^h_{\boldsymbol{b}^t}, \kappa \boldsymbol{n} \times (\varepsilon^I_{\widehat{\boldsymbol{u}}^*} \times \boldsymbol{d})\right\rangle\right| &\leq \kappa \left\|\varepsilon^h_{\boldsymbol{b}^t}\right\|_{\partial \mathcal{T}_h} \left\|\boldsymbol{u}^* - \mathbb{P}_k \boldsymbol{u}^*\right\|_{\partial \mathcal{T}_h} \left\|\boldsymbol{d} - \mathbb{P}_0 \boldsymbol{d}\right\|_{L^\infty(\partial \mathcal{T}_h)} \\ &\lesssim h^2 \kappa \left\|\boldsymbol{d}\right\|_{W^{1,\infty}} \left\|\varepsilon^h_{\boldsymbol{b}}\right\|_0 \left\|\boldsymbol{\theta}, \boldsymbol{\sigma}\right\|_0 , \end{aligned}$$

where we used Lemma 5.7 and the discrete trace inequality. Using the Cauchy–Schwarz inequality, (5.83), and Lemma 5.7, the third term is bounded by

$$h^{\frac{1}{2}} \left(\kappa \left\|\boldsymbol{d}\right\|_{L^\infty} + \alpha_2 + 1\right) \left\|\varepsilon^h_{\widehat{\boldsymbol{b}}^t} - \varepsilon^h_{\boldsymbol{b}^t}\right\|_{\partial \mathcal{T}_h} \left\|\boldsymbol{\sigma}, \boldsymbol{\theta}\right\|_0 .$$

Combining the above estimates we conclude

$$\begin{aligned} |\kappa I_3 + I_8 + I_9| \lesssim \Bigg(& h\kappa \left\|\boldsymbol{d}\right\|_{W^{1,\infty}} \left\|\varepsilon^h_{\boldsymbol{b}}\right\|_0 \\ & + h^{\frac{1}{2}} \left(\kappa \left\|\boldsymbol{d}\right\|_{L^\infty} + \alpha_2 + 1\right) \left\|\varepsilon^h_{\widehat{\boldsymbol{b}}^t} - \varepsilon^h_{\boldsymbol{b}^t}\right\|_{\partial \mathcal{T}_h} \Bigg) \left\|\boldsymbol{\sigma}, \boldsymbol{\theta}\right\|_0 . \end{aligned} \tag{5.91}$$

Estimate for I_{10}: Using the approximation capability of the projector $\boldsymbol{\Pi}$ (see Section 5.5.2) we have

$$\begin{aligned} & \left| \left\langle \boldsymbol{n} \times \varepsilon^I_{\boldsymbol{J}} - \frac{1}{2}\kappa \boldsymbol{n} \times ((\varepsilon^I_{\boldsymbol{u}} + \varepsilon^I_{\widehat{\boldsymbol{u}}}) \times \boldsymbol{d}) + \alpha_2 \varepsilon^I_{\boldsymbol{b}^t}, \Pi^* \boldsymbol{b}^* - \mathbb{P}_e \boldsymbol{b}^* \right\rangle \right| \\ & \lesssim h^{\frac{1}{2}} \left(\left\|\varepsilon^I_{\boldsymbol{J}}\right\|_{\partial \mathcal{T}_h} + \kappa \left\|\boldsymbol{d}\right\|_{L^\infty} \left\|\varepsilon^I_{\boldsymbol{u}}\right\|_{\partial \mathcal{T}_h} + \alpha_2 \left\|\varepsilon^I_{\boldsymbol{b}}\right\|_{\partial \mathcal{T}_h} \right) \left\|\boldsymbol{\theta}, \boldsymbol{\sigma}\right\|_0 . \end{aligned} \tag{5.92}$$

Finally, we take $\boldsymbol{\theta} = \varepsilon^h_{\boldsymbol{u}}$, $\boldsymbol{\sigma} = \varepsilon^h_{\boldsymbol{b}}$ in (5.78). If we use (5.85), the estimates (5.86)–(5.92), and Young's inequality, we can obtain

$$\left\|\varepsilon^h_{\boldsymbol{b}}, \varepsilon^h_{\boldsymbol{u}}\right\|_0 \lesssim \left\|\varepsilon^I_{\boldsymbol{b}}\right\|_0 + h\left\|\varepsilon^I_{\boldsymbol{L}}, \varepsilon^h_{\mathbf{L}}, \varepsilon^I_{\boldsymbol{u}}, \varepsilon^h_{\boldsymbol{u}}, \varepsilon^h_{\boldsymbol{b}}\right\|_0 + h^{\frac{1}{2}}\left\|\varepsilon^I_{\boldsymbol{J}}, \varepsilon^I_{\boldsymbol{u}}, \varepsilon^I_{\boldsymbol{b}}, \varepsilon^h_{\widehat{\boldsymbol{b}}^t} - \varepsilon^h_{\boldsymbol{b}^t}\right\|_{\partial\mathcal{T}_h}. \tag{5.93}$$

5.5.7 Putting It Together

At this point we are ready to estimate the approximation errors for $\mathbf{L}$, $\boldsymbol{u}$, $\boldsymbol{J}$, and $\boldsymbol{b}$. For readability let us absorb α_1, α_2, α_3, Re, Rm, κ, and the norms on $\boldsymbol{d}$ and $\boldsymbol{w}$ into the implicit constants. Note that the error estimates stated in the theorem below are optimal for $\boldsymbol{u}$ and $\boldsymbol{b}$, and suboptimal for $\mathbf{L}$, p, $\boldsymbol{J}$, and r. The results in Section 5.8 indicate that it is possible for numerical results to exceed the suboptimal estimates proven in this work.

Theorem 5.15. *Suppose that $\alpha_1 - \frac{1}{2}\|\boldsymbol{w}\|_{L^\infty}$, α_2, α_3 are positive constants independent of h,* Re, Rm, *κ, $\boldsymbol{d}$, $\boldsymbol{w}$, and suppose that h is sufficiently small, i.e.,*

$$h \leq C \ll 1 \tag{5.94}$$

with C depending on the coefficients in estimates (5.90) *and* (5.91)*. Then it holds that*

$$E_h \lesssim h^{k+\frac{1}{2}}\left\|\mathbf{L}, \boldsymbol{u}, p, \boldsymbol{J}, \boldsymbol{b}, r\right\|_{k+1} \tag{5.95}$$

and the following error estimates hold:

$$\left\|\mathbf{L} - \mathbf{L}_h, \boldsymbol{J} - \boldsymbol{J}_h\right\|_0 \lesssim h^{k+\frac{1}{2}}\left\|\mathbf{L}, \boldsymbol{u}, p, \boldsymbol{J}, \boldsymbol{b}, r\right\|_{k+1}, \tag{5.96}$$

$$\left\|\boldsymbol{u} - \boldsymbol{u}_h, \boldsymbol{b} - \boldsymbol{b}_h\right\|_0 \lesssim h^{k+1}\left\|\mathbf{L}, \boldsymbol{u}, p, \boldsymbol{J}, \boldsymbol{b}, r\right\|_{k+1}. \tag{5.97}$$

Proof. First, we can simplify (5.93) to

$$\left\|\varepsilon^h_{\boldsymbol{b}}, \varepsilon^h_{\boldsymbol{u}}\right\|_0 \lesssim \left\|\varepsilon^I_{\boldsymbol{b}}\right\|_0 + h\left\|\varepsilon^I_{\boldsymbol{L}}, \varepsilon^h_{\mathbf{L}}, \varepsilon^I_{\boldsymbol{u}}\right\|_0 + h^{\frac{1}{2}}\left\|\varepsilon^I_{\boldsymbol{J}}, \varepsilon^I_{\boldsymbol{u}}, \varepsilon^I_{\boldsymbol{b}}, \varepsilon^h_{\widehat{\boldsymbol{b}}^t} - \varepsilon^h_{\boldsymbol{b}^t}\right\|_{\partial\mathcal{T}_h} \tag{5.98}$$

if the constants that multiply $\left\|\varepsilon_{\boldsymbol{u}}^h\right\|_0$ and $\left\|\varepsilon_{\boldsymbol{b}}^h\right\|_0$ in (5.90) and (5.91) are sufficiently small, which is true under the assumptions we have made on α_1, α_2, and α_3 together with (5.94). The approximation error terms on the right hand side of (5.98) (i.e., terms with superscript "h") are bounded by E_h (see definition of E_h in (5.68)). This implies

$$\left\|\varepsilon_{\boldsymbol{b}}^h, \varepsilon_{\boldsymbol{u}}^h\right\|_0 \lesssim \left\|\varepsilon_{\boldsymbol{b}}^I\right\|_0 + h\left\|\varepsilon_{\boldsymbol{L}}^I, \varepsilon_{\boldsymbol{u}}^I\right\|_0 + h^{\frac{1}{2}}\left\|\varepsilon_{\boldsymbol{J}}^I, \varepsilon_{\boldsymbol{u}}^I, \varepsilon_{\boldsymbol{b}}^I\right\|_{\partial\mathcal{T}_h} + h^{\frac{1}{2}}E_h. \tag{5.99}$$

Applying Young's inequality to the right side of (5.77) for $\left\|\varepsilon_{\boldsymbol{u}}^h\right\|_0$, $\left\|\varepsilon_{\boldsymbol{b}}^h\right\|_0$, and using (5.99), we get

$$E_h^2 \lesssim \left\|\varepsilon_{\boldsymbol{J}}^I, \varepsilon_{\boldsymbol{u}}^I, \varepsilon_{\boldsymbol{b}}^I\right\|_{\partial\mathcal{T}_h}^2 + \left\|\varepsilon_{\boldsymbol{L}}^I, \varepsilon_{\boldsymbol{u}}^I, \varepsilon_{\boldsymbol{b}}^I\right\|_0^2.$$

Then (5.95) follows from the approximation properties of $\varepsilon_{\boldsymbol{J}}^I, \varepsilon_{\boldsymbol{u}}^I, \varepsilon_{\boldsymbol{b}}^I, \varepsilon_{\boldsymbol{L}}^I$ with the trace inequality Lemma 5.7 discussed in sections 5.5.2 and 5.5.1, respectively. Further, it gives

$$\left\|\varepsilon_{\mathbf{L}}^h, \varepsilon_{\boldsymbol{J}}^h\right\|_0 + \left\|\varepsilon_{\boldsymbol{u}}^h - \varepsilon_{\widehat{\boldsymbol{u}}}^h, \varepsilon_{\boldsymbol{b}^t}^h - \varepsilon_{\widehat{\boldsymbol{b}}^t}^h, \varepsilon_r^h - \varepsilon_{\widehat{r}}^h\right\|_{\partial\mathcal{T}_h} \lesssim E_h \lesssim h^{k+\frac{1}{2}}\left\|\mathbf{L}, \boldsymbol{u}, p, \boldsymbol{J}, \boldsymbol{b}, r\right\|_{k+1},$$

where the first inequality is from the definition of E_h in (5.68). Then (5.96) follows from the triangle inequality. Finally, the above estimate with (5.99) and the triangle inequality give (5.97). □

What remains is to estimate $\left\|\varepsilon_p^h\right\|_0$ and $\left\|\varepsilon_r^h\right\|_0$.

Theorem 5.16. *There holds:*

$$\left\|\varepsilon_p^h\right\|_0 \lesssim \left\|\varepsilon_{\mathbf{L}}^h, \varepsilon_{\boldsymbol{u}}^h, \varepsilon_{\boldsymbol{b}}^h, \varepsilon_{\boldsymbol{b}}^I\right\|_0 + h^{\frac{1}{2}}E_h \lesssim h^{k+\frac{1}{2}}\left\|\mathbf{L}, \boldsymbol{u}, p, \boldsymbol{J}, \boldsymbol{b}, r\right\|_{k+1}, \quad k \geq 0.$$

Proof. Let $\tilde{\Pi} : [H^1(\Omega)]^d \to [\mathcal{P}_k(\mathcal{T}_h)]^d$ be defined by (see [17, Lemma 4.1])

$$\begin{aligned}\left(\tilde{\Pi}\boldsymbol{\vartheta} - \boldsymbol{\vartheta}, \boldsymbol{v}\right)_K &= 0, \qquad \boldsymbol{v} \in [\mathcal{P}_{k-1}(K)]^d,\\ \left\langle(\tilde{\Pi}\boldsymbol{\vartheta} - \boldsymbol{\vartheta})\cdot\boldsymbol{n}, \widehat{\boldsymbol{v}}\cdot\boldsymbol{n}\right\rangle_{\partial K} &= 0, \qquad \widehat{\boldsymbol{v}} \in \left[\mathcal{P}_k^{\perp}(K)\right]^d,\end{aligned}$$

for $\boldsymbol{\vartheta} \in [H^1(\Omega)]^d$ and $K \in \mathcal{T}_h$, where $\mathcal{P}_k^{\perp}(K)$ is the subspace of $\mathcal{P}_k(K)$ which is orthogonal to $\mathcal{P}_{k-1}(K)$ in $L^2(K)$.

Since Πp is the L^2-projection, we have $\left(\varepsilon_p^h, 1\right) = -(\varepsilon_p^I, 1) = 0$ from (5.28). It is known [30] that there exists $\boldsymbol{\vartheta} \in [H_0^1(\Omega)]^d$ such that $\nabla \cdot \boldsymbol{\vartheta} = \varepsilon_p^h$, $\|\boldsymbol{\vartheta}\|_1 \lesssim \left\|\varepsilon_p^h\right\|_0$. Then

$$\begin{aligned}
\left\|\varepsilon_p^h\right\|_0^2 &= \left(\varepsilon_p^h, \nabla \cdot \boldsymbol{\vartheta}\right) = -\left(\nabla \varepsilon_p^h, \boldsymbol{\vartheta}\right) + \left\langle \varepsilon_p^h, \boldsymbol{\vartheta} \cdot \boldsymbol{n} \right\rangle \\
&= -\left(\nabla \varepsilon_p^h, \tilde{\Pi} \boldsymbol{\vartheta}\right) + \left\langle \varepsilon_p^h, \boldsymbol{\vartheta} \cdot \boldsymbol{n} \right\rangle \\
&= \left(\varepsilon_p^h, \nabla \cdot \tilde{\Pi} \boldsymbol{\vartheta}\right) + \left\langle \varepsilon_p^h \boldsymbol{n}, \boldsymbol{\vartheta} - \tilde{\Pi} \boldsymbol{\vartheta} \right\rangle, \qquad (5.100)
\end{aligned}$$

where we used the integration by parts twice and used the definition $\tilde{\Pi}$. Since the exact solution $(\mathbf{L}, p, \boldsymbol{u}, \boldsymbol{b})$ and its trace also satisfy the HDG local (sub-) equation (5.10b), we can add and subtract the corresponding projections in (5.66) to obtain

$$\begin{aligned}
\left(\varepsilon_p^h, \nabla \cdot \tilde{\Pi} \boldsymbol{\vartheta}\right) &= \left(\varepsilon_{\mathbf{L}}^h, \nabla \tilde{\Pi} \boldsymbol{\vartheta}\right) - \left(\varepsilon_{\boldsymbol{u}}^h, (\boldsymbol{w} \cdot \nabla) \tilde{\Pi} \boldsymbol{\vartheta}\right) + \kappa \left(\varepsilon_{\boldsymbol{b}}^h, \nabla \times \left(\tilde{\Pi} \boldsymbol{\vartheta} \times \boldsymbol{d}\right)\right) \\
&+ \left\langle m \varepsilon_{\boldsymbol{u}}^h - \varepsilon_{\mathbf{L}}^h \boldsymbol{n} + \varepsilon_p^h \boldsymbol{n} + \frac{1}{2} \kappa \boldsymbol{d} \times \left(\boldsymbol{n} \times \left(\varepsilon_{\boldsymbol{b}^t}^h + \varepsilon_{\widehat{\boldsymbol{b}}^t}^h\right)\right) + \alpha_1 \left(\varepsilon_{\boldsymbol{u}}^h - \varepsilon_{\widehat{\boldsymbol{u}}}^h\right), \tilde{\Pi} \boldsymbol{\vartheta} \right\rangle \\
&+ \kappa \left(\varepsilon_{\boldsymbol{b}}^I, \nabla \times \left(\tilde{\Pi} \boldsymbol{\vartheta} \times \boldsymbol{d}\right)\right), \qquad (5.101)
\end{aligned}$$

where we have taken $\tilde{\Pi} \boldsymbol{\vartheta}$ as the test function in (5.10b). Combining (5.100) and (5.101) yields

$$\begin{aligned}
\left\|\varepsilon_p^h\right\|_0^2 &= \left(\varepsilon_{\mathbf{L}}^h, \nabla \tilde{\Pi} \boldsymbol{\vartheta}\right) - \left(\varepsilon_{\boldsymbol{u}}^h, (\boldsymbol{w} \cdot \nabla) \tilde{\Pi} \boldsymbol{\vartheta}\right) + \kappa \left(\varepsilon_{\boldsymbol{b}}^h, \nabla \times \left(\tilde{\Pi} \boldsymbol{\vartheta} \times \boldsymbol{d}\right)\right) \\
&+ \left\langle m \varepsilon_{\boldsymbol{u}}^h - \varepsilon_{\mathbf{L}}^h \boldsymbol{n} + \frac{1}{2} \kappa \boldsymbol{d} \times \left(\boldsymbol{n} \times \left(\varepsilon_{\boldsymbol{b}^t}^h + \varepsilon_{\widehat{\boldsymbol{b}}^t}^h\right)\right) + \alpha_1 \left(\varepsilon_{\boldsymbol{u}}^h - \varepsilon_{\widehat{\boldsymbol{u}}}^h\right), \tilde{\Pi} \boldsymbol{\vartheta} \right\rangle \\
&+ \kappa \left(\varepsilon_{\boldsymbol{b}}^I, \nabla \times \left(\tilde{\Pi} \boldsymbol{\vartheta} \times \boldsymbol{d}\right)\right) + \left\langle \varepsilon_p^h \boldsymbol{n}, \boldsymbol{\vartheta} \right\rangle,
\end{aligned}$$

which can be further simplified using two facts: first, integrating by parts twice and using the definition of $\tilde{\Pi}$ give $\left(\varepsilon_{\mathbf{L}}^h, \nabla \tilde{\Pi} \boldsymbol{\vartheta}\right) = \left(\varepsilon_{\mathbf{L}}^h, \nabla \boldsymbol{\vartheta}\right) - \left\langle \varepsilon_{\mathbf{L}}^h \boldsymbol{n}, \boldsymbol{\vartheta} \right\rangle + \left\langle \varepsilon_{\mathbf{L}}^h \boldsymbol{n}, \tilde{\Pi} \boldsymbol{\vartheta} \right\rangle$; and

second, we combine (5.47g) and (5.66k) to have

$$\begin{aligned}\left\langle -\varepsilon_{\mathbf{L}}^h \boldsymbol{n} + \varepsilon_p^h \boldsymbol{n}, \boldsymbol{\vartheta} \right\rangle &= \left\langle -\varepsilon_{\mathbf{L}}^h \boldsymbol{n} + \varepsilon_p^h \boldsymbol{n}, \mathbb{P}_e \boldsymbol{\vartheta} \right\rangle \\ &= -\left\langle m\varepsilon_{\boldsymbol{u}}^h + \frac{1}{2}\kappa \boldsymbol{d} \times \left(\boldsymbol{n} \times \left(\varepsilon_{\boldsymbol{b}^t}^h + \varepsilon_{\widehat{\boldsymbol{b}}^t}^h \right) \right) + \alpha_1 \left(\varepsilon_{\boldsymbol{u}}^h - \varepsilon_{\widehat{\boldsymbol{u}}}^h \right), \mathbb{P}_e \boldsymbol{\vartheta} \right\rangle.\end{aligned}$$

In particular, we obtain

$$\begin{aligned}\left\| \varepsilon_p^h \right\|_0^2 = &\left(\varepsilon_{\mathbf{L}}^h, \nabla \boldsymbol{\vartheta} \right) - \left(\varepsilon_{\boldsymbol{u}}^h, (\boldsymbol{w} \cdot \nabla) \tilde{\Pi} \boldsymbol{\vartheta} \right) + \kappa \left(\varepsilon_{\boldsymbol{b}}^h, \nabla \times \left(\tilde{\Pi} \boldsymbol{\vartheta} \times \boldsymbol{d} \right) \right) \\ &+ \left\langle m\varepsilon_{\boldsymbol{u}}^h + \frac{1}{2}\kappa \boldsymbol{d} \times \left(\boldsymbol{n} \times \left(\varepsilon_{\boldsymbol{b}^t}^h + \varepsilon_{\widehat{\boldsymbol{b}}^t}^h \right) \right) + \alpha_1 \left(\varepsilon_{\boldsymbol{u}}^h - \varepsilon_{\widehat{\boldsymbol{u}}}^h \right), \tilde{\Pi} \boldsymbol{\vartheta} - \mathbb{P}_e \boldsymbol{\vartheta} \right\rangle \\ &+ \kappa \left(\varepsilon_{\boldsymbol{b}}^I, \nabla \times \left(\tilde{\Pi} \boldsymbol{\vartheta} \times \boldsymbol{d} \right) \right).\end{aligned}$$

By the triangle and Hölder inequalities,

$$\begin{aligned}&\left\| \varepsilon_p^h \right\|_0^2 \lesssim \left\| \varepsilon_{\mathbf{L}}^h \right\|_0 \left\| \nabla \boldsymbol{\vartheta} \right\|_0 + \left\| \boldsymbol{w} \right\|_{L^\infty} \left\| \varepsilon_{\boldsymbol{u}}^h \right\|_0 \left\| \nabla \tilde{\Pi} \boldsymbol{\vartheta} \right\|_0 + \kappa \left\| \boldsymbol{d} \right\|_{W^{1,\infty}} \left\| \varepsilon_{\boldsymbol{b}}^h, \varepsilon_{\boldsymbol{b}}^I \right\|_0 \left\| \nabla \tilde{\Pi} \boldsymbol{\vartheta} \right\|_0 \\ &+ \left(\left\| \boldsymbol{w} \right\|_{L^\infty} \left\| \varepsilon_{\boldsymbol{u}}^h \right\|_{\partial \mathcal{T}_h} + \kappa \left\| \boldsymbol{d} \right\|_{L^\infty} \left\| \varepsilon_{\boldsymbol{b}^t}^h, \varepsilon_{\boldsymbol{b}^t}^h - \varepsilon_{\widehat{\boldsymbol{b}}^t}^h \right\|_{\partial \mathcal{T}_h} + \alpha_1 \left\| \varepsilon_{\boldsymbol{u}}^h - \varepsilon_{\widehat{\boldsymbol{u}}}^h \right\|_{\partial \mathcal{T}_h} \right) \left\| \tilde{\Pi} \boldsymbol{\vartheta} - \mathbb{P}_e \boldsymbol{\vartheta} \right\|_{\partial \mathcal{T}_h} \\ &\lesssim \left(\left\| \varepsilon_{\mathbf{L}}^h, \varepsilon_{\boldsymbol{u}}^h, \varepsilon_{\boldsymbol{b}}^h, \varepsilon_{\boldsymbol{b}}^I \right\|_0 + h^{\frac{1}{2}} E_h \right) \left\| \varepsilon_p^h \right\|_0\end{aligned}$$

where we have used Lemma 5.8, the approximation capability of $\tilde{\Pi}$ and the L^2-projection, definition of E_h in (5.68), the property of $\boldsymbol{\vartheta}$, and we absorb all mesh independent parameters into the implicit constant in the final inequality. As a consequence, we have $\left\| \varepsilon_p^h \right\|_0 \lesssim \left\| \varepsilon_{\mathbf{L}}^h, \varepsilon_{\boldsymbol{u}}^h, \varepsilon_{\boldsymbol{b}}^h, \varepsilon_{\boldsymbol{b}}^I \right\|_0 + h^{\frac{1}{2}} E_h$. Then the conclusion follows from the triangle inequality and the estimates of $\left\| \varepsilon_{\mathbf{L}}^h, \varepsilon_{\boldsymbol{u}}^h, \varepsilon_{\boldsymbol{b}}^h, \varepsilon_{\boldsymbol{b}}^I \right\|_0$ and E_h. □

For an analogous result for $\left\| \varepsilon_r^h \right\|_0$, we need the following result.

Lemma 5.17. *There exists* $\left[\boldsymbol{\vartheta} \in H^1(\Omega) \right]^d$ *such that* $\nabla \cdot \boldsymbol{\vartheta} = \varepsilon_r^h$, $\boldsymbol{n} \times \boldsymbol{\vartheta} = \mathbf{0}$ *on* $\partial\Omega$, *and* $\left\| \boldsymbol{\vartheta} \right\|_1 \lesssim \left\| \varepsilon_r^h \right\|_0$.

Proof. We omit the proof and refer to [47]. □

Theorem 5.18. *There holds:*

$$\|r - r_h\|_0 \lesssim \left\|\varepsilon_{\boldsymbol{J}}^h, \varepsilon_{\boldsymbol{u}}^I, \varepsilon_{\boldsymbol{u}}^h\right\|_0 + h^{\frac{1}{2}} E_h \lesssim h^{k+\frac{1}{2}} \left\|\mathbf{L}, \boldsymbol{H}, \boldsymbol{u}, \boldsymbol{b}, p, r\right\|_{k+1}, \quad k \geq 0.$$

Proof. It is similar to the estimate of $\|p - p_h\|_0$, so we refer to [47] for details. □

5.6 A Nonlinear Solver

In this work, we employ the linear HDG scheme given by Formulation 5.3 in a fixed point Picard iteration to find a numerical solution to the nonlinear problem (5.5). If we consider the linearized MHD equations (5.9) to be a linear map $(\boldsymbol{w}, \boldsymbol{d}) \mapsto (\boldsymbol{u}, \boldsymbol{b})$, then any fixed point of that mapping is a solution to the nonlinear incompressible MHD equations (5.5). With this in mind, we can use the general linearized incompressible MHD HDG scheme (5.10) – (5.12) in an iterative manner to numerically solve the nonlinear incompressible MHD equations. Omitting the specification of trial/test spaces for simplicity, we can express any of the the linearized MHD HDG schemes as solving

$$a\left(\boldsymbol{w}, \boldsymbol{d}; \mathbf{L}_h, \boldsymbol{u}_h, p_h, \boldsymbol{J}_h, \boldsymbol{b}_h, r_h, \widehat{\boldsymbol{U}}_h; \mathbf{G}, \boldsymbol{v}, q, \boldsymbol{H}, \boldsymbol{c}, s, \widehat{\boldsymbol{V}}\right) = \ell\left(\mathbf{G}, \boldsymbol{v}, q, \boldsymbol{H}, \boldsymbol{c}, s, \widehat{\boldsymbol{V}}\right), \tag{5.102}$$

where $\widehat{\boldsymbol{U}}_h$ and $\widehat{\boldsymbol{V}}$ represent the global unknowns and test functions, respectively. For example, for Formulation 5.3, $\widehat{\boldsymbol{U}}_h$ represents $(\widehat{\boldsymbol{u}}_h^i, \widehat{\boldsymbol{b}}_h^{t,i}, \widehat{r}_h^i, \rho_h)$ and $\widehat{\boldsymbol{V}}$ represents $(\widehat{\boldsymbol{v}}, \widehat{\boldsymbol{c}}^t, \widehat{s}, \psi)$, and for Formulation 5.1, $\widehat{\boldsymbol{U}}_h$ represents $(\widehat{\boldsymbol{u}}_h^i, \widehat{\boldsymbol{b}}_h^i, \rho_h, \gamma_h)$ and $\widehat{\boldsymbol{V}}$ represents $(\widehat{\boldsymbol{v}}, \widehat{\boldsymbol{c}}, \psi, \phi)$. This is the case for both the steady state version and time dependent version with fully implicit time stepping. Then, we can define one step of the Picard iteration as solving for $\left(\mathbf{L}_h^m, \boldsymbol{u}_h^m, p_h^m, \boldsymbol{J}_h{}^m, \boldsymbol{b}_h{}^m, r_h{}^m, \widehat{\boldsymbol{U}}_h^m\right)$ using

$$\begin{aligned} a\left(\boldsymbol{u}_h^{m-1}, \boldsymbol{b}_h{}^{m-1}; \mathbf{L}_h^m, \boldsymbol{u}_h^m, p_h^m, \boldsymbol{J}_h{}^m, \boldsymbol{b}_h{}^m, r_h{}^m, \widehat{\boldsymbol{U}}_h^m; \mathbf{G}, \boldsymbol{v}, q, \boldsymbol{H}, \boldsymbol{c}, s, \widehat{\boldsymbol{V}}\right) \\ = \ell\left(\mathbf{G}, \boldsymbol{v}, q, \boldsymbol{H}, \boldsymbol{c}, s, \widehat{\boldsymbol{V}}\right). \end{aligned} \tag{5.103}$$

It remains to define stopping criteria for the nonlinear iteration. One possible stopping criterion involves using a combined nonlinear residual $(\boldsymbol{r}_1^m, \boldsymbol{r}_2^m) \in \boldsymbol{V}_h \times \boldsymbol{C}_h$ to the discretized momentum and induction equations that we define by

$$\begin{aligned}(\boldsymbol{r}_1^m; \boldsymbol{v})_{\mathcal{T}_h} + (\boldsymbol{r}_2^m; \boldsymbol{c})_{\mathcal{T}_h} &= -\ell\left(\boldsymbol{0}, \boldsymbol{v}, 0, \boldsymbol{0}, \boldsymbol{c}, 0, \boldsymbol{0}\right) \\ &\quad + a\left(\boldsymbol{u}_h^m, {\boldsymbol{b}_h}^m; \mathbf{L}_h^m, \boldsymbol{u}_h^m, p_h^m, {\boldsymbol{J}_h}^m, {\boldsymbol{b}_h}^m, {r_h}^m, \widehat{\boldsymbol{U}}_h^m; \boldsymbol{0}, \boldsymbol{v}, 0, \boldsymbol{0}, \boldsymbol{c}, 0, \boldsymbol{0}\right) \end{aligned} \tag{5.104}$$

for all $(\boldsymbol{v}, \boldsymbol{c})$ in $\boldsymbol{V}_h \times \boldsymbol{C}_h$ and stopping when

$$\sqrt{\|\boldsymbol{r}_1^m\|_{L^2(\Omega)}^2 + \|\boldsymbol{r}_2^m\|_{L^2(\Omega)}^2} < \delta \tag{5.105}$$

for some $\delta > 0$. The algorithm is outlined in Algorithm 3

Algorithm 3 Picard Iteration for Steady Incompressible MHD HDG Schemes.

```
set initial guess (u_h^0, b_h^0), choose stopping tolerance δ, and set m = 1
while true do
  solve for (L_h^m, u_h^m, p_h^m, J_h^m, b_h^m, r_h^m, Û_h^m) using (5.103)
  if (5.105) is true then
    break
  end if
  m ← m + 1
end while
```

For time dependent problems with fully implicit time discretization, Algorithm 3 is used at each BDF time step or at each stage of a diagonally implicit Runge-Kutta scheme. For steady state problems a natural initial guess for $(\boldsymbol{u}_h, \boldsymbol{b}_h)$ is zero, and for time dependent problems a natural initial guess is the values of $(\boldsymbol{u}_h, \boldsymbol{b}_h)$ at the previous time step.

There are several generalizations and alternate choices for the volume residual norm based stopping criterion given above. We could use a weighted ℓ^2 norm of the $L^2(\Omega)$ norms of $\boldsymbol{r}_1^m$ and $\boldsymbol{r}_2^m$,

$$\sqrt{\alpha_1 \|\boldsymbol{r}_1^m\|_{L^2(\Omega)}^2 + \alpha_2 \|\boldsymbol{r}_2^m\|_{L^2(\Omega)}^2} < 1, \tag{5.106}$$

that is, we could favor minimizing the residual of the momentum equation over that of the induction equation, or vice versa. We could also include the residual of the conservation equations, or some weighting of that. As an alternative to any of these choices, we could use discrete norms of the residual vector of the matrix system and/or discrete norms of the solution update vector of the matrix system. See [64] for stopping criteria of this type.

5.7 Time Integration

For time dependent problems, HDG spatial discretizations lead to differential-algebraic systems of equations. For these systems, implicit time stepping schemes such as BDF and diagonally implicit Runge-Kutta (DIRK) are suitable.

In this work, for solving problems in MHD, we favor DIRK schemes over the BDF schemes, in part because DIRK schemes are self-starting. An s-stage DIRK scheme involves s implicit solves for the intermediate stage values, followed by an explicit update to compute the solution at t^{n+1}. At each stage, we apply the Picard linearization, which results in linear systems that still take the form (1.10), where we solve for all variables in the usual way. Then, in the explicit update step of the DIRK scheme, we compute $(\boldsymbol{u}^{n+1}, \boldsymbol{b}^{n+1})$ from the intermediate stage values of $\boldsymbol{u}$ and $\boldsymbol{b}$. Finally, because of the nature of unsteady HDG scheme, in order to calculate $\left(\mathbf{L}^{n+1}, p^{n+1}, \boldsymbol{J}^{n+1}, r^{n+1}, \widehat{\boldsymbol{u}}^{n+1}, \widehat{\boldsymbol{b}}^{t,n+1}, \widehat{r}^{n+1}, \rho^{n+1}\right)$ we must perform an additional implicit solve. Note that we can advance in time without performing this additional solve, so we only need to perform this additional implicit solve at time steps of interest. See [54] for details.

The class of *stiffly accurate* DIRK methods has the desirable property (among other desirable properties) that the final intermediate stage coincides with the next

time step. Therefore, when using stiffly accurate DIRK methods, the additional implicit step described above is never necessary. In the numerical simulations that follow, we employ 2 stage, 2nd order and 3 stage, 3rd order stiffly accurate DIRK methods from [2], and 5 stage, 4th order stiffly accurate DIRK method given in Table 22 of [41]. In the remainder of this work, we refer to these methods as DIRK(2,2), DIRK(3,3), and DIRK(5,4), respectively.

5.8 Numerical Results

In this section, we perform a set of numerical experiments to demonstrate the capabilities of the HDG scheme. First, we verify the theoretical order of accuracy results for the linearized scheme by applying the scheme to a problem with a smooth solution. Then we demonstrate that the scheme converges to singular solutions on a nonconvex domain. Finally, we apply the scheme in a Picard iteration to solve nonlinear steady state and transient problems in liquid metal duct flow and in plasma physics.

5.8.1 Smooth Solution

This example illustrates the convergence of the linearized steady-state HDG scheme applied to a smooth manufactured solution problem posed on the non-convex domain $\Omega = (-1,1)\times(-1,1)\backslash[0,1)\times(-1,0]$ shown in Figure 5.1 (similar to Section 5.1.1 in [37]). We take $\mathrm{Re} = \mathrm{Rm} = \kappa = 1$, $\boldsymbol{w} = (2,1)$, and $\boldsymbol{d} = (x_1, -x_2)$. We set $\boldsymbol{f}$ and $\boldsymbol{g}$ such that the manufactured solution for (5.4) is

$$\boldsymbol{u} = \left(-\left[x_2\cos(x_2)+\sin(x_2)\right]e^{x_1}, x_2\sin(x_2)e^{x_1}\right), \quad p = 2e^{x_1}\sin(x_2) - p_0,$$
$$\boldsymbol{b} = \left(-\left[x_2\cos(x_2)+\sin(x_2)\right]e^{x_1}, x_2\sin(x_2)e^{x_1}\right), \quad r = -\sin(\pi x_1)\sin(\pi x_2),$$

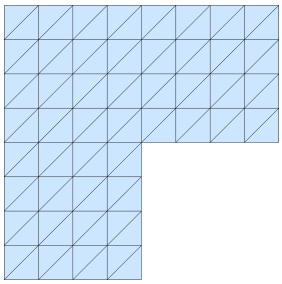

Figure 5.1: Geometry of the non-convex domain with a mesh at refinement level $l = 4$.

where p_0 is the constant that enables p to satisfy the zero average pressure condition $(p, 1)_\Omega = 0$. We use the exact solution to enforce the boundary conditions $\partial\Omega$, i.e., $\boldsymbol{u}_D = \boldsymbol{u}$, $\boldsymbol{b}_D^t = \boldsymbol{b}^t$, and $r_D = r$.

At refinement level l, each quadrant of the domain is subdivided into $l \times l$ squares, each of which is divided into two triangles from top right to bottom left. Mesh parameter h is defined as $h := 1/l$. See Figure 5.1 for an example mesh ($l = 4$). In Figure 5.2 are the convergence plots. For this problem, we observe the optimal convergence rates of $k + 1$ for all of the local variables, which matches or exceeds the rates proven in Section 5.5.

5.8.2 Singular Solution

Although we do not discuss the implications of singular solutions on the theoretical convergence rates of the HDG scheme, applying the scheme to such a problem is instructive in assessing its robustness. This example illustrates the convergence of the HDG scheme using a manufactured solution with a singularity (similar to the example in Section 5.2 of [37]). In particular, we consider the same non-convex domain and mesh refinement as in the previous example (see Figure 5.1). We take $\mathrm{Re} = \mathrm{Rm} = \kappa = 1$, $\boldsymbol{w} = \boldsymbol{0}$, and $\boldsymbol{d} = (-1, 1)$. We choose $\boldsymbol{f}$ and $\boldsymbol{g}$ such that the

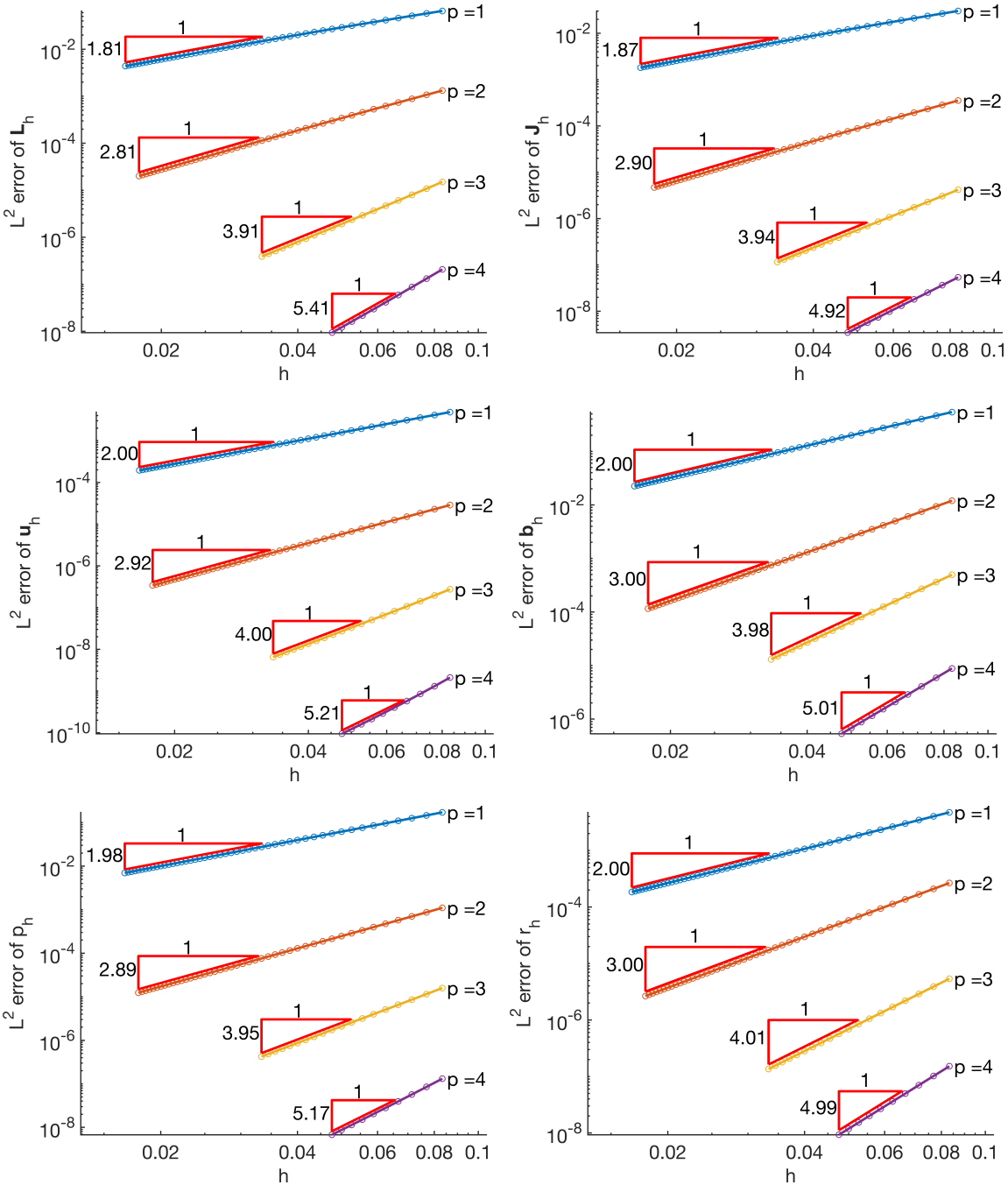

Figure 5.2: MHD smooth solution problem: L^2 convergence.

analytical solution of (5.4) has the form

$$\boldsymbol{u} = \begin{pmatrix} \rho^{\lambda}\left[(1+\lambda)\sin(\phi)\psi(\phi) + \cos(\phi)\psi'(\phi)\right], \\ \rho^{\lambda}\left[-(1+\lambda)\cos(\phi)\psi(\phi) + \sin(\phi)\psi'(\phi)\right] \end{pmatrix}, \qquad \boldsymbol{b} = \nabla\left(\rho^{2/3}\sin\left(\frac{2\phi}{3}\right)\right),$$
$$p = -\rho^{\lambda-1}\frac{(1+\lambda)^2\psi'(\phi) + \psi'''(\phi)}{1-\lambda}, \qquad r = 0,$$

where

$$\psi(\phi) = \cos(\lambda w)\left[\frac{\sin((1+\lambda)\phi)}{1+\lambda} - \frac{\sin((1-\lambda)\phi)}{1-\lambda}\right] - \cos((1+\lambda)\phi) + \cos((1-\lambda)\phi),$$
$$w = \frac{3\pi}{2}, \qquad \lambda \approx 0.54448373678246.$$

On $\partial\Omega$ we use the exact solution to set the boundary condition, i.e., $\boldsymbol{u}_D = \boldsymbol{u}$, ${\boldsymbol{b}^t}_D = \boldsymbol{b}^t$, and $r_D = r$. For this problem, it is known that $\boldsymbol{u} \in \left[H^{1+\lambda}(\Omega)\right]^2$, $p \in H^{\lambda}(\Omega)$, and $\boldsymbol{b} \in \left[H^{2/3}(\Omega)\right]^2$, and that the solution contains magnetic and hydrodynamic singularities that are among the strongest singularities [37].

Convergence results for this problem are shown in Figure 5.3. For the fluid variables $\mathbf{L}_h$, $\boldsymbol{u}_h$, and p_h, we observe convergence rates of approximately λ, 2λ, and λ, respectively. For the magnetic variables $\boldsymbol{J}_h$, $\boldsymbol{b}_h$, and r_h, we observe convergence rates of approximately 1/2, 2/3, and 1/3, respectively.

5.8.3 Hartmann Flow

As a steady state nonlinear verification problem, we consider Hartmann flow. This is the MHD extension of plane Poiseuille flow, and is discussed in detail in [48, 49]. Consider a conducting incompressible fluid (liquid metal, for example) in a domain $[-\infty, \infty] \times [-L, L] \times [-\infty, \infty]$ bounded by infinite parallel plates. The fluid is subject to a uniform pressure gradient $G := -\frac{\partial p}{\partial x}$ in the x direction, and a uniform external magnetic field b_0 in the y direction. If we consider no-slip boundary conditions, the resulting flow pattern is known as *Hartmann flow* and is described by

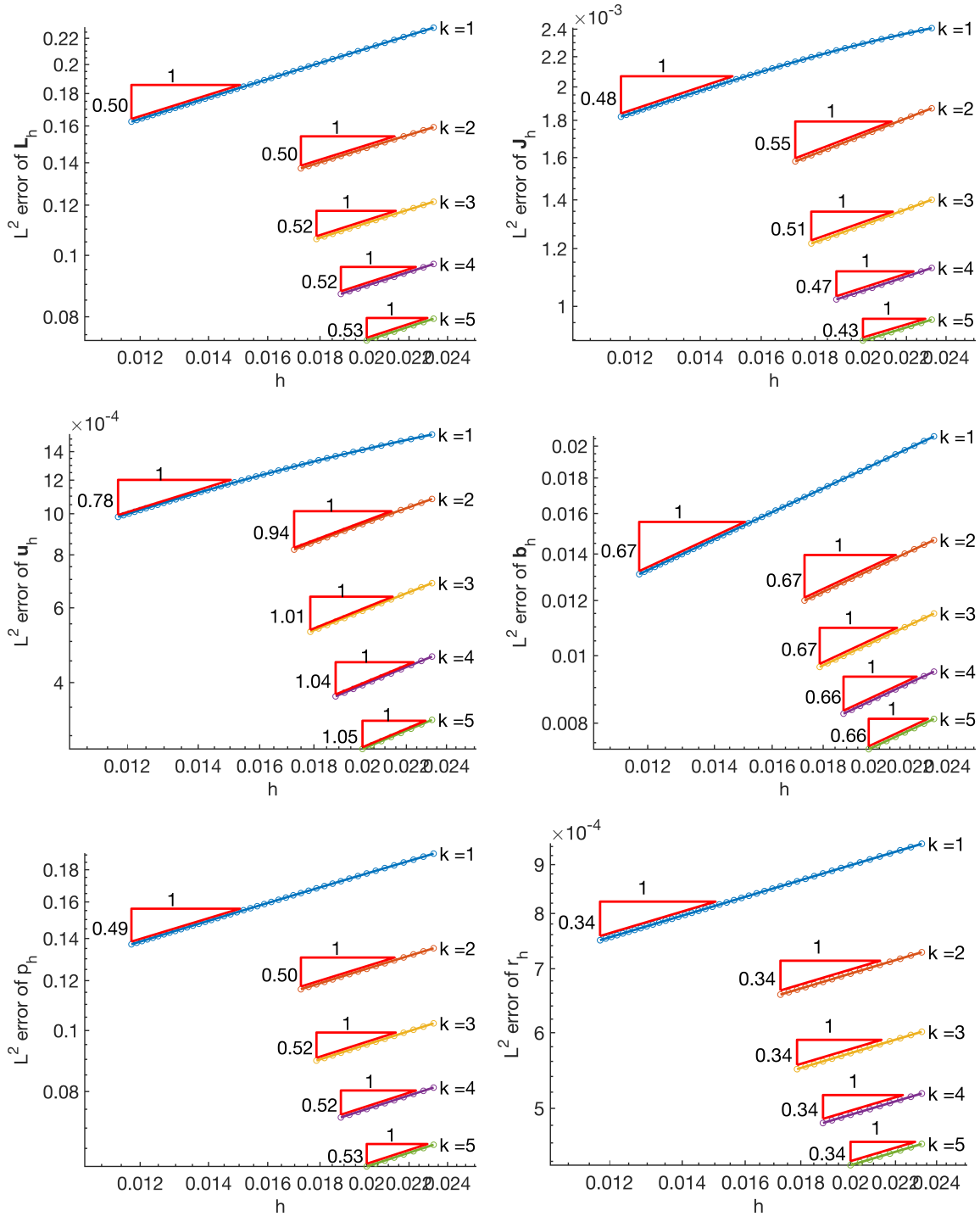

Figure 5.3: MHD singular solution problem: L^2 convergence.

an analytical solution that is 1D in nature. If the infinite parallel plates are perfectly insulating, the analytical solution is given by

$$\begin{aligned}
\boldsymbol{u} &= \left(\frac{GL^2}{\mu \mathrm{Ha} \tanh(\mathrm{Ha})} \left(1 - \frac{\cosh(\frac{x_2}{L}\mathrm{Ha})}{\cosh(\mathrm{Ha})} \right), 0, 0 \right), \\
\boldsymbol{b} &= \left(\frac{GL\mu_0}{b_0} \left(\frac{\sinh(\frac{x_2}{L}\mathrm{Ha})}{\sinh(\mathrm{Ha})} - \frac{x_2}{L} \right), b_0, 0 \right), \\
p &= p_0 - \frac{G^2 L^2 \mu_0}{2b_0^2} \left(\frac{\sinh(\frac{x_2}{L}\mathrm{Ha})}{\sinh(\mathrm{Ha})} - \frac{x_2}{L} \right)^2,
\end{aligned}$$

where p_0 is an arbitrary constant. As it is written above, p does not include the part of the pressure that gives the pressure gradient G. This is because we treat G as part of the forcing when solving the problem. Notice that the solution is independent of the x_1 spatial coordinate.

Remark 5.1. In the setup of the Hartmann flow problem described above, all variables are assumed to be dimensional (not dimensionless). Although Formulation 5.3 is framed in terms of dimensionless quantities and operators, we can use the formulation to solve the fully dimensional MHD equations by making the implicit substitution of all dimensionless variables and operators with their dimensional counterparts, and additionally making the substitutions $\mathrm{Re} \to \frac{\rho}{\mu}$, $\mathrm{Rm} \to \frac{\mu_0}{\eta}$, $\kappa \to \frac{1}{\rho\mu_0}$, $p \to \frac{p}{\rho}$, $\boldsymbol{f} \to \frac{\boldsymbol{f}}{\rho}$, $r \to \rho\mu_0 r$, and $\boldsymbol{g} \to \rho\mu_0 \boldsymbol{g}$.

For this study, we consider a 2D domain $[0, 10] \times [-L, L]$. To replicate the numerical experiments in [62, 64], we choose $L = \rho = \mu = \mu_0 = \eta = 1$, $G = 50$, and vary b_0 to produce velocity and magnetic field profiles with steeper and steeper gradients. Periodic boundary conditions are applied in the x_1 direction. The Picard iteration has demonstrated that it converges for some choices of parameters, but not all. Reintroducing the time derivatives to the momentum and induction equations, and discretizing in time by implicit Euler, the Picard iteration again converges. This is the approach we take in solving the Hartmann flow problem here. Since we are

interested in the steady state solution only, we take large time steps. Initial conditions of zero are given.

Figure 5.4 shows the numerical solutions and exact solutions for the x_1 velocity and x_1 magnetic field profiles for various values of b_0. The plots are made from simulations on a mesh of 1×8 rectangular, fourth order, tensor product elements strategically clustered toward $x_2 = \pm 1$. The figure indicates that the numerical solutions qualitatively match the exact solutions, as the plots coincide.

Since Hartmann flow is the MHD extension to Poiseuille flow in incompressible fluid flow, setting $b_0 = 0$ recovers the parabolic velocity profile of Poiseuille flow. As the magnitude of the transverse magnetic field is increased, the resulting Lorentz force more strongly opposes the motion of the fluid due to the applied pressure gradient, so the magnitude of the fluid velocity becomes smaller. The magnitude of b_1 increases with b_0 at small values of b_0, then decreases with larger values of b_0. Although u_1 and b_1 become smaller at higher and higher b_0, their profiles become steeper, as a thin boundary layer develops at particularly high b_0. The velocity in such cases is effectively constant throughout the duct with a sharp transition to the no-slip boundary condition in the boundary layers. This is illustrated in Figure 5.5, where the solutions from Figure 5.4 are plotted again, but with u_1 is scaled to a maximum value of 1 and with b_1 is scaled by b_0. Without sufficient mesh resolution in the boundary layers, oscillations can appear on the element interiors. In future work, we will consider stabilization/shock capturing [26].

Figure 5.6 demonstrates the optimal spatial convergence of the velocity and magnetic field. For this study, a mesh of $1 \times K$ uniformly spaced quadrilateral elements is used, b_0 is set to 100, and the remaining parameters remain the same as stated above.

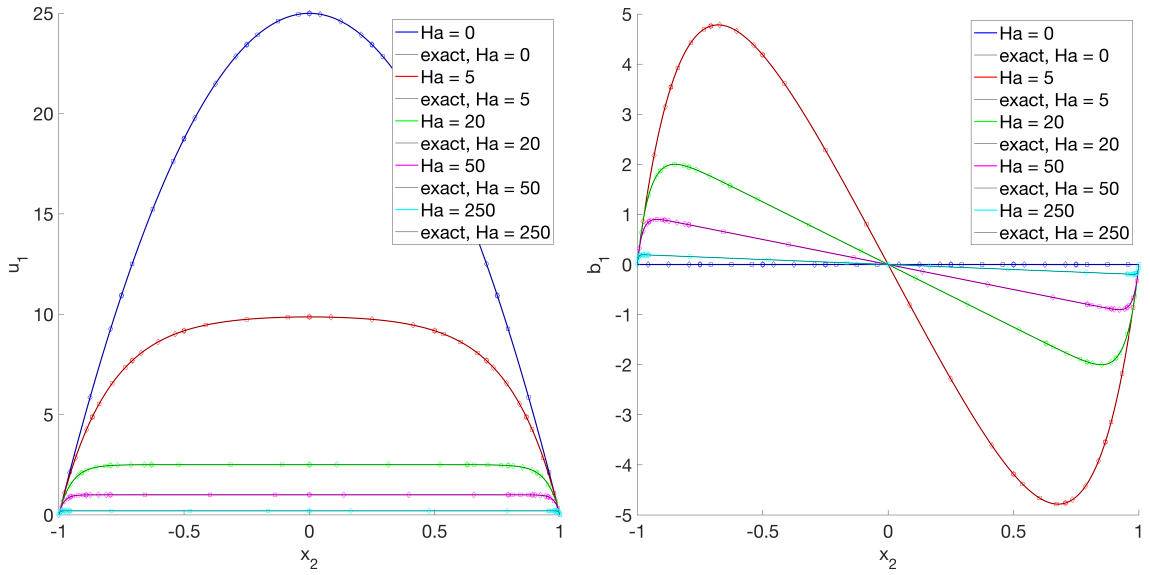

Figure 5.4: Hartmann flow problem: numerical and exact solution for u_1 (left) and b_1 (right).

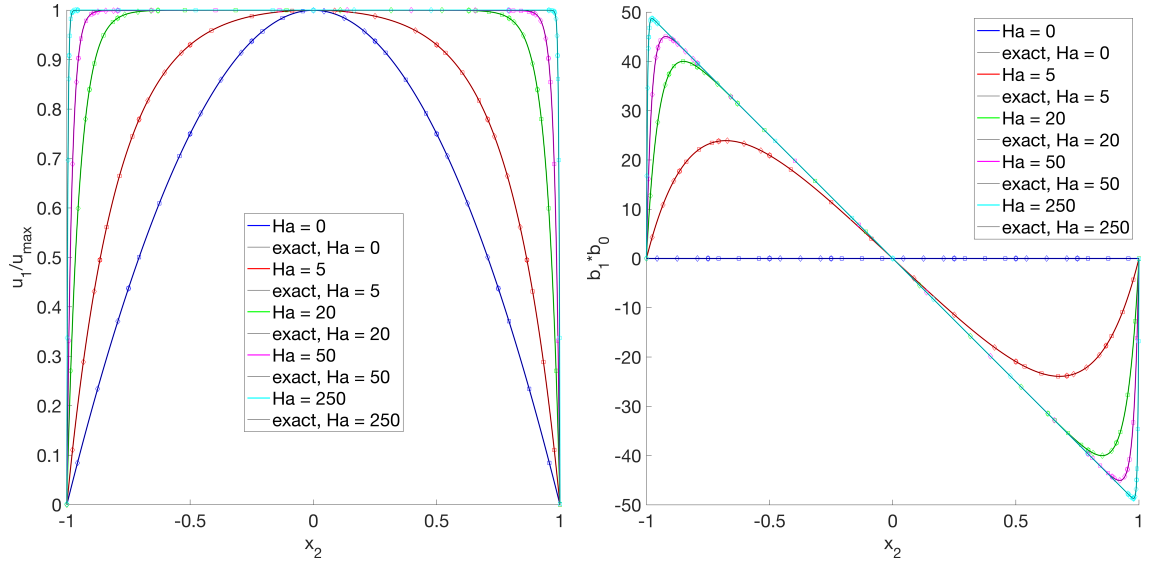

Figure 5.5: Hartmann flow problem: numerical and exact solution for u_1 (left) and b_1 (right), scaled to reveal boundary layers.

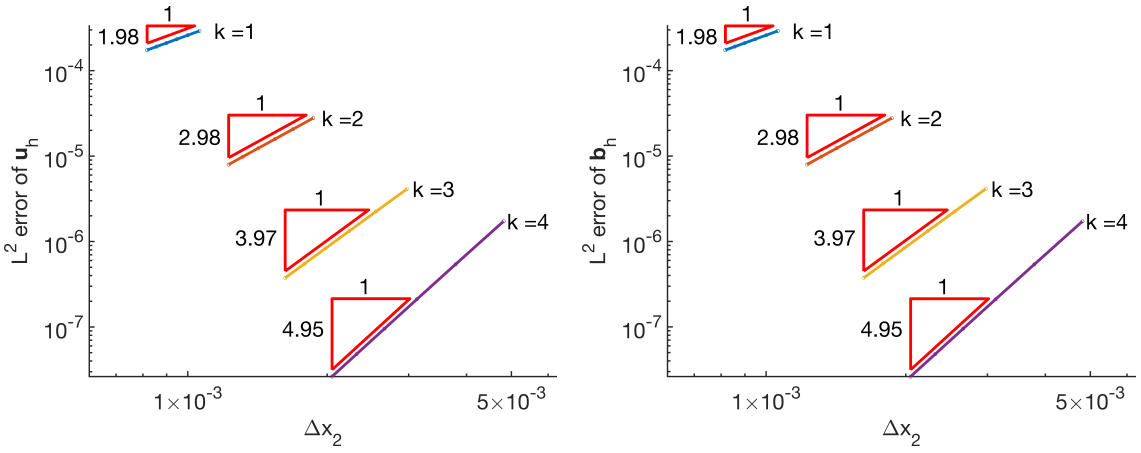

Figure 5.6: Hartmann flow problem: spatial convergence in L^2 norm for velocity and magnetic field.

5.8.4 Rayleigh Flow

As a nonlinear time dependent verification problem, we consider a Rayleigh flow problem with Alfvén wave propagation. This is the MHD extension to Stokes' first problem, and is discussed in detail in [48, 49]. Consider a conducting incompressible fluid in a semi-infinite domain $[-\infty, \infty] \times [0, \infty] \times [-\infty, \infty]$ bounded by an infinite insulating flat plate at $x_2 = 0$, subject to a uniform external magnetic field b_0 in the x_2 direction. The fluid is initially at rest, and the plate is instantaneously set into motion at a velocity U in the x_1 direction. Assuming that the magnetic Prandtl number $Pm := \frac{\mathrm{Rm}}{\mathrm{Re}}$ is equal to one, the resulting flow pattern is described by an analytical solution that is 1D in nature,

$$\boldsymbol{u} = \left(\frac{U}{4} \left[\left(1 + e^{\frac{-u_A y}{D}}\right) \operatorname{erfc}\left(\frac{y - u_A t}{2\sqrt{Dt}}\right) + \left(1 + e^{\frac{u_A y}{D}}\right) \operatorname{erfc}\left(\frac{y + u_A t}{2\sqrt{Dt}}\right) \right], 0, 0 \right),$$

$$\boldsymbol{b} = \left(-\frac{U\sqrt{\mu_0 \rho}}{4} \left(1 - e^{\frac{-u_A y}{D}}\right) \left[\operatorname{erfc}\left(\frac{y - u_A t}{2\sqrt{Dt}}\right) + e^{\frac{u_A y}{D}} \operatorname{erfc}\left(\frac{y + u_A t}{2\sqrt{Dt}}\right) \right], b_0, 0 \right),$$

$$p = p_0 - \frac{\rho U^2}{32} \left(1 - e^{\frac{-u_A y}{D}}\right)^2 \left[\operatorname{erfc}\left(\frac{y - u_A t}{2\sqrt{Dt}}\right) + e^{\frac{u_A y}{D}} \operatorname{erfc}\left(\frac{y + u_A t}{2\sqrt{Dt}}\right) \right]^2,$$

where $u_A := \frac{b_0}{\sqrt{\rho\mu_0}}$ is the Alfvén speed, the parameter $D := \frac{\mu}{\rho} = \frac{\eta}{\mu_0}$ (the equality is a result of the assumption $Pm = 1$), and p_0 is an arbitrary constant. In the above, all the variables are to be interpreted as fully dimensional. As in the Hartmann flow example, Remark 5.1 applies regarding applying the dimensionless HDG schemes to solve the fully dimensional equations.

For this study, we consider a 2D domain $[0, 5] \times [0, L]$, with periodic boundary conditions in the x_1 direction, a no-flow, insulating boundary condition at $x_2 = L$, and a no-slip, insulating boundary condition at $x_2 = 0$. That is, the quiescent fluid far from the moving plate is modeled as a second parallel insulating plate at rest with a no-flow boundary condition, the second plate being sufficiently far away (L large enough) that the flow profile is not affected by the "artificial" boundary condition for the time frame under consideration. We choose $\rho = \mu = \mu_0 = \eta = 1$, and $U = 1$ to replicate the numerical experiments in [62, 64].

As a first test, we choose $b_0 = 10$, and $L = 5$. Figure 5.7 shows the numerical and exact solution for the x_1 velocity and x_1 magnetic field profiles for various times up to $t = 0.1$. Fourth-order tensor-product basis functions are used, with a mesh of 1×32 quadrilateral elements strategically clustered. DIRK(5,4) time stepping was used with a time step of $\Delta t = 5 \times 10^{-3}$.

As a more demanding test of the robustness of the scheme, we apply an external magnetic field of $b_0 = 100$, and set $L = 50$ to accommodate the faster speed of the propagating wave while reasonably representing a semi-infinite domain. Figure 5.8 shows the x_1 velocity and x_1 magnetic field profiles for various times up to $t = 0.1$. Fourth-order tensor-product basis functions are used, with a mesh of 1×288 quadrilateral elements strategically clustered to capture the very steep gradient around $x_2 = 0$, and the propagating wave, which becomes less steep as it travels away from $x_2 = 0$.

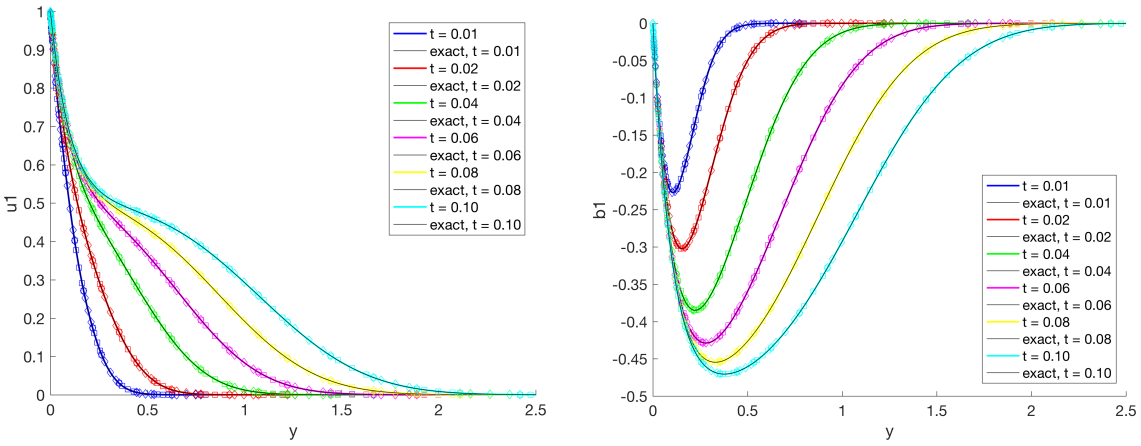

Figure 5.7: Rayleigh flow problem: numerical and exact solution for u_1 (left) and b_1 (right) for $b_0 = 10$.

DIRK(5,4) time stepping was used with a time step of $\Delta t = 5 \times 10^{-4}$.

Figure 5.9 demonstrates the expected temporal convergence of the velocity and magnetic field for stiffly-accurate, L-stable, diagonally-implicit Runge-Kutta methods of order 1 through 4. For this study $b_0 = 10$ and $L = 5$. A mesh of 1×32 strategically clustered 7th-order quadrilateral elements is used, and the system is evolved to $t = 0.01$.

Figure 5.10 demonstrates optimal spatial convergence of the velocity and magnetic field. Again $b_0 = 10$ and $L = 5$. A mesh of $1 \times K$ uniformly spaced quadrilateral elements is used. DIRK(5,4) time stepping was used to step to a final time of 0.01, with a time step of $\Delta t = 5 \times 10^{-4}$.

5.8.5 Magnetic Reconnection - Island Coalescence

We move on to a more challenging test problem that is relevant in plasma physics. Magnetic reconnection is a phenomenon by which a magnetic field configuration changes its topology, accompanied by a release of energy. This phenomenon

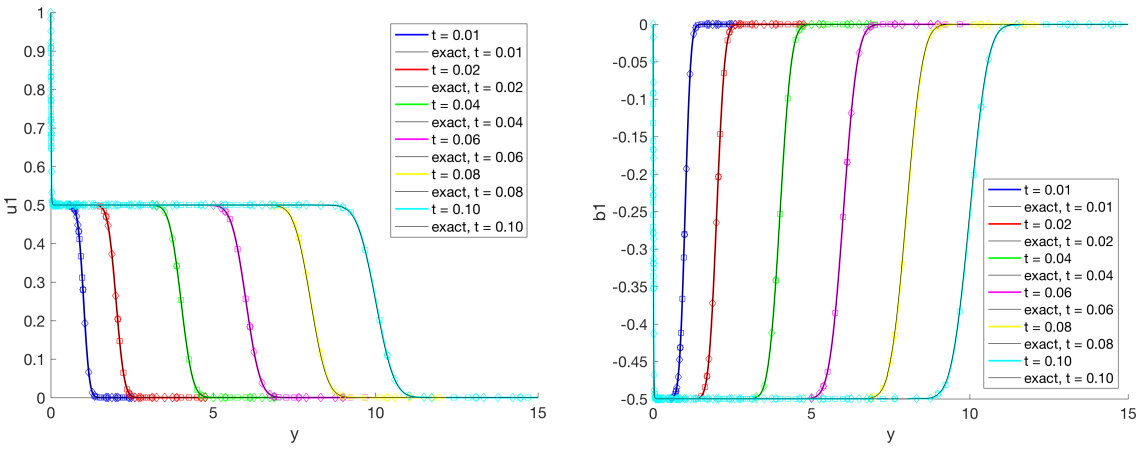

Figure 5.8: Rayleigh flow problem: numerical and exact solution for u_1 (left) and b_1 (right) for $b_0 = 100$.

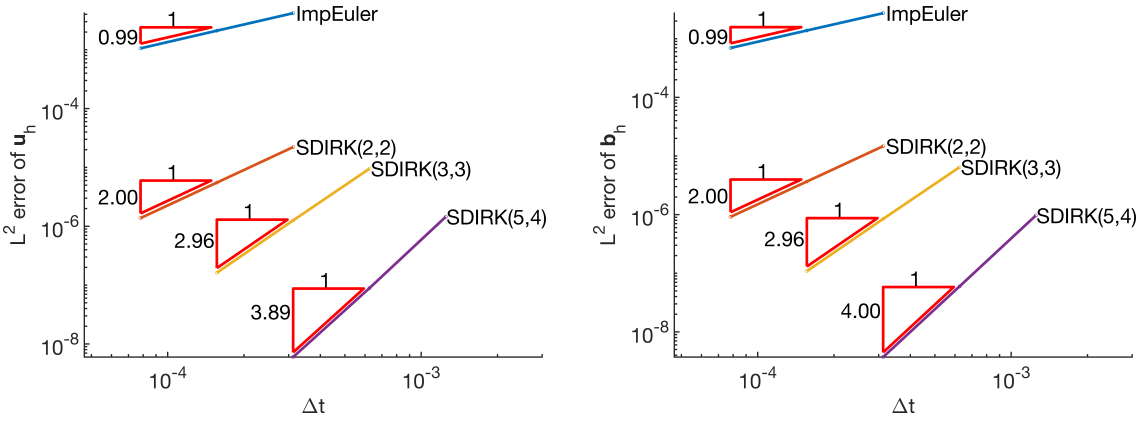

Figure 5.9: Rayleigh flow problem: temporal convergence in L^2 norm for u_1 (left) and b_1 (right).

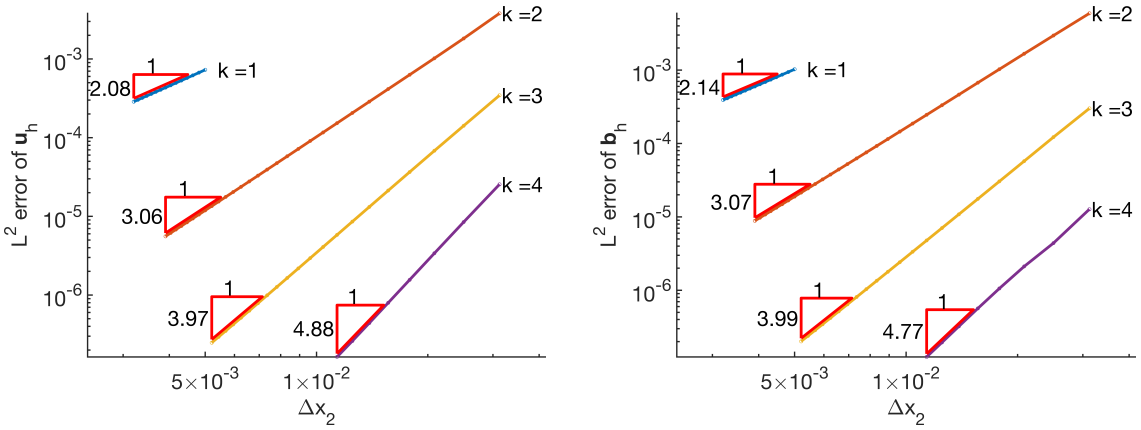

Figure 5.10: Rayleigh flow problem: spatial convergence in L^2 norm for u_1 (left) and b_1 (right).

is observed to occur during solar flares and coronal mass ejections, in the Earth's magnetosphere, and in laboratory plasmas. Magnetic confinement fusion processes rely on the ability to maintain a stable plasma configuration. Magnetic reconnection events can lead to plasma disruption, which can lead to loss of plasma confinement and/or damage to the machine. Thus it is in the interest of the fusion community to better understand the processes behind magnetic reconnection in order to avoid such events in fusion machines.

Ideal MHD (defined by a perfectly conducting fluid) has the property of conservation of magnetic flux, which prevents a change in magnetic topology. With a finite resistivity, reconnection is allowed to take place. The Sweet-Parker theoretical model for reconnection gives a result for the reconnection rate in resistive MHD. The result predicts a reconnection rate that is proportional to the inverse of the square root of the Lundquist number. Reconnection in astrophysical and laboratory plasmas is observed to happen at a much faster rate than what the Sweet-Parker model predicts. Models other than the Sweet-Parker model facilitate faster reconnection rates, and involve, for example, allowing formation of slow shock fronts, using locally higher

resistivities in the current sheet, or extending the resistive MHD model to account for small length scale electron effects. For details on magnetic reconnection, we refer the reader to [31, 32, 58, 7]

Numerical simulations using resistive MHD with a uniform resistivity have demonstrated good agreement with the *peak* reconnection rate with the Sweet-Parker model within a certain range of Lundquist numbers [43, 62, 1]. As a test of our HDG MHD scheme, we aim to replicate these results here. The initial equilibrium configuration is a Harris current sheet with a chain of "islands" of current density embedded in the current sheet. The configuration is initially in an equilibrium, but a perturbation from equilibrium draws two current islands (whose centers are "O-points") with the same orientation toward each other. Reconnection of magnetic field lines occurs at an "X-point", and the two islands coalesce resulting in one larger island. The manner in which the islands coalesce depends on the Lundquist number. Lower Lundquist numbers (higher resistivities) give coalescence of the islands where the O-points approach each other monotonically, and the rate of reconnection is more or less independent of the Lundquist number itself. At higher Lundquist numbers, the reconnection rate agrees well with the Sweet-Parker theory. Also at higher Lundquist numbers, as the islands move toward each other, a thin current sheet builds up at the X-point, and a pressure build-up causes the O-points to momentarily move away from each other. This oscillatory behavior is referred to as "sloshing". Below we describe the problem setup in more detail.

The domain and boundary conditions: The problem is described by the pairwise merging of islands in a chain of islands. We model two islands along the x_1 direction in a domain of $[-1,1]\times[-1,1]$ that is periodic in the x_1 direction. On the top and bottom edges of the domain, the fluid boundary conditions are mirror boundary conditions, and the magnetic boundary conditions are those of a perfect conductor.

Note that on the left and right edges, instead of periodicity, we could apply mirror fluid boundary conditions and perfectly insulating magnetic boundary conditions. It is also possible to exploit symmetry and to simulate the problem on a half domain or quarter domain. For the right half domain $[0,1] \times [-1,1]$, mirror fluid boundary conditions are applied on all edges, while perfectly conducting magnetic boundary conditions are applied on the top and bottom boundaries and perfectly insulating magnetic boundary conditions are applied on the left and right boundaries. For the top-right quarter domain $[0,1] \times [0,1]$, mirror fluid boundary conditions are applied on all edges, while perfectly conducting magnetic boundary conditions are applied on the top boundary and perfectly insulating magnetic boundary conditions are applied on the remaining three boundaries.

In the above, a mirror fluid boundary condition is described by zero normal velocity and zero shear stress,

$$\boldsymbol{u} \cdot \boldsymbol{n} = 0, \quad \mathbf{T}\left(\nabla \boldsymbol{u}\right) \boldsymbol{n} = \mathbf{0}.$$

A perfect insulating boundary is described by zero tangential magnetic field, which is equivalent to

$$\boldsymbol{n} \times \boldsymbol{b} = 0.$$

A perfect conducting boundary is described by zero normal magnetic field $\boldsymbol{b} \cdot \boldsymbol{n} = 0$, and zero tangential electric field, which is equivalent to $\boldsymbol{n} \times \boldsymbol{E} = \mathbf{0}$. From Ohm's law (5.3), this gives $\boldsymbol{n} \times \boldsymbol{J} + \boldsymbol{n} \times (\boldsymbol{u} \times \boldsymbol{b}) = \mathbf{0}$. Through cross product identities, the second term becomes $\boldsymbol{n} \times (\boldsymbol{u} \times \boldsymbol{b}) = \boldsymbol{b}(\boldsymbol{u} \cdot \boldsymbol{n}) - \boldsymbol{u}(\boldsymbol{b} \cdot \boldsymbol{n}) = \boldsymbol{b}(\boldsymbol{u} \cdot \boldsymbol{n})$, which is zero from the mirror boundary condition. Thus, a perfectly conducting boundary, along with zero flow normal to the boundary, is given by

$$\boldsymbol{b} \cdot \boldsymbol{n} = 0, \quad \boldsymbol{n} \times \boldsymbol{J} = \mathbf{0}.$$

The initial conditions and forcing current: The plasma is initially at rest

$$\boldsymbol{u}^0 := \boldsymbol{u}(t=0) = \mathbf{0}. \tag{5.107}$$

The initial magnetic field configuration is determined by the vector potential

$$A^0 := A(t=0) = \frac{1}{2\pi}\log\left[\cosh\left(2\pi x_2\right) + \epsilon\cos\left(2\pi x_1\right)\right], \tag{5.108}$$

where ϵ is the island width. Recalling how we define the curl of a scalar, we define the initial magnetic field by $\boldsymbol{b} = \nabla \times A = \left(\frac{\partial A}{\partial x_2}, -\frac{\partial A}{\partial x_1}\right)$ giving

$$\boldsymbol{b}^0 := \boldsymbol{b}(t=0) = \left(\frac{\sinh\left(2\pi x_2\right)}{\cosh\left(2\pi x_2\right) + \epsilon\sinh\left(2\pi x_1\right)}, \frac{\epsilon\sin\left(2\pi x_1\right)}{\cosh\left(2\pi x_2\right) + \epsilon\sinh\left(2\pi x_1\right)}\right). \tag{5.109}$$

The resulting initial current $\boldsymbol{J} = \frac{\kappa}{\mathrm{Rm}}\nabla \times \boldsymbol{b} = \frac{\kappa}{\mathrm{Rm}}\left(\frac{\partial b_2}{\partial x_1} - \frac{\partial b_1}{\partial x_2}\right)$ is

$$\boldsymbol{J}^0 := \boldsymbol{J}(t=0) = -\frac{2\pi\kappa\left(1-\epsilon^2\right)}{\mathrm{Rm}\left(\cosh\left(2\pi x_2\right) + \epsilon\sinh\left(2\pi x_1\right)\right)}. \tag{5.110}$$

Figures 5.11 and 5.12 show the initial conditions for A^0, b_1^0, b_2^0, and $\boldsymbol{J}^0$ with the island width $\epsilon = 0.2$ on a domain of $[-1,1]\times[-1,1]$, where for $\boldsymbol{J}^0$, the scale is shown with $\kappa = 1$ and $\mathrm{Rm} = 10^3$.

In order for the initial configuration to be in resistive equilibrium, we ensure $\frac{\partial \boldsymbol{b}}{\partial t}(t=0) = \mathbf{0}$ in (5.4c) by applying a constant (in time) external current equal to $\boldsymbol{J}(t=0)$. That is, we set

$$\boldsymbol{g} = \nabla \times \boldsymbol{J}^0. \tag{5.111}$$

It can also be shown that the momentum equation is in equilibrium without any additional forcing. This can be shown by proving that the initial Lorentz force

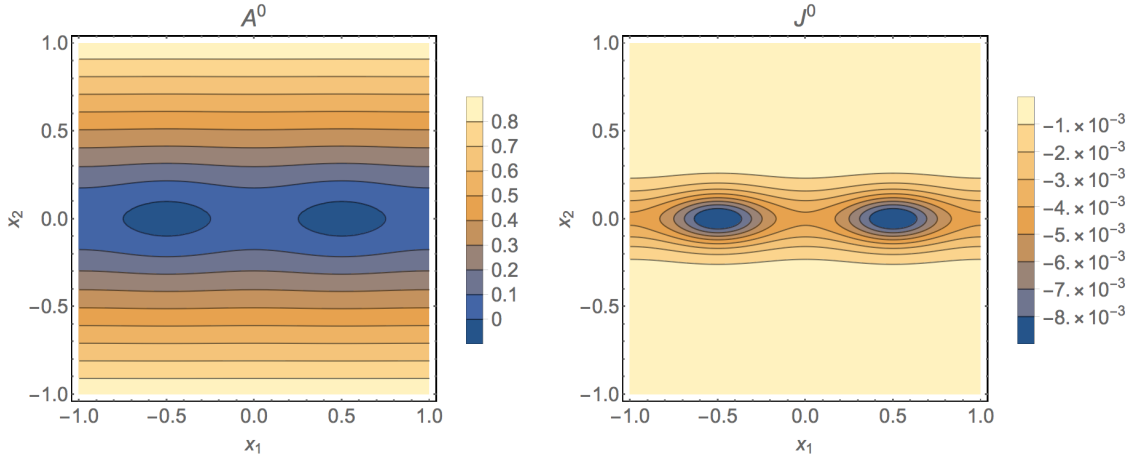

Figure 5.11: Magnetic island coalescence problem: initial magnetic vector potential (left), and initial current (right).

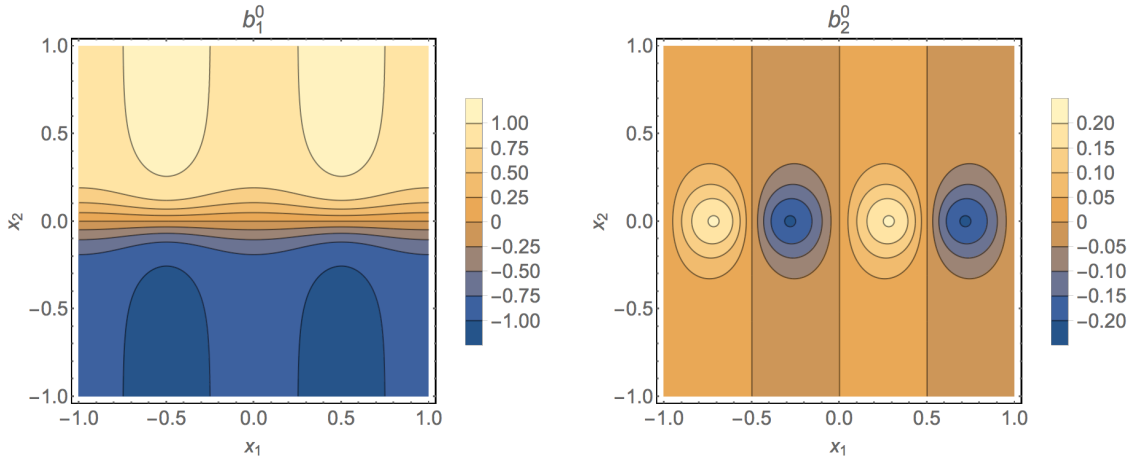

Figure 5.12: Magnetic island coalescence problem: initial magnetic field configuration.

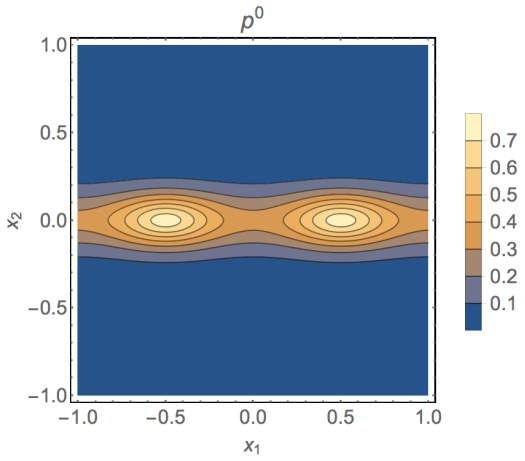

Figure 5.13: Magnetic island coalescence problem: initial pressure profile.

$\kappa \boldsymbol{b}^0 \times \left(\nabla \times \boldsymbol{b}^0\right)$ can be expressed as the gradient of a scalar. Expressing the Lorentz force as a function of the vector potential, we have

$$\kappa \boldsymbol{b}^0 \times \left(\nabla \times \boldsymbol{b}^0\right) = -\kappa \left(\nabla \times A^0\right) \times \Delta A^0 = \kappa \Delta A^0 \nabla A^0. \tag{5.112}$$

We can write $A^0 = \frac{1}{2\pi} \ln\left(F\right)$, where $F := \cosh\left(2\pi x_2\right) + \epsilon\left(2\pi x_1\right)$. Then it can be shown that

$$\Delta A^0 = \frac{F\Delta F - \nabla F \cdot \nabla F}{2\pi F^2} = \frac{2\pi\left(1-\epsilon^2\right)}{F^2} \tag{5.113}$$

and since $\nabla A^0 = \frac{\nabla F}{2\pi F}$ that

$$\Delta A^0 \nabla A^0 = \frac{\left(1-\epsilon^2\right)\nabla F}{F^3} = \nabla\left(-\frac{1-\epsilon^2}{2F^2}\right). \tag{5.114}$$

Thus, with $\boldsymbol{f} = \boldsymbol{0}$, the system is in equilibrium with the initial balancing pressure

$$p^0 := p(t=0) = \tilde{p} + \frac{\kappa\left(1-\epsilon^2\right)}{2\left[\cosh\left(2\pi x_2\right) + \epsilon \sinh\left(2\pi x_1\right)\right]^2} \tag{5.115}$$

for some arbitrary constant $\tilde{p}$. This can be visualized in Figure 5.13 for $\tilde{p}$ that gives a $p^0 = 0$ at the corners of the domain.

The perturbation: With the initial conditions and forcing just described, the fluid and magnetic field would theoretically remain constant in time. The islands of current density (directed in the x_3 direction) shown in Figure 5.11 attract each other, but they are equally attracted to their neighboring island on the other side of the periodic boundary. The equilibrium is unstable, however, so that in a numerical simulation a slight asymmetry resulting for example from long time roundoff error may cause the islands to be set into motion in the x_1 direction either toward the center ($x_1 = 0$) or toward the edge of the periodic domain ($x_1 = \pm 1$).

To set the islands into motion faster, and in a reproducible way, we perturb the initial magnetic configuration. We choose a perturbation that is described by the vector potential

$$\delta A^0 = -\sigma \cos(\pi x_1) \cos\left(\frac{\pi x_2}{2}\right), \tag{5.116}$$

for some small constant σ. The resulting perturbations in the magnetic field and current are

$$\delta \boldsymbol{b}^0 = \sigma \left(\frac{\pi}{2} \cos(\pi x_1) \sin\left(\frac{\pi x_2}{2}\right), -\pi \sin(\pi x_1) \cos\left(\frac{\pi x_2}{2}\right)\right), \tag{5.117}$$

$$\delta \boldsymbol{J}^0 = -\sigma \frac{5\pi^2 \kappa}{4\mathrm{Rm}} \cos(\pi x_1) \cos\left(\frac{\pi x_2}{2}\right). \tag{5.118}$$

Note that this perturbation satisfies the same symmetry conditions as the initial conditions. Plotting the perturbation of the current can give us confidence that the perturbation will indeed set the islands into motion. Other choices of perturbations may not follow the same symmetries as the initial conditions and/or may stretch/compress or twist the configuration without setting the islands into motion. The plot of $\delta \boldsymbol{J}^0$ (with $\sigma = 10^{-3}$) in Figure 5.14 indicates that the islands will be attracted to the current perturbation in the center of the domain, thus being set into motion in that

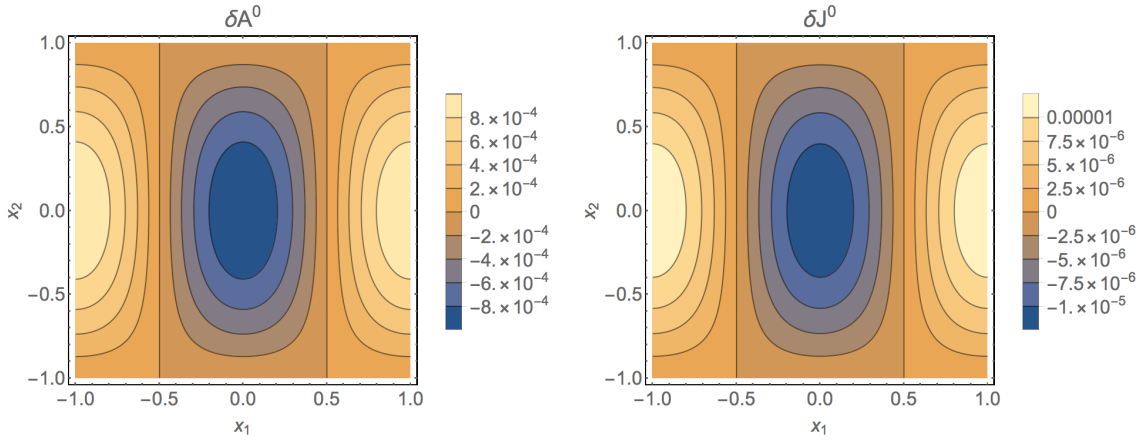

Figure 5.14: Magnetic island coalescence problem: perturbation in the initial magnetic vector potential (left), and perturbation in the initial current (right).

direction. Figure 5.15 shows the perturbation in the initial magnetic field configuration, which adheres to the symmetries described in the discussion on the domain and boundary conditions.

Applying the HDG Scheme: We next describe the problem setup within the context of the HDG scheme. We choose the characteristic velocity as the Alfvén speed, so $\kappa = 1$. We choose the island width to be $\epsilon = 0.2$, the perturbation magnitude to be $\sigma = 10^{-3}$, and set the fluid and magnetic Reynolds number (Lundquist number in this case) equal to each other. We set the forcing function for the momentum equation to be $\boldsymbol{f} = \boldsymbol{0}$, set $\boldsymbol{g}$ to the curl of the initial current as specified by (5.111), define the initial velocity by $\boldsymbol{u}_h = \boldsymbol{0}$, and define the initial magnetic field by the L^2 projection on each element

$$(\boldsymbol{b}_h, \boldsymbol{c})_{\mathcal{T}_h} = \left(\boldsymbol{b}^0 + \delta\boldsymbol{b}^0, \boldsymbol{c}\right)_{\mathcal{T}_h}. \tag{5.119}$$

Here, the problem is modeled on the quarter domain. Mirror fluid boundary condi-

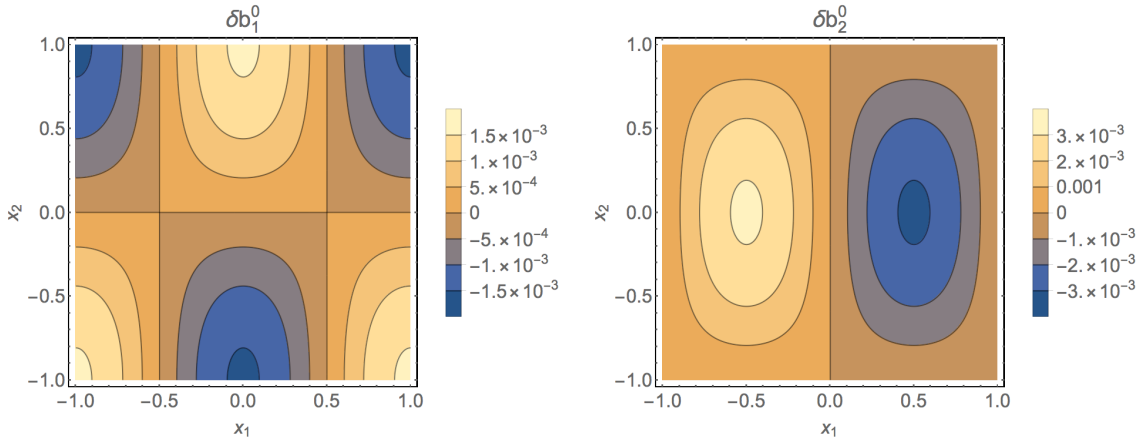

Figure 5.15: Magnetic island coalescence problem: perturbation in the initial magnetic field configuration.

tions are applied through $\boldsymbol{u}_h^* \cdot \boldsymbol{n}$ and $\mathbf{T}\left(\mathbf{L}_h^* \boldsymbol{n}\right)$, by

$$\langle \boldsymbol{u}_h^* \cdot \boldsymbol{n}, \widehat{v}^n \rangle_{\partial\Omega} = \langle \widehat{\boldsymbol{u}}_h \cdot \boldsymbol{n}, \widehat{v}^n \rangle_{\partial\Omega} = 0, \tag{5.120}$$

$$\begin{aligned} \left\langle -\mathbf{T}\mathbf{L}_h^* \boldsymbol{n}, \widehat{\boldsymbol{v}}^t \right\rangle_{\partial\Omega} = \Bigg\langle & -\mathbf{L}_h \boldsymbol{n} + \left(\tau_t + \frac{1}{2}\boldsymbol{w} \cdot \boldsymbol{n}\right)\left(\boldsymbol{u}_h - \widehat{\boldsymbol{u}}_h\right) \\ & + \xi\kappa \boldsymbol{d} \times \left(\boldsymbol{n} \times \left(\boldsymbol{b}_h^t - \widehat{\boldsymbol{b}}_h^t\right)\right), \widehat{\boldsymbol{v}}^t \Bigg\rangle_{\partial\Omega} = 0. \end{aligned} \tag{5.121}$$

Perfect insulating boundary conditions on the magnetic variables are enforced through $\mathbf{T}\boldsymbol{b}_h^*$ and r_h^*, as

$$\left\langle \widehat{\boldsymbol{b}}_h^t, \widehat{\boldsymbol{c}}^t \right\rangle_{\partial\Omega_I} = 0, \tag{5.122}$$

$$\langle \widehat{r}_h, \widehat{s} \rangle_{\partial\Omega_I} = 0, \tag{5.123}$$

where $\partial\Omega_I$ is the portion of the boundary on which insulating boundary conditions are applied. Perfect conducting boundary conditions on the magnetic variables are

enforced through $\boldsymbol{b}_h^* \cdot \boldsymbol{n}$ and $\boldsymbol{n} \times \boldsymbol{J}_h^*$, as

$$\langle \boldsymbol{b}_h^* \cdot \boldsymbol{n}, \widehat{s} \rangle_{\partial\Omega_C} = \left\langle \boldsymbol{b}_h \cdot \boldsymbol{n} + \frac{1}{\beta_n} \left(r_h - \widehat{r}_h \right), \widehat{s} \right\rangle_{\partial\Omega_C} = 0, \tag{5.124}$$

$$\left\langle \boldsymbol{n} \times \boldsymbol{J}_h^*, \widehat{\boldsymbol{c}}^t \right\rangle_{\partial\Omega_C} =$$

$$\left\langle \boldsymbol{n} \times \boldsymbol{J}_h + \beta_t \left(\boldsymbol{b}_h^t - \widehat{\boldsymbol{b}}_h^t \right) - [1 - \xi] \kappa \boldsymbol{n} \times \left((\boldsymbol{u}_h - \widehat{\boldsymbol{u}}_h) \times \boldsymbol{d} \right), \widehat{\boldsymbol{c}}^t \right\rangle_{\partial\Omega_C} = 0, \tag{5.125}$$

where $\partial\Omega_C$ is the portion of the boundary on which conducting boundary conditions are applied. Finally, HDG scheme parameters are chosen as $\xi = \frac{1}{2}$, $\tau_t = \tau_t^O$, $\tau_n = \tau_n^O$, $\beta_t = \beta_t^M$, and $\beta_n = \beta_n^M$.

The results: We ran the simulation with DIRK(5,4) time stepping with an adaptive time step size, with all of the parameters set to the values mentioned above, and with the Lundquist number of 10^a, a ranging between 2 and 5. Figure 5.18 shows a filled color contour plot of the current density for Lundquist number Rm = $10^{3.5}$. The mesh used for this simulation is a structured mesh of 91 rectangular elements with a 9th order tensor-product basis, with the elements strategically clustered. The X structure is clearly visible, as is the current sheet at its center. Figure 5.19 shows a filled color contour plot of the pressure for Lundquist number Rm = $10^{3.5}$. Here it is easier to see the O-points as they move toward each other. A modest pressure buildup is observed at the location of the current sheet. Plots for the current density and pressure with Rm = $10^{4.5}$ are shown in Figures 5.20 and 5.21, respectively. For this higher Lundquist number, the current sheet and the X structure are thinner than for the lower Lundquist number, putting a higher demand on spatial resolution, though for this particular simulation the same mesh was used as for the Rm = $10^{3.5}$ case. The pressure buildup in the current sheet is more apparent, and movement away from each other of the O-points can be seen between times 7 and 8. Note that the color scale for the two pressure plots is the same, but the color scales are different between the two current density plots.

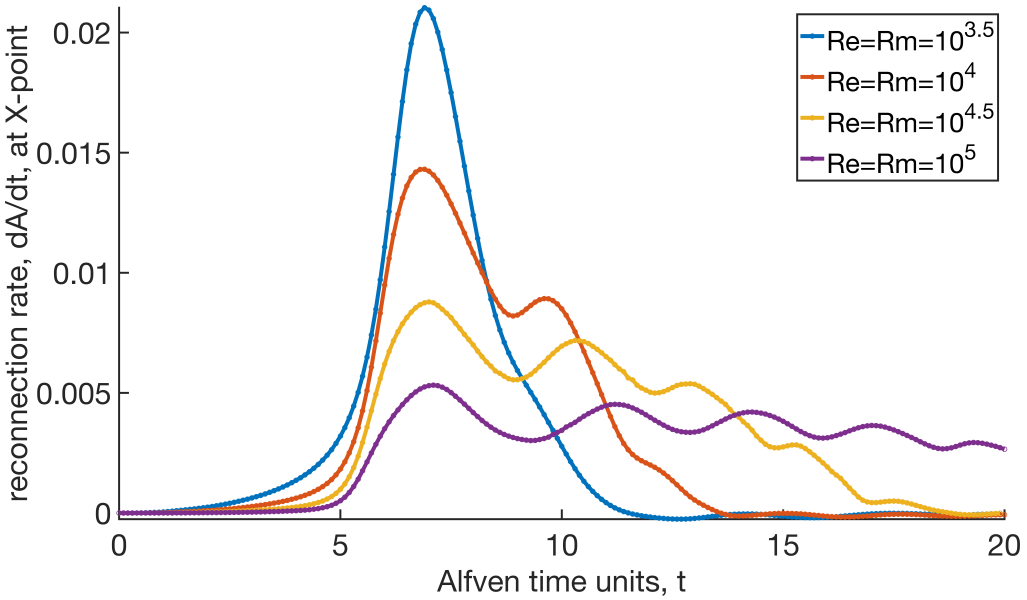

Figure 5.16: Magnetic island coalescence problem: reconnection rates.

The reconnection rate is defined as the rate of change of the magnetic vector potential (in the x_3 direction), $\frac{\partial A}{\partial t}$. Through the induction equation with a vector potential, we have

$$\frac{\partial A}{\partial t} = -\frac{1}{\kappa}\left(\boldsymbol{J} - \boldsymbol{J}^0\right) + \boldsymbol{u} \times \boldsymbol{b},$$

so we calculate a numerical reconnection rate as

$$\left(\frac{\partial A}{\partial t}\right)_h = -\frac{1}{\kappa}\left(\boldsymbol{J}_h - \boldsymbol{J}^0\right) + \boldsymbol{u}_h \times \boldsymbol{b}_h.$$

Figure 5.16 shows the reconnection rate over time at the X-point for a selection of Lundquist numbers. The oscillatory behavior of the island movement can be seen for the higher Lundquist numbers. Figure 5.17 shows the peak reconnection rates for all simulations. It shows reasonably good agreement with the Sweet-Parker theory for the higher Lundquist numbers.

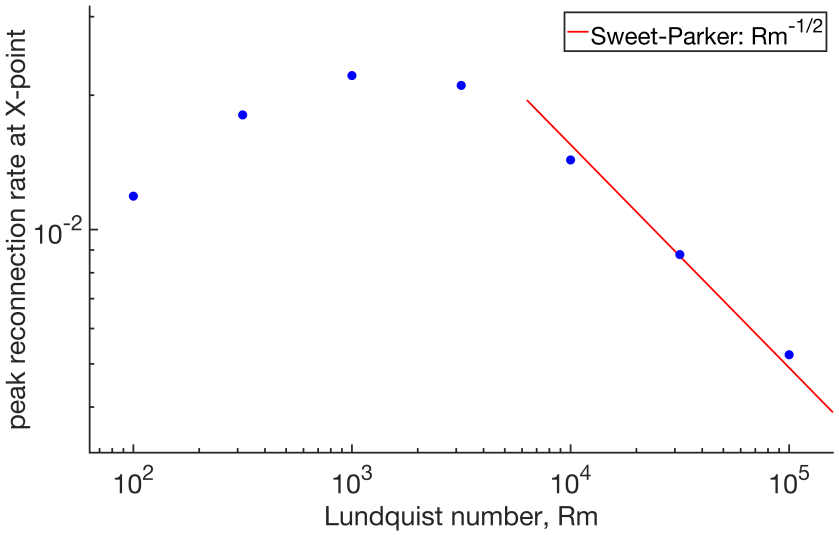

Figure 5.17: Magnetic island coalescence problem: peak reconnection rates.

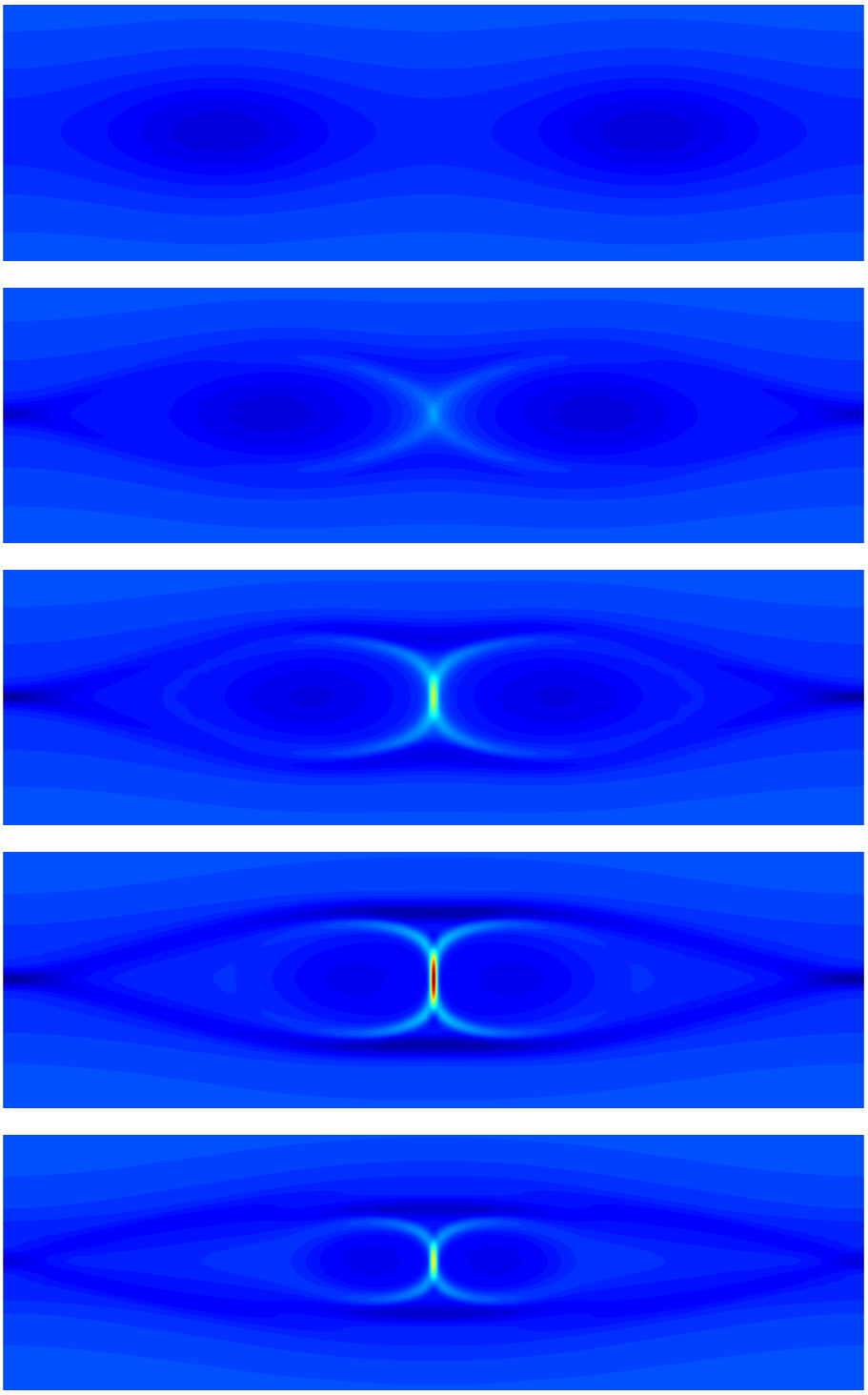

Figure 5.18: Magnetic island coalescence problem: current density $\boldsymbol{J}_h$ in x_3 direction with $Re = Rm = 10^{3.5}$ for $t = 0, 5, 6, 7, 8$ (top to bottom).

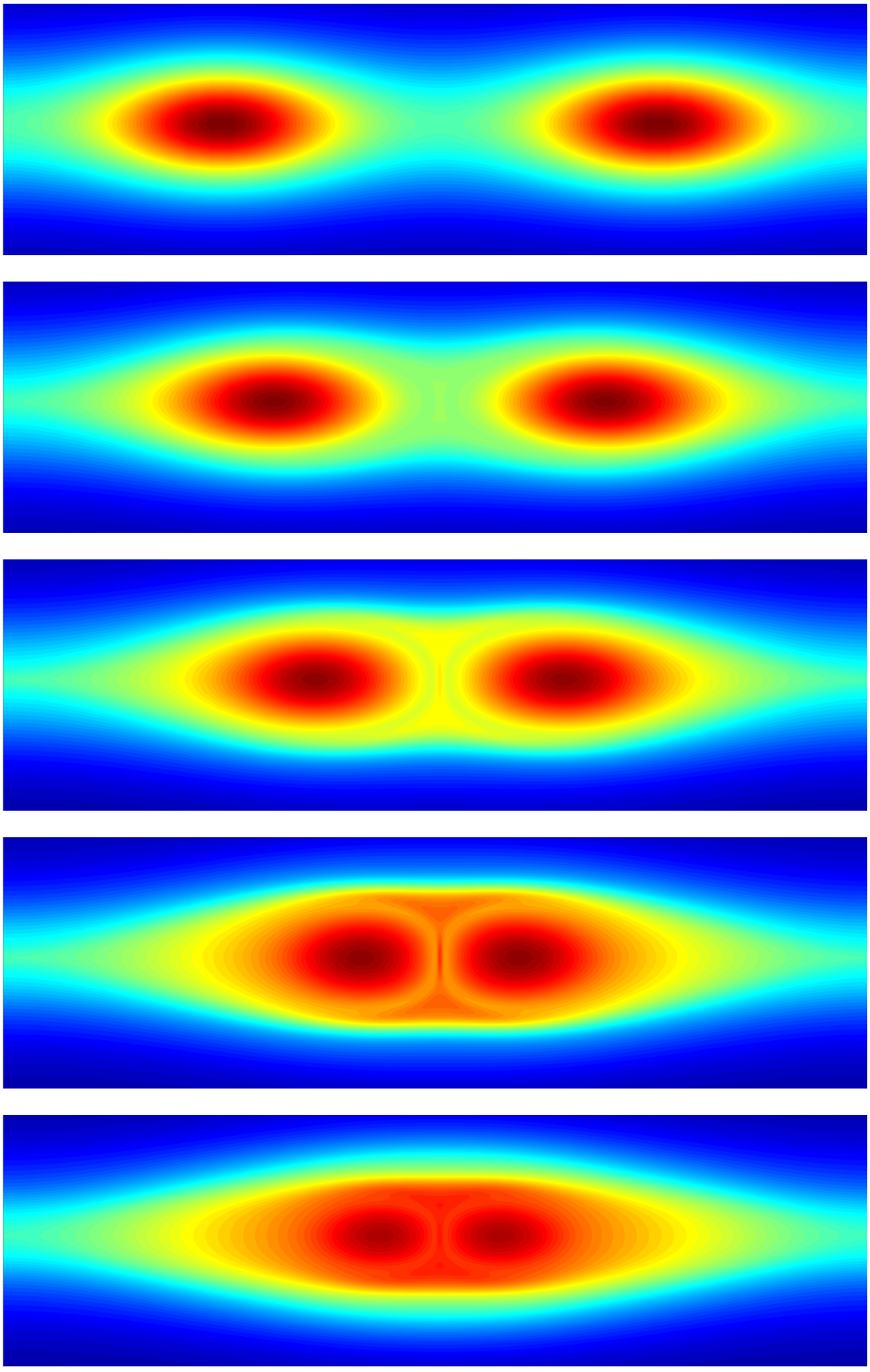

Figure 5.19: Magnetic island coalescence problem: pressure p_h with $Re = Rm = 10^{3.5}$ for $t = 0, 5, 6, 7, 8$ (top to bottom).

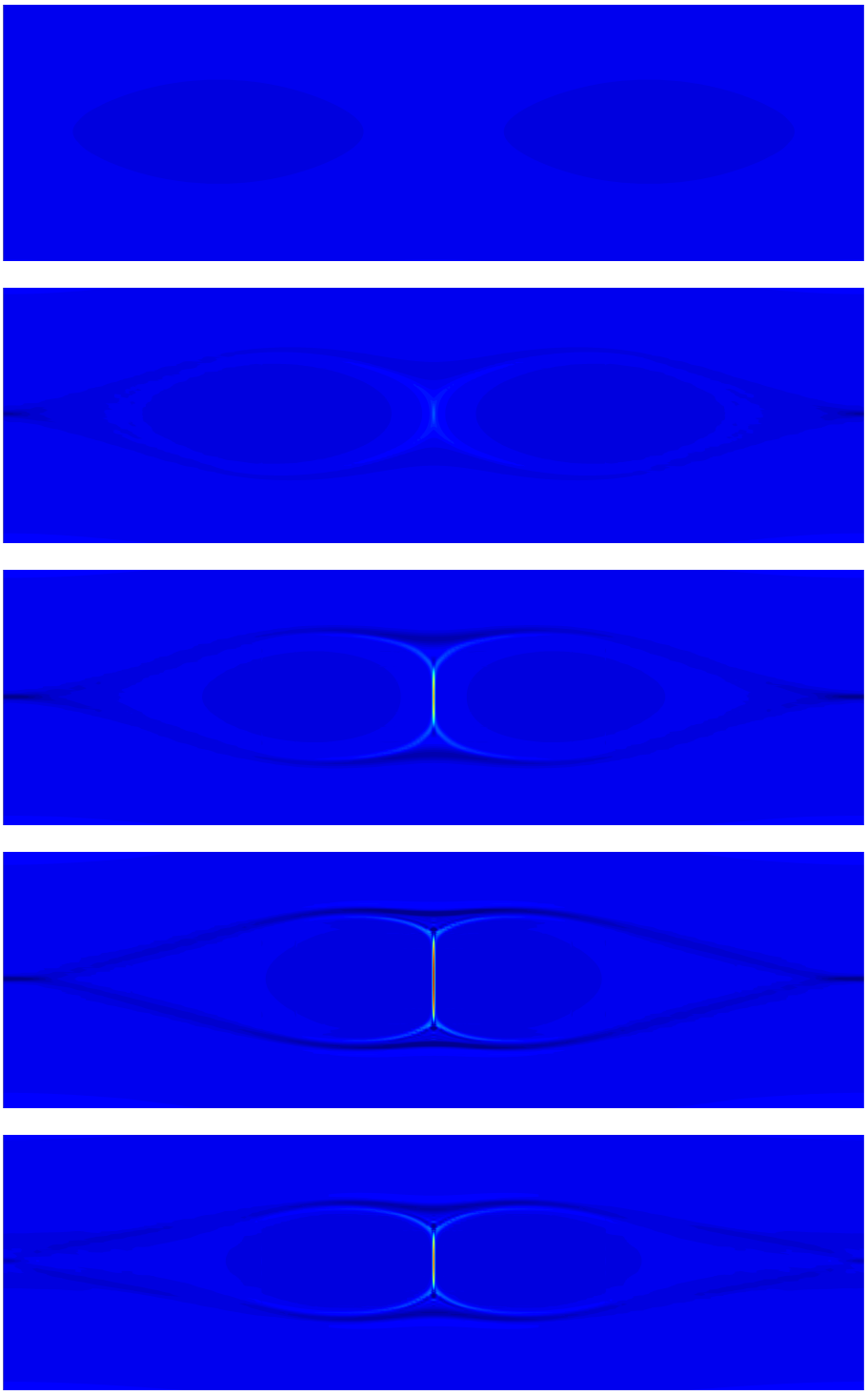

Figure 5.20: Magnetic island coalescence problem: current density $\boldsymbol{J}_h$ in x_3 direction with $Re = Rm = 10^{4.5}$ for $t = 0, 5, 6, 7, 8$ (top to bottom).

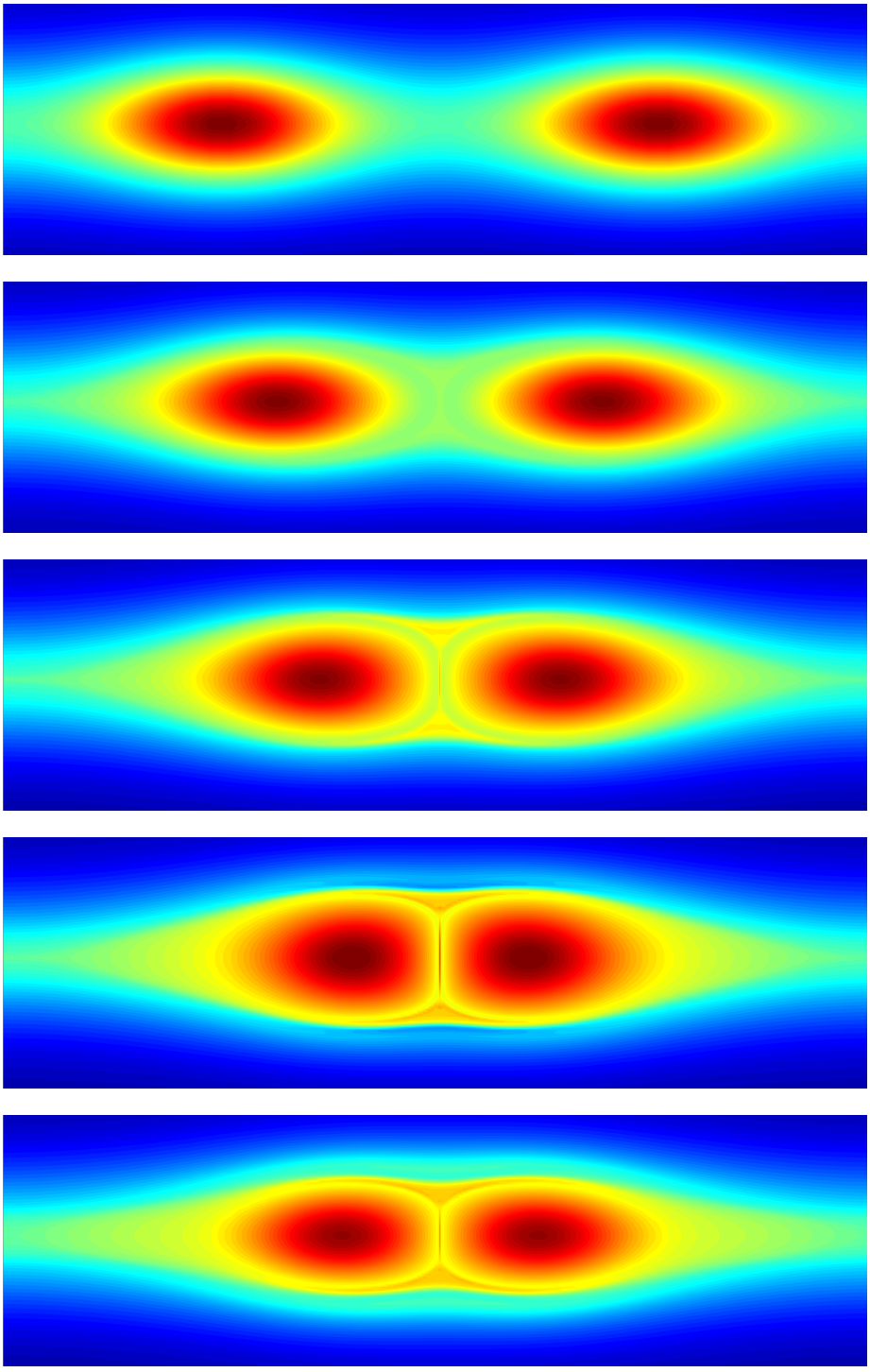

Figure 5.21: Magnetic island coalescence problem: pressure p_h with $Re = Rm = 10^{4.5}$ for $t = 0, 5, 6, 7, 8$ (top to bottom).

Chapter 6

Conclusions and Future Work

In this work, we have developed the first known HDG schemes for linearized visco-resistive incompressible magnetohydrodynamics. The MHD HDG schemes were constructed by piecing together numerical fluxes based on the Oseen equations and the induction equation in the limit of zero velocity. We used the upwind HDG framework, based on a first order form of the underlying equations, to derive the aforementioned HDG schemes for the Oseen equations and the induction equation. The four HDG schemes for the induction equation that we developed coincide with four schemes developed by Cockburn and Gopalakrishnan for the velocity-vorticity-pressure formulation for the Stokes equations. Of the four HDG schemes for the Oseen equations that we have derived through the upwind HDG framework, one of them is related to existing HDG schemes, whereas the other three schemes are new. The existing HDG schemes, which use the trace of the velocity as the trace unknown, require some form of modification in order for the local solver of the scheme to be well-posed. One method of modification requires solving the velocity trace system multiple times, and another method involves introducing additional global unknowns of a different nature (elementwise constant) than the velocity trace unknowns and solving a resulting saddle point system. Of the three new HDG schemes for the Oseen equations, one of them gives a local solver that is well-posed without modification and results in a matrix for the global trace system without zeros on the block diagonal. We proved well-posedness and demonstrated convergence for this scheme, which uses the *tan-*

gential velocity in addition to a scalar as trace unknowns. Additionally, we defined and employed a Picard iteration to solve the (nonlinear) steady state incompressible Navier-Stokes equations, and demonstrated convergence (with respect to mesh refinement) of the nonlinear scheme.

The methodology we used to combine the Oseen and induction fluxes for the MHD equations leads to ten possible forms of the HDG flux, each with a different combination of trace variables. We concretized three of the schemes which we see as particularly useful. For the scheme with the $(\widehat{\boldsymbol{u}}_h, \widehat{\boldsymbol{b}}_h^t, \widehat{r}_h)$ flux, we rigorously analyzed and performed numerical experiments. We proved well-posedness, and we proved asymptotic L^2 error estimates for the volume unknowns on simplicial meshes, assuming a smooth exact solution, through a projection-based analysis and a duality argument. The results are optimal (order h^{k+1}) for the velocity and magnetic field variables, and quasi-optimal (order $h^{k+\frac{1}{2}}$) for the remaining volume variables.

We have implemented the MHD HDG scheme with the $(\widehat{\boldsymbol{u}}_h, \widehat{\boldsymbol{b}}_h^t, \widehat{r}_h)$ flux. A first implementation is in MATLAB with triangular elements. This implementation was used to verify the error estimates. A second MATLAB implementation uses 2D and 3D tensor product elements (quadrilateral and hexahedral elements). With this implementation we have tested the HDG scheme with steady state and time dependent benchmark problems in MHD, where we use the linearized scheme as a substep in a Picard iteration to solve the nonlinear incompressible visco-resistive MHD equations. A third implementation is a C++ implementation built on the dealII finite element library [6, 3]. This implementation provides the opportunity to tackle larger problems on large distributed memory computers.

While this work provides a foundation for developing HDG schemes for magnetohydrodynamics, there are plenty of opportunities to extend this work. Some

suggested future research directions are listed here.

- **Linear solvers:** We have discussed the nature of HDG schemes; that the volume unknowns are coupled across elements only through the trace unknowns and so the volume unknowns can be condensed out of the global linear system.The advantage of HDG over DG, in terms of linear system size, is seen for implicit time discretization and is magnified for high spatial polynomial order. Ultimately, though, a linear system must still be solved. Solving this linear system, especially in 3D, very quickly becomes the most expensive part of an HDG implementation as we increase the size of the problem we are solving. To be able to solve large-scale problems, it is critical that efficient scalable iterative linear solvers and preconditioners be applied to the linear system. Development of such solvers and preconditioners is an ongoing research topic, and an active research topic in the Computational Engineering and Optimization Group at UT Austin [50, 52, 72, 51].

- **Adaptive mesh refinement:** As we have seen in the benchmark problems, very fine scale features and sharp gradients can occur in MHD flows. Local and adaptive mesh refinement is the logical strategy to efficiently deal with these features as they appear and/or move across the computational domain. HDG is naturally suited for solving problems on a mesh with geometric nonconformities, as we already have a tool in the mesh skeleton faces that act very naturally as *mortars* as they are defined in a traditional mortar method. The definition and well-posedness of the HDG schemes presented in this work do not require that the mesh is conforming; that is, hanging nodes are allowed. Beyond choosing/defining error indicators for refinement, this research topic is mainly an implementation issue.

- **Nonlinear solvers based on Newton's method:** The linearized incompressible MHD system that we developed and analyzed is naturally suited for use in a Picard iteration to solve the nonlinear equations. As Newton's method is known to converge faster than a Picard iteration, it could prove useful to extend the MHD HDG methods developed in this work to a Newton linearization with the goal of reducing the number of linear system solves in the solution process.

- **Implicit-explicit (IMEX) time discretization:** Implicit-explicit (IMEX) Runge-Kutta schemes aim to combine the advantages of implicit and explicit time stepping schemes. In such a scheme, the nonlinear operator in the PDE is split into a linear part containing the fast waves, and a nonlinear part with the fast waves removed. If the nonlinear part is advanced explicitly in time and the linear part is advanced implicitly in time, then the number of linear system solves per time step is reduced to one, as opposed to however many linear system solves it otherwise takes for a Picard or Newton iteration to converge. A logical way to apply this idea with discontinuous Galerkin is to discretize the linear operator with (implicit) HDG and to discretize the nonlinear operator with (explicit) traditional DG [40].

- **Postprocessing:** Postprocessing of the HDG volume solution has been proposed in various works as an element-local (and thus inexpensive) means to find solutions that conform to some desired property that the HDG solution does not fulfill and/or to gain an additional order of convergence. For example, in [56] for the incompressible Navier-Stokes equations, a postprocessing procedure is proposed that takes an "un-postprocessed" velocity that is weakly divergence-free and approximately $H(div, \Omega)$-conforming and recovers a postprocessed veloc-

ity that is pointwise divergence-free, exactly $H(div, \Omega)$-conforming, and converges with an additional order of accuracy. In our HDG schemes, we have assumed that the linearized velocity $\boldsymbol{w}$ is pointwise divergence free and resides in $H(div, \Omega)$. When we employ a Picard iteration taking $\boldsymbol{w}$ as the previous un-postprocessed iteration of $\boldsymbol{u}_h$, we are violating some of the assumptions of the well-posedness analysis. A similar statement applies to the assumption that the known magnetic field $\boldsymbol{d}$ about which the equations are linearized has normal and tangential components that are continuous across element interfaces, whereas the previous un-postprocessed iteration of $\boldsymbol{b}_h$ does not. Although the Picard iteration appears to be effective without postprocessing these variables, it is not guaranteed that this will always lead to a stable solution procedure. For these reasons, mathematical development and numerical implementation of a postprocessing procedure for $\boldsymbol{u}_h$ and $\boldsymbol{b}_h$ is suggested as a research topic [47].

- **Alternate HDG formulations:** An HDG flux based on the exact upwind flux of the visco-resistive MHD equations involves roots of 6th order polynomials, which cannot be expressed analytically, and so HDG schemes of this type were not further pursued. All of the HDG schemes in this work for MHD are based on piecing together the upwind fluxes of the Oseen equations and induction equation in the zero-velocity limit. The resulting HDG schemes are not upwind, as the coupling between the fluid and magnetic subsystems in the flux were done in a way only to ensure stability of the scheme. Piecing together of the Oseen and induction equation fluxes is not necessarily the only way we could have proceeded. For many astrophysical and laboratory plasmas, the viscosity and resistivity are very small. This leads to the idea that an alternate flux derivation based on the upwind flux of the ideal MHD equations (zero resistivity and zero viscosity), and piecing together the diffusive terms to ensure

stability, could lead to an HDG scheme that exhibits good behavior. The upwind flux of the incompressible ideal MHD equations involves roots of fourth order polynomials, which do have analytical expressions. These expressions are cumbersome, especially when attempting to express the flux in terms of a minimal number of trace unknowns, and so up to this point no serious attempts to develop such schemes have been made.

- **Extending the error analysis:** Several extensions to the error analysis presented in this work are possible. The error analysis performed in this work assumes sufficient regularity of the exact solution so that the polynomial order of numerical solution is the limiting factor that determines the error convergence rate. Removing this assumption would provide a more complete estimate. Beyond this, it is possible to keep track of the parameters rather than absorbing them into the inequalities, and to relax the assumption that all variables are represented with the same polynomial order. Finally, error analysis can be performed for different forms of the parameters τ_n, τ_t, β_n, β_t, and ξ, or for different numerical fluxes altogether.

- **Formulations beyond incompressible MHD:** Extending the schemes beyond incompressible MHD would allow us to solve more interesting problems in plasma physics.

Appendices

Appendix A

Common Notation

In this appendix we review common notation and conventions that apply to the entirety of this work. The spatial dimension of the problem under consideration is denoted by d. Let $\Omega \subset \mathbb{R}^d$, $d = 2, 3$, be a bounded domain and its boundary $\partial\Omega$ is a Lipschitz manifold. We partition Ω into disjoint elements K (simplices or quadrilaterals/hexahedra), and define $\mathcal{T}_h := \{K\}$ as the collection of elements. We define $\partial\mathcal{T} := \{\partial K : K \in \mathcal{T}\}$ as the collection of element faces (where we use the term "face" regardless of the spatial dimension). For any K, $e = \partial K \cap \partial\Omega$ is a ($d-1$ dimensional) boundary face if e has a nonzero $d-1$ Lebesgue measure. For any two distinct elements K^- and K^+, $e = \partial K^- \cap \partial K^+$ is an interior face if e has a nonzero $d-1$ Lebesgue measure. The collection of all interior faces is denoted by $\mathcal{E}_h^o$ and the collection of all boundary faces is denoted by $\mathcal{E}_h^\partial$. The mesh skeleton $\mathcal{E}_h := \mathcal{E}_h^o \cup \mathcal{E}_h^\partial$ is the collection of all faces, boundary and interior. The mesh size of triangulations is $h := \max_{K\in\mathcal{T}_h} \operatorname{diam}(K)$.

We use $(\cdot,\cdot)_D$ or $\langle\cdot,\cdot\rangle_D$ to denote the L^2-inner product on D if D is a d or $(d-1)$ dimensional domain, respectively. The standard notation $W^{s,p}(D)$, $s \geq 0$, $1 \leq p \leq \infty$, is used for the Sobolev space on D based on L^p-norm with differentiability s (see, e.g., [27]) and $\|\cdot\|_{W^{s,p}(D)}$ denotes the associated norm. In particular, if $p = 2$, we use $H^s(D) := W^{s,2}(D)$ and $\|\cdot\|_{s,D}$. $W^{s,p}(\mathcal{T}_h)$ denotes the space of functions whose restrictions on K reside in $W^{s,p}(K)$ for each $K \in \mathcal{T}_h$ and its norm is $\|u\|^p_{W^{s,p}(\mathcal{T}_h)} := \sum_{K\in\mathcal{T}_h} \|u|_K\|^p_{W^{s,p}(K)}$ if $1 \leq p < \infty$ and $\|u\|_{W^{s,\infty}(\mathcal{T}_h)} := \max_{K\in\mathcal{T}_h} \|u|_K\|_{W^{s,\infty}(K)}$. For

simplicity, we use $\|\cdot\|_s$ for $\|\cdot\|_{s,\mathcal{T}_h}$, and we use $\|\cdot\|_{\partial\mathcal{T}_h}$ for $\|\cdot\|_{0,\partial\mathcal{T}_h}$. We define $\|u,v\| := \|u\| + \|v\|$. Furthermore, we denote by $A \lesssim B$ the inequality $A \leq \lambda B$ with a constant $\lambda > 0$ independent of the mesh size, and by $A \sim B$ the combination of $A \lesssim B$ and $B \lesssim A$.

For vector (first order tensor) valued functions or second order tensor valued functions, these notations are naturally extended with a component-wise inner product. We define the gradient of a vector (first order tensor), the divergence of a second order tensor, and the outer product symbol $\otimes$ as

$$(\nabla \boldsymbol{u})_{ij} = \frac{\partial u_i}{\partial x_j}, \quad (\nabla \cdot \mathbf{L})_i = \sum_{j=1}^{d} \frac{\partial \mathbf{L}_{ij}}{\partial x_j}, \quad (\boldsymbol{a} \otimes \boldsymbol{b})_{ij} = a_i b_j = \left(\boldsymbol{a}\boldsymbol{b}^\top\right)_{ij}.$$

The curl of a vector when $d = 3$ takes its standard form, $(\nabla \times \boldsymbol{b})_i = \sum_{j,k} \epsilon_{ijk} \frac{\partial \boldsymbol{b}_k}{\partial x_j}$, where ϵ is the Levi-Civita symbol. When $d = 2$, let us explicitly define the curl of a vector as the scalar quantity $\nabla \times \boldsymbol{b} = \frac{\partial \boldsymbol{b}_2}{\partial x_1} - \frac{\partial \boldsymbol{b}_1}{\partial x_2}$, and the curl of a scalar as the vector quantity $\nabla \times a = \left(\frac{\partial a}{\partial x_2}, -\frac{\partial a}{\partial x_1}\right)$. This first definition is consistent with applying the 3D curl operator to a 2D vector extended by zero in the third dimension, then restricting the result to the third dimension, as the result is necessarily zero in the other two dimensions. Similarly, the second definition is consistent with applying the 3D curl operator to a scalar, interpreted as a 3D vector whose value is zero in the first two dimensions, and then restricting the result to two dimensions. Similar definitions hold for the cross product of two 2D vectors, $\boldsymbol{n} \times \boldsymbol{b} = n_1 b_2 - n_2 b_1$, and for the cross product of a 2D vector with a scalar $\boldsymbol{n} \times a = (n_2 a, -n_1 a)$. The symbol $\tilde{d}$ is used to denote the dimension of the curl of a d dimensional vector, i.e., $\tilde{d} = 3$ when $d = 3$ and $\tilde{d} = 1$ when $d = 2$. In general, we denote vectors by bold, italicized symbols, and we denote matrices and tensors by non-italicized, bold, uppercase letters. When relevant, vectors are to be interpreted as column vectors $\boldsymbol{v} = (v_1; v_2; v_3)$, and $\mathbf{A}^\top$ denotes the vector or matrix transpose.

In this work $\boldsymbol{n}$ denotes a unit normal vector field on a face of ∂K, and it points outward relative to the element K with which ∂K is associated. If $\partial K^- \cap \partial K^+ \in \mathcal{E}_h$ for two distinct simplices K^-, K^+, then $\boldsymbol{n}^-$ and $\boldsymbol{n}^+$ denote the outward unit normal vector fields on ∂K^- and ∂K^+, respectively, and $\boldsymbol{n}^- = -\boldsymbol{n}^+$ on $\partial K^- \cap \partial K^+$. We simply use $\boldsymbol{n}$ to denote either $\boldsymbol{n}^-$ or $\boldsymbol{n}^+$ in an expression that is valid for both cases, and this convention is also used for other quantities restricted to a face $e \in \mathcal{E}_h$. We use $\tilde{\boldsymbol{n}}$ to define a unique normal vector associated with the face $\partial K^- \cap \partial K^+$. That is, $\tilde{\boldsymbol{n}}$ is chosen arbitrarily as either $\boldsymbol{n}^-$ or $\boldsymbol{n}^+$, so that either $\tilde{\boldsymbol{n}} = \boldsymbol{n}^- = -\boldsymbol{n}^+$ or $\tilde{\boldsymbol{n}} = -\boldsymbol{n}^- = \boldsymbol{n}^+$. We define the double valued sgn $:= \boldsymbol{n} \cdot \tilde{\boldsymbol{n}}$ associated with each skeleton face, which is either positive or negative 1. We define $\mathbf{N} := \boldsymbol{n} \otimes \boldsymbol{n}$ so that the normal component of some vector $\boldsymbol{b}$ can be written as $\boldsymbol{b}^n := (\boldsymbol{b} \cdot \boldsymbol{n})\, \boldsymbol{n} = \mathbf{N}\boldsymbol{b}$. Similarly, we define $\mathbf{T} := \mathbf{I} - \mathbf{N} = -\boldsymbol{n} \times (\boldsymbol{n} \times \cdot)$, where $\mathbf{I}$ is the identity matrix, so that the tangential component of some vector $\boldsymbol{b}$ can be written as $\boldsymbol{b}^t := -\boldsymbol{n} \times (\boldsymbol{n} \times \boldsymbol{b}) = \mathbf{T}\boldsymbol{b}$. For a quantity which is double-valued on a face e, the jump term on e is defined by $[\![f]\!] := f^- + f^+$, and is typically used for quantities involving the normal vectors, e.g., $[\![u\boldsymbol{n}]\!] = \boldsymbol{n}^- u^- + \boldsymbol{n}^+ u^+$.

We define $\mathcal{P}_k(K)$ as the space of polynomials of degree at most k on a K, with $k \geq 0$ and we define

$$\mathcal{P}_k(\mathcal{T}_h) = \left\{ u \in L^2(\Omega) \ : \ u|_K \in \mathcal{P}_k(K) \ \forall K \in \mathcal{T}_h \right\}.$$

The space of polynomials on the mesh skeleton $\mathcal{P}_k(\mathcal{E}_h)$ is similarly defined, and their extensions to vector- or matrix-valued polynomials $[\mathcal{P}_k(\mathcal{T}_h)]^d$, $[\mathcal{P}_k(\mathcal{T}_h)]^{d\times d}$, $[\mathcal{P}_k(\mathcal{E}_h)]^d$, etc, are straightforward.

Finally, in the derivation of numerical fluxes for HDG schemes with second order tensor valued auxiliary variables, for conciseness and convenience we will use the Kronecker product and vectorization operator [35, 71]. The Kronecker product is

typically denoted by the same symbol ($\otimes$) as the tensor product. Because we use both the tensor product and Kronecker product in this work, in order to avoid confusion we will denote the Kronecker product by $\otimes_K$ (where the subscript refers to "Kronecker"). For an arbitrary $m \times n$ matrix $\mathbf{A}$ and $p \times q$ matrix $\mathbf{B}$, the Kronecker product $\mathbf{A} \otimes_K \mathbf{B}$ is defined by

$$\mathbf{A} \otimes_K \mathbf{B} = \begin{bmatrix} a_{11}\mathbf{B} & \dots & a_{1n}\mathbf{B} \\ \vdots & \ddots & \vdots \\ a_{m1}\mathbf{B} & \dots & a_{mn}\mathbf{B} \end{bmatrix},$$

or, more concisely, $(\mathbf{A} \otimes_K \mathbf{B})_{p(i-1)+k,q(j-1)+l} = \mathbf{A}_{ij}\mathbf{B}_{kl}$. Among the useful properties of the Kronecker product are the following:

$$(\mathbf{A} \otimes_K \mathbf{B})^\top = \mathbf{A}^\top \otimes_K \mathbf{B}^\top,$$
$$(\mathbf{A} \otimes_K \mathbf{B})(\mathbf{C} \otimes_K \mathbf{D}) = (\mathbf{AC}) \otimes_K (\mathbf{BD}).$$

The vectorization operator, vec, maps a matrix to a vector that is composed of the columns of the matrix "stacked" on top of each other. For example a 3×3 matrix $\mathbf{L}$ is mapped to the vector $\mathrm{vec}(\mathbf{L}) = (L_{11}; L_{21}; L_{31}; L_{12}; L_{22}; L_{32}; L_{13}; L_{23}; L_{33})$. A convenient relationship between the Kronecker product and the vectorization operator is

$$\mathrm{vec}(\mathbf{ABC}) = \left(\mathbf{C}^\top \otimes_K \mathbf{A}\right) \mathrm{vec}(\mathbf{B}). \tag{A.1}$$

Appendix B

Characterization of HDG Schemes for the Stokes Equations

For conforming finite element methods, it is a relatively easy task to determine the form that the matrix structure will take. For the Stokes equations with homogeneous Dirichlet boundary conditions, a conforming finite element method looks like: find $(\boldsymbol{u}_h, p_h) \in \boldsymbol{V}_h \times Q_h \subset H_0^1(\Omega) \times L_0^2(\Omega)$ such that

$$\frac{1}{\mathrm{Re}} (\nabla \boldsymbol{u}_h, \nabla \boldsymbol{v})_\Omega - (p_h, \nabla \cdot \boldsymbol{v})_\Omega = (\boldsymbol{f}, \boldsymbol{v})_\Omega , \tag{B.1}$$

$$- (\nabla \cdot \boldsymbol{u}_h, q)_\Omega = 0, \tag{B.2}$$

for all $(\boldsymbol{v}, q) \in \boldsymbol{V}_h \times Q_h$ for some stable finite element space pair $(\boldsymbol{V}_h, Q_h)$. Here the letters $\boldsymbol{V}_h$ and Q_h are reused and are not meant to refer to (2.20), and $L_0^2(\Omega)$ refers to functions in $L^2(\Omega)$ with zero average. It is clear that the matrix associated with (B.1) will take the form

$$\begin{bmatrix} A & B^\top \\ B & 0 \end{bmatrix} \begin{Bmatrix} U \\ P \end{Bmatrix} = F. \tag{B.3}$$

For the HDG schemes for the Stokes equations in Chapter 2, it is not clear what form the condensed global system will take just by looking at the weak form of the HDG scheme. In this appendix, we prove the properties of the condensed global matrices for the Stokes HDG schemes discussed in Chapter 2.

B.1 Characterization of Formulation 2.2

In the following, we characterize the statically condensed global system of the Stokes HDG scheme Formulation 2.2, which uses the $\widehat{\boldsymbol{u}}_h$ flux (2.16) and the augmented Lagrangian modification for well-posedness of the local solver. The following characterization sheds light on the matrix system associated with this formulation. Toward this goal, we define the following local solvers, where $\mathbf{S}$ is a stabilization tensor defined in (2.26).

For $\boldsymbol{\mu} \in \widehat{\boldsymbol{V}}_h^i$, we define $(\mathbf{L}_h^{\boldsymbol{\mu}}, \boldsymbol{u}_h^{\boldsymbol{\mu}}, p_h^{\boldsymbol{\mu}})$ in $\mathbf{G}_h \times \boldsymbol{V}_h \times Q_h$ as the solution to

$$\operatorname{Re}\left(\mathbf{L}_h^{\boldsymbol{\mu}}, \mathbf{G}\right)_{\mathcal{T}_h} + \left(\boldsymbol{u}_h^{\boldsymbol{\mu}}, \nabla \cdot \mathbf{G}\right)_{\mathcal{T}_h} - \left\langle \boldsymbol{\mu}, \mathbf{G}\boldsymbol{n}\right\rangle_{\partial\mathcal{T}_h \setminus \partial\Omega_D} = 0, \quad \text{(B.4a)}$$

$$-\left(\nabla \cdot \mathbf{L}_h^{\boldsymbol{\mu}}, \boldsymbol{v}\right)_{\mathcal{T}_h} + \left(\nabla p_h^{\boldsymbol{\mu}}, \boldsymbol{v}\right)_{\mathcal{T}_h} + \left\langle \mathbf{S}\left(\boldsymbol{u}_h^{\boldsymbol{\mu}} - \boldsymbol{\mu}\right), \boldsymbol{v}\right\rangle_{\partial\mathcal{T}_h \setminus \partial\Omega_D} + \left\langle \mathbf{S}\boldsymbol{u}_h^{\boldsymbol{\mu}}, \boldsymbol{v}\right\rangle_{\partial\Omega_D} = 0, \quad \text{(B.4b)}$$

$$\frac{1}{\Delta\tau}\left(p_h^{\boldsymbol{\mu}}, q\right)_{\mathcal{T}_h} - \left(\boldsymbol{u}_h^{\boldsymbol{\mu}}, \nabla q\right)_{\mathcal{T}_h} + \left\langle \boldsymbol{\mu} \cdot \boldsymbol{n}, q\right\rangle_{\partial\mathcal{T}_h \setminus \partial\Omega_D} = 0, \quad \text{(B.4c)}$$

for all $(\mathbf{G}, \boldsymbol{v}, q)$ in $\mathbf{G}_h \times \boldsymbol{V}_h \times Q_h$.

For $\boldsymbol{U} \in \widehat{\boldsymbol{V}}_h(\partial\Omega_D)$, we define $\left(\mathbf{L}_h^{\boldsymbol{U}}, \boldsymbol{u}_h^{\boldsymbol{U}}, p_h^{\boldsymbol{U}}\right)$ in $\mathbf{G}_h \times \boldsymbol{V}_h \times Q_h$ as the solution to

$$\operatorname{Re}\left(\mathbf{L}_h^{\boldsymbol{U}}, \mathbf{G}\right)_{\mathcal{T}_h} + \left(\boldsymbol{u}_h^{\boldsymbol{U}}, \nabla \cdot \mathbf{G}\right)_{\mathcal{T}_h} - \left\langle \boldsymbol{U}, \mathbf{G}\boldsymbol{n}\right\rangle_{\partial\Omega_D} = 0, \quad \text{(B.5a)}$$

$$-\left(\nabla \cdot \mathbf{L}_h^{\boldsymbol{U}}, \boldsymbol{v}\right)_{\mathcal{T}_h} + \left(\nabla p_h^{\boldsymbol{U}}, \boldsymbol{v}\right)_{\mathcal{T}_h} + \left\langle \mathbf{S}\boldsymbol{u}_h^{\boldsymbol{U}}, \boldsymbol{v}\right\rangle_{\partial\mathcal{T}_h \setminus \partial\Omega_D} + \left\langle \mathbf{S}\left(\boldsymbol{u}_h^{\boldsymbol{U}} - \boldsymbol{U}\right), \boldsymbol{v}\right\rangle_{\partial\Omega_D} = 0, \quad \text{(B.5b)}$$

$$\frac{1}{\Delta\tau}\left(p_h^{\boldsymbol{U}}, q\right)_{\mathcal{T}_h} - \left(\boldsymbol{u}_h^{\boldsymbol{U}}, \nabla q\right)_{\mathcal{T}_h} + \left\langle \boldsymbol{U} \cdot \boldsymbol{n}, q\right\rangle_{\partial\Omega_D} = 0, \quad \text{(B.5c)}$$

for all $(\mathbf{G}, \boldsymbol{v}, q)$ in $\mathbf{G}_h \times \boldsymbol{V}_h \times Q_h$.

For $\boldsymbol{g} \in L^2(\Omega)$, we define $(\mathbf{L}_h^{\boldsymbol{g}}, \boldsymbol{u}_h^{\boldsymbol{g}}, p_h^{\boldsymbol{g}})$ in $\mathbf{G}_h \times \boldsymbol{V}_h \times Q_h$ as the solution to

$$\operatorname{Re}\left(\mathbf{L}_h^{\boldsymbol{g}}, \mathbf{G}\right)_{\mathcal{T}_h} + \left(\boldsymbol{u}_h^{\boldsymbol{g}}, \nabla \cdot \mathbf{G}\right)_{\mathcal{T}_h} = 0, \quad \text{(B.6a)}$$

$$-\left(\nabla \cdot \mathbf{L}_h^{\boldsymbol{g}}, \boldsymbol{v}\right)_{\mathcal{T}_h} + \left(\nabla p_h^{\boldsymbol{g}}, \boldsymbol{v}\right)_{\mathcal{T}_h} + \left\langle \mathbf{S}\boldsymbol{u}_h^{\boldsymbol{g}}, \boldsymbol{v}\right\rangle_{\partial\mathcal{T}_h} = \left(\boldsymbol{g}, \boldsymbol{v}\right)_{\mathcal{T}_h}, \quad \text{(B.6b)}$$

$$\frac{1}{\Delta\tau}\left(p_h^{\boldsymbol{g}}, q\right)_{\mathcal{T}_h} - \left(\boldsymbol{u}_h^{\boldsymbol{g}}, \nabla q\right)_{\mathcal{T}_h} = 0, \quad \text{(B.6c)}$$

for all $(\mathbf{G}, \boldsymbol{v}, q)$ in $\mathbf{G}_h \times \boldsymbol{V}_h \times Q_h$.

For $r \in Q_h$, we define $(\mathbf{L}_h^r, \boldsymbol{u}_h^r, p_h^r)$ in $\mathbf{G}_h \times \boldsymbol{V}_h \times Q_h$ as the solution to

$$\mathrm{Re}\,(\mathbf{L}_h^r, \mathbf{G})_{\mathcal{T}_h} + (\boldsymbol{u}_h^r, \nabla \cdot \mathbf{G})_{\mathcal{T}_h} = 0, \tag{B.7a}$$

$$-(\nabla \cdot \mathbf{L}_h^r, \boldsymbol{v})_{\mathcal{T}_h} + (\nabla p_h^r, \boldsymbol{v})_{\mathcal{T}_h} + \langle \mathbf{S}\boldsymbol{u}_h^r, \boldsymbol{v}\rangle_{\partial\mathcal{T}_h} = 0, \tag{B.7b}$$

$$\frac{1}{\Delta\tau}(p_h^r, q)_{\mathcal{T}_h} - (\boldsymbol{u}_h^r, \nabla q)_{\mathcal{T}_h} = \frac{1}{\Delta\tau}(r, q)_{\mathcal{T}_h}, \tag{B.7c}$$

for all $(\mathbf{G}, \boldsymbol{v}, q)$ in $\mathbf{G}_h \times \boldsymbol{V}_h \times Q_h$.

The local solvers (B.4) – (B.7) can be shown to be well-posed in an identical manner to how the well-posedness of the local solver of Formulation 2.2 is shown in Chapter 2.

At this point, we are in a position to state the main result.

Theorem B.1. *(characterization of condensed global system for Formulation 2.2) The combined jump condition and Neumann boundary condition* (2.36d) *can be written as*

$$a\left(\widehat{\boldsymbol{u}}_h^{i,k}, \widehat{\boldsymbol{v}}\right) = \ell\left(\widehat{\boldsymbol{v}}\right), \tag{B.8}$$

where

$$\begin{aligned} a\left(\widehat{\boldsymbol{u}}_h^{i,k}, \widehat{\boldsymbol{v}}\right) := &\left(\mathrm{Re}\mathbf{L}_h^{\widehat{\boldsymbol{u}}_h^{i,k}}, \mathbf{L}_h^{\widehat{\boldsymbol{v}}}\right)_{\mathcal{T}_h} + \frac{1}{\Delta\tau}\left(p_h^{\widehat{\boldsymbol{u}}_h^{i,k}}, p_h^{\widehat{\boldsymbol{v}}}\right)_{\mathcal{T}_h} + \left\langle \mathbf{S}\boldsymbol{u}_h^{\widehat{\boldsymbol{u}}_h^{i,k}}, \boldsymbol{u}_h^{\widehat{\boldsymbol{v}}}\right\rangle_{\partial\Omega_D} \\ &+ \left\langle \mathbf{S}\left(\boldsymbol{u}_h^{\widehat{\boldsymbol{u}}_h^{i,k}} - \widehat{\boldsymbol{u}}_h^{i,k}\right), \boldsymbol{u}_h^{\widehat{\boldsymbol{v}}} - \widehat{\boldsymbol{v}}\right\rangle_{\partial\mathcal{T}_h\setminus\partial\Omega_D} \end{aligned} \tag{B.9}$$

and

$$\begin{aligned} l_1\left(\widehat{\boldsymbol{v}}\right) := &-\langle \boldsymbol{f}_N, \widehat{\boldsymbol{v}}\rangle_{\partial\Omega_N} + \left\langle -\mathbf{L}_h^{\widehat{\boldsymbol{u}}_h^D}\boldsymbol{n} + p_h^{\widehat{\boldsymbol{u}}_h^D}\boldsymbol{n} + \mathbf{S}\boldsymbol{u}_h^{\widehat{\boldsymbol{u}}_h^D}, \widehat{\boldsymbol{v}}\right\rangle_{\partial\mathcal{T}_h\setminus\partial\Omega_D} \\ &+ \left\langle -\mathbf{L}_h^{\boldsymbol{f}}\boldsymbol{n} + p_h^{\boldsymbol{f}}\boldsymbol{n} + \mathbf{S}\boldsymbol{u}_h^{\boldsymbol{f}}, \widehat{\boldsymbol{v}}\right\rangle_{\partial\mathcal{T}_h\setminus\partial\Omega_D} \\ &+ \left\langle -\mathbf{L}_h^{\frac{1}{\Delta\tau}p_h^{k-1}}\boldsymbol{n} + p_h^{\frac{1}{\Delta\tau}p_h^{k-1}}\boldsymbol{n} + \mathbf{S}\boldsymbol{u}_h^{\frac{1}{\Delta\tau}p_h^{k-1}}, \widehat{\boldsymbol{v}}\right\rangle_{\partial\mathcal{T}_h\setminus\partial\Omega_D}. \end{aligned} \tag{B.10}$$

Proof. Due to the linearity of the local solver (2.36a) – (2.36c) , we can decompose the volume solution to (2.36a) – (2.36c) as

$$\begin{aligned}\left(\mathbf{L}_h^k, \boldsymbol{u}_h^k, p_h^k\right) = &\left(\mathbf{L}_h^{\widehat{\boldsymbol{u}}_h^{i,k}}, \boldsymbol{u}_h^{\widehat{\boldsymbol{u}}_h^{i,k}}, p_h^{\widehat{\boldsymbol{u}}_h^{i,k}}\right) + \left(\mathbf{L}_h^{\widehat{\boldsymbol{u}}_h^{D}}, \boldsymbol{u}_h^{\widehat{\boldsymbol{u}}_h^{D}}, p_h^{\widehat{\boldsymbol{u}}_h^{D}}\right) \\ &+ \left(\mathbf{L}_h^{\boldsymbol{f}}, \boldsymbol{u}_h^{\boldsymbol{f}}, p_h^{\boldsymbol{f}}\right) + \left(\mathbf{L}_h^{\frac{1}{\Delta\tau}p_h^{k-1}}, \boldsymbol{u}_h^{\frac{1}{\Delta\tau}p_h^{k-1}}, p_h^{\frac{1}{\Delta\tau}p_h^{k-1}}\right).\end{aligned}$$

That is, $\left(\mathbf{L}_h^k, \boldsymbol{u}_h^k, p_h^k\right)$ is the sum of the solutions to (B.4) – (B.7) with $\boldsymbol{\mu} = \widehat{\boldsymbol{u}}_h^{i,k}$, $\boldsymbol{U} = \widehat{\boldsymbol{u}}_h^D$, $\boldsymbol{g} = \boldsymbol{f}$, and $\boldsymbol{r} = \frac{1}{\Delta\tau}p_h^{k-1}$. Then, the combined jump and Neumann boundary condition (2.36d) can be written as

$$\begin{aligned}&-\left\langle -\mathbf{L}_h^{\widehat{\boldsymbol{u}}_h^{i,k}}\boldsymbol{n} + p_h^{\widehat{\boldsymbol{u}}_h^{i,k}}\boldsymbol{n} + \mathbf{S}\left(\boldsymbol{u}_h^{\widehat{\boldsymbol{u}}_h^{i,k}} - \widehat{\boldsymbol{u}}_h^{i,k}\right), \widehat{\boldsymbol{v}}\right\rangle_{\partial\mathcal{T}_h\setminus\partial\Omega_D} \\ &-\left\langle -\mathbf{L}_h^{\widehat{\boldsymbol{u}}_h^{D}}\boldsymbol{n} + p_h^{\widehat{\boldsymbol{u}}_h^{D}}\boldsymbol{n} + \mathbf{S}\boldsymbol{u}_h^{\widehat{\boldsymbol{u}}_h^{D}}, \widehat{\boldsymbol{v}}\right\rangle_{\partial\mathcal{T}_h\setminus\partial\Omega_D} - \left\langle -\mathbf{L}_h^{\boldsymbol{f}}\boldsymbol{n} + p_h^{\boldsymbol{f}}\boldsymbol{n} + \mathbf{S}\boldsymbol{u}_h^{\boldsymbol{f}}, \widehat{\boldsymbol{v}}\right\rangle_{\partial\mathcal{T}_h\setminus\partial\Omega_D} \\ &-\left\langle -\mathbf{L}_h^{\frac{1}{\Delta\tau}p_h^{k-1}}\boldsymbol{n} + p_h^{\frac{1}{\Delta\tau}p_h^{k-1}}\boldsymbol{n} + \mathbf{S}\boldsymbol{u}_h^{\frac{1}{\Delta\tau}p_h^{k-1}}, \widehat{\boldsymbol{v}}\right\rangle_{\partial\mathcal{T}_h\setminus\partial\Omega_D} = -\left\langle \boldsymbol{f}_N, \widehat{\boldsymbol{v}}\right\rangle_{\partial\Omega_N}.\end{aligned}$$

It remains to show $-\left\langle -\mathbf{L}_h^{\widehat{\boldsymbol{u}}_h^{i,k}}\boldsymbol{n} + p_h^{\widehat{\boldsymbol{u}}_h^{i,k}}\boldsymbol{n} + \mathbf{S}\left(\boldsymbol{u}_h^{\widehat{\boldsymbol{u}}_h^{i,k}} - \widehat{\boldsymbol{u}}_h^{i,k}\right), \widehat{\boldsymbol{v}}\right\rangle_{\partial\mathcal{T}_h\setminus\partial\Omega_D} = a\left(\widehat{\boldsymbol{u}}_h^{i,k}, \widehat{\boldsymbol{v}}\right)$ as defined by (B.9). In (B.4a) take $\boldsymbol{\mu} = \widehat{\boldsymbol{v}}$ and $\mathbf{G} = \mathbf{L}_h^{\widehat{\boldsymbol{u}}_h^{i,k}}$, in (B.4b) take $\boldsymbol{\mu} = \widehat{\boldsymbol{u}}_h^{i,k}$ and $\boldsymbol{v} = \boldsymbol{u}_h^{\widehat{\boldsymbol{v}}}$, and in (B.4c) take $\boldsymbol{\mu} = \widehat{\boldsymbol{v}}$ and $q = p_h^{\widehat{\boldsymbol{u}}_h^{i,k}}$. Summing the result, we have

$$\begin{aligned}&\left(\mathrm{Re}\mathbf{L}_h^{\widehat{\boldsymbol{u}}_h^{i,k}}, \mathbf{L}_h^{\widehat{\boldsymbol{v}}}\right)_{\mathcal{T}_h} + \frac{1}{\Delta\tau}\left(p_h^{\widehat{\boldsymbol{u}}_h^{i,k}}, p_h^{\widehat{\boldsymbol{v}}}\right)_{\mathcal{T}_h} + \left\langle \mathbf{S}\left(\boldsymbol{u}_h^{\widehat{\boldsymbol{u}}_h^{i,k}} - \widehat{\boldsymbol{u}}_h^{i,k}\right), \boldsymbol{u}_h^{\widehat{\boldsymbol{v}}}\right\rangle_{\partial\mathcal{T}_h\setminus\partial\Omega_D} \\ &\quad + \left\langle \mathbf{S}\boldsymbol{u}_h^{\widehat{\boldsymbol{u}}_h^{i,k}}, \boldsymbol{u}_h^{\widehat{\boldsymbol{v}}}\right\rangle_{\partial\Omega_D} - \left\langle \mathbf{L}_h^{\widehat{\boldsymbol{u}}_h^{i,k}}\boldsymbol{n}, \widehat{\boldsymbol{v}}\right\rangle_{\partial\mathcal{T}_h\setminus\partial\Omega_D} + \left\langle p_h^{\widehat{\boldsymbol{u}}_h^{i,k}}, \widehat{\boldsymbol{v}}\cdot\boldsymbol{n}\right\rangle_{\partial\mathcal{T}_h\setminus\partial\Omega_D} = 0.\end{aligned}$$

Therefore,

$$\begin{aligned}&\left\langle \mathbf{L}_h^{\widehat{\boldsymbol{u}}_h^{i,k}}\boldsymbol{n}, \widehat{\boldsymbol{v}}\right\rangle_{\partial\mathcal{T}_h\setminus\partial\Omega_D} - \left\langle p_h^{\widehat{\boldsymbol{u}}_h^{i,k}}, \widehat{\boldsymbol{v}}\cdot\boldsymbol{n}\right\rangle_{\partial\mathcal{T}_h\setminus\partial\Omega_D} \\ &\quad - \left\langle \mathbf{S}\left(\boldsymbol{u}_h^{\widehat{\boldsymbol{u}}_h^{i,k}} - \widehat{\boldsymbol{u}}_h^{i,k}\right), \widehat{\boldsymbol{v}}\right\rangle_{\partial\mathcal{T}_h\setminus\partial\Omega_D} = a\left(\widehat{\boldsymbol{u}}_h^{i,k}, \widehat{\boldsymbol{v}}\right).\end{aligned}$$

□

We can conclude from Theorem B.1 that the condensed global system will take the form

$$A\widehat{U}^k = F^{k-1}.$$

Inspecting (B.9), we can see that the block matrix A is symmetric and positive semi-definite. We can further claim that A is positive definite. To support this claim we must show $a\left(\widehat{\boldsymbol{u}}_h^{i,k}, \widehat{\boldsymbol{u}}_h^{i,k}\right) = 0 \Rightarrow \widehat{\boldsymbol{u}}_h^{i,k} = \mathbf{0}$. Indeed, $a\left(\widehat{\boldsymbol{u}}_h^{i,k}, \widehat{\boldsymbol{u}}_h^{i,k}\right) = 0$ implies $\mathbf{L}_h^{\widehat{\boldsymbol{u}}_h^{i,k}} = \mathbf{0}$, $p_h^{\widehat{\boldsymbol{u}}_h^{i,k}} = 0$, $\boldsymbol{u}_h^{\widehat{\boldsymbol{u}}_h^{i,k}} = 0$ on $\partial\Omega_D$, and $\boldsymbol{u}_h^{\widehat{\boldsymbol{u}}_h^{i,k}} = \widehat{\boldsymbol{u}}_h^{i,k}$ on $\mathcal{E}_h \backslash \partial\Omega_D$. Then, with $\boldsymbol{\mu} = \widehat{\boldsymbol{u}}_h^{i,k}$ in (B.4a), integrating by parts reveals that $\boldsymbol{u}_h^{\widehat{\boldsymbol{u}}_h^{i,k}}$ is elementwise constant, and therefore globally constant since $\boldsymbol{u}_h^{\widehat{\boldsymbol{u}}_h^{i,k}} = \widehat{\boldsymbol{u}}_h^{i,k}$ on $\mathcal{E}_h \backslash \partial\Omega_D$. Since $\partial\Omega_D \neq \emptyset$ then $\boldsymbol{u}_h^{\widehat{\boldsymbol{u}}_h^{i,k}} = 0$ and therefore $\widehat{\boldsymbol{u}}_h^{i,k} = 0$.

B.2 Characterization of Formulation 2.3

In the following, we characterize the statically condensed global system of the Stokes HDG scheme Formulation 2.3, which uses the $\widehat{\boldsymbol{u}}_h$ flux (2.16) and the average edge-pressure modification for well-posedness of the local solver. The following characterization sheds light on the matrix system associated with this formulation. Toward this goal, we define the following local solvers, where $\mathbf{S}$ is a stabilization tensor defined in (2.26).

For $\boldsymbol{\mu} \in \widehat{\boldsymbol{V}}_h^i$, we define $(\mathbf{L}_h^{\boldsymbol{\mu}}, \boldsymbol{u}_h^{\boldsymbol{\mu}}, p_h^{\boldsymbol{\mu}})$ in $\mathbf{G}_h \times \boldsymbol{V}_h \times Q_h$ as the solution to

$$\mathrm{Re}\left(\mathbf{L}_h^{\boldsymbol{\mu}}, \mathbf{G}\right)_{\mathcal{T}_h} + \left(\boldsymbol{u}_h^{\boldsymbol{\mu}}, \nabla \cdot \mathbf{G}\right)_{\mathcal{T}_h} - \left\langle \boldsymbol{\mu}, \mathbf{G}\boldsymbol{n}\right\rangle_{\partial\mathcal{T}_h \backslash \partial\Omega_D} = 0, \quad \text{(B.11a)}$$

$$-\left(\nabla \cdot \mathbf{L}_h^{\boldsymbol{\mu}}, \boldsymbol{v}\right)_{\mathcal{T}_h} + \left(\nabla p_h^{\boldsymbol{\mu}}, \boldsymbol{v}\right)_{\mathcal{T}_h} + \left\langle \mathbf{S}\boldsymbol{u}_h^{\boldsymbol{\mu}}, \boldsymbol{v}\right\rangle_{\partial\Omega_D} + \left\langle \mathbf{S}\left(\boldsymbol{u}_h^{\boldsymbol{\mu}} - \boldsymbol{\mu}\right), \boldsymbol{v}\right\rangle_{\partial\mathcal{T}_h \backslash \partial\Omega_D} = 0, \quad \text{(B.11b)}$$

$$-\left(\boldsymbol{u}_h^{\boldsymbol{\mu}}, \nabla q\right)_{\mathcal{T}_h} + \left\langle \boldsymbol{\mu} \cdot \boldsymbol{n}, q - \overline{q}\right\rangle_{\partial\mathcal{T}_h \backslash \partial\Omega_D} + \left\langle \overline{p}_h^{\boldsymbol{\mu}}, \overline{q}\right\rangle_{\partial\mathcal{T}_h} = 0, \quad \text{(B.11c)}$$

for all $(\mathbf{G}, \boldsymbol{v}, q)$ in $\mathbf{G}_h \times \boldsymbol{V}_h \times Q_h$.

For $\beta \in \mathcal{P}_0(\partial\mathcal{T}_h)$, we define $\left(\mathbf{L}_h^\beta, \boldsymbol{u}_h^\beta, p_h^\beta\right)$ in $\mathbf{G}_h \times \boldsymbol{V}_h \times Q_h$ as the solution to

$$\mathrm{Re}\left(\mathbf{L}_h^\beta, \mathbf{G}\right)_{\mathcal{T}_h} + \left(\boldsymbol{u}_h^\beta, \nabla\cdot\mathbf{G}\right)_{\mathcal{T}_h} = 0, \tag{B.12a}$$

$$-\left(\nabla\cdot\mathbf{L}_h^\beta, \boldsymbol{v}\right)_{\mathcal{T}_h} + \left(\nabla p_h^\beta, \boldsymbol{v}\right)_{\mathcal{T}_h} + \left\langle \mathbf{S}\boldsymbol{u}_h^\beta, \boldsymbol{v}\right\rangle_{\partial\mathcal{T}_h} = 0, \tag{B.12b}$$

$$-\left(\boldsymbol{u}_h^\beta, \nabla q\right)_{\mathcal{T}_h} + \left\langle \overline{p}_h^\beta, \overline{q}\right\rangle_{\partial\mathcal{T}_h} - \langle\beta, \overline{q}\rangle_{\partial\mathcal{T}_h} = 0, \tag{B.12c}$$

for all $(\mathbf{G}, \boldsymbol{v}, q)$ in $\mathbf{G}_h \times \boldsymbol{V}_h \times Q_h$.

For $\boldsymbol{U} \in \widehat{\boldsymbol{V}}_h(\partial\Omega_D)$, we define $\left(\mathbf{L}_h^{\boldsymbol{U}}, \boldsymbol{u}_h^{\boldsymbol{U}}, p_h^{\boldsymbol{U}}\right)$ in $\mathbf{G}_h \times \boldsymbol{V}_h \times Q_h$ as the solution to

$$\mathrm{Re}\left(\mathbf{L}_h^{\boldsymbol{U}}, \mathbf{G}\right)_{\mathcal{T}_h} + \left(\boldsymbol{u}_h^{\boldsymbol{U}}, \nabla\cdot\mathbf{G}\right)_{\mathcal{T}_h} - \langle\boldsymbol{U}, \mathbf{G}\boldsymbol{n}\rangle_{\partial\Omega_D} = 0, \tag{B.13a}$$

$$\begin{aligned}-\left(\nabla\cdot\mathbf{L}_h^{\boldsymbol{U}}, \boldsymbol{v}\right)_{\mathcal{T}_h} + \left(\nabla p_h^{\boldsymbol{U}}, \boldsymbol{v}\right)_{\mathcal{T}_h} + \left\langle \mathbf{S}\boldsymbol{u}_h^{\boldsymbol{U}}, \boldsymbol{v}\right\rangle_{\partial\mathcal{T}_h\setminus\partial\Omega_D} \\ + \left\langle \mathbf{S}\left(\boldsymbol{u}_h^{\boldsymbol{U}} - \boldsymbol{U}\right), \boldsymbol{v}\right\rangle_{\partial\Omega_D} = 0,\end{aligned} \tag{B.13b}$$

$$-\left(\boldsymbol{u}_h^{\boldsymbol{U}}, \nabla q\right)_{\mathcal{T}_h} + \langle\boldsymbol{U}\cdot\boldsymbol{n}, q\rangle_{\partial\Omega_D} + \left\langle \overline{p}_h^{\boldsymbol{U}}, \overline{q}\right\rangle_{\partial\mathcal{T}_h} = 0, \tag{B.13c}$$

for all $(\mathbf{G}, \boldsymbol{v}, q)$ in $\mathbf{G}_h \times \boldsymbol{V}_h \times Q_h$.

For $\boldsymbol{g} \in L^2(\Omega)$, we define $(\mathbf{L}_h^{\boldsymbol{g}}, \boldsymbol{u}_h^{\boldsymbol{g}}, p_h^{\boldsymbol{g}})$ in $\mathbf{G}_h \times \boldsymbol{V}_h \times Q_h$ as the solution to

$$\mathrm{Re}\left(\mathbf{L}_h^{\boldsymbol{g}}, \mathbf{G}\right)_{\mathcal{T}_h} + \left(\boldsymbol{u}_h^{\boldsymbol{g}}, \nabla\cdot\mathbf{G}\right)_{\mathcal{T}_h} = 0, \tag{B.14a}$$

$$-\left(\nabla\cdot\mathbf{L}_h^{\boldsymbol{g}}, \boldsymbol{v}\right)_{\mathcal{T}_h} + \left(\nabla p_h^{\boldsymbol{g}}, \boldsymbol{v}\right)_{\mathcal{T}_h} + \left\langle \mathbf{S}\boldsymbol{u}_h^{\boldsymbol{g}}, \boldsymbol{v}\right\rangle_{\partial\mathcal{T}_h} = \left(\boldsymbol{g}, \boldsymbol{v}\right)_{\mathcal{T}_h}, \tag{B.14b}$$

$$-\left(\boldsymbol{u}_h^{\boldsymbol{g}}, \nabla q\right)_{\mathcal{T}_h} + \left\langle \overline{p}_h^{\boldsymbol{g}}, \overline{q}\right\rangle_{\partial\mathcal{T}_h} = 0, \tag{B.14c}$$

for all $(\mathbf{G}, \boldsymbol{v}, q)$ in $\mathbf{G}_h \times \boldsymbol{V}_h \times Q_h$.

The local solvers (B.11) – (B.14) can be shown to be well-posed in an identical manner to how the well-posedness of the local solver of Formulation 2.3 is shown in Chapter 2.

At this point, we are in a position to state the main result.

Theorem B.2. *(characterization of condensed global system for Formulation 2.3) The combined jump condition and Neumann boundary condition* (2.40d) *with the additional condition* (2.40e) *can be written as*

$$a\left(\widehat{\boldsymbol{u}}_h^i, \widehat{\boldsymbol{v}}\right) + b\left(\widehat{\boldsymbol{v}}, \rho_h\right) = l_1\left(\widehat{\boldsymbol{v}}\right), \tag{B.15a}$$

$$-b\left(\widehat{\boldsymbol{u}}_h^i, \psi\right) = l_2\left(\psi\right), \tag{B.15b}$$

where

$$\begin{aligned} a\left(\widehat{\boldsymbol{u}}_h^i, \widehat{\boldsymbol{v}}\right) := & \left(\mathrm{Re}\mathbf{L}_h^{\widehat{\boldsymbol{u}}_h^i}, \mathbf{L}_h^{\widehat{\boldsymbol{v}}}\right)_{\mathcal{T}_h} + \left\langle \mathbf{S}\boldsymbol{u}_h^{\widehat{\boldsymbol{u}}_h^i}, \boldsymbol{u}_h^{\widehat{\boldsymbol{v}}}\right\rangle_{\partial\Omega_D} \\ & + \left\langle \mathbf{S}\left(\boldsymbol{u}_h^{\widehat{\boldsymbol{u}}_h^i} - \widehat{\boldsymbol{u}}_h^i\right), \boldsymbol{u}_h^{\widehat{\boldsymbol{v}}} - \widehat{\boldsymbol{v}}\right\rangle_{\partial\mathcal{T}_h\setminus\partial\Omega_D}, \end{aligned} \tag{B.16}$$

$$b\left(\widehat{\boldsymbol{v}}, \psi\right) := -\left\langle \widehat{\boldsymbol{v}}\cdot\boldsymbol{n}, \psi\right\rangle_{\partial\mathcal{T}_h\setminus\partial\Omega_D}, \tag{B.17}$$

$$\begin{aligned} l_1\left(\widehat{\boldsymbol{v}}\right) := & -\left\langle \boldsymbol{f}_N, \widehat{\boldsymbol{v}}\right\rangle_{\partial\Omega_N}, + \left\langle -\mathbf{L}_h^{\widehat{\boldsymbol{u}}_h^D}\boldsymbol{n} + p_h^{\widehat{\boldsymbol{u}}_h^D}\boldsymbol{n} + \mathbf{S}\boldsymbol{u}_h^{\widehat{\boldsymbol{u}}_h^D}, \widehat{\boldsymbol{v}}\right\rangle_{\partial\mathcal{T}_h\setminus\partial\Omega_D} \\ & + \left\langle -\mathbf{L}_h^{\boldsymbol{f}}\boldsymbol{n} + p_h^{\boldsymbol{f}}\boldsymbol{n} + \mathbf{S}\boldsymbol{u}_h^{\boldsymbol{f}}, \widehat{\boldsymbol{v}}\right\rangle_{\partial\mathcal{T}_h\setminus\partial\Omega_D}, \end{aligned} \tag{B.18}$$

and

$$l_2\left(\psi\right) := -\left\langle \psi, \widehat{\boldsymbol{u}}_h^D\cdot\boldsymbol{n}\right\rangle_{\partial\Omega_D}. \tag{B.19}$$

Proof. Due to the linearity of the local solver (2.40a) – (2.40c) , we can decompose the volume solution to (2.40a) – (2.40c) as

$$\left(\mathbf{L}_h, \boldsymbol{u}_h, p_h\right) = \left(\mathbf{L}_h^{\widehat{\boldsymbol{u}}_h^i}, \boldsymbol{u}_h^{\widehat{\boldsymbol{u}}_h^i}, p_h^{\widehat{\boldsymbol{u}}_h^i}\right) + \left(\mathbf{L}_h^{\rho_h}, \boldsymbol{u}_h^{\rho_h}, p_h^{\rho_h}\right) \quad + \left(\mathbf{L}_h^{\widehat{\boldsymbol{u}}_h^D}, \boldsymbol{u}_h^{\widehat{\boldsymbol{u}}_h^D}, p_h^{\widehat{\boldsymbol{u}}_h^D}\right) + \left(\mathbf{L}_h^{\boldsymbol{f}}, \boldsymbol{u}_h^{\boldsymbol{f}}, p_h^{\boldsymbol{f}}\right).$$

That is, $\left(\mathbf{L}_h, \boldsymbol{u}_h, p_h\right)$ is the sum of the solutions to (B.11) – (B.14) with $\boldsymbol{\mu} = \widehat{\boldsymbol{u}}_h^i$, $\beta = \rho_h$, $\boldsymbol{U} = \widehat{\boldsymbol{u}}_h^D$, and $\boldsymbol{g} = \boldsymbol{f}$. Then, the combined jump and Neumann boundary

condition (2.40d) can be written as

$$
\begin{aligned}
&-\left\langle -\mathbf{L}_h^{\widehat{\boldsymbol{u}}_h^i}\boldsymbol{n}+p_h^{\widehat{\boldsymbol{u}}_h^i}\boldsymbol{n}+\mathbf{S}\left(\boldsymbol{u}_h^{\widehat{\boldsymbol{u}}_h^i}-\widehat{\boldsymbol{u}}_h^i\right),\widehat{\boldsymbol{v}}\right\rangle_{\partial\mathcal{T}_h\setminus\partial\Omega_D}\\
&\quad-\langle -\mathbf{L}_h^{\rho_h}\boldsymbol{n}+p_h^{\rho_h}\boldsymbol{n}+\mathbf{S}\boldsymbol{u}_h^{\rho_h},\widehat{\boldsymbol{v}}\rangle_{\partial\mathcal{T}_h\setminus\partial\Omega_D}-\left\langle -\mathbf{L}_h^{\widehat{\boldsymbol{u}}_h^D}\boldsymbol{n}+p_h^{\widehat{\boldsymbol{u}}_h^D}\boldsymbol{n}+\mathbf{S}\boldsymbol{u}_h^{\widehat{\boldsymbol{u}}_h^D},\widehat{\boldsymbol{v}}\right\rangle_{\partial\mathcal{T}_h\setminus\partial\Omega_D}\\
&\quad-\left\langle -\mathbf{L}_h^{\boldsymbol{f}}\boldsymbol{n}+p_h^{\boldsymbol{f}}\boldsymbol{n}+\mathbf{S}\boldsymbol{u}_h^{\boldsymbol{f}},\widehat{\boldsymbol{v}}\right\rangle_{\partial\mathcal{T}_h\setminus\partial\Omega_D}=-\langle \boldsymbol{f}_N,\widehat{\boldsymbol{v}}\rangle_{\partial\Omega_N}\,. \qquad \text{(B.20)}
\end{aligned}
$$

It remains to show that $-\left\langle -\mathbf{L}_h^{\widehat{\boldsymbol{u}}_h^i}\boldsymbol{n}+p_h^{\widehat{\boldsymbol{u}}_h^i}\boldsymbol{n}+\mathbf{S}\left(\boldsymbol{u}_h^{\widehat{\boldsymbol{u}}_h^i}-\widehat{\boldsymbol{u}}_h^i\right),\widehat{\boldsymbol{v}}\right\rangle_{\partial\mathcal{T}_h\setminus\partial\Omega_D}=a\left(\widehat{\boldsymbol{u}}_h^i,\widehat{\boldsymbol{v}}\right)$ as defined by (B.16) and that $-\langle -\mathbf{L}_h^{\rho_h}\boldsymbol{n}+p_h^{\rho_h}\boldsymbol{n}+\mathbf{S}\boldsymbol{u}_h^{\rho_h},\widehat{\boldsymbol{v}}\rangle_{\partial\mathcal{T}_h\setminus\partial\Omega_D}=b\left(\widehat{\boldsymbol{v}},\rho_h\right)$ as defined by (B.17).

Step 1: Taking q equal to a (nonzero) elementwise constant in (B.12c) gives

$$\overline{p}_h^{\beta}=\beta \qquad \text{(B.21)}$$

and

$$-\left(\boldsymbol{u}_h^{\beta},\nabla q\right)_{\mathcal{T}_h}=0. \qquad \text{(B.22)}$$

Then setting $(\mathbf{G},\boldsymbol{v},q)=\left(\mathbf{L}_h^{\beta},\boldsymbol{u}_h^{\beta},p_h^{\beta}\right)$ in (B.12a), (B.12b), and (B.22), we conclude by summing the results that

$$\left(\mathrm{Re}\mathbf{L}_h^{\beta},\mathbf{L}_h^{\beta}\right)_{\mathcal{T}_h}+\left\langle \mathbf{S}\boldsymbol{u}_h^{\beta},\boldsymbol{u}_h^{\beta}\right\rangle_{\partial\mathcal{T}_h}=0$$

and therefore that $\mathbf{L}_h^{\beta}=\mathbf{0}$, and $\boldsymbol{u}_h^{\beta}=\mathbf{0}$ on $\partial\mathcal{T}_h$. Integrating what remains of (B.12a) by parts, we conclude that $\boldsymbol{u}_h^{\beta}$ is elementwise constant and therefore zero. Then what remains of (B.12b) implies that p_h^{β} is elementwise constant, and therefore $p_h^{\beta}=\beta$. Summarizing, we have that for any β in $\mathcal{P}_0(\partial\mathcal{T}_h)$, that $\left(\mathbf{L}_h^{\beta},\boldsymbol{u}_h^{\beta},p_h^{\beta}\right)=(\mathbf{0},\mathbf{0},\beta)$. Therefore $-\langle -\mathbf{L}_h^{\rho_h}\boldsymbol{n}+p_h^{\rho_h}\boldsymbol{n}+\mathbf{S}\boldsymbol{u}_h^{\rho_h},\widehat{\boldsymbol{v}}\rangle_{\partial\mathcal{T}_h\setminus\partial\Omega_D}=b\left(\rho_h,\widehat{\boldsymbol{v}}\right)$.

Step 2: Taking q equal to a (nonzero) constant in (B.11c) gives

$$\overline{p}_h^{\boldsymbol{\mu}}=0 \qquad \text{(B.23)}$$

and

$$-\left(\boldsymbol{u}_h^{\boldsymbol{\mu}}, \nabla q\right)_{\mathcal{T}_h} + \left\langle \boldsymbol{\mu}\cdot\boldsymbol{n}, q-\overline{q}\right\rangle_{\partial\mathcal{T}_h\backslash\partial\Omega_D} = 0. \tag{B.24}$$

In (B.11a) take $\boldsymbol{\mu} = \widehat{\boldsymbol{v}}$ and $\mathbf{G} = \mathbf{L}_h^{\widehat{\boldsymbol{u}}_h^i}$, in (B.11b) take $\boldsymbol{\mu} = \widehat{\boldsymbol{u}}_h^i$ and $\boldsymbol{v} = \boldsymbol{u}_h^{\widehat{\boldsymbol{v}}}$, and in (B.24) take $\boldsymbol{\mu} = \widehat{\boldsymbol{v}}$ and $q = p_h^{\widehat{\boldsymbol{u}}_h^i}$. Summing the result, and recalling (B.23), we have

$$\begin{aligned}\left(\mathrm{Re}\mathbf{L}_h^{\widehat{\boldsymbol{u}}_h^i}, \mathbf{L}_h^{\widehat{\boldsymbol{v}}}\right)_{\mathcal{T}_h} + \left\langle \mathbf{S}\boldsymbol{u}_h^{\widehat{\boldsymbol{u}}_h^i}, \boldsymbol{u}_h^{\widehat{\boldsymbol{v}}}\right\rangle_{\partial\Omega_D} + \left\langle \mathbf{S}\left(\boldsymbol{u}_h^{\widehat{\boldsymbol{u}}_h^i} - \widehat{\boldsymbol{u}}_h^i\right), \boldsymbol{u}_h^{\widehat{\boldsymbol{v}}}\right\rangle_{\partial\mathcal{T}_h\backslash\partial\Omega_D} \\ - \left\langle \mathbf{L}_h^{\widehat{\boldsymbol{u}}_h^i}\boldsymbol{n}, \widehat{\boldsymbol{v}}\right\rangle_{\partial\mathcal{T}_h\backslash\partial\Omega_D} + \left\langle p_h^{\widehat{\boldsymbol{u}}_h^i}, \widehat{\boldsymbol{v}}\cdot\boldsymbol{n}\right\rangle_{\partial\mathcal{T}_h\backslash\partial\Omega_D} = 0.\end{aligned} \tag{B.25}$$

Therefore,

$$\left\langle \mathbf{L}_h^{\widehat{\boldsymbol{u}}_h^i}\boldsymbol{n}, \widehat{\boldsymbol{v}}\right\rangle_{\partial\mathcal{T}_h\backslash\partial\Omega_D} - \left\langle p_h^{\widehat{\boldsymbol{u}}_h^i}, \widehat{\boldsymbol{v}}\cdot\boldsymbol{n}\right\rangle_{\partial\mathcal{T}_h\backslash\partial\Omega_D} - \left\langle \mathbf{S}\left(\boldsymbol{u}_h^{\widehat{\boldsymbol{u}}_h^i} - \widehat{\boldsymbol{u}}_h^i\right), \widehat{\boldsymbol{v}}\right\rangle_{\partial\mathcal{T}_h\backslash\partial\Omega_D} = a\left(\widehat{\boldsymbol{u}}_h^i, \widehat{\boldsymbol{v}}\right).$$

□

We can conclude from Theorem B.2 that the condensed global system will take the form

$$\begin{bmatrix} A & B^\top \\ -B & 0 \end{bmatrix}\begin{Bmatrix} \widehat{U} \\ \rho \end{Bmatrix} = \begin{Bmatrix} F_1 \\ F_2 \end{Bmatrix}.$$

Inspecting (B.16), we can see that the block matrix A is symmetric and positive semi-definite. We can further claim that A is positive definite. To claim this we must show $a\left(\widehat{\boldsymbol{u}}_h^i, \widehat{\boldsymbol{u}}_h^i\right) = 0 \Rightarrow \widehat{\boldsymbol{u}}_h^i = \mathbf{0}$. Indeed, $a\left(\widehat{\boldsymbol{u}}_h^i, \widehat{\boldsymbol{u}}_h^i\right) = 0$ implies $\mathbf{L}_h^{\widehat{\boldsymbol{u}}_h^i} = \mathbf{0}$, $\boldsymbol{u}_h^{\widehat{\boldsymbol{u}}_h^i} = 0$ on $\partial\Omega_D$, and $\boldsymbol{u}_h^{\widehat{\boldsymbol{u}}_h^i} = \widehat{\boldsymbol{u}}_h^i$ on $\mathcal{E}_h\backslash\partial\Omega_D$. Then, with $\boldsymbol{\mu} = \widehat{\boldsymbol{u}}_h^i$ in (B.11a), integrating by parts reveals that $\boldsymbol{u}_h^{\widehat{\boldsymbol{u}}_h^i}$ is elementwise constant, and therefore globally constant since $\boldsymbol{u}_h^{\widehat{\boldsymbol{u}}_h^i} = \widehat{\boldsymbol{u}}_h^i$ on $\mathcal{E}_h\backslash\partial\Omega_D$. Since $\partial\Omega_D \neq \emptyset$, then $\boldsymbol{u}_h^{\widehat{\boldsymbol{u}}_h^{i,k}} = 0$ and therefore $\widehat{\boldsymbol{u}}_h^i = 0$.

B.3 Characterization of Formulation 2.4

In the following, we characterize the statically condensed global system of the Stokes HDG scheme Formulation 2.4, which uses the $(\widehat{\boldsymbol{u}}_h^t, \widehat{f}_h)$ flux (2.18). The following characterization sheds light on the matrix system associated with this formulation.

Toward this goal, we define the following local solvers, where

$$f_h^{\widehat{\boldsymbol{u}}_h^{t,i}} := -\boldsymbol{n}\cdot\mathbf{L}_h^{\widehat{\boldsymbol{u}}_h^{t,i}}\boldsymbol{n} + p_h^{\widehat{\boldsymbol{u}}_h^{t,i}}\boldsymbol{n},$$

$$f_h^{\boldsymbol{\mu}} := -\boldsymbol{n}\cdot\mathbf{L}_h^{\boldsymbol{\mu}}\boldsymbol{n} + p_h^{\boldsymbol{\mu}}\boldsymbol{n},$$

etc.

For $\boldsymbol{\mu}\in\widehat{\boldsymbol{V}}_h^{t,i}$, we define $(\mathbf{L}_h^{\boldsymbol{\mu}},\boldsymbol{u}_h^{\boldsymbol{\mu}},p_h^{\boldsymbol{\mu}})$ in $\mathbf{G}_h\times\boldsymbol{V}_h\times Q_h$ as the solution to

$$\begin{aligned}
&\mathrm{Re}\,(\mathbf{L}_h^{\boldsymbol{\mu}},\mathbf{G})_{\mathcal{T}_h} - (\nabla\boldsymbol{u}_h^{\boldsymbol{\mu}},\mathbf{G})_{\mathcal{T}_h} + \langle\mathbf{T}\boldsymbol{u}_h^{\boldsymbol{\mu}},\mathbf{G}\boldsymbol{n}\rangle_{\partial\Omega_D}\\
&\quad+\langle\mathbf{T}\boldsymbol{u}_h^{\boldsymbol{\mu}}-\boldsymbol{\mu},\mathbf{G}\boldsymbol{n}\rangle_{\partial\mathcal{T}_h\backslash\partial\Omega_D} + \left\langle\frac{1}{\tau_n}f_h^{\boldsymbol{\mu}},-\boldsymbol{n}\cdot\mathbf{G}\boldsymbol{n}\right\rangle_{\partial\mathcal{T}_h} = 0, \qquad \text{(B.26a)}\\
&(\mathbf{L}_h^{\boldsymbol{\mu}},\nabla\boldsymbol{v})_{\mathcal{T}_h} - (p_h^{\boldsymbol{\mu}},\nabla\cdot\boldsymbol{v})_{\mathcal{T}_h} + \left\langle-\mathbf{L}_h^{\boldsymbol{\mu}}\boldsymbol{n}+\tau_t\mathbf{T}\boldsymbol{u}_h^{\boldsymbol{\mu}},\boldsymbol{v}^t\right\rangle_{\partial\Omega_D}\\
&\quad+\left\langle-\mathbf{L}_h^{\boldsymbol{\mu}}\boldsymbol{n}+\tau_t\left(\mathbf{T}\boldsymbol{u}_h^{\boldsymbol{\mu}}-\boldsymbol{\mu}\right),\boldsymbol{v}^t\right\rangle_{\partial\mathcal{T}_h\backslash\partial\Omega_D} = 0, \qquad \text{(B.26b)}\\
&(\nabla\cdot\boldsymbol{u}_h^{\boldsymbol{\mu}},q)_{\mathcal{T}_h} + \left\langle\frac{1}{\tau_n}f_h^{\boldsymbol{\mu}},q\right\rangle_{\partial\mathcal{T}_h} = 0, \qquad \text{(B.26c)}
\end{aligned}$$

for all $(\mathbf{G},\boldsymbol{v},q)$ in $\mathbf{G}_h\times\boldsymbol{V}_h\times Q_h$.

For $\gamma\in\widehat{F}_h^i$, we define $(\mathbf{L}_h^{\gamma},\boldsymbol{u}_h^{\gamma},p_h^{\gamma})$ in $\mathbf{G}_h\times\boldsymbol{V}_h\times Q_h$ as the solution to

$$\begin{aligned}
&\mathrm{Re}\,(\mathbf{L}_h^{\gamma},\mathbf{G})_{\mathcal{T}_h} - (\nabla\boldsymbol{u}_h^{\gamma},\mathbf{G})_{\mathcal{T}_h} + \langle\mathbf{T}\boldsymbol{u}_h^{\gamma},\mathbf{G}\boldsymbol{n}\rangle_{\partial\mathcal{T}_h}\\
&+\left\langle\frac{1}{\tau_n}\left(f_h^{\gamma}-\gamma\right),-\boldsymbol{n}\cdot\mathbf{G}\boldsymbol{n}\right\rangle_{\partial\mathcal{T}_h\backslash\partial\Omega_N} + \left\langle\frac{1}{\tau_n}f_h^{\gamma},-\boldsymbol{n}\cdot\mathbf{G}\boldsymbol{n}\right\rangle_{\partial\Omega_N} = 0, \qquad \text{(B.27a)}\\
&(\mathbf{L}_h^{\gamma},\nabla\boldsymbol{v})_{\mathcal{T}_h} - (p_h^{\gamma},\nabla\cdot\boldsymbol{v})_{\mathcal{T}_h}\\
&\quad+\left\langle-\mathbf{L}_h^{\gamma}\boldsymbol{n}+\tau_t\mathbf{T}\boldsymbol{u}_h^{\gamma},\boldsymbol{v}^t\right\rangle_{\partial\mathcal{T}_h} + \langle\gamma,\boldsymbol{v}\cdot\boldsymbol{n}\rangle_{\partial\mathcal{T}_h\backslash\partial\Omega_N} = 0, \qquad \text{(B.27b)}\\
&(\nabla\cdot\boldsymbol{u}_h^{\gamma},q)_{\mathcal{T}_h} + \left\langle\frac{1}{\tau_n}\left(f_h^{\gamma}-\gamma\right),q\right\rangle_{\partial\mathcal{T}_h\backslash\partial\Omega_N} + \left\langle\frac{1}{\tau_n}f_h^{\gamma},q\right\rangle_{\partial\Omega_N} = 0, \qquad \text{(B.27c)}
\end{aligned}$$

for all $(\mathbf{G},\boldsymbol{v},q)$ in $\mathbf{G}_h\times\boldsymbol{V}_h\times Q_h$.

For $\boldsymbol{U}\in\widehat{\boldsymbol{V}}_h^{t}(\partial\Omega_D)$, we define $\left(\mathbf{L}_h^{\boldsymbol{U}},\boldsymbol{u}_h^{\boldsymbol{U}},p_h^{\boldsymbol{U}}\right)$ in $\mathbf{G}_h\times\boldsymbol{V}_h\times Q_h$ as the solution

to

$$\begin{aligned}
\operatorname{Re}\left(\mathbf{L}_h^{\boldsymbol{U}}, \mathbf{G}\right)_{\mathcal{T}_h} - \left(\nabla \boldsymbol{u}_h^{\boldsymbol{U}}, \mathbf{G}\right)_{\mathcal{T}_h} + \left\langle \mathbf{T}\boldsymbol{u}_h^{\boldsymbol{U}}, \mathbf{G}\boldsymbol{n}\right\rangle_{\partial\mathcal{T}_h\setminus\partial\Omega_D} \\
+ \left\langle \mathbf{T}\boldsymbol{u}_h^{\boldsymbol{U}} - \boldsymbol{U}, \mathbf{G}\boldsymbol{n}\right\rangle_{\partial\Omega_D} + \left\langle \frac{1}{\tau_n} f_h^{\boldsymbol{U}}, -\boldsymbol{n}\cdot\mathbf{G}\boldsymbol{n}\right\rangle_{\partial\mathcal{T}_h} = 0, \qquad \text{(B.28a)} \\
\left(\mathbf{L}_h^{\boldsymbol{U}}, \nabla\boldsymbol{v}\right)_{\mathcal{T}_h} - \left(p_h^{\boldsymbol{U}}, \nabla\cdot\boldsymbol{v}\right)_{\mathcal{T}_h} + \left\langle -\mathbf{L}_h^{\boldsymbol{U}}\boldsymbol{n} + \tau_t \mathbf{T}\boldsymbol{u}_h^{\boldsymbol{U}}, \boldsymbol{v}^t\right\rangle_{\partial\mathcal{T}_h\setminus\partial\Omega_D} \\
+ \left\langle -\mathbf{L}_h^{\boldsymbol{U}}\boldsymbol{n} + \tau_t\left(\mathbf{T}\boldsymbol{u}_h^{\boldsymbol{U}} - \boldsymbol{U}\right), \boldsymbol{v}^t\right\rangle_{\partial\Omega_D} = 0, \qquad \text{(B.28b)} \\
\left(\nabla\cdot\boldsymbol{u}_h^{\boldsymbol{U}}, q\right)_{\mathcal{T}_h} + \left\langle \frac{1}{\tau_n} f_h^{\boldsymbol{U}}, q\right\rangle_{\partial\mathcal{T}_h} = 0, \qquad \text{(B.28c)}
\end{aligned}$$

for all $(\mathbf{G}, \boldsymbol{v}, q)$ in $\mathbf{G}_h \times \boldsymbol{V}_h \times Q_h$.

For $F \in \widehat{F}_h(\partial\Omega_N)$, we define $\left(\mathbf{L}_h^F, \boldsymbol{u}_h^F, p_h^F\right)$ in $\mathbf{G}_h \times \boldsymbol{V}_h \times Q_h$ as the solution to

$$\begin{aligned}
\operatorname{Re}\left(\mathbf{L}_h^F, \mathbf{G}\right)_{\mathcal{T}_h} - \left(\nabla \boldsymbol{u}_h^F, \mathbf{G}\right)_{\mathcal{T}_h} + \left\langle \mathbf{T}\boldsymbol{u}_h^F, \mathbf{G}\boldsymbol{n}\right\rangle_{\partial\mathcal{T}_h} \\
+ \left\langle \frac{1}{\tau_n} f_h^F, -\boldsymbol{n}\cdot\mathbf{G}\boldsymbol{n}\right\rangle_{\partial\mathcal{T}_h\setminus\partial\Omega_N} + \left\langle \frac{1}{\tau_n}\left(f_h^F - F\right), -\boldsymbol{n}\cdot\mathbf{G}\boldsymbol{n}\right\rangle_{\partial\Omega_N} = 0, \qquad \text{(B.29a)} \\
\left(\mathbf{L}_h^F, \nabla\boldsymbol{v}\right)_{\mathcal{T}_h} - \left(p_h^F, \nabla\cdot\boldsymbol{v}\right)_{\mathcal{T}_h} \\
+ \left\langle -\mathbf{L}_h^F\boldsymbol{n} + \tau_t\mathbf{T}\boldsymbol{u}_h^F, \boldsymbol{v}^t\right\rangle_{\partial\mathcal{T}_h} + \left\langle F, \boldsymbol{v}\cdot\boldsymbol{n}\right\rangle_{\partial\Omega_N} = 0, \qquad \text{(B.29b)} \\
\left(\nabla\cdot\boldsymbol{u}_h^F, q\right)_{\mathcal{T}_h} + \left\langle \frac{1}{\tau_n} f_h^F, q\right\rangle_{\partial\mathcal{T}_h\setminus\partial\Omega_N} + \left\langle \frac{1}{\tau_n}\left(f_h^F - F\right), q\right\rangle_{\partial\Omega_N} = 0, \qquad \text{(B.29c)}
\end{aligned}$$

for all $(\mathbf{G}, \boldsymbol{v}, q)$ in $\mathbf{G}_h \times \boldsymbol{V}_h \times Q_h$.

For $\boldsymbol{g} \in L^2(\Omega)$, we define $(\mathbf{L}_h^{\boldsymbol{g}}, \boldsymbol{u}_h^{\boldsymbol{g}}, p_h^{\boldsymbol{g}})$ in $\mathbf{G}_h \times \boldsymbol{V}_h \times Q_h$ as the solution to

$$\begin{aligned}
\operatorname{Re}\left(\mathbf{L}_h^{\boldsymbol{g}}, \mathbf{G}\right)_{\mathcal{T}_h} - \left(\nabla \boldsymbol{u}_h^{\boldsymbol{g}}, \mathbf{G}\right)_{\mathcal{T}_h} + \left\langle \mathbf{T}\boldsymbol{u}_h^{\boldsymbol{g}}, \mathbf{G}\boldsymbol{n}\right\rangle_{\partial\mathcal{T}_h} + \left\langle \frac{1}{\tau_n} f_h^{\boldsymbol{g}}, -\boldsymbol{n}\cdot\mathbf{G}\boldsymbol{n}\right\rangle_{\partial\mathcal{T}_h} = 0 \qquad \text{(B.30a)} \\
\left(\mathbf{L}_h^{\boldsymbol{g}}, \nabla\boldsymbol{v}\right)_{\mathcal{T}_h} - \left(p_h^{\boldsymbol{g}}, \nabla\cdot\boldsymbol{v}\right)_{\mathcal{T}_h} + \left\langle -\mathbf{L}_h^{\boldsymbol{g}}\boldsymbol{n} + \tau_t\mathbf{T}\boldsymbol{u}_h^{\boldsymbol{g}}, \boldsymbol{v}^t\right\rangle_{\partial\mathcal{T}_h} = \left(\boldsymbol{g}, \boldsymbol{v}\right)_{\mathcal{T}_h} \qquad \text{(B.30b)} \\
\left(\nabla\cdot\boldsymbol{u}_h^{\boldsymbol{g}}, q\right)_{\mathcal{T}_h} + \left\langle \frac{1}{\tau_n} f_h^{\boldsymbol{g}}, q\right\rangle_{\partial\mathcal{T}_h} = 0, \qquad \text{(B.30c)}
\end{aligned}$$

for all $(\mathbf{G}, \boldsymbol{v}, q)$ in $\mathbf{G}_h \times \boldsymbol{V}_h \times Q_h$.

The local solvers (B.26) – (B.30) can be shown to be well-posed in an identical manner to how the well-posedness of the local solver of Formulation 2.4 is shown in Chapter 2.

At this point, we are in a position to state the main result.

Theorem B.3. *(characterization of condensed global system for Formulation 2.4) The jump conditions* (2.54d) – (2.54e) *can be written as*

$$a\left(\widehat{\boldsymbol{u}}_h^{t,i},\widehat{\boldsymbol{v}}^t\right)+b\left(\widehat{\boldsymbol{v}}^t,\widehat{f}_h^i\right)=l_1\left(\widehat{\boldsymbol{v}}^t\right), \tag{B.31a}$$

$$-b\left(\widehat{\boldsymbol{u}}_h^{t,i},\widehat{g}\right)+d\left(\widehat{f}_h^i,\widehat{g}\right)=l_2\left(\widehat{g}\right), \tag{B.31b}$$

where

$$\begin{aligned}a\left(\widehat{\boldsymbol{u}}_h^{t,i},\widehat{\boldsymbol{v}}^t\right):=&\left(\mathrm{Re}\mathbf{L}_h^{\widehat{\boldsymbol{u}}_h^{t,i}},\mathbf{L}_h^{\widehat{\boldsymbol{v}}^t}\right)_{\mathcal{T}_h}+\left\langle\tau_t\left(\mathbf{T}\boldsymbol{u}_h^{\widehat{\boldsymbol{u}}_h^{t,i}}-\widehat{\boldsymbol{u}}_h^{t,i}\right),\mathbf{T}\boldsymbol{u}_h^{\widehat{\boldsymbol{v}}^t}-\widehat{\boldsymbol{v}}^t\right\rangle_{\partial\mathcal{T}_h\backslash\partial\Omega_D}\\&+\left\langle\frac{1}{\tau_n}f_h^{\widehat{\boldsymbol{u}}_h^{t,i}},f_h^{\widehat{\boldsymbol{v}}^t}\right\rangle_{\partial\mathcal{T}_h}+\left\langle\tau_t\mathbf{T}\boldsymbol{u}_h^{\widehat{\boldsymbol{u}}_h^{t,i}},\mathbf{T}\boldsymbol{u}_h^{\widehat{\boldsymbol{v}}^t}\right\rangle_{\partial\Omega_D},\end{aligned} \tag{B.32}$$

$$\begin{aligned}d\left(\widehat{f}_h^i,\widehat{g}\right):=&\left(\mathrm{Re}\mathbf{L}_h^{\widehat{f}_h^i},\mathbf{L}_h^{\widehat{g}}\right)_{\mathcal{T}_h}+\left\langle\tau_t\mathbf{T}\boldsymbol{u}_h^{\widehat{f}_h^i},\mathbf{T}\boldsymbol{u}_h^{\widehat{g}}\right\rangle_{\partial\mathcal{T}_h}\\&+\left\langle\frac{1}{\tau_n}\left(f_h^{\widehat{f}_h^i}-\widehat{f}_h^i\right),f_h^{\widehat{g}}-\widehat{g}\right\rangle_{\partial\mathcal{T}_h\backslash\partial\Omega_N}+\left\langle\frac{1}{\tau_n}f_h^{\widehat{f}_h^i},f_h^{\widehat{g}}\right\rangle_{\partial\Omega_N},\end{aligned} \tag{B.33}$$

$$\begin{aligned}b\left(\widehat{\boldsymbol{v}}^t,\widehat{g}\right):=&\left(\mathrm{Re}\mathbf{L}_h^{\widehat{\boldsymbol{v}}^t},\mathbf{L}_h^{\widehat{g}}\right)_{\mathcal{T}_h}-\left(\nabla\boldsymbol{u}_h^{\widehat{\boldsymbol{v}}^t},\mathbf{L}_h^{\widehat{g}}\right)_{\mathcal{T}_h}-\left(\mathbf{L}_h^{\widehat{\boldsymbol{v}}^t},\nabla\boldsymbol{u}_h^{\widehat{g}}\right)_{\mathcal{T}_h}+\left(p_h^{\widehat{\boldsymbol{v}}^t},\nabla\cdot\boldsymbol{u}_h^{\widehat{g}}\right)_{\mathcal{T}_h}\\&+\left(\nabla\cdot\boldsymbol{u}_h^{\widehat{\boldsymbol{v}}^t},p_h^{\widehat{g}}\right)_{\mathcal{T}_h}+\left\langle\mathbf{T}\boldsymbol{u}_h^{\widehat{\boldsymbol{v}}^t},\mathbf{L}_h^{\widehat{g}}\boldsymbol{n}\right\rangle_{\partial\mathcal{T}_h}+\left\langle\mathbf{L}_h^{\widehat{\boldsymbol{v}}^t}\boldsymbol{n},\mathbf{T}\boldsymbol{u}_h^{\widehat{g}}\right\rangle_{\partial\mathcal{T}_h}\\&-\left\langle\tau_t\mathbf{T}\boldsymbol{u}_h^{\widehat{\boldsymbol{v}}^t},\mathbf{T}\boldsymbol{u}_h^{\widehat{g}}\right\rangle_{\partial\mathcal{T}_h}+\left\langle\frac{1}{\tau_n}f_h^{\widehat{\boldsymbol{v}}^t},f_h^{\widehat{g}}\right\rangle_{\partial\mathcal{T}_h},\end{aligned} \tag{B.34}$$

$$\begin{aligned}l_1\left(\widehat{\boldsymbol{v}}^t\right):=&-\left\langle\mathbf{T}\boldsymbol{f}_N,\widehat{\boldsymbol{v}}^t\right\rangle_{\partial\Omega_N}+\left\langle-\mathbf{L}_h^{\widehat{\boldsymbol{u}}_h^D}\boldsymbol{n}+\tau_t\mathbf{T}\boldsymbol{u}_h^{\widehat{\boldsymbol{u}}_h^D},\widehat{\boldsymbol{v}}^t\right\rangle_{\partial\mathcal{T}_h\backslash\partial\Omega_D}\\&+\left\langle-\mathbf{L}_h^{\widehat{f}_h^N}\boldsymbol{n}+\tau_t\mathbf{T}\boldsymbol{u}_h^{\widehat{f}_h^N},\widehat{\boldsymbol{v}}^t\right\rangle_{\partial\mathcal{T}_h\backslash\partial\Omega_D}+\left\langle-\mathbf{L}_h^{\boldsymbol{f}}\boldsymbol{n}+\tau_t\mathbf{T}\boldsymbol{u}_h^{\boldsymbol{f}},\widehat{\boldsymbol{v}}^t\right\rangle_{\partial\mathcal{T}_h\backslash\partial\Omega_D},\end{aligned} \tag{B.35}$$

and

$$\begin{aligned}l_2\left(\widehat{g}\right):=&-\left\langle\boldsymbol{u}_D\cdot\boldsymbol{n},\widehat{g}\right\rangle_{\partial\Omega_D}+\left\langle\boldsymbol{u}_h^{\widehat{\boldsymbol{u}}_h^D}\cdot\boldsymbol{n}+\frac{1}{\tau_n}f_h^{\widehat{\boldsymbol{u}}_h^D},\widehat{g}\right\rangle_{\partial\mathcal{T}_h\backslash\partial\Omega_N}\\&+\left\langle\boldsymbol{u}_h^{\widehat{f}_h^N}\cdot\boldsymbol{n}+\frac{1}{\tau_n}f_h^{\widehat{f}_h^N},\widehat{g}\right\rangle_{\partial\mathcal{T}_h\backslash\partial\Omega_N}+\left\langle\boldsymbol{u}_h^{\boldsymbol{f}}\cdot\boldsymbol{n}+\frac{1}{\tau_n}f_h^{\boldsymbol{f}},\widehat{g}\right\rangle_{\partial\mathcal{T}_h\backslash\partial\Omega_N}.\end{aligned} \tag{B.36}$$

Proof. Due to the linearity of the local solver (2.54a) – (2.54c) , we can decompose the volume solution to (2.54a) – (2.54c) as

$$
\begin{aligned}
(\mathbf{L}_h, \boldsymbol{u}_h, p_h) = &\left(\mathbf{L}_h^{\widehat{\boldsymbol{u}}_h^{t,i}}, \boldsymbol{u}_h^{\widehat{\boldsymbol{u}}_h^{t,i}}, p_h^{\widehat{\boldsymbol{u}}_h^{t,i}}\right) + \left(\mathbf{L}_h^{\widehat{f}_h^i}, \boldsymbol{u}_h^{\widehat{f}_h^i}, p_h^{\widehat{f}_h^i}\right) \\
&+ \left(\mathbf{L}_h^{\widehat{\boldsymbol{u}}_h^D}, \boldsymbol{u}_h^{\widehat{\boldsymbol{u}}_h^D}, p_h^{\widehat{\boldsymbol{u}}_h^D}\right) + \left(\mathbf{L}_h^{\widehat{f}_h^N}, \boldsymbol{u}_h^{\widehat{f}_h^N}, p_h^{\widehat{f}_h^N}\right) + \left(\mathbf{L}_h^{\boldsymbol{f}}, \boldsymbol{u}_h^{\boldsymbol{f}}, p_h^{\boldsymbol{f}}\right).
\end{aligned}
$$

That is, it is the sum of the solutions to (B.26) – (B.30) with $\boldsymbol{\mu} = \widehat{\boldsymbol{u}}_h^{t,i}$, $\gamma = \widehat{f}_h^i$, $\boldsymbol{U} = \widehat{\boldsymbol{u}}_h^{t,D}$, $F = \widehat{f}_h^N$, and $\boldsymbol{g} = \boldsymbol{f}$. Then, the jump conditions and partial boundary condition imposition (2.54d) – (2.54e) can be written as

$$
\begin{aligned}
&-\left\langle -\mathbf{L}_h^{\widehat{\boldsymbol{u}}_h^{t,i}}\boldsymbol{n} + \tau_t\left(\mathbf{T}\boldsymbol{u}_h^{\widehat{\boldsymbol{u}}_h^{t,i}} - \widehat{\boldsymbol{u}}_h^{t,i}\right), \widehat{\boldsymbol{v}}^t\right\rangle_{\partial\mathcal{T}_h\setminus\partial\Omega_D} - \left\langle \boldsymbol{u}_h^{\widehat{\boldsymbol{u}}_h^{t,i}}\cdot\boldsymbol{n} + \frac{1}{\tau_n} f_h^{\widehat{\boldsymbol{u}}_h^{t,i}}, \widehat{g}\right\rangle_{\partial\mathcal{T}_h\setminus\partial\Omega_N} \\
&- \left\langle -\mathbf{L}_h^{\widehat{f}_h^i}\boldsymbol{n} + \tau_t\mathbf{T}\boldsymbol{u}_h^{\widehat{f}_h^i}, \widehat{\boldsymbol{v}}^t\right\rangle_{\partial\mathcal{T}_h\setminus\partial\Omega_D} - \left\langle \boldsymbol{u}_h^{\widehat{f}_h^i}\cdot\boldsymbol{n} + \frac{1}{\tau_n}\left(f_h^{\widehat{f}_h^i} - \widehat{f}_h^i\right), \widehat{g}\right\rangle_{\partial\mathcal{T}_h\setminus\partial\Omega_N} \\
&- \left\langle -\mathbf{L}_h^{\widehat{\boldsymbol{u}}_h^D}\boldsymbol{n} + \tau_t\mathbf{T}\boldsymbol{u}_h^{\widehat{\boldsymbol{u}}_h^D}, \widehat{\boldsymbol{v}}^t\right\rangle_{\partial\mathcal{T}_h\setminus\partial\Omega_D} - \left\langle \boldsymbol{u}_h^{\widehat{\boldsymbol{u}}_h^D}\cdot\boldsymbol{n} + \frac{1}{\tau_n} f_h^{\widehat{\boldsymbol{u}}_h^D}, \widehat{g}\right\rangle_{\partial\mathcal{T}_h\setminus\partial\Omega_N} \\
&- \left\langle -\mathbf{L}_h^{\widehat{f}_h^N}\boldsymbol{n} + \tau_t\mathbf{T}\boldsymbol{u}_h^{\widehat{f}_h^N}, \widehat{\boldsymbol{v}}^t\right\rangle_{\partial\mathcal{T}_h\setminus\partial\Omega_D} - \left\langle \boldsymbol{u}_h^{\widehat{f}_h^N}\cdot\boldsymbol{n} + \frac{1}{\tau_n} f_h^{\widehat{f}_h^N}, \widehat{g}\right\rangle_{\partial\mathcal{T}_h\setminus\partial\Omega_N} \\
&- \left\langle -\mathbf{L}_h^{\boldsymbol{f}}\boldsymbol{n} + \tau_t\mathbf{T}\boldsymbol{u}_h^{\boldsymbol{f}}, \widehat{\boldsymbol{v}}^t\right\rangle_{\partial\mathcal{T}_h\setminus\partial\Omega_D} - \left\langle \boldsymbol{u}_h^{\boldsymbol{f}}\cdot\boldsymbol{n} + \frac{1}{\tau_n} f_h^{\boldsymbol{f}}, \widehat{g}\right\rangle_{\partial\mathcal{T}_h\setminus\partial\Omega_N} \\
&= -\left\langle \mathbf{T}\boldsymbol{f}_N, \widehat{\boldsymbol{v}}^t\right\rangle_{\partial\Omega_N} - \left\langle \boldsymbol{u}_D\cdot\boldsymbol{n}, \widehat{g}\right\rangle_{\partial\Omega_D}.
\end{aligned}
$$

It remains to show that $-\left\langle -\mathbf{L}_h^{\widehat{\boldsymbol{u}}_h^{t,i}}\boldsymbol{n} + \tau_t\left(\mathbf{T}\boldsymbol{u}_h^{\widehat{\boldsymbol{u}}_h^{t,i}} - \widehat{\boldsymbol{u}}_h^{t,i}\right), \widehat{\boldsymbol{v}}^t\right\rangle_{\partial\mathcal{T}_h\setminus\partial\Omega_D} = a\left(\widehat{\boldsymbol{u}}_h^{t,i}, \widehat{\boldsymbol{v}}^t\right)$ as defined by (B.32), that $-\left\langle \boldsymbol{u}_h^{\widehat{f}_h^i}\cdot\boldsymbol{n} + \frac{1}{\tau_n}\left(f_h^{\widehat{f}_h^i} - \widehat{f}_h^i\right), \widehat{g}\right\rangle_{\partial\mathcal{T}_h\setminus\partial\Omega_N} = d\left(\widehat{f}_h^i, \widehat{g}\right)$ as defined by (B.33), that $-\left\langle \boldsymbol{u}_h^{\widehat{\boldsymbol{u}}_h^{t,i}}\cdot\boldsymbol{n} + \frac{1}{\tau_n} f_h^{\widehat{\boldsymbol{u}}_h^{t,i}}, \widehat{g}\right\rangle_{\partial\mathcal{T}_h\setminus\partial\Omega_N} = -b\left(\widehat{\boldsymbol{u}}_h^{t,i}, \widehat{g}\right)$ as defined by (B.34), and that $-\left\langle -\mathbf{L}_h^{\widehat{f}_h^i}\boldsymbol{n} + \tau_t\mathbf{T}\boldsymbol{u}_h^{\widehat{f}_h^i}, \widehat{\boldsymbol{v}}^t\right\rangle_{\partial\mathcal{T}_h\setminus\partial\Omega_D} = b\left(\widehat{\boldsymbol{v}}^t, \widehat{f}_h^i\right)$ as defined by (B.34).

Step 1: In (B.26a) take $\boldsymbol{\mu} = \widehat{\boldsymbol{v}}^t$ and $\mathbf{G} = \mathbf{L}_h^{\widehat{\boldsymbol{u}}_h^{t,i}}$, in (B.26b) take $\boldsymbol{\mu} = \widehat{\boldsymbol{u}}_h^{t,i}$ and $\boldsymbol{v} = \boldsymbol{u}_h^{\widehat{\boldsymbol{v}}^t}$, and in (B.26c) take $\boldsymbol{\mu} = \widehat{\boldsymbol{v}}^t$ and $q = p_h^{\widehat{\boldsymbol{u}}_h^{t,i}}$. Summing the result, we have

$$
\begin{aligned}
&\left(\mathrm{Re}\mathbf{L}_h^{\widehat{\boldsymbol{u}}_h^{t,i}}, \mathbf{L}_h^{\widehat{\boldsymbol{v}}^t}\right)_{\mathcal{T}_h} + \left\langle \frac{1}{\tau_n} f_h^{\widehat{\boldsymbol{u}}_h^{t,i}}, f_h^{\widehat{\boldsymbol{v}}^t}\right\rangle_{\partial\mathcal{T}_h} + \left\langle \tau_t\mathbf{T}\boldsymbol{u}_h^{\widehat{\boldsymbol{u}}_h^{t,i}}, \mathbf{T}\boldsymbol{u}_h^{\widehat{\boldsymbol{v}}^t}\right\rangle_{\partial\Omega_D} \\
&\quad + \left\langle \tau_t\left(\mathbf{T}\boldsymbol{u}_h^{\widehat{\boldsymbol{u}}_h^{t,i}} - \widehat{\boldsymbol{u}}_h^{t,i}\right), \mathbf{T}\boldsymbol{u}_h^{\widehat{\boldsymbol{v}}^t}\right\rangle_{\partial\mathcal{T}_h\setminus\partial\Omega_D} - \left\langle \mathbf{L}_h^{\widehat{\boldsymbol{u}}_h^{t,i}}\boldsymbol{n}, \widehat{\boldsymbol{v}}^t\right\rangle_{\partial\mathcal{T}_h\setminus\partial\Omega_D} = 0. \qquad \text{(B.37)}
\end{aligned}
$$

Therefore, $\left\langle \mathbf{L}_h^{\widehat{\boldsymbol{u}}_h^{t,i}}\boldsymbol{n}, \widehat{\boldsymbol{v}}^t\right\rangle_{\partial\mathfrak{T}_h\setminus\partial\Omega_D} - \left\langle \tau_t\left(\mathbf{T}\boldsymbol{u}_h^{\widehat{\boldsymbol{u}}_h^{t,i}} - \widehat{\boldsymbol{u}}_h^{t,i}\right), \widehat{\boldsymbol{v}}^t\right\rangle_{\partial\mathfrak{T}_h\setminus\partial\Omega_D} = a\left(\widehat{\boldsymbol{u}}_h^{t,i}, \widehat{\boldsymbol{v}}^t\right)$.

Step 2: In (B.27a) take $\gamma = \widehat{f}_h^i$ and $\mathbf{G} = \mathbf{L}_h^{\widehat{g}}$, in (B.27b) take $\gamma = \widehat{g}$ and $\boldsymbol{v} = \boldsymbol{u}_h^{\widehat{f}_h^i}$, and in (B.27c) take $\gamma = \widehat{f}_h^i$ and $q = p_h^{\widehat{g}}$. Summing the result, we have

$$\begin{aligned}&\left(\mathrm{Re}\mathbf{L}_h^{\widehat{f}_h^i}, \mathbf{L}_h^{\widehat{g}}\right)_{\mathfrak{T}_h} + \left\langle \tau_t\mathbf{T}\boldsymbol{u}_h^{\widehat{f}_h^i}, \mathbf{T}\boldsymbol{u}_h^{\widehat{g}}\right\rangle_{\partial\mathfrak{T}_h} + \left\langle \frac{1}{\tau_n}f_h^{\widehat{f}_h^i}, f_h^{\widehat{g}}\right\rangle_{\partial\Omega_N}\\ &\quad + \left\langle \frac{1}{\tau_n}\left(f_h^{\widehat{f}_h^i} - \widehat{f}_h^i\right), f_h^{\widehat{g}}\right\rangle_{\partial\mathfrak{T}_h\setminus\partial\Omega_N} + \left\langle \boldsymbol{u}_h^{\widehat{f}_h^i}\cdot\boldsymbol{n}, \widehat{g}\right\rangle_{\partial\mathfrak{T}_h\setminus\partial\Omega_N} = 0.\end{aligned} \tag{B.38}$$

Therefore, $-\left\langle \boldsymbol{u}_h^{\widehat{f}_h^i}\cdot\boldsymbol{n}, \widehat{g}\right\rangle_{\partial\mathfrak{T}_h\setminus\partial\Omega} - \left\langle \frac{1}{\tau_n}\left(f_h^{\widehat{f}_h^i} - \widehat{f}_h^i\right), \widehat{g}\right\rangle_{\partial\mathfrak{T}_h\setminus\partial\Omega} = d\left(\widehat{f}_h^i, \widehat{g}\right)$.

Step 3: In (B.27) take $\gamma = \widehat{g}$ and $(\mathbf{G}, \boldsymbol{v}, q) = \left(-\mathbf{L}_h^{\widehat{\boldsymbol{u}}_h^{t,i}}, \boldsymbol{u}_h^{\widehat{\boldsymbol{u}}_h^{t,i}}, -p_h^{\widehat{\boldsymbol{u}}_h^{t,i}}\right)$. Summing the result, we have

$$\begin{aligned}&-\left(\mathbf{L}_h^{\widehat{g}}, \mathbf{L}_h^{\widehat{\boldsymbol{u}}_h^{t,i}}\right)_{\mathfrak{T}_h} + \left(\mathbf{L}_h^{\widehat{g}}, \nabla\boldsymbol{u}_h^{\widehat{\boldsymbol{u}}_h^{t,i}}\right)_{\mathfrak{T}_h} + \left(\nabla\boldsymbol{u}_h^{\widehat{g}}, \mathbf{L}_h^{\widehat{\boldsymbol{u}}_h^{t,i}}\right)_{\mathfrak{T}_h} - \left(\nabla\cdot\boldsymbol{u}_h^{\widehat{g}}, p_h^{\widehat{\boldsymbol{u}}_h^{t,i}}\right)_{\mathfrak{T}_h}\\ &\quad - \left(p_h^{\widehat{g}}, \nabla\cdot\boldsymbol{u}_h^{\widehat{\boldsymbol{u}}_h^{t,i}}\right)_{\mathfrak{T}_h} - \left\langle \mathbf{L}_h^{\widehat{g}}\boldsymbol{n}, \mathbf{T}\boldsymbol{u}_h^{\widehat{\boldsymbol{u}}_h^{t,i}}\right\rangle_{\partial\mathfrak{T}_h} - \left\langle \mathbf{T}\boldsymbol{u}_h^{\widehat{g}}, \mathbf{L}_h^{\widehat{\boldsymbol{u}}_h^{t,i}}\boldsymbol{n}\right\rangle_{\partial\mathfrak{T}_h} + \left\langle \tau_t\mathbf{T}\boldsymbol{u}_h^{\widehat{g}}, \mathbf{T}\boldsymbol{u}_h^{\widehat{\boldsymbol{u}}_h^{t,i}}\right\rangle_{\partial\mathfrak{T}_h}\\ &\quad - \left\langle \frac{1}{\tau_n}f_h^{\widehat{g}}, f_h^{\widehat{\boldsymbol{u}}_h^{t,i}}\right\rangle_{\partial\mathfrak{T}_h} + \left\langle \frac{1}{\tau_n}\widehat{g}, f_h^{\widehat{\boldsymbol{u}}_h^{t,i}}\right\rangle_{\partial\mathfrak{T}_h\setminus\partial\Omega_N} + \left\langle \widehat{g}, \boldsymbol{u}_h^{\widehat{\boldsymbol{u}}_h^{t,i}}\cdot\boldsymbol{n}\right\rangle_{\partial\mathfrak{T}_h\setminus\partial\Omega_N} = 0.\end{aligned} \tag{B.39}$$

Therefore, $-\left\langle \boldsymbol{u}_h^{\widehat{\boldsymbol{u}}_h^{t,i}}\cdot\boldsymbol{n}, \widehat{g}\right\rangle_{\partial\mathfrak{T}_h\setminus\partial\Omega_N} - \left\langle \frac{1}{\tau_n}f_h^{\widehat{\boldsymbol{u}}_h^{t,i}}, \widehat{g}\right\rangle_{\partial\mathfrak{T}_h\setminus\partial\Omega_N} = -b\left(\widehat{\boldsymbol{u}}_h^{t,i}, \widehat{g}\right)$.

Step 4: In (B.26) take $\boldsymbol{\mu} = \widehat{\boldsymbol{v}}^t$ and $(\mathbf{G}, \boldsymbol{v}, q) = \left(\mathbf{L}_h^{\widehat{f}_h^i}, -\boldsymbol{u}_h^{\widehat{f}_h^i}, p_h^{\widehat{f}_h^i}\right)$. Summing the result, we have

$$\begin{aligned}&\left(\mathbf{L}_h^{\widehat{f}_h^i}, \mathbf{L}_h^{\widehat{\boldsymbol{v}}^t}\right)_{\mathfrak{T}_h} - \left(\mathbf{L}_h^{\widehat{f}_h^i}, \nabla\boldsymbol{u}_h^{\widehat{\boldsymbol{v}}^t}\right)_{\mathfrak{T}_h} - \left(\nabla\boldsymbol{u}_h^{\widehat{f}_h^i}, \mathbf{L}_h^{\widehat{\boldsymbol{v}}^t}\right)_{\mathfrak{T}_h} + \left(\nabla\cdot\boldsymbol{u}_h^{\widehat{f}_h^i}, p_h^{\widehat{\boldsymbol{v}}^t}\right)_{\mathfrak{T}_h}\\ &\quad + \left(p_h^{\widehat{f}_h^i}, \nabla\cdot\boldsymbol{u}_h^{\widehat{\boldsymbol{v}}^t}\right)_{\mathfrak{T}_h} + \left\langle \mathbf{L}_h^{\widehat{f}_h^i}\boldsymbol{n}, \mathbf{T}\boldsymbol{u}_h^{\widehat{\boldsymbol{v}}^t}\right\rangle_{\partial\mathfrak{T}_h} + \left\langle \mathbf{T}\boldsymbol{u}_h^{\widehat{f}_h^i}, \mathbf{L}_h^{\widehat{\boldsymbol{v}}^t}\boldsymbol{n}\right\rangle_{\partial\mathfrak{T}_h} - \left\langle \tau_t\mathbf{T}\boldsymbol{u}_h^{\widehat{f}_h^i}, \mathbf{T}\boldsymbol{u}_h^{\widehat{\boldsymbol{v}}^t}\right\rangle_{\partial\mathfrak{T}_h}\\ &\quad + \left\langle \frac{1}{\tau_n}f_h^{\widehat{f}_h^i}, f_h^{\widehat{\boldsymbol{v}}^t}\right\rangle_{\partial\mathfrak{T}_h} - \left\langle \mathbf{L}_h^{\widehat{f}_h^i}\boldsymbol{n}, \widehat{\boldsymbol{v}}^t\right\rangle_{\partial\mathfrak{T}_h\setminus\partial\Omega_D} + \left\langle \tau_t\mathbf{T}\boldsymbol{u}_h^{\widehat{f}_h^i}, \widehat{\boldsymbol{v}}^t\right\rangle_{\partial\mathfrak{T}_h\setminus\partial\Omega_D} = 0.\end{aligned} \tag{B.40}$$

Therefore, $\left\langle \mathbf{L}_h^{\widehat{f}_h^i}\boldsymbol{n}, \widehat{\boldsymbol{v}}^t\right\rangle_{\partial\mathfrak{T}_h\setminus\partial\Omega_D} - \left\langle \tau_t\mathbf{T}\boldsymbol{u}_h^{\widehat{f}_h^i}, \widehat{\boldsymbol{v}}^t\right\rangle_{\partial\mathfrak{T}_h\setminus\partial\Omega_D} = b\left(\widehat{\boldsymbol{v}}^t, \widehat{f}_h^i\right)$. □

We can conclude from Theorem B.3 that the condensed global system will take

the form

$$\begin{bmatrix} A & B^\top \\ -B & D \end{bmatrix} \begin{bmatrix} \widehat{U}^t \\ \widehat{F} \end{bmatrix} = \begin{bmatrix} F_1 \\ F_2 \end{bmatrix}.$$

Inspecting (B.32) and (B.33), we can see that the block matrices A and D are symmetric and positive semi-definite. We can further claim that the matrix D is positive definite. To claim this we must show $d\left(\widehat{f}_h^i, \widehat{f}_h^i\right) = 0 \Rightarrow \widehat{f}_h^i = 0$. Indeed, $d\left(\widehat{f}_h^i, \widehat{f}_h^i\right) = 0$ implies $\mathbf{L}_h^{\widehat{f}_h^i} = \mathbf{0}$, $p_h^{\widehat{f}_h^i} = \widehat{f}_h^i$ on $\mathcal{E}_h \backslash \partial\Omega_N$, $p_h^{\widehat{f}_h^i} = 0$ on $\partial\Omega_N$, and $\mathbf{T}\boldsymbol{u}_h^{\widehat{f}_h^i} = \mathbf{0}$ on $\mathcal{E}_h$. Then, with $\gamma = \widehat{f}_h^i$ in (B.27b), integrating by parts reveals that $p_h^{\widehat{f}_h^i}$ is elementwise constant, and therefore globally constant since $p_h^{\widehat{f}_h^i} = \widehat{f}_h^i$ on $\mathcal{E}_h \backslash \partial\Omega_N$. If $\partial\Omega_N \neq \emptyset$, then $p_h^{\widehat{f}_h^i} = 0$ and therefore $\widehat{f}_h^i = 0$. Otherwise, constraining one value of $\widehat{f}_h^i$ to zero gives that $p_h = \widehat{f}_h^i = 0$. In this case, we can only claim positive definiteness for the D matrix that results from reducing the matrix by the one constrained degree of freedom.

Appendix C

Additional Fluxes for the Oseen Equations

In Chapter 3, we derived HDG schemes for the Oseen equations, where four different fluxes can be used. These four fluxes are based on four different forms of the upwind flux. These four forms of the upwind flux are not the only ways we can express the upwind flux, but they are the four that we know lead to well-posed HDG schemes when used on all faces of the mesh skeleton. When the problem being solved has boundary conditions on $-\frac{1}{\mathrm{Re}}\left[\nabla \boldsymbol{u}\right]\boldsymbol{n}+p\boldsymbol{n}$, or its normal or tangential components, it could be feasible to use an HDG flux that directly approximates these quantities so that the boundary conditions can be directly prescribed to the hatted trace variables. We present three numerical fluxes in this appendix that can serve such a purpose. First we rewrite the numerical flux (3.11) using the identities (3.18).

The $-\mathbf{L}^*\boldsymbol{n}+p^*\boldsymbol{n}$ flux: The quantity $\boldsymbol{u}^*$ can be eliminated from (3.11) so that (3.11) can be written as

$$\boldsymbol{F}_n^* = \begin{pmatrix} -\left(\boldsymbol{u}+\left(\frac{1}{\tau_t^O+\frac{m}{2}}\mathbf{T}+\frac{1}{\tau_n^O+\frac{m}{2}}\mathbf{N}\right)\left[-\left(\mathbf{L}-\mathbf{L}^*\right)\boldsymbol{n}+\left(p-p^*\right)\boldsymbol{n}\right]\right)\otimes\boldsymbol{n}, \\ -\mathbf{L}^*\boldsymbol{n}+p^*\boldsymbol{n}+m\boldsymbol{u} \\ +m\left(\frac{1}{\tau_t^O+\frac{m}{2}}\mathbf{T}+\frac{1}{\tau_n^O+\frac{m}{2}}\mathbf{N}\right)\left(-\left(\mathbf{L}-\mathbf{L}^*\right)\boldsymbol{n}+\left(p-p^*\right)\boldsymbol{n}\right), \\ \boldsymbol{u}\cdot\boldsymbol{n}+\frac{1}{\tau_n^O+\frac{m}{2}}\left[-\boldsymbol{n}\cdot\left(\mathbf{L}-\mathbf{L}^*\right)\boldsymbol{n}+\left(p-p^*\right)\right] \end{pmatrix}. \quad \text{(C.1)}$$

The $(\mathbf{T}\boldsymbol{u}^*, h^*)$ flux: The quantities $\mathbf{T}\mathbf{L}^*\boldsymbol{n}$ and $\mathbf{N}\boldsymbol{u}^*$ can be eliminated from (3.11)

so that (3.11) can be written as

$$\boldsymbol{F}_n^* = \begin{pmatrix} -\left(\mathbf{T}\boldsymbol{u}^* + \mathbf{N}\boldsymbol{u} + \frac{1}{\tau_n^O + \frac{m}{2}}\left(-\boldsymbol{n}\cdot\mathbf{L}\boldsymbol{n} + p - h^*\right)\boldsymbol{n}\right)\otimes\boldsymbol{n}, \\ h^*\boldsymbol{n} - \mathbf{T}\mathbf{L}\boldsymbol{n} + m\mathbf{N}\boldsymbol{u} + \frac{m}{2}\mathbf{T}\boldsymbol{u}^* + \frac{m}{2}\mathbf{T}\boldsymbol{u} \\ +\tau_t^O\mathbf{T}\left(\boldsymbol{u} - \boldsymbol{u}^*\right) + m\frac{1}{\tau_n^O + \frac{m}{2}}\left(-\boldsymbol{n}\cdot\mathbf{L}\boldsymbol{n} + p - h^*\right)\boldsymbol{n}, \\ \boldsymbol{u}\cdot\boldsymbol{n} + \frac{1}{\tau_n^O + \frac{m}{2}}\left(-\boldsymbol{n}\cdot\mathbf{L}\boldsymbol{n} + p - h^*\right) \end{pmatrix}, \tag{C.2}$$

where $h^* := -\boldsymbol{n}\cdot\mathbf{L}^*\boldsymbol{n} + p^*$.

The $(\mathbf{N}\boldsymbol{u}^*, \mathbf{T}\mathbf{L}^*)$ flux: The quantities $\mathbf{N}\left(-\mathbf{L}^*\boldsymbol{n} + p^*\boldsymbol{n}\right)$ and $\mathbf{T}\boldsymbol{u}^*$ can be eliminated from (3.11) so that (3.11) can be written as

$$\boldsymbol{F}_n^* = \begin{pmatrix} -\left(\mathbf{N}\boldsymbol{u}^* + \mathbf{T}\boldsymbol{u} - \frac{1}{\tau_t^O + \frac{m}{2}}\left(\mathbf{L} - \mathbf{L}^*\right)\boldsymbol{n}\right)\otimes\boldsymbol{n}, \\ -\mathbf{N}\mathbf{L}\boldsymbol{n} + p\boldsymbol{n} - \mathbf{T}\mathbf{L}^*\boldsymbol{n} + \frac{m}{2}\mathbf{N}\boldsymbol{u}^* + \frac{m}{2}\mathbf{N}\boldsymbol{u} + m\mathbf{T}\boldsymbol{u} \\ +\tau_n^O\mathbf{N}\left(\boldsymbol{u} - \boldsymbol{u}^*\right) - m\frac{1}{\tau_t^O + \frac{m}{2}}\mathbf{T}\left(\mathbf{L} - \mathbf{L}^*\right)\boldsymbol{n}, \\ \boldsymbol{u}^*\cdot\boldsymbol{n} \end{pmatrix}. \tag{C.3}$$

As before, in order to define the numerical flux (3.19) we append a subscript h to the terms in (C.1) – (C.3), replace the starred quantities on the right side of (C.1) – (C.3) with hatted unknown quantities residing on the mesh skeleton, and replace τ_t^O and τ_n^O with τ_t and τ_n. The following numerical fluxes are the result.

The $\widehat{\boldsymbol{h}}_h$ flux (where $\widehat{\boldsymbol{h}}_h$ approximates $-\mathbf{L}^*\tilde{\boldsymbol{n}} + p^*\tilde{\boldsymbol{n}}$):

$$\boldsymbol{F}_{n,h}^* := \begin{pmatrix} -\left(\boldsymbol{u}_h + \left(\frac{1}{\tau_t + \frac{m}{2}}\mathbf{T} + \frac{1}{\tau_n + \frac{m}{2}}\mathbf{N}\right)\left(-\mathbf{L}_h\boldsymbol{n} + p_h\boldsymbol{n} - \mathrm{sgn}\widehat{\boldsymbol{h}}_h\right)\right)\otimes\boldsymbol{n}, \\ -\mathrm{sgn}\widehat{\boldsymbol{h}}_h + m\boldsymbol{u} \\ +m\left(\frac{1}{\tau_t + \frac{m}{2}}\mathbf{T} + \frac{1}{\tau_n + \frac{m}{2}}\mathbf{N}\right)\left(-\mathbf{L}_h\boldsymbol{n} + p_h\boldsymbol{n} - \mathrm{sgn}\widehat{\boldsymbol{h}}_h\right), \\ \boldsymbol{u}_h\cdot\boldsymbol{n} + \frac{1}{\tau_n + \frac{m}{2}}\left[-\boldsymbol{n}\cdot\left(\mathbf{L}_h\boldsymbol{n}\right) + p_h - \widehat{\boldsymbol{h}}_h\cdot\tilde{\boldsymbol{n}}\right] \end{pmatrix}. \tag{C.4}$$

The $(\widehat{\boldsymbol{u}}_h^t, \widehat{h}_h)$ flux (where $\widehat{h}_h$ approximates $-\boldsymbol{n}\cdot\mathbf{L}^*\boldsymbol{n} + p^*$):

$$\boldsymbol{F}_{n,h}^* = \begin{pmatrix} -\left(\widehat{\boldsymbol{u}}_h^t + \mathbf{N}\boldsymbol{u}_h + \frac{1}{\tau_n + \frac{m}{2}}\left(-\boldsymbol{n}\cdot\mathbf{L}_h\boldsymbol{n} + p_h - \widehat{h}_h\right)\boldsymbol{n}\right)\otimes\boldsymbol{n}, \\ \widehat{h}_h\boldsymbol{n} - \mathbf{T}\mathbf{L}_h\boldsymbol{n} + m\mathbf{N}\boldsymbol{u} + \frac{m}{2}\widehat{\boldsymbol{u}}_h^t + \frac{m}{2}\boldsymbol{u}_h^t \\ +\tau_t\mathbf{T}\left(\boldsymbol{u}_h - \widehat{\boldsymbol{u}}_h\right) + m\frac{1}{\tau_n + \frac{m}{2}}\left(-\boldsymbol{n}\cdot\mathbf{L}_h\boldsymbol{n} + p_h - \widehat{h}_h\right)\boldsymbol{n}, \\ \boldsymbol{u}_h\cdot\boldsymbol{n} + \frac{1}{\tau_n + \frac{m}{2}}\left(-\boldsymbol{n}\cdot\mathbf{L}_h\boldsymbol{n} + p_h - \widehat{h}_h\right) \end{pmatrix}. \tag{C.5}$$

The $(\widehat{u}_h^{\tilde{n}}, \widehat{\boldsymbol{h}}_h^t)$ **flux** (where $\widehat{u}_h^{\tilde{n}}$ approximates $\boldsymbol{u}^* \cdot \tilde{\boldsymbol{n}}$ and $\widehat{\boldsymbol{h}}_h^t$ approximates $-\mathbf{T}\mathbf{L}^* \tilde{\boldsymbol{n}}$):

$$\boldsymbol{F}^*_{n,h} = \begin{pmatrix} -\left(\widehat{u}_h^{\tilde{n}} \tilde{\boldsymbol{n}} + \boldsymbol{u}_h^t + \frac{1}{\tau_t + \frac{m}{2}} \left(-\mathbf{L}_h \boldsymbol{n} - \mathrm{sgn} \widehat{\boldsymbol{h}}_h^t\right)\right) \otimes \boldsymbol{n}, \\ -\mathbf{N}\mathbf{L}_h \boldsymbol{n} + p_h \boldsymbol{n} + \mathrm{sgn} \widehat{\boldsymbol{h}}_h^t + \frac{m}{2} \widehat{u}_h^{\tilde{n}} \tilde{\boldsymbol{n}} + \frac{m}{2} \mathbf{N} \boldsymbol{u}_h + m \mathbf{T} \boldsymbol{u}_h \\ +\tau_n \left(\mathbf{N} \boldsymbol{u}_h - \widehat{u}_h^{\tilde{n}} \tilde{\boldsymbol{n}}\right) + m \frac{1}{\tau_t + \frac{m}{2}} \left(-\mathbf{T}\mathbf{L}_h \boldsymbol{n} - \mathrm{sgn} \widehat{\boldsymbol{h}}_h^t\right), \\ \mathrm{sgn} \widehat{u}_h^{\tilde{n}} \end{pmatrix}. \tag{C.6}$$

In (C.4) and (C.6), we rely on an arbitrarily chosen normal direction $\tilde{\boldsymbol{n}}$ associated with a skeleton face e, and

$$\mathrm{sgn} := \mathrm{sgn}(\boldsymbol{n}) = \begin{cases} 1, & \text{if } \boldsymbol{n} = \tilde{\boldsymbol{n}}, \\ -1, & \text{if } \boldsymbol{n} = -\tilde{\boldsymbol{n}} \end{cases}$$

associated with each face of each element K in order to allow the unknowns on the mesh skeleton to be single-valued.

Appendix D

Proofs of Properties of Projections

In this appendix, we prove the optimality of the projections and adjoint projections used in the error analysis for the MHD HDG scheme in Formulation 5.3.

First, to understand the approximation capability of the coupled projection $\Pi(\mathbf{L}, \boldsymbol{u}) := (\Pi\mathbf{L}, \Pi\boldsymbol{u})$ as defined in (5.66), we recall a result in [22, Lemma A.1].

Lemma D.1. *Suppose that $w \in \mathcal{P}_k^{\perp}(K)$. Then, for any $e \subset \partial K$, the map $w \mapsto w|_e \in \mathcal{P}_k(e)$ is an isomorphism and $\|w\|_{0,K}^2 \sim h_K \|w\|_{0,e}^2$ holds with a constant independent of h_K.*

Proof of Lemma 5.9 (estimate for $\varepsilon_{\boldsymbol{u}}^I$). We extend the proof of a result in [11]. To begin, we define $\boldsymbol{g} := -\frac{1}{2}\kappa \boldsymbol{d} \times \left(\boldsymbol{n} \times \left(\varepsilon_{\boldsymbol{b}^t}^I + \varepsilon_{\hat{\boldsymbol{b}}^t}^I\right)\right)$, take $\boldsymbol{\mu} = \boldsymbol{v}|_{\partial K}$ for some $\boldsymbol{v} \in \boldsymbol{\mathcal{P}}_k^{\perp}(K)$ which will be determined later, and rewrite (5.66k) as

$$\begin{aligned}
\left\langle (\alpha_1 + m)\, \varepsilon_{\boldsymbol{u}}^I, \boldsymbol{v} \right\rangle_{\partial K} &= \left\langle \varepsilon_{\mathbf{L}}^I \boldsymbol{n} - \varepsilon_p^I \boldsymbol{n} + \boldsymbol{g}, \boldsymbol{v} \right\rangle_{\partial K} \\
&= \left(\nabla \cdot \varepsilon_{\mathbf{L}}^I, \boldsymbol{v}\right)_K + \left(\varepsilon_{\mathbf{L}}^I, \nabla \boldsymbol{v}\right)_K - \left(\nabla \varepsilon_p^I, \boldsymbol{v}\right)_K - \left(\varepsilon_p^I, \nabla \cdot \boldsymbol{v}\right)_K + \langle \boldsymbol{g}, \boldsymbol{v} \rangle_{\partial K} \\
&= \left(\nabla \cdot \mathbf{L} - \nabla p, \boldsymbol{v}\right)_K + \left(\varepsilon_{\boldsymbol{u}}^I \otimes \boldsymbol{w}, \nabla \boldsymbol{v}\right)_K + \langle \boldsymbol{g}, \boldsymbol{v} \rangle_{\partial K}, \qquad \text{(D.1)}
\end{aligned}$$

where we have used the integration by parts in the second equality, definitions of the projections $\Pi\mathbf{L}$, $\Pi\boldsymbol{u}$, and Πp, the orthogonality between $\nabla \cdot (\Pi\mathbf{L}), \nabla(\Pi p)$ and $\boldsymbol{v} \in \boldsymbol{\mathcal{P}}_k^{\perp}(K)$, and the orthogonality $\varepsilon_p^I \perp \nabla \cdot \boldsymbol{v}$ in the last equality. Now, let $\mathbb{P}_k \boldsymbol{u}$ be the L^2 projection of $\boldsymbol{u}$ and define $\delta_{\boldsymbol{u}}^I := \boldsymbol{u} - \mathbb{P}_k \boldsymbol{u}$. By the triangle inequality, it suffices to

estimate the approximation capability of $\delta_{\boldsymbol{u}} := \mathbb{P}_k \boldsymbol{u} - \Pi \boldsymbol{u}$. From the above formula, we have

$$\begin{aligned}
&\langle (\alpha_1 + m)\, \delta_{\boldsymbol{u}}, \boldsymbol{v} \rangle_{\partial K} - (\delta_{\boldsymbol{u}} \otimes \boldsymbol{w}, \nabla \boldsymbol{v})_K \\
&\quad = \underbrace{- \left\langle (\alpha_1 + m)\, \delta_{\boldsymbol{u}}^I, \boldsymbol{v} \right\rangle_{\partial K} + \left(\delta_{\boldsymbol{u}}^I \otimes \boldsymbol{w}, \nabla \boldsymbol{v} \right)_K}_{=: F_{\boldsymbol{u}}(\boldsymbol{v})} + \underbrace{(\nabla \cdot \mathbf{L} - \nabla p, \boldsymbol{v})_K}_{=: F_{\mathbf{L}}(\boldsymbol{v})} + \underbrace{\langle \boldsymbol{g}, \boldsymbol{v} \rangle_{\partial K}}_{=: F_{\boldsymbol{g}}(\boldsymbol{v})}.
\end{aligned}$$

Since $\delta_{\boldsymbol{u}} \in \boldsymbol{\mathcal{P}}_k^{\perp}(K)$, we can take $\boldsymbol{v} = \delta_{\boldsymbol{u}}$ to obtain

$$\left\langle \left(\alpha_1 + \frac{m}{2} \right) \delta_{\boldsymbol{u}}, \delta_{\boldsymbol{u}} \right\rangle_{\partial K} = F_{\boldsymbol{u}}(\delta_{\boldsymbol{u}}) + F_{\mathbf{L}}(\delta_{\boldsymbol{u}}) + F_{\boldsymbol{g}}(\delta_{\boldsymbol{u}})$$

where we have used $\nabla \cdot \boldsymbol{w} = 0$ in the integration by parts

$$\begin{aligned}
- (\delta_{\boldsymbol{u}} \otimes \boldsymbol{w}, \nabla \delta_{\boldsymbol{u}})_K &= -\frac{1}{2} (\boldsymbol{w}, \nabla (\delta_{\boldsymbol{u}} \cdot \delta_{\boldsymbol{u}}))_K \\
= \frac{1}{2} ((\nabla \cdot \boldsymbol{w}) \delta_{\boldsymbol{u}}, \delta_{\boldsymbol{u}})_K - \frac{1}{2} \langle \boldsymbol{w} \cdot \boldsymbol{n} \delta_{\boldsymbol{u}}, \delta_{\boldsymbol{u}} \rangle_{\partial K} &= - \left\langle \frac{m}{2} \delta_{\boldsymbol{u}}, \delta_{\boldsymbol{u}} \right\rangle_{\partial K}.
\end{aligned}$$

By Lemma D.1 and the fact that $\alpha_1 > \frac{1}{2} \|\boldsymbol{w}\|_{L^\infty}$, we have

$$\begin{aligned}
\|\delta_{\boldsymbol{u}}\|_{0,K}^2 \lesssim h_K \|\delta_{\boldsymbol{u}}\|_{0,\partial K}^2 &\lesssim \frac{h_K}{\alpha_1 - \frac{1}{2} \|\boldsymbol{w}\|_{L^\infty(K)}} \left\langle \left(\alpha_1 + \frac{m}{2} \right) \delta_{\boldsymbol{u}}, \delta_{\boldsymbol{u}} \right\rangle_{\partial K} \\
&= \frac{h_K}{\alpha_1 - \frac{1}{2} \|\boldsymbol{w}\|_{L^\infty(K)}} \left(F_{\boldsymbol{u}}(\delta_{\boldsymbol{u}}) + F_{\mathbf{L}}(\delta_{\boldsymbol{u}}) + F_{\boldsymbol{g}}(\delta_{\boldsymbol{u}}) \right). \qquad \text{(D.2)}
\end{aligned}$$

We now estimate $|F_{\boldsymbol{u}}(\delta_{\boldsymbol{u}})|$. Defining $\delta_{\boldsymbol{w}} = \boldsymbol{w} - \mathbb{P}_0 \boldsymbol{w}$, note that $(\delta_{\boldsymbol{u}}^I \otimes \boldsymbol{w}, \nabla \delta_{\boldsymbol{u}})_K = (\delta_{\boldsymbol{u}}^I \otimes \delta_{\boldsymbol{w}}, \nabla \delta_{\boldsymbol{u}})_K$ holds due to the definition of $\delta_{\boldsymbol{u}}^I$. Thus, we have

$$\begin{aligned}
|F_{\boldsymbol{u}}(\delta_{\boldsymbol{u}})| &= \left| \left\langle (m + \alpha_1) \delta_{\boldsymbol{u}}^I, \delta_{\boldsymbol{u}} \right\rangle_{\partial K} + \left(\delta_{\boldsymbol{u}}^I \otimes \delta_{\boldsymbol{w}}, \nabla \delta_{\boldsymbol{u}} \right)_K \right| \\
&\lesssim (\|\boldsymbol{w}\|_{L^\infty(\partial K)} + \alpha_1) h_K^{-1} \left(\|\delta_{\boldsymbol{u}}^I\|_{0,K} + h_K \|\nabla \delta_{\boldsymbol{u}}^I\|_{0,K} \right) \|\delta_{\boldsymbol{u}}\|_{0,K} \\
&\quad + \|\delta_{\boldsymbol{u}}^I\|_{0,K} \|\boldsymbol{w}\|_{W^{1,\infty}(K)} \|\delta_{\boldsymbol{u}}\|_{0,K}
\end{aligned}$$

where we have used $\|\delta_{\boldsymbol{w}}\|_{L^\infty(K)} \lesssim h_K \|\boldsymbol{w}\|_{W^{1,\infty}(K)}$, the inverse inequality, and the continuous and discrete trace inequalities ((5.63) and (5.64), respectively) in the last step. Taking the approximation capability of $\mathbb{P}_k \boldsymbol{u}$ into account, we get

$$|F_{\boldsymbol{u}}(\delta_{\boldsymbol{u}})| \lesssim \left(\alpha_1 + \|\boldsymbol{w}\|_{L^\infty(\partial K)} + h_K \|\boldsymbol{w}\|_{W^{1,\infty}(K)} \right) h_K^k \|\boldsymbol{u}\|_{k+1,K} \|\delta_{\boldsymbol{u}}\|_{0,K}. \qquad \text{(D.3)}$$

The estimate of $|F_{\mathbf{L}}(\delta_{\boldsymbol{u}})|$ is straightforward since $\delta_{\boldsymbol{u}} \in \boldsymbol{\mathcal{P}}_k^{\perp}(K)$:

$$\begin{aligned} |F_{\mathbf{L}}(\delta_{\boldsymbol{u}})| &\leq \|\nabla \cdot \mathbf{L} - \nabla p - \mathbb{P}_{k-1}(\nabla \cdot \mathbf{L} - \nabla p)\|_{0,K} \|\delta_{\boldsymbol{u}}\|_{0,K} \\ &\lesssim h_K^k \|\nabla \cdot \mathbf{L} - \nabla p\|_{k,K} \|\delta_{\boldsymbol{u}}\|_{0,K}. \end{aligned} \tag{D.4}$$

For the estimate of $|F_{\boldsymbol{g}}(\delta_{\boldsymbol{u}})|$, note that

$$\begin{aligned} \left\|\nabla \varepsilon_{\boldsymbol{b}}^I\right\|_{0,K} &\leq \|\nabla (\boldsymbol{b} - \mathbb{P}_k \boldsymbol{b})\|_{0,K} + \|\nabla (\mathbb{P}_k \boldsymbol{b} - \Pi \boldsymbol{b})\|_{0,K} \\ &\lesssim \|\boldsymbol{b} - \mathbb{P}_k \boldsymbol{b}\|_{1,K} + h_K^{-1} \|\mathbb{P}_k \boldsymbol{b} - \Pi \boldsymbol{b}\|_{0,K} \\ &\lesssim \|\boldsymbol{b} - \mathbb{P}_k \boldsymbol{b}\|_{1,K} + h_K^{-1} \|\mathbb{P}_k \boldsymbol{b} - \boldsymbol{b}\|_{0,K} + h_K^{-1} \|\boldsymbol{b} - \Pi \boldsymbol{b}\|_{0,K} \\ &\lesssim h_K^k \|\boldsymbol{b}\|_{k+1,K} + h_K^{-1} \left\|\varepsilon_{\boldsymbol{b}}^I\right\|_{0,K}. \end{aligned} \tag{D.5}$$

Using the definition of $\Pi^* \widehat{\boldsymbol{b}}^t$ as the L^2-projection, the continuous and discrete trace inequalities ((5.63) and (5.64), respectively), the above estimate of $\left\|\nabla \varepsilon_{\boldsymbol{b}}^I\right\|_{0,K}$ (D.5), and finally the estimate of $\left\|\varepsilon_{\boldsymbol{b}}^I\right\|_{0,K}$ in (5.67a), we have

$$\begin{aligned} |F_{\boldsymbol{g}}(\delta_{\boldsymbol{u}})| &\lesssim \kappa \|\boldsymbol{d}\|_{L^\infty(\partial K)} \left(\left\|\varepsilon_{\boldsymbol{b}^t}^I\right\|_{0,\partial K} + \left\|\varepsilon_{\widehat{\boldsymbol{b}}^t}^I\right\|_{0,\partial K} \right) \|\delta_{\boldsymbol{u}}\|_{0,\partial K} \\ &\lesssim \kappa \|\boldsymbol{d}\|_{L^\infty(\partial K)} \left\|\varepsilon_{\boldsymbol{b}^t}^I\right\|_{0,\partial K} \|\delta_{\boldsymbol{u}}\|_{0,\partial K} \\ &\lesssim \kappa \|\boldsymbol{d}\|_{L^\infty(\partial K)} \left(h_K^{-1} \|\varepsilon_{\boldsymbol{b}}^I\|_{0,K} + \|\nabla \varepsilon_{\boldsymbol{b}}^I\|_{0,K} \right) \|\delta_{\boldsymbol{u}}\|_{0,K} \\ &\lesssim \kappa \|\boldsymbol{d}\|_{L^\infty(\partial K)} \left(h_K^{-1} \|\varepsilon_{\boldsymbol{b}}^I\|_{0,K} + h_K^k \|\boldsymbol{b}\|_{k+1,K} \right) \|\delta_{\boldsymbol{u}}\|_{0,K} \\ &\lesssim \kappa \|\boldsymbol{d}\|_{L^\infty(\partial K)} h_K^k \left(\|\boldsymbol{b}\|_{k+1,K} + \alpha_3 \|r\|_{k+1,K} \right) \|\delta_{\boldsymbol{u}}\|_{0,K}. \end{aligned} \tag{D.6}$$

Using (D.3), (D.4), and (D.6) in (D.2), and using the triangle inequality $\|\varepsilon_{\boldsymbol{u}}^I\|_{0,K} \lesssim \|\boldsymbol{u} - \mathbb{P}_k \boldsymbol{u}\|_{0,K} + \|\delta_{\boldsymbol{u}}\|_{0,K}$ ends the proof. □

To estimate $\left\|\varepsilon_{\mathbf{L}}^I\right\|_0$, we need some auxiliary results. We first recall a result with a sketch of its proof.

Lemma D.2. *Let e_K be a fixed face of the simplex K. For $\boldsymbol{R} \in [L^2(K)]^d$ and $g \in L^2(\partial K)$, we define $\Pi(\boldsymbol{R}, g) \in \boldsymbol{\mathcal{P}}_k(K)$ as*

$$\begin{aligned} (\Pi(\boldsymbol{R}, g), \boldsymbol{\tau})_K &= (\boldsymbol{R}, \boldsymbol{\tau})_K, & \forall \boldsymbol{\tau} \in \boldsymbol{\mathcal{P}}_{k-1}(K), \\ \langle \Pi(\boldsymbol{R}, g) \cdot \boldsymbol{n}, \mu \rangle_e &= \langle g, \mu \rangle_e, & \forall \mu \in \mathcal{P}_k(e) \quad \textit{for } e \neq e_K. \end{aligned}$$

Then, $\|\Pi(\boldsymbol{R}, g)\|_K \lesssim \|\boldsymbol{R}\|_K + h_K^{1/2} \|g\|_{\partial K}$.

Proof. We refer to [20] for the existence and uniqueness of $\Pi(\boldsymbol{R}, g)$. Let $\boldsymbol{\sigma}_1 = \Pi(\boldsymbol{R}, 0)$ and $\boldsymbol{\sigma}_2 = \Pi(\boldsymbol{0}, g)$. By the standard scaling argument,

$$\|\boldsymbol{\sigma}_1\|_{0,K} \lesssim \|\mathbb{P}_{k-1} \boldsymbol{\sigma}_1\|_{0,K} \leq \|\boldsymbol{R}\|_{0,K}.$$

To estimate $\boldsymbol{\sigma}_2$, note that there exists $a_e \in \mathbb{R}$, $e \neq e_K$ such that $(1; 0; 0) = \sum_{e, e \neq e_K} a_e \boldsymbol{n}_e$, and the first component of $\boldsymbol{\sigma}_2$, say $\boldsymbol{\sigma}_2^1$, is

$$\boldsymbol{\sigma}_2^1 = \sum_{e, e \neq e_K} a_e (\boldsymbol{\sigma}_2 \cdot \boldsymbol{n}_e).$$

Since $\boldsymbol{\sigma}_2 \cdot \boldsymbol{n}_e \perp \mathcal{P}_{k-1}(K)$ by the definition of $\boldsymbol{\sigma}_2$, $\|\boldsymbol{\sigma}_2 \cdot \boldsymbol{n}_e\|_{0,K} \lesssim h_K^{1/2} \|\boldsymbol{\sigma}_2 \cdot \boldsymbol{n}_e\|_{0,e} \lesssim h_K^{1/2} \|g\|_{0,e}$ by Lemma D.1. The estimate $\|\boldsymbol{\sigma}_2\|_{0,K} \lesssim h_K^{1/2} \|g\|_{0,\partial K}$ follows easily by using this inequality to each component of $\boldsymbol{\sigma}_2$. □

We now recall other known facts without proofs (cf. Lemma 4.8 in [24]).

Lemma D.3. *For a face e of K, let $\mathcal{B}_e$ be an orthogonal basis of the vectors orthogonal to $\boldsymbol{n}_e$, and let $\mathcal{B} = \{\mathbb{I}_d\} \cup \{\boldsymbol{t} \otimes \boldsymbol{n}_e, \boldsymbol{t} \in \mathcal{B}_e\}$. This $\mathcal{B}$ is a basis of the space of $d \times d$ matrices.*

Proof of 5.10 (estimate for $\varepsilon_{\mathbf{L}}^I$). We proceed in a manner similar to [11, Theorem 2.3] with adaptations corresponding to our more complicated projectors $\boldsymbol{\Pi}(\mathbf{L}, \boldsymbol{u})$.

The dual basis of $\mathcal{B}$ (see Lemma D.3) can be written as

$$\mathcal{B}^* = \left\{ \frac{1}{d}\mathbb{I}_d \right\} \cup \{ W_{e,\boldsymbol{t}} \ : \ e \subset \partial K, \boldsymbol{t} \in \mathcal{B}_e \},$$

where $W_{e,\boldsymbol{t}} : (\boldsymbol{t} \otimes \boldsymbol{n}_e) = 1$ for the e and $\boldsymbol{t}$ corresponding to the subscripts of W, and 0 otherwise. Any $d \times d$ matrix, A, can be written as

$$A = \sum_e \sum_{\boldsymbol{t} \in \mathcal{B}_e} (A : (\boldsymbol{t} \otimes \boldsymbol{n}_e)) W_{e,\boldsymbol{t}} + \frac{\operatorname{tr} A}{d}\mathbb{I}_d = \sum_e \sum_{\boldsymbol{t} \in \mathcal{B}_e} (A\boldsymbol{n}_e \cdot \boldsymbol{t}) W_{e,\boldsymbol{t}} + \frac{\operatorname{tr} A}{d}\mathbb{I}_d,$$

so

$$\varepsilon^I_{\mathbf{L}} = \sum_e \sum_{\boldsymbol{t} \in \mathcal{B}_e} (\varepsilon^I_{\mathbf{L}} \boldsymbol{n}_e \cdot \boldsymbol{t}) W_{e,\boldsymbol{t}} + \frac{\operatorname{tr} \varepsilon^I_{\mathbf{L}}}{d}\mathbb{I}_d. \tag{D.7}$$

Since $W_{e,\boldsymbol{t}}$ is an element of $\mathcal{B}^*$ independent of mesh size, this identity reduces the estimate of $\|\varepsilon^I_{\mathbf{L}}\|_{0,K}$ to the estimates of $\|\varepsilon^I_{\mathbf{L}} \boldsymbol{n}_e \cdot \boldsymbol{t}\|_{0,K}$ with $\boldsymbol{t} \in \mathcal{B}_e$ and $\|\operatorname{tr} \varepsilon^I_{\mathbf{L}}\|_{0,K}$.

We first estimate $\|\varepsilon^I_{\mathbf{L}} \boldsymbol{n} \cdot \boldsymbol{t}\|_{0,K}$ with $\boldsymbol{n} = \boldsymbol{n}_e$ for some e. Let e_K be a fixed face of K and define $\Pi_1 \mathbf{L}, \Pi_2 \mathbf{L} \in \tilde{\boldsymbol{\mathcal{P}}}_1(K)$ as

$$(\Pi_1 \mathbf{L}, \mathbf{G})_K = (\mathbf{L}, \mathbf{G})_K, \qquad \forall \mathbf{G} \in \tilde{\boldsymbol{\mathcal{P}}}_{k-1}(K), \tag{D.8a}$$

$$\langle \Pi_1 \mathbf{L}\boldsymbol{n}, \boldsymbol{\mu} \rangle_e = \langle \mathbf{L}\boldsymbol{n}, \boldsymbol{\mu} \rangle_e, \qquad \forall \boldsymbol{\mu} \in \boldsymbol{\mathcal{P}}_k(e), e \neq e_K. \tag{D.8b}$$

and

$$(\Pi_2 \mathbf{L}, \mathbf{G})_K = (\mathbf{L}, \mathbf{G})_K - \left(\varepsilon^I_{\boldsymbol{u}} \otimes \delta_{\boldsymbol{w}}, \mathbf{G}\right)_K, \qquad \forall \mathbf{G} \in \tilde{\boldsymbol{\mathcal{P}}}_{k-1}(K), \tag{D.9a}$$

$$\langle \Pi_2 \mathbf{L}\boldsymbol{n}, \boldsymbol{\mu} \rangle_e = \langle \mathbf{L}\boldsymbol{n}, \boldsymbol{\mu} \rangle_e, \qquad \forall \boldsymbol{\mu} \in \boldsymbol{\mathcal{P}}_k(e), e \neq e_K. \tag{D.9b}$$

The existence and uniqueness of $\Pi_1 \mathbf{L}$ and $\Pi_2 \mathbf{L}$ follow from Lemma D.2. By the triangle inequality,

$$\begin{aligned} &\|\varepsilon^I_{\mathbf{L}} \boldsymbol{n} \cdot \boldsymbol{t}\|_{0,K} \\ &\quad \leq \|\mathbf{L}\boldsymbol{n} \cdot \boldsymbol{t} - \Pi_1 \mathbf{L}\boldsymbol{n} \cdot \boldsymbol{t}\|_{0,K} + \|(\Pi_1 - \Pi_2)\mathbf{L}\boldsymbol{n} \cdot \boldsymbol{t}\|_{0,K} + \|(\Pi_2 - \Pi)\mathbf{L}\boldsymbol{n} \cdot \boldsymbol{t}\|_{0,K}. \end{aligned} \tag{D.10}$$

Again by the triangle inequality, we bound the first term in (D.10) as

$$\begin{aligned}\|\mathbf{L}\boldsymbol{n}\cdot\boldsymbol{t}-\Pi_1\mathbf{L}\boldsymbol{n}\cdot\boldsymbol{t}\|_{0,K} &\le \|\mathbf{L}-\Pi_1\mathbf{L}\|_{0,K}\\ &\le \left\|\mathbf{L}-\Pi^{RTN}\mathbf{L}\right\|_{0,K}+\left\|\Pi^{RTN}\mathbf{L}-\Pi_1\mathbf{L}\right\|_{0,K},\end{aligned}\tag{D.11}$$

where Π^{RTN} is the row-wise canonical Raviart-Thomas-Nédélec (RTN) interpolation operator into the row-wise $(k+1)$-th order RTN element, which contains $\tilde{\boldsymbol{\mathcal{P}}}_k(K)$ for all $K\in\mathcal{T}_h$. From [20, Proposition 2.1 (vi)], we have that $\left\|\Pi^{RTN}\mathbf{L}-\Pi_1\mathbf{L}\right\|_{0,K}\lesssim h_K^{k+1}\left\|\mathbb{P}_k\nabla\cdot\mathbf{L}\right\|_k$, and from a well known property of the canonical RTN interpolation operator we have that $\left\|\mathbf{L}-\Pi^{RTN}\mathbf{L}\right\|_{0,K}\lesssim h_K^{k+1}\left\|\mathbf{L}\right\|_{k+1}$. Therefore, for the first term of (D.10) we have

$$\|\mathbf{L}-\Pi_1\mathbf{L}\|_{0,K}\lesssim h_K^{k+1}\left\|\mathbf{L}\right\|_{k+1,K}.$$

Note that $\Pi^{RTN}\mathbf{L}$ is not necessarily in $\tilde{\boldsymbol{\mathcal{P}}}_k(\mathcal{T}_h)$ but the above argument does not require $\Pi^{RTN}\mathbf{L}\in\tilde{\boldsymbol{\mathcal{P}}}_k(\mathcal{T}_h)$.

For the estimate of the second term in (D.10), note that the definitions of Π_1 and Π_2 give

$$(\Pi_1\mathbf{L}-\Pi_2\mathbf{L},\mathbf{G})_K=\left(\varepsilon^I_{\boldsymbol{u}}\otimes\delta_{\boldsymbol{w}},\mathbf{G}\right)_K,\qquad\forall\mathbf{G}\in\tilde{\boldsymbol{\mathcal{P}}}_{k-1}(K),\tag{D.12a}$$

$$\langle\Pi_1\mathbf{L}\boldsymbol{n}-\Pi_2\mathbf{L}\boldsymbol{n},\boldsymbol{\mu}\rangle_e=0,\qquad\forall\boldsymbol{\mu}\in\boldsymbol{\mathcal{P}}_k(e),e\neq e_K.\tag{D.12b}$$

By Lemma D.2, we can estimate the second term in (D.10) as

$$\begin{aligned}\|(\Pi_1-\Pi_2)\mathbf{L}\boldsymbol{n}\cdot\boldsymbol{t}\|_{0,K}\le\|\Pi_1\mathbf{L}-\Pi_2\mathbf{L}\|_{0,K}&\lesssim\|\varepsilon^I_{\boldsymbol{u}}\otimes\delta_{\boldsymbol{w}}\|_{0,K}\\ &\lesssim h_K\|\varepsilon^I_{\boldsymbol{u}}\|_{0,K}\|\boldsymbol{w}\|_{W^{1,\infty}(K)}.\end{aligned}\tag{D.13}$$

For the estimate of the third term in (D.10), recalling (5.66i), (5.66j), and (D.9a), we derive $(\Pi_2\mathbf{L}-\Pi\mathbf{L},\mathbf{G})_K=0$ for all $\mathbf{G}\in\tilde{\boldsymbol{\mathcal{P}}}_{k-1}(K)$. Selecting $\mathbf{G}=(\boldsymbol{t}\otimes\boldsymbol{n})\,q$

with $q \in \mathcal{P}_{k-1}(K)$, we have that $(\Pi_2 - \Pi)\,\mathbf{L}\boldsymbol{n}\cdot\boldsymbol{t} \in \mathcal{P}_k^{\perp}(K)$, and by Lemma D.1,

$$\|(\Pi_2 - \Pi)\,\mathbf{L}\boldsymbol{n}\cdot\boldsymbol{t}\|_{0,K} \lesssim h_K^{\frac{1}{2}} \|(\Pi_2 - \Pi)\,\mathbf{L}\boldsymbol{n}\cdot\boldsymbol{t}\|_{0,e}$$

for any e of ∂K. From (5.66k) and (D.9b), we have, for $e \neq e_K$

$$\langle(\Pi_2 - \Pi))\,\mathbf{L}\boldsymbol{n}, \boldsymbol{\mu}\rangle_e = \left\langle (m+\alpha_1)\varepsilon_{\boldsymbol{u}}^I + \varepsilon_p^I \boldsymbol{n} - \boldsymbol{g}, \boldsymbol{\mu}\right\rangle_e \quad \forall \boldsymbol{\mu} \in \boldsymbol{\mathcal{P}}_k(e),$$

with $\boldsymbol{g} := -\frac{1}{2}\kappa \boldsymbol{d} \times \left(\boldsymbol{n} \times \left(\varepsilon_{\boldsymbol{b}^t}^I + \varepsilon_{\widehat{\boldsymbol{b}}^t}^I\right)\right)$. Choosing $\boldsymbol{\mu} = [(\Pi_2 - \Pi)\,\mathbf{L}\boldsymbol{n}\cdot\boldsymbol{t}]\,\boldsymbol{t}$ and applying the Cauchy-Schwarz inequality to the above expression, we have

$$\begin{aligned}
\|(\Pi_2 - \Pi)\,\mathbf{L}\boldsymbol{n}\cdot\boldsymbol{t}\|_{0,e} &\lesssim \left\|(m+\alpha_1)\varepsilon_{\boldsymbol{u}}^I - \boldsymbol{g}\right\|_{0,e} \\
&\lesssim \left(\alpha_1 + \|\boldsymbol{w}\|_{L^\infty(K)}\right)\left\|\varepsilon_{\boldsymbol{u}}^I\right\|_{0,e} + \kappa\|\boldsymbol{d}\|_{L^\infty(K)}\left\|\varepsilon_{\boldsymbol{b}}^I\right\|_{0,e} \\
&\lesssim \left(\alpha_1 + \|\boldsymbol{w}\|_{L^\infty(K)}\right)\left(h_K^{-\frac{1}{2}}\left\|\varepsilon_{\boldsymbol{u}}^I\right\|_{0,K} + h_K^{\frac{1}{2}}\left\|\nabla\varepsilon_{\boldsymbol{u}}^I\right\|_{0,K}\right) \\
&\quad + \kappa\|\boldsymbol{d}\|_{L^\infty(K)}\left(h_K^{-\frac{1}{2}}\left\|\varepsilon_{\boldsymbol{b}}^I\right\|_{0,K} + h_K^{\frac{1}{2}}\left\|\nabla\varepsilon_{\boldsymbol{b}}^I\right\|_{0,K}\right) \\
&\lesssim \left(\alpha_1 + \|\boldsymbol{w}\|_{L^\infty(K)}\right)\left(h_K^{-\frac{1}{2}}\left\|\varepsilon_{\boldsymbol{u}}^I\right\|_{0,K} + h_K^{k+\frac{1}{2}}\|\boldsymbol{u}\|_{k+1,K}\right) \\
&\quad + \kappa\|\boldsymbol{d}\|_{L^\infty(K)}\left(h_K^{-\frac{1}{2}}\left\|\varepsilon_{\boldsymbol{b}}^I\right\|_{0,K} + h_K^{k+\frac{1}{2}}\|\boldsymbol{b}\|_{k+1,K}\right),
\end{aligned}$$

where we have used the fact that $\left\|\varepsilon_{\widehat{\boldsymbol{b}}^t}^I\right\|_{0,e} \leq \left\|\varepsilon_{\boldsymbol{b}^t}^I\right\|_{0,e}$, the continuous trace inequality (5.63), the bound on $\left\|\nabla\varepsilon_{\boldsymbol{b}}^I\right\|_{0,K}$ given by (D.5), and a similar bound for $\left\|\nabla\varepsilon_{\boldsymbol{u}}^I\right\|_{0,K}$ given by

$$\left\|\nabla\varepsilon_{\boldsymbol{u}}^I\right\|_{0,K} \lesssim h_K^k\|\boldsymbol{u}\|_{k+1,K} + h_K^{-1}\left\|\varepsilon_{\boldsymbol{u}}^I\right\|_{0,K}. \tag{D.14}$$

Combining the previous expressions, we have

$$\begin{aligned}
\|(\Pi_2 - \Pi)\,\mathbf{L}\boldsymbol{n}\cdot\boldsymbol{t}\|_{0,K} &\lesssim \left(\alpha_1 + \|\boldsymbol{w}\|_{L^\infty(K)}\right)\left(\left\|\varepsilon_{\boldsymbol{u}}^I\right\|_{0,K} + h_K^{k+1}\|\boldsymbol{u}\|_{k+1,K}\right) \\
&\quad + \kappa\|\boldsymbol{d}\|_{L^\infty(K)}\left(\left\|\varepsilon_{\boldsymbol{b}}^I\right\|_{0,K} + h_K^{k+1}\|\boldsymbol{b}\|_{k+1,K}\right) \\
&\lesssim \left(\alpha_1 + \|\boldsymbol{w}\|_{L^\infty(K)}\right)\left(\left\|\varepsilon_{\boldsymbol{u}}^I\right\|_{0,K} + h_K^{k+1}\|\boldsymbol{u}\|_{k+1,K}\right) \\
&\quad + \kappa\|\boldsymbol{d}\|_{L^\infty(K)}\left(h_K^{k+1}\|\boldsymbol{b}\|_{k+1,K} + \alpha_3 h_K^{k+1}\|r\|_{k+1,K}\right),
\end{aligned} \tag{D.15}$$

where we have used (5.67a) in the final step, but for simplicity in writing have not expanded $\left\|\varepsilon_{\boldsymbol{u}}^I\right\|_{0,K}$. Thus, from the three estimates (D.11), (D.13), (D.15) with (D.10), we have

$$\begin{aligned}\left\|\varepsilon_{\mathbf{L}}^I \boldsymbol{n}\cdot\boldsymbol{t}\right\|_{0,K} \lesssim\; & h_K^{k+1}\left\|\mathbf{L}\right\|_{k+1,K} + \left(\alpha_1 + \left\|\boldsymbol{w}\right\|_{L^\infty(K)}\right) h_K^{k+1}\left\|\boldsymbol{u}\right\|_{k+1,K} \\ & + \left(\alpha_1 + \left\|\boldsymbol{w}\right\|_{L^\infty(K)} + h_K\left\|\boldsymbol{w}\right\|_{W^{1,\infty}(K)}\right)\left\|\varepsilon_{\boldsymbol{u}}^I\right\|_{0,K} \\ & + \kappa\left\|\boldsymbol{d}\right\|_{L^\infty(K)}\left(h_K^{k+1}\left\|\boldsymbol{b}\right\|_{k+1,K} + \alpha_3 h_K^{k+1}\left\|r\right\|_{k+1,K}\right). \end{aligned} \tag{D.16}$$

To complete the estimate of $\|\varepsilon_{\mathbf{L}}^I\|_{0,K}$, we need to estimate $\|\operatorname{tr}\varepsilon_{\mathbf{L}}^I\|_{0,K}$. First, by taking $\mathbf{G} = q\mathbb{I}$ in (5.66i) with $q \in \mathcal{P}_{k-1}(K)$, we get

$$\left(\operatorname{tr}\varepsilon_{\mathbf{L}}^I, q\right)_K = \left(\operatorname{tr}(\varepsilon_{\boldsymbol{u}}^I \otimes \delta_{\boldsymbol{w}}), q\right)_K = \left(\mathbb{P}_{k-1}\operatorname{tr}(\varepsilon_{\boldsymbol{u}}^I \otimes \delta_{\boldsymbol{w}}), q\right)_K, \qquad q \in \mathcal{P}_{k-1}(K) \tag{D.17}$$

where $\mathbb{P}_{k-1}$ is the orthogonal L^2 projection into $\mathcal{P}_{k-1}(K)$. For a fixed $e_K \subset \partial K$, taking $\boldsymbol{\mu} = w\boldsymbol{n}_{e_K}$ with $w \in \mathcal{P}_k^\perp(K)$ in (5.66k) and using (D.7), we also get

$$\left\langle \operatorname{tr}\varepsilon_{\mathbf{L}}^I, w\right\rangle_{e_K} = \left\langle \zeta, w\right\rangle_{e_K} = \left\langle \mathbb{P}_{e_K}\zeta, w\right\rangle_{e_K}, \tag{D.18}$$

where ζ is a scalar function on K defined by

$$\zeta := -\left(\left(\sum_e \sum_{\boldsymbol{t}\in\mathcal{B}_e} (\varepsilon_{\mathbf{L}}^I \boldsymbol{n}_e\cdot\boldsymbol{t}) W_{e,\boldsymbol{t}}\right)\boldsymbol{n}_{e_K}\right)\cdot\boldsymbol{n}_{e_K} + \varepsilon_p^I|_{e_K} + (\alpha_1+m)\varepsilon_{\boldsymbol{u}}^I\cdot\boldsymbol{n}_{e_K} - \boldsymbol{g}\cdot\boldsymbol{n}_{e_K}$$

and $\mathbb{P}_{e_K}$ is the orthogonal L^2 projection into $\mathcal{P}_k(e_K)$. We define $\Pi_{e_K}(f,g) \in \mathcal{P}_k(K)$ for $f \in L^2(K)$ and $g \in L^2(e_K)$ as

$$\begin{aligned} \left(\Pi_{e_K}(f,g), q\right)_K &= \left(f, q\right)_K, && \forall q \in \mathcal{P}_{k-1}(K), \\ \left\langle \Pi_{e_K}(f,g), \mu\right\rangle_e &= \left\langle g, \mu\right\rangle_e, && \forall \mu \in \mathcal{P}_k(e), e = e_K. \end{aligned}$$

We refer to [20, Lemma 3.1] for well-posedness of this interpolation and optimal approximation property. By an argument similar to Lemma D.2, we have

$$\left\|\Pi_{e_K}(f,g)\right\|_{0,K} \lesssim \left\|f\right\|_{0,K} + h_K^{\frac{1}{2}}\left\|g\right\|_{0,e_K}.$$

For simplicity, we will use $\Pi_{e_K} f$ if $g = f|_{e_K}$.

Note that $\operatorname{tr} \varepsilon_{\mathbf{L}}^I$ is an element-wise polynomial because $\operatorname{tr} \mathbf{L} = 0$, so $\operatorname{tr} \varepsilon_{\mathbf{L}}^I = \Pi_{e_K} \operatorname{tr} \varepsilon_{\mathbf{L}}^I$. From this, the identities (D.17) and (D.18), and the above inequalities from scaling argument, we have

$$\left\|\operatorname{tr} \varepsilon_{\mathbf{L}}^I\right\|_{0,K} = \left\|\Pi_{e_K} \operatorname{tr} \varepsilon_{\mathbf{L}}^I\right\|_{0,K} \lesssim \left\|\mathbb{P}_{k-1} \operatorname{tr}(\varepsilon_{\boldsymbol{u}}^I \otimes \delta_{\boldsymbol{w}})\right\|_{0,K} + h_K^{\frac{1}{2}} \left\|\mathbb{P}_{e_K} \zeta\right\|_{0,e_K}.$$

The optimality of the orthogonal L^2 projection and the inverse trace inequality give

$$h_K^{\frac{1}{2}} \left\|\mathbb{P}_{e_K} \zeta\right\|_{0,e_K} \leq h_K^{\frac{1}{2}} \left\|\mathbb{P}_k \zeta\right\|_{0,e_K} \lesssim \left\|\mathbb{P}_k \zeta\right\|_{0,K} \leq \left\|\zeta\right\|_{0,K},$$

and using this and the previous estimate, we can write

$$\begin{aligned}
\left\|\operatorname{tr} \varepsilon_{\mathbf{L}}^I\right\|_{0,K} &\lesssim \left\|\varepsilon_{\boldsymbol{u}}^I \otimes \delta_{\boldsymbol{w}}\right\|_{0,K} + \left\|\zeta\right\|_{0,K} \\
&\lesssim h_K \left\|\boldsymbol{w}\right\|_{W^{1,\infty}(K)} \left\|\varepsilon_{\boldsymbol{u}}^I\right\|_{0,K} + h_K^{k+1} \left\|p\right\|_{k+1,K} \\
&\quad + \sum_e \sum_{\boldsymbol{t} \in \mathcal{B}_e} \left\|(\varepsilon_{\mathbf{L}}^I \boldsymbol{n}_e) \cdot \boldsymbol{t}\right\|_{0,K} + \left\|(\alpha_1 + m)\varepsilon_{\boldsymbol{u}}^I - \boldsymbol{g}\right\|_{0,K} \\
&\lesssim h_K^{k+1} \left\|p\right\|_{k+1,K} + h_K^{k+1} \left\|\mathbf{L}\right\|_{k+1,K} + \left(\alpha_1 + \left\|\boldsymbol{w}\right\|_{L^\infty(K)}\right) h_K^{k+1} \left\|\boldsymbol{u}\right\|_{k+1,K} \\
&\quad + \kappa \left\|\boldsymbol{d}\right\|_{L^\infty(K)} \left(h_K^{k+1} \left\|\boldsymbol{b}\right\|_{k+1,K} + \alpha_3 h_K^{k+1} \left\|r\right\|_{k+1,K}\right) \\
&\quad + \left(\alpha_1 + \left\|\boldsymbol{w}\right\|_{L^\infty(K)} + h_K \left\|\boldsymbol{w}\right\|_{W^{1,\infty}(K)}\right) \left\|\varepsilon_{\boldsymbol{u}}^I\right\|_{0,K}
\end{aligned}$$

and here we used previous results on $\left\|\varepsilon_{\mathbf{L}}^I \boldsymbol{n}\right\|_{0,K}$ and $\left\|(\alpha_1 + m)\varepsilon_{\boldsymbol{u}}^I - \boldsymbol{g}\right\|_{0,K}$ in the final inequality. We completed the estimate of $\|\varepsilon_{\mathbf{L}}^I\|_{0,K}$. □

Bibliography

[1] J. Adler, M. Brezina, T. A. Manteuffel, S. F. McCormick, J. W. Ruge, and L. Tang. Island coalescence using parallel first-order system least squares on incompressible resistive magnetohydrodynamics. *SIAM Journal on Scientific Computing*, 35(5):S171–S191, 2013.

[2] R. Alexander. Diagonally implicit Runge-Kutta methods for stiff ODE's. *SIAM Journal on Numerical Analysis*, 14(6):1006–1021, 1977.

[3] G. Alzetta, D. Arndt, W. Bangerth, V. Boddu, B. Brands, D. Davydov, R. Gassmoeller, T. Heister, L. Heltai, K. Kormann, M. Kronbichler, M. Maier, J.-P. Pelteret, B. Turcksin, and D. Wells. The `deal.II` library, version 9.0. *Journal of Numerical Mathematics*, 2018, accepted.

[4] D. N. Arnold, F. Brezzi, B. Cockburn, and L. D. Marini. Unified analysis of discontinuous galerkin methods for elliptic problems. *SIAM journal on numerical analysis*, 39(5):1749–1779, 2002.

[5] S. Badia, R. Codina, and R. Planas. On an unconditionally convergent stabilized finite element approximation of resistive magnetohydrodynamics. *Journal of Computational Physics*, 234:399–416, 2013.

[6] W. Bangerth, R. Hartmann, and G. Kanschat. deal.II – a general purpose object oriented finite element library. *ACM Trans. Math. Softw.*, 33(4):24/1–24/27, 2007.

[7] D. Biskamp. *Magnetic reconnection in plasmas*. Cambridge University Press, 2000.

[8] S. C. Brenner and L. R. Scott. *The Mathematical Theory of Finite Element Methods*. Springer, Third edition, 2008.

[9] T. Bui-Thanh. From Godunov to a unified hybridized discontinuous Galerkin framework for partial differential equations. *Journal of Computational Physics*, 295:114–146, 2015.

[10] T. Bui-Thanh. Construction and analysis of HDG methods for linearized shallow water equations. *SIAM Journal on Scientific Computing*, 38(6):A3696–A3719, 2016.

[11] A. Cesmelioglu, B. Cockburn, N. C. Nguyen, and J. Peraire. Analysis of HDG methods for Oseen equations. *Journal of Scientific Computing*, 55(2):392–431, 2013.

[12] L. Chacón. A non-staggered, conservative, $\nabla \cdot \mathbf{B} = \mathbf{0}$, finite-volume scheme for 3D implicit extended magnetohydrodynamics in curvilinear geometries. *Comput. Phys. Comm.*, 163:143–171, 2004.

[13] L. Chacón. An optimal, parallel, fully implicit Newton-Krylov solver for three-dimensional visco-resistive magnetohydrodynamics. *Phys. Plasmas*, 2008. accepted.

[14] L. Chacón, D. A. Knoll, and J. M. Finn. Implicit, nonlinear reduced resistive MHD nonlinear solver. *J. Comput. Phys.*, 178(1):15–36, 2002.

[15] L. Chacón, D. A. Knoll, and J. M. Finn. An implicit nonlinear reduced resistive MHD solver. *J. Comput. Phys.*, 178:15–36, 2002.

[16] B. Cockburn and J. Gopalakrishnan. The derivation of hybridizable discontinuous Galerkin methods for Stokes flow. *SIAM Journal on Numerical Analysis*, 47 (2):1092–1125, 2009.

[17] B. Cockburn and F.-J. Sayas. Divergence-conforming HDG methods for Stokes flows. *Mathematics of Computation*, 83(288):1571–1598, 2014.

[18] B. Cockburn, G. Kanschat, D. Schötzau, and C. Schwab. Local discontinuous Galerkin methods for the Stokes system. *SIAM Journal on Numerical Analysis*, 40(1):319–343, 2002.

[19] B. Cockburn, G. Kanschat, and D. Schötzau. A locally conservative LDG method for the incompressible Navier-Stokes equations. *Mathematics of Computation*, 74 (251):1067–1095, 2005.

[20] B. Cockburn, B. Dong, and J. Guzmán. A superconvergent LDG-hybridizable Galerkin method for second-order elliptic problems. *Mathematics of Computation*, 77(264):1887–1916, 2008.

[21] B. Cockburn, J. Gopalakrishnan, and R. Lazarov. Unified hybridization of discontinuous Galerkin, mixed, and continuous galerkin methods for second order elliptic problems. *SIAM Journal on Numerical Analysis*, 47(2):1319–1365, 2009.

[22] B. Cockburn, J. Gopalakrishnan, and F.-J. Sayas. A projection-based error analysis of HDG methods. *Mathematics of Computation*, 79(271):1351–1367, 2010.

[23] B. Cockburn, N. C. Nguyen, and J. Peraire. A comparison of HDG methods for Stokes flow. *Journal of Scientific Computing*, 45(1):215–237, 2010.

[24] B. Cockburn, J. Gopalakrishnan, N. Nguyen, J. Peraire, and F.-J. Sayas. Analysis of HDG methods for Stokes flow. *Mathematics of Computation*, 80(274):723–760, 2011.

[25] R. Codina and N. Hernández-Silva. Stabilized finite element approximation of the stationary magneto-hydrodynamics equations. *Computational Mechanics*, 38 (4-5):344–355, 2006.

[26] M. Dumbser, O. Zanotti, R. Loubère, and S. Diot. A posteriori subcell limiting of the discontinuous Galerkin finite element method for hyperbolic conservation laws. *Journal of Computational Physics*, 278:47–75, 2014.

[27] L. C. Evans. *Partial differential equations*, volume 19 of *Graduate Studies in Mathematics*. American Mathematical Society, Providence, RI, 1998. ISBN 0-8218-0772-2.

[28] J.-F. Gerbeau. A stabilized finite element method for the incompressible magnetohydrodynamic equations. *Numerische Mathematik*, 87(1):83–111, 2000.

[29] J.-F. Gerbeau, C. Le Bris, and T. Lelièvre. *Mathematical methods for the magnetohydrodynamics of liquid metals*. Clarendon Press, 2006.

[30] V. Girault and P.-A. Raviart. *Finite element methods for Navier-Stokes equations: Theory and Algorithms*, volume 5 of *Springer Series in Computational Mathematics*. Springer-Verlag, Berlin, 1986.

[31] J. P. Goedbloed and S. Poedts. *Principles of magnetohydrodynamics: with applications to laboratory and astrophysical plasmas*. Cambridge University Press, 2004.

[32] J. P. Goedbloed, R. Keppens, and S. Poedts. *Advanced magnetohydrodynamics: with applications to laboratory and astrophysical plasmas*. Cambridge University Press, 2010.

[33] M. D. Gunzburger, A. J. Meir, and J. S. Peterson. On the existence, uniqueness, and finite element approximation of solutions of the equations of stationary, incompressible magnetohydrodynamics. *Mathematics of Computation*, 56(194): 523–563, 1991.

[34] U. Hasler, A. Schneebeli, and D. Schötzau. Mixed finite element approximation of incompressible MHD problems based on weighted regularization. *Applied Numerical Mathematics*, 51(1):19–45, 2004.

[35] H. V. Henderson and S. R. Searle. The vec-permutation matrix, the vec operator and Kronecker products: A review. *Linear and Multilinear Algebra*, 9(4):271–288, 1981.

[36] J. S. Hesthaven and T. Warburton. *Nodal discontinuous Galerkin methods: algorithms, analysis, and applications*. Springer Science & Business Media, 2007.

[37] P. Houston, D. Schötzau, and X. Wei. A mixed DG method for linearized incompressible magnetohydrodynamics. *Journal of Scientific Computing*, 40(1): 281–314, 2009.

[38] A. Hujeirat. IRMHD: an implicit radiative and magnetohydrodynamical solver for self-gravitating systems. *Mon. Not. R. Astron. Soc.*, 298:310–320, 1998.

[39] S. C. Jardin. Review of implicit methods for the magnetohydrodynamic description of magnetically confined plasmas. *J. Comp. Physics*, 231:822–838, 2012.

[40] S. Kang, F. X. Giraldo, and T. Bui-Thanh. IMEX HDG-DG: a coupled implicit hybridized discontinuous Galerkin (HDG) and explicit discontinuous Galerkin (DG) approach for shallow water systems. *arXiv preprint arXiv:1711.02751*, 2017.

[41] C. A. Kennedy and M. H. Carpenter. Diagonally implicit Runge-Kutta methods for ordinary differential equations. A review. 2016.

[42] R. Keppens, G. Tóth, M. A. Botchev, and A. V. D. Ploeg. Implicit and semi-implicit schemes: algorithms. *Int. J. Numer. Meth. Fluids*, 30:335–352, 1999.

[43] D. Knoll and L. Chacón. Coalescence of magnetic islands, sloshing, and the pressure problem. *Physics of Plasmas*, 13(3):032307, 2006.

[44] D. A. Knoll and L. Chacón. Coalescence of magnetic islands in the low-resistivity, Hall-MHD regime. *Phys. Rev. Lett.*, 96(13):135001 – 4, 2006.

[45] L. Kovasznay. Laminar flow behind a two-dimensional grid. In *Mathematical Proceedings of the Cambridge Philosophical Society*, volume 44, pages 58–62. Cambridge University Press, 1948.

[46] J. J. Lee, S. Shannon, T. Bui-Thanh, and J. N. Shadid. Analysis of an HDG method for linearized incompressible resistive MHD equations. *submitted*, 2017.

[47] J. J. Lee, S. J. Shannon, T. Bui-Thanh, and J. N. Shadid. Analysis of an HDG method for linearized incompressible resistive MHD equations. *arXiv preprint arXiv:1702.05124*, 2017.

[48] R. J. Moreau. *Magnetohydrodynamics*. Springer Science & Business Media, 1990.

[49] U. Müller and L. Bühler. *Magnetofluiddynamics in Channels and Containers*. Springer Science & Business Media, 2013.

[50] S. Muralikrishnan, M.-B. Tran, and T. Bui-Thanh. iHDG: An iterative HDG framework for partial differential equations. *SIAM Journal on Scientific Computing*, 39(5):S782–S808, 2017.

[51] S. Muralikrishnan, T. Bui-Thanh, and J. N. Shadid. A multilevel solver for HDG methods. *In Preparation*, 2018.

[52] S. Muralikrishnan, M.-B. Tran, and T. Bui-Thanh. An improved iterative HDG approach for partial differential equations. *Journal of Computational Physics*, 367:295–321, 2018.

[53] N. Nguyen, J. Peraire, and B. Cockburn. A hybridizable discontinuous Galerkin method for Stokes flow. *Computer Methods in Applied Mechanics and Engineering*, 199(9):582–597, 2010.

[54] N. C. Nguyen and J. Peraire. Hybridizable discontinuous Galerkin methods for partial differential equations in continuum mechanics. *Journal of Computational Physics*, 231(18):5955–5988, 2012.

[55] N. C. Nguyen, J. Peraire, and B. Cockburn. An implicit high-order hybridizable discontinuous Galerkin method for linear convection–diffusion equations. *Journal of Computational Physics*, 228(9):3232–3254, 2009.

[56] N. C. Nguyen, J. Peraire, and B. Cockburn. An implicit high-order hybridizable discontinuous Galerkin method for the incompressible Navier–Stokes equations. *Journal of Computational Physics*, 230(4):1147–1170, 2011.

[57] D. A. D. Pietro and A. Ern. *Mathematical aspects of Discontinuous Galerkin methods*. Springer, 2012.

[58] E. Priest and T. Forbes. Magnetic reconnection; MHD theory and applications. 2000.

[59] W. H. Reed and T. Hill. Triangular mesh methods for the neutron transport equation. Technical report, Los Alamos Scientific Lab., N. Mex.(USA), 1973.

[60] N. B. Salah, A. Soulaimani, W. G. Habashi, and M. Fortin. A conservative stabilized finite element method for the magneto-hydrodynamic equations. *International Journal for Numerical Methods in Fluids*, 29(5):535–554, 1999.

[61] D. Schötzau. Mixed finite element methods for stationary incompressible magneto–hydrodynamics. *Numerische Mathematik*, 96(4):771–800, 2004.

[62] J. N. Shadid, R. P. Pawlowski, J. W. Banks, L. Chacón, P. T. Lin, and R. S. Tuminaro. Towards a scalable fully-implicit fully-coupled resistive MHD formulation with stabilized FE methods. *Journal of Computational Physics*, 229(20): 7649–7671, 2010.

[63] J. N. Shadid, R. P. Pawlowski, E. C. Cyr, R. S. Tumiaro, L. Chacon, and P. D. Weber. Scalable implicit incompressible resistive MHD with stabilized FE and fully-coupled Newton-Krylov-AMG. *Comput. Methods Appl. Mech. Engrg*, 304: 1–25, 2016.

[64] J. N. Shadid, R. P. Pawlowski, E. C. Cyr, R. S. Tuminaro, L. Chacón, and P. D. Weber. Scalable implicit incompressible resistive MHD with stabilized FE and fully-coupled Newton–Krylov-AMG. *Computer Methods in Applied Mechanics and Engineering*, 304:1–25, 2016.

[65] J. N. Shadid, R. P. Pawlowski, J. W. Banks, L. Chacón, P. T. Lin, and R. S. Tuminaro. Towards a scalable fully-implicit fully-coupled resistive MHD formu-

lation with stabilized FE methods. *J. Comput. Phys.*, 229(20):7649–7671, OCT 1 2010.

[66] S. Shannon, J. N. Shadid, T. Bui-Thanh, and J. J. Lee. A hybridized discontinuous Galerkin method for resistive incompressible magnetohydrodynamics. *The Center for Computing Research at Sandia National Laboratories; Summer Proceedings*, 2016.

[67] U. Shumlak and J. Loverich. Approximate Riemann solver for the two-fluid plasma model. *J. Comp. Phy.*, 187:620–638, 2003.

[68] U. Shumlak, R. Lilly, N. Reddell, E. Sousa, and B. Srinivasan. Advanced physics calculations using a multi-fluid plasma model. *Computer Physics Comm.*, 182: 1767–1770, 2011.

[69] C. Sovinec, A. Glasser, T. Gianakon, D. Barnes, R. Nebel, S. Kruger, D. Schnack, S. Plimpton, A. Tarditi, M. Chu, et al. Nonlinear magnetohydrodynamics simulation using high-order finite elements. *Journal of Computational Physics*, 195 (1):355–386, 2004.

[70] G. Tóth, R. Keppens, and M. A. Botchev. Implicit and semi-implicit schemes in the Versatile Advection Code: numerical tests. *Astron. Astrophys.*, 332:1159–1170, 1998.

[71] C. F. Van Loan. The ubiquitous Kronecker product. *Journal of Computational and Applied Mathematics*, 123(1-2):85–100, 2000.

[72] T. Wildey, S. Muralikrishnan, and T. Bui-Thanh. Unified geometric multigrid algorithm for hybridized high-order finite element methods. *SIAM Journal on Scientific Computing (Under Revision)*, 2018.